



n. 1 – 2020

Italian Journal of Agrometeorology

Rivista Italiana di Agrometeorologia



SCIENTIFIC DIRECTOR

Simone Orlandini

Department of Agriculture, Food, Environment and Forestry (DAGRI)
University of Florence
Piazzale delle Cascine 18 – 50144, Firenze (FI), Italia
Tel. +39 055 2755755
simone.orlandini@unifi.it

PUBLICATION DIRECTOR

Francesca Ventura

Dipartimento di Scienze e Tecnologie Agro-alimentari
Università di Bologna
Via Fanin, 44 – 40127 Bologna (BO), Italia
Tel. +39 051 20 96 658
francesca.ventura@unibo.it

FIELD EDITORS

CROP PROTECTION

Antonello Cossu

ARPAS - Servizio Valutazione Analisi
Ambientale (Sassari)

Federico Spanna

Phytosanitary sector and technical-scientific
services - Piemonte region (Turin)

CLIMATOLOGY

Emanuele Eccel

Fondazione Edmund Mach di San Michele
all'Adige (Trento)

Valentina Pavan

Arpae – Emilia Romagna (Bologna)

CLIMATE CHANGE

Domenico Ventrella

Environment Research Center Agriculture –
CREA (Bari)

Vittorio Marletto

Arpae – Emilia Romagna (Bologna)

CROP GROWING, PRODUCTION AND AGRO- MANAGEMENT

Roberto Confalonieri

Department of Plant Production -
University of Milano

Anna Dalla Marta

Department of Agriculture, Food,
Environment and Forestry (DAGRI) -
University of Florence

PHENOLOGY

Alessandro Chiaudani

Department of Engineering and Geology –
University of Chieti

Gabriele Cola

Department of Plant Production -
University of Milano

MICRO-METEOROLOGY

Simona Consoli

Department of Agriculture, Food and
Environment (Di3A) - University of Catania

WATER RELATIONS AND IRRIGATION

Marco Napoli

Department of Agriculture, Food,
Environment and Forestry (DAGRI) -
University of Florence

SPATIALIZATION, GIS

Fabio Zottele

Fondazione Edmund Mach di San Michele
all'Adige (TN)

OPERATIVE TECHNIQUES

Luigi Pasotti

Regional Department of Agriculture and
Forests of the Sicily Region

EDITORIAL BOARD

Marco Acutis, University of Milan, Milan (Italy)

Vesselin Alexandrov, National Institute of Meteorology and Hydrology, Sofia (Bulgaria)

Marco Bindi, University of Florence, Florence (Italy)

Stefano Bocchi, University of Milan, Milan (Italy)

Maurizio Borin, University of Padua, Padua (Italy)

Orivaldo Brunini, Center of Ecology and Biophysics - Agronomic Institute, Campinas (Brazil)

Pierluigi Calanca, Agroscope Reckenholz-Tänikon, Zurich (Switzerland)

Raffaele Casa, Tuscia University, Viterbo (Italy)

Francesco Danuso, University of Udine, Udine (Italy)

Josef Eitzinger, University of Boku, Wien (Austria)

Lee Byong-Lyol, Korea Meteorological Administration, Suwon (Republic of Korea)

Vittorio Marletto, ARPA - Emilia Romagna, Bologna (Italy)

Raymond Motha, United States Department of Agriculture, Washington (USA)

Pavol Nejedlik, Slovak Hydrometeorological Institute, Bratislava (Slovakia)

Luigi Perini, CRA – CMA, Rome (Italy)

Laxman Singh Rathore, Agromet Division, India Meteorological Department, New Delhi (India)

Federica Rossi, CNR - IBIMET, Bologna (Italy)

Paola Rossi Pisa, University of Bologna, Bologna (Italy)

Paulo Cesar Sentelhas, Department of Exact Sciences ESALQ - University of São Paulo, Piracicaba, SP, (Brazil)

Donatella Spano, University of Sassari, Sassari (Italy)

Robert Stefanski, WMO, Geneva (Switzerland)

Roger Stone, University of Southern Australia, Toowoomba (Australia)

Italian Journal of Agrometeorology

n. 1 - 2020

Firenze University Press

The *Italian Journal of Agrometeorology (IJAm - Rivista Italiana di Agrometeorologia)* is the official periodical of the Italian Association of Agrometeorology (AIAM) and aims to publish original scientific contributions in English on agrometeorology, as a science that studies the interactions of hydrological and meteorological factors with the agricultural and forest ecosystems, and with agriculture in its broadest sense (including livestock and fisheries).

Italian Association of Agrometeorology (AIAM)

Presidente: Francesca Ventura (francesca.ventura@unibo.it)

Vicepresidente: Federica Rossi

Consiglieri: Filiberto Altobelli, Anna dalla Marta, Emanuele Scalcione, Federico Spanna, Domenico Ventrella

Revisori dei conti: Bruno Di Lena, Chiara Epifani, Marcello Giovanni Onorato

Segreteria: Simone Falzoi, Emanuela Forni, Tiziana La Iacona, Mattia Sanna, Irene Vercellino

e-mail AIAM: segreteria@agrometeorologia.it

Sede legale: via Caproni, 8 - 50144 Firenze

web: www.agrometeorologia.it

e-mail Italian Journal of Agrometeorology: ijagrometeorology@agrometeorologia.it

SUBSCRIPTION INFORMATION

IJAm articles are freely available online, but print editions are available to paying subscribers. Subscription rates are in Eur and are applicable worldwide.

Annual Subscription: € 50,00 Single Issue: € 25,00

CONTACT INFORMATION

Please contact ordini@fupress.com, if you have any questions about your subscription or if you would like to place an order for the print edition. Information on payment methods will be provided after your initial correspondence.

Published by

Firenze University Press – University of Florence, Italy

Via Cittadella, 7 - 50144 Florence - Italy

<http://www.fupress.com/ijam>

Copyright © 2020 **Authors**. The authors retain all rights to the original work without any restrictions.

Open Access. This issue is distributed under the terms of the [Creative Commons Attribution 4.0 International License \(CC-BY-4.0\)](https://creativecommons.org/licenses/by/4.0/) which permits unrestricted use, distribution, and reproduction in any medium, provided you give appropriate credit to the original author(s) and the source, provide a link to the Creative Commons license, and indicate if changes were made. The Creative Commons Public Domain Dedication (CC0 1.0) waiver applies to the data made available in this issue, unless otherwise stated.



OPEN ACCESS

Citation: S. Yeşilköy, L. Şaylan (2020) Assessment and modelling of crop yield and water footprint of winter wheat by aquacrop. *Italian Journal of Agrometeorology* (1): 3-14. doi: 10.13128/ijam-859

Received: February 25, 2020

Accepted: April 21, 2020

Published: June 23, 2020

Copyright: © 2020 S. Yeşilköy, L. Şaylan. This is an open access, peer-reviewed article published by Firenze University Press (<http://www.fupress.com/ijam>) and distributed under the terms of the Creative Commons Attribution License, which permits unrestricted use, distribution, and reproduction in any medium, provided the original author and source are credited.

Data Availability Statement: All relevant data are within the paper and its Supporting Information files.

Competing Interests: The Author(s) declare(s) no conflict of interest.

Assessment and modelling of crop yield and water footprint of winter wheat by aquacrop

SERHAN YEŞILKÖY^{1,2,*}, LEVENT ŞAYLAN²

1 İstanbul Directorate of Provincial Agriculture and Forestry, Ministry of Agriculture and Forestry – İstanbul, Turkey

2 Department of Meteorological Engineering, Faculty of Aeronautics and Astronautics, İstanbul Technical University – İstanbul, Turkey

* Corresponding author: yesilkoy@itu.edu.tr

Abstract. Agriculture has a considerable impact on water resources and it is strongly affected by climate change. It is important to determine and forecast crop water use for controlling and planning water resources while ensuring agricultural sustainability. Crop Water Footprint (WF) is an indicator of water consumed for crop production. The aim of the study is to calculate WF of winter wheat using Water Footprint Assessment (WFA) and to simulate future WFs by means of AquaCrop model for the Thrace region in Turkey. Although winter wheat does not require irrigation, the estimation of the WF is of importance due to its extensive production throughout the country. The WFs is estimated using meteorological and CORDEX data. The emerging findings indicate an increase in average temperature between 0.9 and 4.0°C. Precipitation is expected to increase by 15% under the optimistic scenario (RCP 4.5) and decrease by 17% under the worst-case scenario (RCP 8.5) by 2099. Winter wheat yield will positively be affected by increasing temperatures by up to 17% under RCP 4.5 and 26% under RCP 8.5 scenarios.

Keywords. Climate Change, Green Water Consumption, Crop Productivity, Crop Growth Simulation Model, Cereal.

INTRODUCTION

Climate projections emphasize that water scarcity will be one of the most important problem in the future. Therefore, determination of water consumption of crops has a crucial importance especially in arid and semi-arid countries in the world. To determine direct and indirect water use, the water footprint is widely used (Hoekstra, 2003). The WF represents the volume of freshwater used to production process and it is measured on all levels of the supply chain. Showing water consumption and polluted water volumes by source and type of pollution, WF comprises of components like blue, green and grey WFs. Blue WF is estimated in crop production with irrigated agriculture while green WF is determined in rainfed agriculture conditions. Grey WF involves the information about groundwater pollution because of fertilization.

Crop-climate models indicate that crop production may decrease because of high temperatures, while crop yield may increase as a consequence of rising CO₂ concentrations in the atmosphere (Caldag and Saylan, 2005; Nakagawa et al., 2007; Özdoğan, 2011). Moreover, agricultural activities consume nearly 70% of global water resources (Huang et al., 2018; Taheri et al., 2019). In this study, WF of winter wheat is estimated and WF's future projections are realized by means of AquaCrop model developed by Food and Agriculture Organization (FAO). AquaCrop bases on soil-water balance method and it is one of the most common used models to determine crop yield and WF (Raes et al., 2009; Steduto et al., 2009). The input requirements of the model are soil, climate, crop and agricultural management data.

There are many applications of the AquaCrop model for estimating the WF and yield. For instance, Gobin et al. (2017) have analyzed variability of arable crop production in some parts of Europe. Results showed that WF of cereals was much bigger than WF of tuber and root crops and the biggest part of WF belongs to green WF. Variability of arable crops was mainly related to variability of crop yield and variability of crop water use. Others, Chouchane et al. (2018) assessed the WF of wheat, barley, potatoes, dates, olives and tomatoes for the period 1981-2010. The model is better in explaining net virtual water import (NVWI) of wheat, barley and potatoes than NVWI of dates, olives, and tomatoes. Alvarez et al. (2016) estimated the green and blue WF of maize in Argentina, observing a WF decrease with an increase in irrigation and fertilization. They have determined that green WF represented 92% of total WF. Zhuo and Hoekstra (2017) have analyzed the effect of different agricultural applications on green and

blue WF, irrigation efficiency and of crop water usage efficiency. The results indicated that the deficit irrigation improved irrigation efficiency by 5% and decreased blue WF by 38%. Zhou et al. (2016) simulated WF of winter wheat production considering only water stress. According to their findings, the WF for irrigated winter wheat was 8-10% larger than rainfed winter wheat and the WF criteria for rainy years were 1-3% smaller than the dry years, 7-8% for the WF criteria for the hot years. Moreover, it was mentioned that WF criteria showed 10-12% differences in different soil types. Karandish and Hoekstra (2017) have predicted WF of 26 crops by means of AquaCrop in Iran. In the 1980-2010 period, it was determined that crop production, total crop production WF and blue WF have increased by 175%, 122%, 20%, respectively. During this period, the population has increased by 92%, while the crop consumption per person has grown by 20%, whereas the total crop consumption and total WF by 130 and 110%, respectively. Additionally, Lalic et al. (2018) have investigated monthly forecast of green water components and summer crops yield in Serbia and Austria using AquaCrop model and ensemble weather forecast. Tsakmakis et al. (2018) analyzed the effects of different irrigation schedules on WF of cotton with AquaCrop and CROPWAT for the north of Greece. The results showed that the effect of irrigation technology and strategy in green, blue and total WF were better predicted by the AquaCrop model, while the CROPWAT model can only evaluate changes in the irrigation strategy. Nouri et al. (2019) examined the reduction of WF with different soil mulching and drip irrigation methods. In the previous study, AquaCrop model and global Water Footprint Assessment (WFA) was used for estimating blue and green WF of ten major crops. The results showed that WF of crop production was more sensitive to climate and soil type. They have found that that the annual blue WF of the summer season was highest when water availability was lowest. Mulching has reduced the blue WF by 3.6% and mulching with drip irrigation have decreased the WF by 4.7%. Bakanogullari et al. (2017) used AquaCrop model and estimated that sunflower is more sensitive to soil water content than winter wheat.

For the estimation of winter wheat WF, different models such as linear and nonlinear regression model (Ye et al., 2019), Agro-Ecological Zones model (Wang et al., 2015), Soil and Water Assessment Tool (Luan et al., 2018), AquaCrop (Gobin et al., 2017; Zhuo and Hoekstra, 2017; Chouchane et al., 2018), Markov chain (Feng et al., 2017), CWUModel (De Miguel et al., 2015), global gridded crop model (Deryng et al., 2016), CROPWAT (Muratoglu, 2019), DSSAT (Ventrella et al., 2018), crop models

within ensemble approach (Palosuo et al., 2011; Garofalo et al., 2019) and WFA methodology have been used (Ababaei and Etedali, 2017; Santos et al., 2017; Huang et al., 2019; Zhai et al., 2019).

The aim of this study was to investigate WF and yield of winter wheat for northwestern part of Turkey (for Edirne, Kırklareli and Tekirdağ cities) using WFA and AquaCrop model. Firstly, WF of winter wheat was calculated by means of WFA with meteorological variables. Secondly, AquaCrop model was performed under RCP (Representative Concentration Pathway) 4.5 and 8.5 scenarios to forecast potential WFs and yields in the future. As input EURO-CORDEX (Coordinated Regional Climate Downscaling Experiment) data, HadGEM2-ES global climate model data and HIRHAM5 regional climate model data were used. Finally, WF and yield from calculations and simulations were compared and evaluated.

MATERIALS AND METHODS

Study Area

This study covers the agricultural areas of the Edirne, Kırklareli and Tekirdağ provinces of Thrace region, in the northwestern part of Turkey. As shown by elevation data reported in figure 1, Istranca mountains are the highest ones of the region with 1032 m and locate in the north of the Kırklareli city. The blue dots and red triangles on the map represent the locations of the meteorological stations used to correct CORDEX data. AquaCrop was performed according to RCP 4.5 and 8.5 scenarios in grids (0.11° horizontal resolution) with the red triangles. AquaCrop was not performed in grids with blue dots because necessary input data such as meteorological, soil and crop phenological data for the model were insufficient. For this

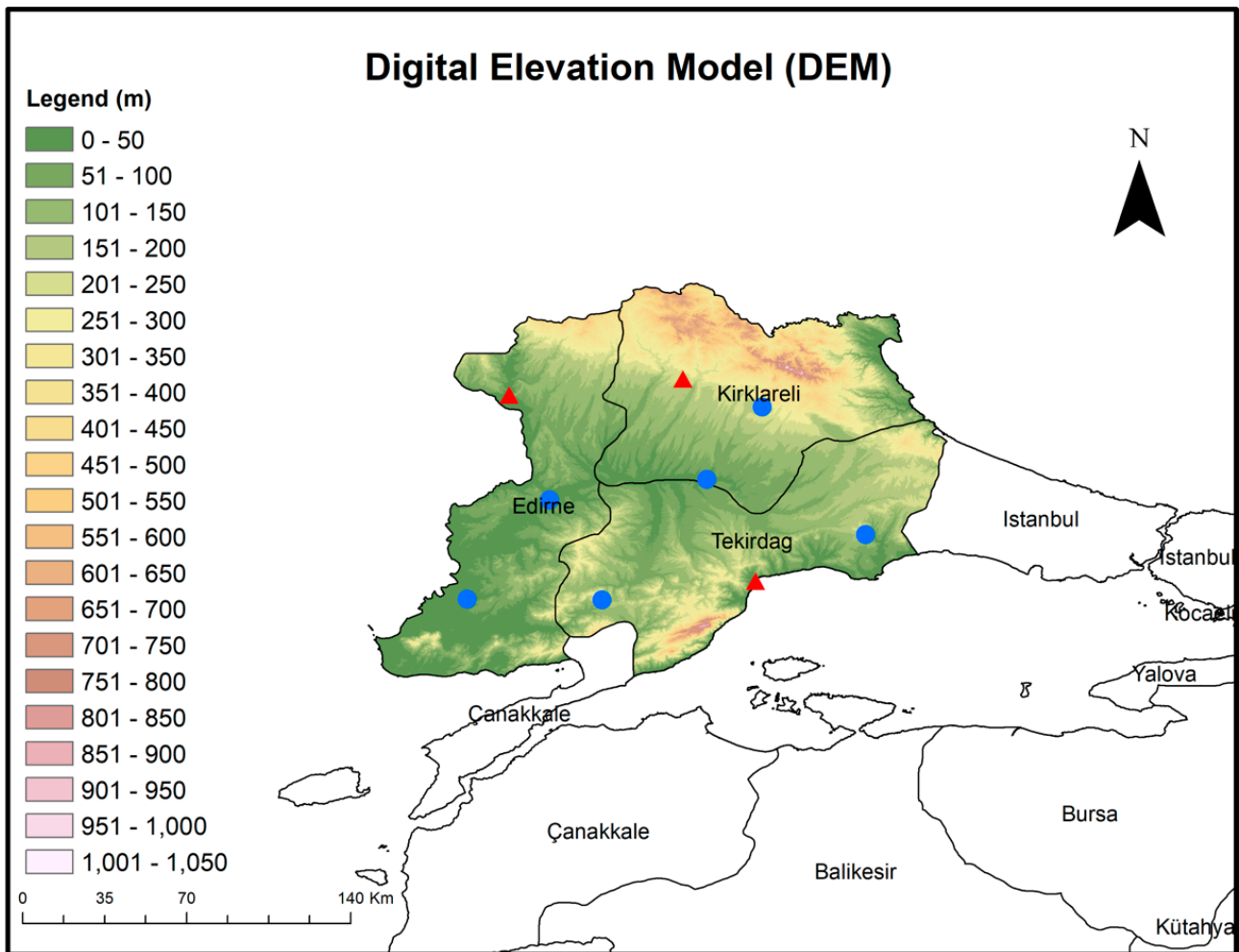


Fig. 1. Study area.

reason, AquaCrop model results were examined for each grid in 3 locations.

Data

Meteorological Data

Daily temperature (mean, maximum, and minimum), precipitation, global solar radiation, relative humidity and wind speed measurements were obtained from meteorological stations located in Edirne, Kırklareli (connected to Atatürk Soil Water and Agricultural Meteorology Research Institute, AMRI) and Tekirdağ (connected to Turkish State Meteorological Service, TSMS). Besides, meteorological data in between the reference years (1971-2000) were used for correction of CORDEX data. Table 1 contains the longitude, latitude, and mean sea level (msl) information of meteorological stations.

In Fig. 2, annual mean air temperature and total precipitation maps are illustrated for reference years (1971-2000).

The annual mean air temperature was 13.2°C and the annual total precipitation was 588 mm. Mean temperature and precipitation values of southwestern part of Thrace were about 0.5°C and 100 mm higher than the region average, respectively. In the reference years, Kırklareli had about 60 mm lower precipitation and about 0.5°C lower than the region's mean precipitation and temperature, respectively. Similarly, Fig. 3 shows the mean air temperature, precipitation and effective precipitation in the growing season of winter wheat.

Tab. 1. Locations of Selected Meteorological Stations.

Stations	Longitude (°)	Latitude (°)	Msl (m)
Pınarhisar (TSMS)	27.52	41.63	225
Edirne (TSMS)	26.55	41.68	48
Kırklareli (TSMS)	27.22	41.74	232
Çorlu (TSMS)	27.92	41.14	153
Tekirdağ (TSMS)	27.50	40.96	14
Lüleburgaz (TSMS)	27.31	41.35	45
İpsala (TSMS)	26.39	40.89	73
Uzunköprü (TSMS)	26.71	41.27	22
Malkara (TSMS)	26.91	40.89	202
Kırklareli (AMRI)	27.21	41.70	170
Edirne (AMRI)	26.64	40.73	30

During the winter wheat growing season, the Thrace region recorded an annual temperature of and precipitation of were 9.9°C and 463 mm, respectively. Moreover, effective precipitation was calculated as 217 mm. The mean temperature and the precipitation during the growing period in the southwestern part of the region were higher than the region average.

According to TSMS measurements, Average temperatures of wheat during growing season between 1971-2000 were measured in Edirne, Kırklareli and Tekirdağ as 10.4, 10.0 and 10.9°C, respectively. However, after 2000s, the average temperature in wheat growing season increased by 1°C in the region (Fig. 4).

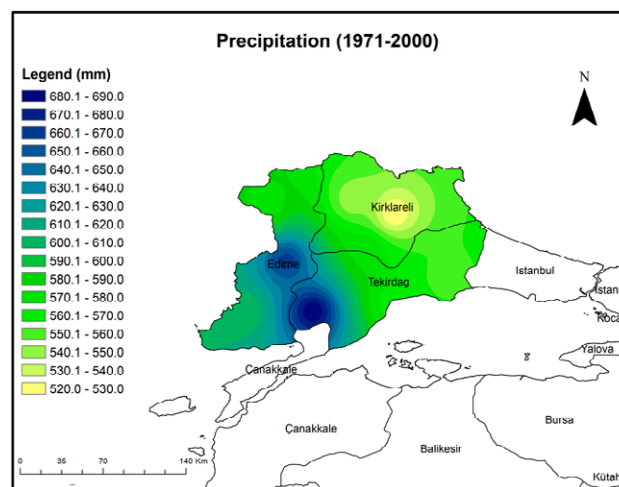
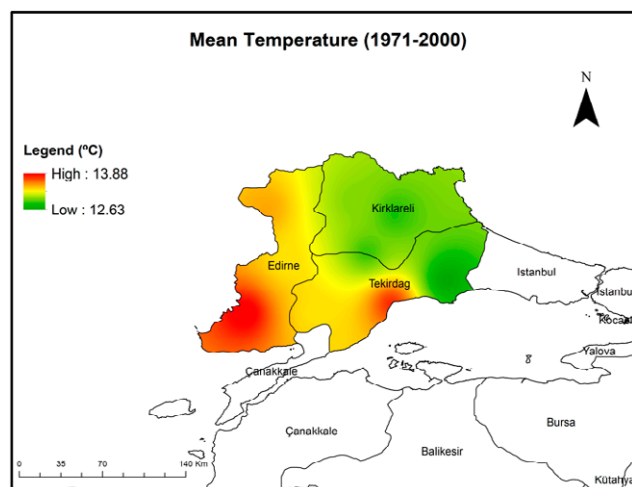


Fig. 2. Annual Mean Temperature and Total Precipitation Maps.

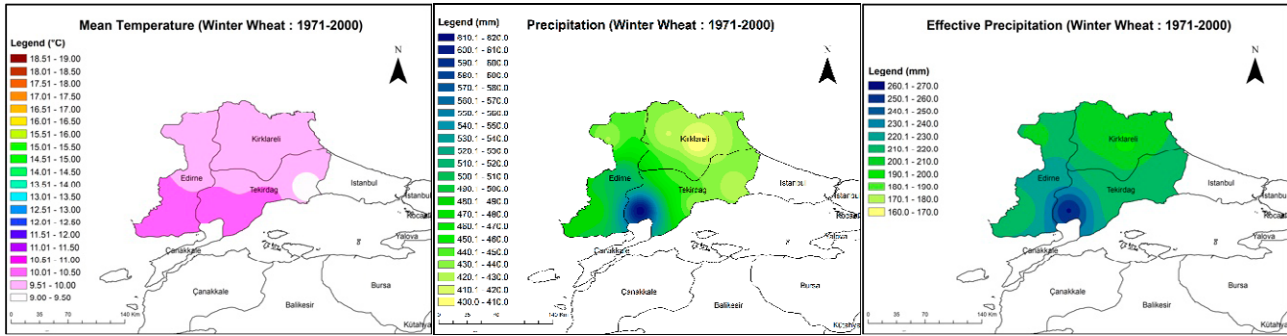


Fig. 3. Mean Temperature, Precipitation and Effective Precipitation in Winter Wheat Growing Season (Reference Years).

Soil and Crop Data

Physical properties of locations’ dominant soils are given in table 2 (Gobin et al., 2017; Gürbüz et al., 2019). Table 3 shows the reference sowing and harvest data for winter wheat (Gelibolu cultivar) cultivated in the region in 2015-2016 and 2017-2018 agricultural years.

CORDEX Data

In the study, projection data of RCP 4.5 (optimistic) and RCP 8.5 (worst-case) scenarios were provided between the years of 1971 and 2099. Developed with the Hadley Meteorology Office and designed for the scenarios in the IPCC’s 5th Assessment Report (AR5), the HadGEM2-ES global climate model, whose outputs are downscaled with HIRHAM5 (Christensen et al., 2007) regional climate model with a horizontal resolution of 0.11° (~12.5 km) and EURO-CORDEX temperature, precipitation, relative humidity, global radiation, and wind speed data were provided in the daily time interval.

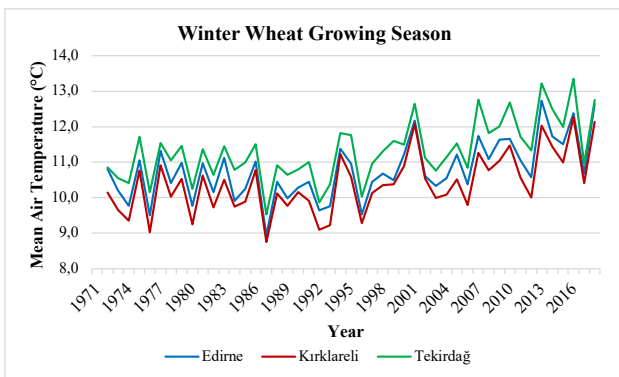


Fig. 4. Time Series of Mean Temperature of Winter Wheat Growing Seasons from 1971 to 2018.

Bias Correction

The data produced by climate models generally do not match the measurement data in the reference period. These errors affect the simulations for the future. Future reliability of climate models is increased with bias correction. Due to the nature of meteorological variables, their distributions are different and different bias correction methods are used (Feigenwinter et al., 2018; Soriano et al., 2019; Zapata et al., 2020).

Simple Mean Seasonal Bias Correction

Climate projection data require bias correction (Teng et al., 2015; Qian et al., 2015; Macadam et al., 2016; Mostafa et al., 2019). In the study, simple mean seasonal bias correction was used for daily mean, maximum, and minimum temperature data. Differences between measured and modelled data for both RCP 4.5 and 8.5 were corrected as computed as follows:

Tab. 2. Texture and hydrological parameters of dominant soils in the Thrace region.

Location	Soil Type	Field Capacity (%)	Wilting Point (%)
Edirne	Clay	37	23
Kırklareli	Sandy Loam	35	17
Tekirdağ	Loamy	39	28

Tab. 3. Sowing and harvest date for winter wheat cultivation.

Practice	Edirne	Kırklareli	Tekirdağ
Planting	20-October	20-October	20-October
Harvest	20-June	25-June	20-June

$$T_{i,cor} = T_i + \Delta T_i, \quad (1)$$

where T_i is the temperature (mean, max, min) in a given month i , ΔT is the difference between the mean temperature of the climate model and the observations in a given month i , and $T_{i,cor}$ is the corrected temperature in month i .

Quantile Mapping Bias Correction

Quantile Mapping (QM) method is a widely used method for correcting projection data not only precipitation but also global solar radiation, relative humidity, wind speed correction (Thiemeßl et al., 2011; Teutschbein and Siebert, 2012; Gudmundsson et al., 2012; Chen et al., 2013; Feigenwinter et al., 2018). This method is based on the application of the measurement values of the cumulative distribution function (CDF) of the reference years from the models to the projection distribution functions by mapping them over the cumulative distribution functions (Heo et al., 2019; Soriano et al., 2019). Bias corrected data was calculated by using the following Eq. 2.

$$Q_m(t) = F_0^{-1}[F_s(Q_s(t))] \quad (2)$$

where $Q_m(t)$ and $Q_s(t)$ are the bias corrected and simulated data from the regional climate model (RCM) during the reference period, F_s and F_0^{-1} are the CDF of the raw data from the RCM and the inverse CDF of the observed data, respectively.

AquaCrop Model

The AquaCrop model has been developed by the FAO, based on the principles of soil-water balance method and widely used by researchers, and was preferred in determining the WF and crop parameters (Alvarez et al., 2016; Zhuo et al., 2016; Gobin et al., 2017; Karandish and Hoekstra, 2017; Zhuo and Hoekstra, 2017; Chouchane et al., 2018; Lalic et al., 2018; Tsakmakis et al., 2018; Nouri et al., 2019). Input data required in this model are soil (soil type, field capacity, wilting point, initial soil water content etc.)-crop (phenological date, seed number etc.)-climate parameters (max and min temperature, global solar radiation, precipitation, relative humidity, ET_0) information on agricultural practices (fertilizer, cultivation etc.) with particular reference to irrigation (Raes et al., 2009; Steduto et al., 2009). In this study, AquaCrop model v6.1 was used in order to model of yield and WF of winter wheat.

Water Footprint Calculations

The WF [$m^3 \text{ ha}^{-1}$] has 3 different components: blue, green and gray WF. The blue WF shows irrigated agriculture, while the green rainfed conditions (Mekonnen and Hoekstra, 2011), and the grey the amount of groundwater contaminated by fertilization. The WF of crops is the sum of blue and green WFs (Eq. 3). In this study, the amount of green WF was calculated since the winter wheat is grown in rainfed conditions in Thrace Region.

$$WF = WF_{Blue} + WF_{Green} \quad (3)$$

Blue and green WFs are calculated with Equations 4 and 5 (Hoekstra et al., 2011; Bocchiola et al. 2013).

$$WF_{Blue} = 10 \times \frac{ET_{Blue}}{Yield} \quad (4)$$

$$WF_{Green} = 10 \times \frac{ET_{Green}}{Yield} \quad (5)$$

The coefficient 10 is used to convert the specified ET quantity unit from mm to $m^3 \text{ ha}^{-1}$, yield ($t \text{ ha}^{-1}$) and WF is used in $m^3 \text{ t}^{-1}$. Blue and green ET calculations from WF components are calculated with Equations 6 and 7, respectively.

$$ET_{Blue} = \max(0, ET_c - P_{eff}) \quad (6)$$

$$ET_{Green} = \min(ET_c, P_{eff}) \quad (7)$$

where ET_c , crop evapotranspiration (mm); P_{eff} , efficient precipitation (mm). In order to determine P_{eff} , USDA SCS method (Nearing et al., 1989) is used in daily time step (Eq. 8 and 9).

$$P_{total} < 8.3 \text{ mm}, P_{eff} = \frac{P_{total}(4.17 - 0.2P_{total})}{4.17} \quad (8)$$

$$P_{total} \geq 8.3 \text{ mm}, P_{eff} = 4.17 + 0.1P_{total} \quad (9)$$

ET_c is calculated from modified Penman&Monteith (P&M) ET_0 approach (Allen et al., 1998), detailed information can be found in Raes et al. (2009) and Steduto et al. (2009). Using soil water content measurements, the actual ET values of winter wheat are determined by the Soil Water Balance (SWB) method (Allen et al., 1998).

RESULTS

Yield and Water Footprint

The calibration of AquaCrop for winter wheat was performed on the basis of grain yield of 2015-2016 and 2017-2018 growing seasons. Measured mean temperature, total precipitation and effective precipitation during the growing seasons are also shown in Tab. 4.

According to Table 4, the daily mean temperature in the wheat development period in the reference years (1971-2000) was 9.9°C, while the mean temperature in the periods of model calibration was calculated as 12.9°C. The total precipitation in the years when the model was calibrated and in the reference years were 481.8 and 462.9 mm (approximately 19 mm lower in reference years), respectively. Although the amount of precipitation in the years when model calibration was performed is higher than the reference years, the effective rainfall amount is approximately 5 mm lower. When the actual and predicted yields were compared, the average relative errors (REs) in the cities of Edirne, Kırklareli and Tekirdağ were -2.4%, -1.6% and 5.6%, respectively.

Figure 5 shows the green WFs calculated from the measurements and estimated by the AquaCrop model. According to Figure 5, the REs between the WF calculated with SWB and the modelled green WF were 17.1%, -28.7% and -52.4% in Edirne, Kırklareli and Tekirdağ, respectively. The average green WF of the region was calculated as 452.7 m³ t⁻¹ with SWB method and it was 359.0 m³ t⁻¹ for modelled green WF. The reason of this difference is that the ET values were calculated using the P&M method through meteorological variables while the SWB method uses the changes of soil water content values. Besides, infiltration and runoff were not taken into account in the calculation of SWB. WF differences between the provinces may be resulted from these assumptions and differences of the soil structure.

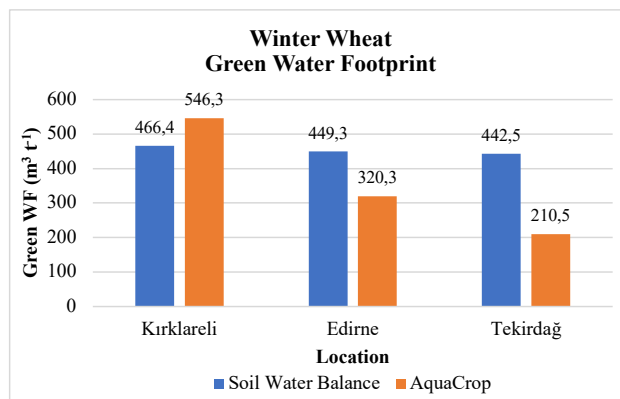


Fig. 5. Comparison of Winter Wheat Water Footprints.

Future Scenarios

While making simulations for the future with the AquaCrop model, the concentration amount of RCP 4.5 and 8.5 scenarios was used as atmospheric CO₂ concentration. It is projected that the increase in temperatures in recent years will continue in the RCP 4.5 and 8.5 scenarios. The mean temperature in the region is expected to increase by 0.9-1.6°C and 2.0-4.0°C under the RCP 4.5 and 8.5, respectively, by 2099. Variation of mean temperature for different scenarios in three periods (P1: 2020-2040, P2: 2041-2070, P3: 2071-2099) during the winter wheat growing seasons are shown in Figures 6 and 7, respectively.

The analysis of future precipitation (RCP 4.5) trends show that precipitation during the winter wheat season will increase 15% compared to baseline scenario, while a decrease of 17% is expected in the worst-case scenario (RCP 8.5). Effective precipitation changes in winter wheat growing season is expected to increase by 12% in the RCP 4.5 and 21% decrease in the RCP 8.5. In Figure 8, there are projected effective precipitation maps according to the RCP 4.5 scenario.

According to the RCP 4.5, effective precipitation is increased between 3% and 22% in P1. The lowest

Tab. 4. Statistics of 2015-2016 and 2017-2018 Winter Wheat Growing Seasons.

	Actual Yield (t ha ⁻¹)	AquaCrop Yield (t ha ⁻¹)	Mean Temperature (°C)	Precipitation (mm)	Peff (mm)
Edirne	4.86	4.74	12.5 (10.8*)	518.8 (499.2*)	225.4 (234.9*)
Kırklareli	4.67	4.59	12.2 (10.4*)	503.0 (492.1*)	218.9 (231.7*)
Tekirdağ	3.85	4.06	13.1 (11.3*)	423.7 (495.7*)	191.7 (232.1*)
Region Average (1971-2000)	-	-	9.9	462.9	216.9

*Average of 1971-2019 in winter wheat growing seasons.

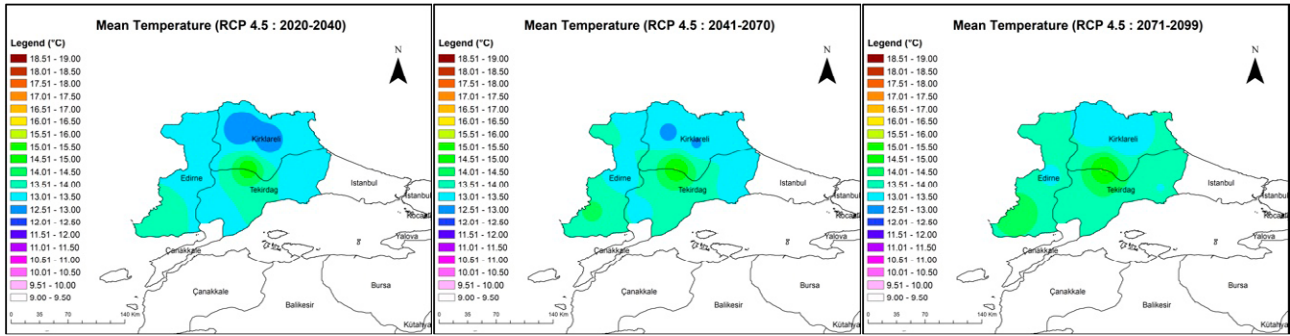


Fig. 6. Mean Air Temperatures in Winter Wheat Growing Season (RCP 4.5 Scenario).

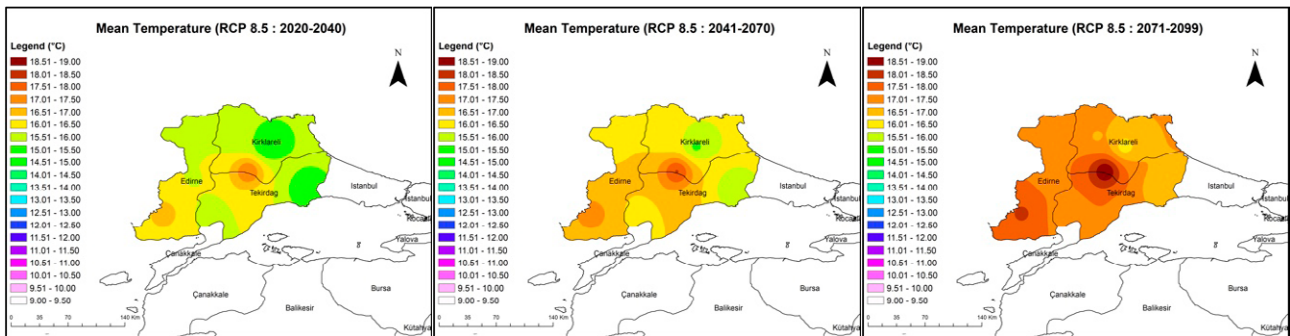


Fig. 7. Mean Air Temperatures in Winter Wheat Growing Season (RCP 8.5 Scenario).

increase is expected to be in the northeast and southwest of the region whereas the highest increase is expected to occur in Tekirdağ city center and some parts of Edirne. The changes in the effective precipitation that occurred in the P2 and P3 periods have similar increase patterns. In P2, the increases in effective precipitation are between 0.3% and 20%. Moreover, the increases in the period of P3 are between 5% and 26%. In Fig. 9, it can be seen maps of the effective precipitation according to the RCP 8.5, with the effective precipitation decreasing in con-

trast to the RCP 4.5. The percentage of such changes were estimated in a range of -14% and -26% in P1, -18% and -28% in P2, and 20% and -30% in P3.

Potential Yield and Water Footprint Estimations

Potential yields and WF calculations of winter wheat in Edirne, Kırklareli and Tekirdağ are reported in Tab. 5.

According to Tab. 5, winter wheat yields show an upward trend in all scenarios except in P1 period in

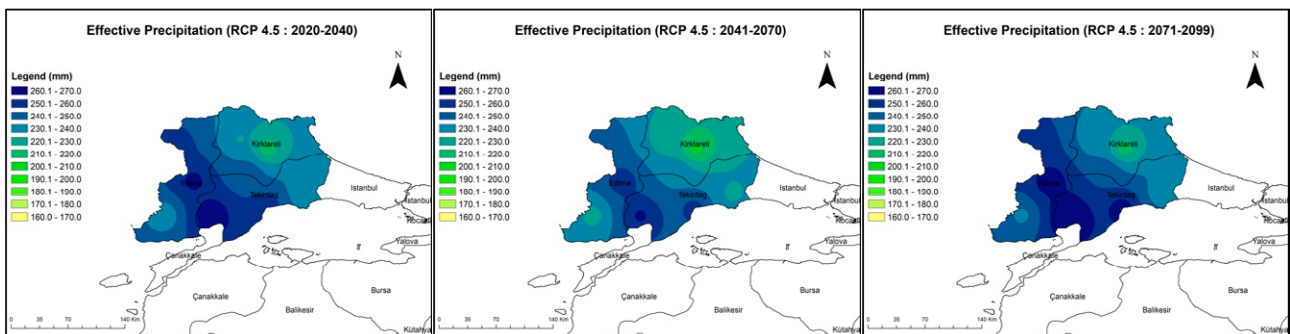


Fig. 8. Effective Precipitation Amount in Winter Wheat Growing Season (RCP 4.5 Scenario).

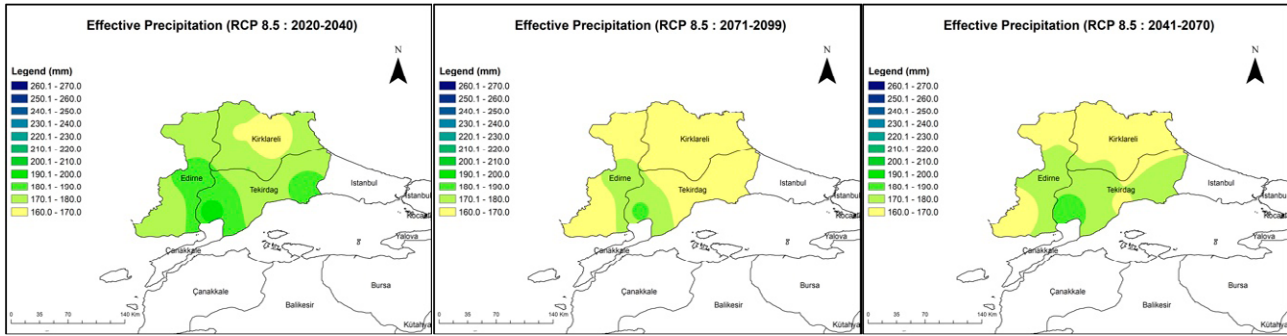


Fig. 9. Effective Precipitation Amounts in Winter Wheat Growing Season (RCP 8.5 Scenario).

Tab. 5. Potential Crop Yield of Winter Wheat by AquaCrop.

Years	Winter Wheat Yield for RCP 4.5 (t ha ⁻¹)			Winter Wheat Yield for RCP 8.5 (t ha ⁻¹)		
	Edirne	Kırklareli	Tekirdağ	Edirne	Kırklareli	Tekirdağ
Actual Yield	4.86	4.67	3.85	4.86	4.67	3.85
2020-2040	5.46 ± 0.72	4.61 ± 0.24	4.52 ± 0.45	5.23 ± 0.77	4.72 ± 0.27	4.48 ± 0.44
2041-2070	5.94 ± 0.80	4.96 ± 0.26	4.88 ± 0.45	6.13 ± 0.82	5.29 ± 0.35	5.11 ± 0.41
2071-2099	6.28 ± 0.86	5.11 ± 0.30	5.05 ± 0.39	7.53 ± 0.84	6.19 ± 0.34	5.89 ± 0.44

Kırklareli. In this period, the decrease in the yield is estimated as 1.3%. Winter wheat yield was positively affected by the increase of temperatures and atmospheric CO₂ concentrations. The decrease in precipitation did not have a considerable effect on yield. The largest increase in wheat yield was reported under RCP 4.5 in Tekirdağ. Average yield increases in Edirne, Kırklareli and Tekirdağ were calculated as 21%, 5% and 25%, respectively. When yields were analyzed by periods, it was predicted that the winter wheat yields in the region will increase by 9% in P1 (4.86±0.79 t ha⁻¹), 18% in P2 (5.26±0.26 t ha⁻¹) and 23% in P3 (5.48±0.42 t ha⁻¹).

Additionally, winter wheat yield may increase more in RCP 8.5 than in RCP 4.5. The reason of this situa-

tion can be explained by the fact that the atmospheric CO₂ concentration and the temperatures will be about 1-2.5°C higher for RCP 8.5 than the RCP 4.5. Average yield increment in Edirne, Kırklareli and Tekirdağ were calculated as 29.6%, 15.6% and 34.0%, respectively. When the yields were analyzed by periods, it is predicted that the winter wheat yields in the region will increase by 8.3% in P1 (4.81±0.81 t ha⁻¹), 24.0% in P2 (5.51±0.32 t ha⁻¹) and 46.8% in P3 (6.54±0.42 t ha⁻¹). In addition to the yield of winter wheat, WF were also calculated with the AquaCrop model and shown in Tab. 6.

According to Tab. 6, the potential WFs of winter wheat decreases in all scenarios and for different time horizons. This is explained by an increase in win-

Tab. 6. Forecasted WF of Winter Wheat by AquaCrop.

Years	Winter Wheat WF for RCP 4.5 (m ³ t ⁻¹)			Winter Wheat WF for RCP 8.5 (m ³ t ⁻¹)		
	Edirne	Kırklareli	Tekirdağ	Edirne	Kırklareli	Tekirdağ
SWB Method	449	466	442	449	466	442
2020-2040	169.7 ± 28.4	177.6 ± 32.8	212.9 ± 37.1	140.5 ± 29.7	143.6 ± 31.2	143.1 ± 26.7
2041-2070	147.0 ± 28.4	153.7 ± 27.7	179.4 ± 41.9	105.5 ± 31.1	109.6 ± 29.5	109.0 ± 28.0
2071-2099	137.6 ± 24.2	145.5 ± 29.6	166.4 ± 32.9	73.1 ± 18.1	77.9 ± 18.4	86.8 ± 22.0

ter wheat yield. The winter wheat WF decrease throughout the region in the periods of P1, P2 and P3 by 58.7% ($186.7 \pm 0.27 \text{ m}^3 \text{ t}^{-1}$), 64.6% ($160.1 \pm 0.30 \text{ m}^3 \text{ t}^{-1}$) and 66.9% ($149.9 \pm 0.37 \text{ m}^3 \text{ t}^{-1}$) in RCP 4.5, respectively. When compared the result of increases in yields between RCP 4.5 and 8.5, it can be said that the WFs in RCP 8.5 is lower than WFs in RCP 4.5. WFs of winter wheat decrease as 68.5% in P1 ($142.4 \pm 0.29 \text{ m}^3 \text{ t}^{-1}$), 76.1% in P2 ($108.0 \pm 0.26 \text{ m}^3 \text{ t}^{-1}$) and 82.5% in P3 ($79.3 \pm 0.25 \text{ m}^3 \text{ t}^{-1}$). The reason for this situation in WF can be explained not only by the increase in yield and atmospheric CO_2 concentration in RCP 8.5, but also with the decrease in the effective precipitation.

CONCLUSION

In this study, actual crop yield and WF of winter wheat grown under rainfed conditions were compared by using AquaCrop model for two growing seasons.

RCP 4.5 and 8.5 scenario results produced by HadGEM2-ES model were used as input data to estimate the crop yield and water footprint of the future by AquaCrop. According to the AquaCrop simulation results, it is predicted that winter wheat yield would increase for the future in the Thrace part of Turkey. Although the precipitation decreased and temperature increased in the RCP 8.5 scenario, crop yield would be affected positively. On the other hand, increases in the crop yield would cause decreasing WF of winter wheat.

The results of our study were compared with other related studies. In the Kersebaum et al. (2016) study, the total WF of wheat ($556 \text{ m}^3 \text{ t}^{-1}$) is 23% more than our WF ($452 \text{ m}^3 \text{ t}^{-1}$) and their wheat yield was 28% higher (5.78 t ha^{-1}) than our research area (4.46 t ha^{-1}). Similarly, estimated WF by Zhuo et al. (2016) for winter wheat ($1074 \pm 133 \text{ m}^3 \text{ t}^{-1}$) in China is higher than our WF. Additionally, green WF of wheat determined by Zhuo and Hoekstra (2017) is also higher than our WF. As can be seen from these studies, dissimilarity of yield and WF of winter wheat can be attributed to the climatic characteristics, soil hydrological parameters, cultural genotype and management practices.

In future studies, current and potential crop yield and WF of winter wheat can be evaluated comparatively using different regional climate model results and crop growth simulation models in this study area. Performing the same processes in different regions and crop types are also important in terms of effective use of water in agricultural ecosystems. In order to enhance such studies, the input and output data required for the models must be continuously monitored and recorded in the countries. Data infrastructure should be created for better results.

ACKNOWLEDGMENT

We would like to thank the Research Fund of Istanbul Technical University for their support by the project number MDK-2018-41436. In addition, we would like to thank all the employees who contributed to field works from Atatürk Soil Water and Agricultural Meteorology Research Institute.

REFERENCES

- Ababaei, B., Etedali, H. R. 2017., Water footprint assessment of main cereals in Iran. *Agricultural Water Management*, **179**, 401-411.
- Allen, R. G., Pereira, L. S., Raes, D., and Smith, M., 1998. Guidelines for computing crop water requirements. *Irrigation and drainage Paper*, **56**, 300.
- Alvarez, A., Morabito, J. A., and Schilardi, C., 2016. Green and blue water footprint of corn (*Zea mays*) production in central and northeastern provinces of Argentina. *Revista de la Facultad de Ciencias Agrarias, Universidad Nacional de Cuyo*, **48** (1), 161-177.
- Bakanogullari, F., Yesilkoy, S., Akataş, N., Saylan, L., and Çaldağ, B., 2018. Modelling the Adaptation Capabilities of Sunflower and Winter Wheat to Crop Rotation and Possible Climatic Change in Thrace. *International Scientific for Agriculture and Food*, 135-139.
- Bocchiola, D., Nana, E., and Soncini, A., 2013. Impact of climate change scenarios on crop yield and water footprint of maize in the Po valley of Italy. *Agricultural Water Management*, **116**, 50-61.
- Caldag, B. and Saylan, L. 2005. Sensitivity analysis of the CERES-wheat model for variations in CO_2 and meteorological factors in Northwest Turkey. *International journal of environment and pollution*, **23** (3), 300-313.
- Casolani, N., Pattara, C., and Liberatore, L., 2016. Water and carbon footprint perspective in Italian durum wheat production. *Land Use Policy*, **58**, 394-402.
- Chen, J., Brissette, F. P., Chaumont, D., and Braun, M., 2013. Finding appropriate bias correction methods in downscaling precipitation for hydrologic impact studies over North America. *Water Resources Research*, **49** (7), 4187-4205.
- Christensen, O. B., Drews, M., Christensen, J. H., Dethloff, K., Ketelsen, K., Hebestadt, I., and Rinke, A., 2007. The HIRHAM regional climate model. Version 5 (beta).
- Chouchane, H., Krol, M. S., and Hoekstra, A. Y., 2018. Virtual water trade patterns in relation to environmental and socioeconomic factors: A case study for Tunisia. *Science of the total environment*, **613**, 287-297.

- De Miguel, Á., Kallache, M., and García-Calvo, E., 2015. The water footprint of agriculture. In: Duero River Basin. *Sustainability*, **7** (6), 6759-6780.
- Deryng, D., Elliott, J., Folberth, C., Müller, C., Pugh, T. A., Boote, K. J., ... and Khabarov, N., 2016. Regional disparities in the beneficial effects of rising CO₂ concentrations on crop water productivity. *Nature Climate Change*, **6** (8), 786-790.
- Feigenwinter, I., Kotlarski, S., Casanueva, A., Schwierz, C., and Liniger, M. A., 2018. Exploring quantile mapping as a tool to produce user-tailored climate scenarios for Switzerland. *MeteoSchweiz*.
- Feng, L., Chen, B., Hayat, T., Alsaedi, A., and Ahmad, B., 2017. Dynamic forecasting of agricultural water footprint based on Markov Chain—a case study of the Heihe River Basin. *Ecological Modelling*, **353**, 150-157.
- Garofalo, P., Ventrella, D., Kersebaum, K. C., Gobin, A., Trnka, M., Giglio, L., ... Castellini, M., 2019. Water footprint of winter wheat under climate change: Trends and uncertainties associated to the ensemble of crop models. *Science of The Total Environment*, **658**, 1186-1208.
- Gobin, A., Kersebaum, K. C., Eitzinger, J., Trnka, M., Hlavinka, P., Takáč, J., ... and Lalić, B., 2017. Variability in the water footprint of arable crop production across European regions. *Water*, **9** (2), 93.
- Gudmundsson, L., Bremnes, J. B., Haugen, J. E., and Engen-Skaugen, T., 2012. Downscaling RCM precipitation to the station scale using statistical transformations: a comparison of methods. *Hydrology and Earth System Sciences*, **16** (9), 3383-3390.
- Gürbüz, M. A., Kayalı, E., Bahar, E., Öz, T. A., and Kurşun, İ., 2019. Composing the Database of Thrace Soils and Some Soil Characteristics. *Toprak Bilimi ve Bitki Besleme Dergisi*, **7**(1), 28-36.
- Heo, J. H., Ahn, H., Shin, J. Y., Kjeldsen, T. R., and Jeong, C. (2019). Probability distributions for a quantile mapping technique for a bias correction of precipitation data: A case study to precipitation data under climate change. *Water*, **11** (7), 1475.
- Hoekstra, A. Y., 2003. Virtual water: An introduction. In: *Virtual water trade: Proceedings of the international expert meeting on virtual water trade*. Value of water research report series, IHE Delft, **11**, 13-23.
- Hoekstra, A. Y., Chapagain, A. K., Mekonnen, M. M., and Aldaya, M. M., 2011. *The water footprint assessment manual: Setting the global standard*. Routledge.
- Huang, Z., Hejazi, M., Li, X., Tang, Q., Leng, G., Liu, Y., ... and Wada, Y., 2018. Reconstruction of global gridded monthly sectoral water withdrawals for 1971-2010 and analysis of their spatiotemporal patterns. *Hydrology and Earth System Sciences Discussions*, **22**, 2117-2133.
- Huang, J., Ridoutt, B. G., Thorp, K. R., Wang, X., Lan, K., Liao, J., ... and Scherer, L., 2019. Water-scarcity footprints and water productivities indicate unsustainable wheat production in China. *Agricultural Water Management*, **224**, 105744.
- Thiemeßl, M. J., Gobiet, A., and Leuprecht, A., 2011. Empirical-statistical downscaling and error correction of daily precipitation from regional climate models. *International Journal of Climatology*, **31** (10), 1530-1544.
- Karandish, F., & Hoekstra, A., 2017. Informing national food and water security policy through water footprint assessment: the case of Iran. *Water*, **9** (11), 831.
- Kersebaum, K. C., Kroes, J., Gobin, A., Takáč, J., Hlavinka, P., Trnka, M., ... and Dalla Marta, A., 2016. Assessing uncertainties of water footprints using an ensemble of crop growth models on winter wheat. *Water*, **8** (12), 571.
- Lalić, B., Sremac, A. F., Eitzinger, J., Stričević, R., Thaler, S., Maksimović, I., ... and Dekić, L., 2018. Seasonal forecasting of green water components and crop yield of summer crops in Serbia and Austria. *The Journal of agricultural science*, **156** (5), 658-672.
- Luan, X., Wu, P., Sun, S., Wang, Y., and Gao, X., 2018. Quantitative study of the crop production water footprint using the SWAT model. *Ecological Indicators*, **89**, 1-10.
- Macadam, I., Argüeso, D., Evans, J. P., Liu, D. L., and Pitman, A. J., 2016. The effect of bias correction and climate model resolution on wheat simulations forced with a regional climate model ensemble. *International Journal of Climatology*, **36** (14), 4577-4591.
- Mekonnen, M. M., & Hoekstra, A. Y., 2011. The green, blue and grey water footprint of crops and derived crop products. *Hydrology & Earth System Sciences Discussions*, **8** (1).
- Mostafa, A. N., Wheida, A., El Nazer, M., Adel, M., El Leithy, L., Siour, G., ... and Saad-Hussein, A., 2019. Past (1950–2017) and future (– 2100) temperature and precipitation trends in Egypt. *Weather and Climate Extremes*, **26**, 100225.
- Muratoglu, A., 2019. Water footprint assessment within a catchment: A case study for Upper Tigris River Basin. *Ecological Indicators*, **106**, 105467.
- Nakagawa, H., Kobata, T., Yano, T., Barutçular, C., Koç M., Tanaka, K., ... and Watanabe, T., 2007. Predicting the Impact of Global Warming on Wheat Production in Adana. *The Final Report of ICCAP*, **14**.
- Nearing, M. A., Foster, G. R., Lane, L. J., and Finkner, S. C., 1989. A process-based soil erosion model for

- USDA-Water Erosion Prediction Project technology. *Transactions of the ASAE*, **32** (5), 1587-1593.
- Nouri, H., Stokvis, B., Galindo, A., Blatchford, M., and Hoekstra, A. Y., 2019. Water scarcity alleviation through water footprint reduction in agriculture: the effect of soil mulching and drip irrigation. *Science of the total environment*, **653**, 241-252.
- Özdoğan, M., 2011. Modeling the impacts of climate change on wheat yields in Northwestern Turkey. *Agriculture, ecosystems & environment*, **141** (1-2), 1-12.
- Palosuo, T., Kersebaum, K. C., Angulo, C., Hlavinka, P., Moriondo, M., Olesen, J. E., ... and Trnka, M., 2011. Simulation of winter wheat yield and its variability in different climates of Europe: a comparison of eight crop growth models. *European Journal of Agronomy*, **35** (3), 103-114.
- Qian, B., Wang, H., He, Y., Liu, J., and De Jong, R., 2016. Projecting spring wheat yield changes on the Canadian Prairies: effects of resolutions of a regional climate model and statistical processing. *International Journal of Climatology*, **36** (10), 3492-3506.
- Raes, D., Steduto, P., Hsiao, T. C., & Fereres, E., 2009. AquaCrop—the FAO crop model to simulate yield response to water: II. Main algorithms and software description. *Agronomy Journal*, **101** (3), 438-447.
- Santos, N., Hess, S., & Jaghdani, T. J., 2017. Turkey. Water along the food chain. Towards water-smart agrifood policies: the case of red meat processing. Turkey. Water along the food chain. Towards water-smart agrifood policies: the case of red meat processing.
- Soriano, E., Mediero, L., & Garijo, C., 2019. Selection of Bias Correction Methods to Assess the Impact of Climate Change on Flood Frequency Curves. In: *Multi-disciplinary Digital Publishing Institute Proceedings*, Vol. 7, N° 1, p. 14).
- Steduto, P., Hsiao, T. C., Raes, D., & Fereres, E., 2009. AquaCrop—The FAO crop model to simulate yield response to water: I. Concepts and underlying principles. *Agronomy Journal*, **101** (3), 426-437.
- Taheri, M., Emadzadeh, M., Gholizadeh, M., Tajrishi, M., Ahmadi, M., & Moradi, M., 2019. Investigating the temporal and spatial variations of water consumption in Urmia Lake River Basin considering the climate and anthropogenic effects on the agriculture in the basin. *Agricultural water management*, **213**, 782-791.
- Teng, J., Potter, N. J., Chiew, F. H. S., Zhang, L., Wang, B., Vaze, J., & Evans, J. P., 2015. How does bias correction of regional climate model precipitation affect modelled runoff? *Hydrology & Earth System Sciences*, **19** (2).
- Teutschbein, C., & Seibert, J., 2012. Bias correction of regional climate model simulations for hydrological climate-change impact studies: Review and evaluation of different methods. *Journal of hydrology*, **456**, 12-29.
- Tsakmakis, I. D., Zidou, M., Gikas, G. D., & Sylaios, G. K. (2018). Impact of irrigation technologies and strategies on cotton water footprint using AquaCrop and CROPWAT models. *Environmental Processes*, **5** (1), 181-199.
- Ventrella, D., Giglio, L., Garofalo, P., & Dalla Marta, A. (2018). Regional assessment of green and blue water consumption for tomato cultivated in Southern Italy. *The Journal of Agricultural Science*, **156** (5), 689-701.
- Wang, X., Li, X., Fischer, G., Sun, L., Tan, M., Xin, L., & Liang, Z., 2015. Impact of the changing area sown to winter wheat on crop water footprint in the North China Plain. *Ecological Indicators*, **57**, 100-109.
- Ye, Q., Li, Y., Zhang, W., & Cai, W., 2019. Influential factors on water footprint: A focus on wheat production and consumption in virtual water import and export regions. *Ecological indicators*, **102**, 309-315.
- Pastén-Zapata, E., Jones, J. M., Moggridge, H., & Widmann, M., 2020. Evaluation of the performance of Euro-CORDEX Regional Climate Models for assessing hydrological climate change impacts in Great Britain: A comparison of different spatial resolutions and quantile mapping bias correction methods. *Journal of Hydrology*, **584**, 124653.
- Zhai, Y., Tan, X., Ma, X., An, M., Zhao, Q., Shen, X., & Hong, J., 2019. Water footprint analysis of wheat production. *Ecological indicators*, **102**, 95-102.
- Zhuo, L., & Hoekstra, A. Y., 2017. The effect of different agricultural management practices on irrigation efficiency, water use efficiency and green and blue water footprint. *Frontiers of Agricultural Science and Engineering*, **4** (2), 185-194.
- Zhuo, L., Mekonnen, M. M., & Hoekstra, A. Y., 2016. Benchmark levels for the consumptive water footprint of crop production for different environmental conditions: a case study for winter wheat in China. *Hydrology and earth system sciences*, **20** (11), 4547-4559.



Citation: B. Parisse, A. Pontrandolfi, C. Epifani, R. Alilla, F. De Natale (2020) An agrometeorological analysis of weather extremes supporting decisions for the agricultural policies in Italy. *Italian Journal of Agrometeorology* (1): 15-30. doi: 10.13128/ijam-790

Received: December 20, 2019

Accepted: January 20, 2020

Published: June 23, 2020

Copyright: © 2020 B. Parisse, A. Pontrandolfi, C. Epifani, R. Alilla, F. De Natale. This is an open access, peer-reviewed article published by Firenze University Press (<http://www.fupress.com/ijam>) and distributed under the terms of the Creative Commons Attribution License, which permits unrestricted use, distribution, and reproduction in any medium, provided the original author and source are credited.

Data Availability Statement: All relevant data are within the paper and its Supporting Information files.

Competing Interests: The Author(s) declare(s) no conflict of interest.

An agrometeorological analysis of weather extremes supporting decisions for the agricultural policies in Italy

BARBARA PARISSÉ, ANTONELLA PONTRANDOLFI, CHIARA EPIFANI*, ROBERTA ALILLA, FLORA DE NATALE

Council for Agricultural Research and Economics (CREA) - Research Centre for Agriculture and Environment

*Corresponding author. Email: barbara.pariisse@crea.gov.it, antonella.pontrandolfi@crea.gov.it, roberta.alilla@crea.gov.it, flora.denatale@crea.gov.it

Abstract. The future European Common Agricultural Policy foresees Strategic National Plans founded on recognised needs for intervention and indicators in order to select the more effective policy measures. The Strategic plans start from a “context analysis”, describing the current-starting conditions. In support to the policy theme on climate change, the authors proposed a context analysis on the main agrometeorological variables and weather extreme events, both at national and subnational (NUTS1) level. This paper describes the methodological choices made and the results obtained, considering the contents required by the European Commission for the context analysis (agrometeorological indicators and an indicator of economic damages due to natural disasters). The data source chosen is ERA5, the climate reanalysis dataset produced within the Copernicus project. The study demonstrates the importance of cross-reading data on hazards and data on vulnerability for policy decisions. In particular this is shown for the resulted most impacting weather condition: the drought, measured through the SPEI index, affecting all the country. There are also other hazards frequent and quite impacting, first of all heavy rain. Further improvements of the analysis are programmed in terms of spatial scale, time scale (seasonal approach) and in terms of correlation hazard-vulnerability.

Keywords. Agrometeorology, climate indices, decision support systems, ETCCDI, climate-related risks.

INTRODUCTION

The Common Agricultural Policy (CAP) was launched in 1962 as a strategy to provide affordable food for European citizens and a fair standard of living for farmers¹. During the last decades, several reforms have been necessary in order to ensure the general goals of the policy in a changing context, in particular referring to the main issues of the environmental protection, the globalization and the challenges posed by climate change (CC), in general covering almost all the United Nations Sustainable Development Goals (SDGs). Given the importance of these global issues for the future CAP 2021-2027, in the new proposal of regulation, the European Parliament introduced, among other innovations, the realization of strategic national plans that reflect a comprehensive intervention logic, a “policy cycle concept” founded on identified and recognised intervention needs, deriving objectives and indicators (at all levels of evaluation) and consequent selected measures that can effectively contribute to reach the targets (European Parliament, 2018). The strategic plans need to start from a “context analysis”, describing through objective studies the current conditions, strengths, weaknesses, opportunities and threats (SWOT analysis) with respect to the objectives of the CAP. The context analysis has a core role for the rural development policy, of the CAP, in which the choice of the measures is linked to specific goals to be pursued (environment, climate change, etc.) and to local conditions.

In Italy, the rural development policy has always been programmed and applied at administrative regional level (21 regional programmes, NUTS2), while the new CAP cycle requires a national programming phase, based on a context analysis at national level. This innovation represents an important step forward to have a more coherent and consistent programming phase compared with the past 21 separate regional programmes, nevertheless it also represents a challenge because of the heterogeneity of environmental and agricultural conditions of the Italian territory. For these reasons, a task force has been established by the Italian Ministry of Agricultural and Forestry Policies (MIPAAF), which involves representatives from the Regions, with the idea of a common work path, identifying the analyses to be carried out at national and regional level. The task is supported by technical analyses performed by research institutions, including the Council of Agricultural Research and Economics (CREA) with its researchers involved in the National Rural Network project².

As a starting point, it was agreed to deal with the proposal of regulation containing context indicators and with the thematic documents produced by the European Commission (EC) on the objectives of the future CAP (policy briefs), which provides guidance on how to set the contents required for the context analysis.

A specific thematic policy brief has been proposed by the EC on the general objective 2 “*to strengthen environmental protection and action for the climate and contributing to the achievement of the Union’s environmental and climate objectives*”, among whose a specific objective 2.1 is “*contributing to the mitigation of climate change and adaptation to them, as well as to the development of sustainable energy*” (EC, 2019; EEA, 2019). The article describes the specific study carried out to contribute to the Italian policy brief on climate change and to the context analysis for future CAP. The objective of the study is also a first attempt to assess the relationships between the agrometeorological context and the impacts on agricultural productions and practices, considering the scenarios currently taking shape, showing an increase in uncertainty of climate conditions directly influencing the agricultural production. The sector is indeed the most exposed and vulnerable to climate change referring to the higher likelihood of weather events extreme and non-extreme leading to natural disasters (IPCC, 2012). At last, the study intends to contribute in exploring the potentialities in agrometeorological analyses of new data sources offered by the European project Copernicus³.

MATERIALS AND METHODS

General criteria adopted for the context analysis

Referring to the objectives of the study, the first step has been to analyse the EC requirements regarding the contents needed in the context analysis with reference to the climate and the impact of CC in agriculture. As explained in the introduction, the reference documents are the proposal of regulation and the EC policy brief on climate change.

The policy brief reports what it is expected from the context indicators in terms of information: a) changes in precipitation; b) changes in temperatures; c) frequency and intensity of extreme events; d) other references, such as changes in agricultural yields, the period of flowering and in the agricultural calendar.

Moreover, in the proposal of regulation, an impact indicator is requested in the “climate” section: the indi-

¹ https://ec.europa.eu/info/food-farming-fisheries/key-policies/common-agricultural-policy/cap-glance_en.

² <https://www.reterurale.it/flex/cm/pages/ServeBLOB.php/L/IT/IDPagina/1>.

³ <https://www.copernicus.eu/en>.

cator c.45 “Direct losses in agriculture attributed to disasters”.

The methods for this study were chosen so as to reflect both the EC expectations for the context analysis of the National strategic plan, and the need to ensure a good agrometeorological analysis at national and sub-national level, with a specific and new focus on extreme events connected to climate-related disasters risks in agriculture.

The main choice criteria were the following:

- availability of data for the calculations;
- descriptive capacity of the relations between agriculture and weather-climate conditions;
- possibility of representing the indicators with respect to the climate (“changes” of temperature and precipitation);
- preference for statistical distributions at a local scale (percentiles) and not for fixed value thresholds for the estimation of extreme events. This choice is linked to the climatic and agricultural heterogeneity of Italy, which makes the fixed thresholds unsuitable to adequately describe the different conditions.

In addition to the EC approach to the context analysis, the main references for the study are the works of the Intergovernmental Panel on Climate Change (IPCC) and of the Expert Team on Climate Change Detection and Indices (ETCCDI)⁴. Following the IPCC approach, the indicators are divided into: context indicators, corresponding to the indicators of “hazard” and “exposure”; impact indicators, representing the “vulnerability” (IPCC, 2007 and 2012). The context and hazard indicators chosen for the information on “extreme events” derive from the work of ETCCDI, that proposed a set of 27 main indices, based on daily temperature (maximum and minimum) and precipitation values.

Moreover, two specific indices have been added to improve the context description, in relation to the drought conditions and the changes of the phenological calendar, respectively.

As above explained, in relation to the objectives of the analysis, it has been proposed to enrich the analysis of hazards and climatic conditions with an impact indicator, a “vulnerability” indicator in the IPCC approach, defined as “Direct losses in agriculture attributed to disasters” in the proposal of regulation. In fact, the concept of “climate extremes” discussed within the IPCC works is particularly important in agriculture, because the increase of climate extremes likely will lead to more “disasters” defined as “*severe alterations in the normal functioning due to hazardous physical events interact-*

ing with vulnerable conditions, that require immediate emergency response” (IPCC, 2012). In the context of climate change, the disaster risk is influenced not only by hazard, but also by exposure and vulnerability, where the exposure refers to the presence of productive systems where hazard may occur, while the vulnerability is the predisposition to be adversely affected (economic damages due to lack of resilience and low capacities to cope with/adapt to). In the IPCC approach, the climate-related risks should be faced through the improvement of two components of risk management: measures of risk reduction (more stringent where the vulnerability is high) and disaster management (more stringent where the hazard is high). For these reasons, it is important to start changing the approach in policy decisions, integrating the weather and climatic analyses with a vulnerability component (IPCC, 2012; UNISDR, 2015; EEA, 2017). This study is also a first attempt to introduce these integrated concepts in the policy analyses in the agricultural sector.

The indicators have been calculated at sub-national scale, using the classification of territorial units for statistics (NUTS), a geocode standard for referencing the administrative divisions of countries for statistics, developed by the European Union⁵. The first-level NUTS regions (hereinafter also called “areas”), based on major socio-economic areas, has been adopted, precisely for Italy: North-West (Aosta Valley, Liguria, Lombardy, Piedmont); North-East (Emilia-Romagna, Friuli Venezia Giulia, Trentino-Alto Adige/Südtirol and Veneto); Centre (Lazio, Marche, Tuscany and Umbria); South (Abruzzo, Apulia, Basilicata, Calabria, Campania and Molise); Islands (Sardinia and Sicily). Although aware that the agrometeorological analyses poorly adapt to areas on administrative basis, this choice seemed the most suitable compromise to be used in this kind of analysis with institutional purposes at national scale.

The climate reference period (hereinafter referred to as “climate period”) is 1981-2010, according to the World Meteorological Organization (WMO) that defines the “normal standard climates” as the averages of climatic variables calculated for a uniform period of 3 consecutive decades. In 2017, the WMO established that, in addition to the 1961-1990 period, which remains the standard reference period for long-term assessments of climate change, it is possible and recommended to use the new “climatological standard normal” 1981-2010, able to describe more coherently the current climate (WMO, 2017). The need to provide a description as representative as possible of the current climate variability led to choose 1981-2010 as the climate reference period.

⁴ http://etccdi.pacificclimate.org/list_27_indices.shtml.

⁵ <https://ec.europa.eu/eurostat/web/nuts/nuts-maps-.pdf>.

The period chosen for the analysis is 2003-2018, covering enough time (16 years) to describe the current context of the application of a mid-term policy like CAP (7 years cycles).

Data

All the elaborations and analyses of data here presented are original and are based on data from three main sources: a climate reanalysis dataset, for meteorological data, a phenological observation dataset, a database on damages on agriculture due to adverse events derived from the Italian ministerial decrees on damages.

The data source chosen for the meteorological analysis, is ERA5, the hourly climate reanalysis data, available on a regular grid at a resolution of 0.25°. ERA5 is the latest climate reanalysis produced by the European Centre for Medium-Range Weather Forecasts (ECMWF), providing hourly data on many atmospheric, land-surface and sea-state parameters together with estimates of uncertainty (C3S - Copernicus Climate Change Service, 2017).

The choice of the ERA5 dataset is due to several reasons:

- climate reanalysis combines past observations with weather models to generate gridded datasets of consistent and complete time series of multiple climate variables at sub-daily intervals, which are currently the most used datasets in the climate extreme studies (Donat et al., 2014);
- the data are public, produced by a European institutional project (Copernicus);
- the available dataset starts from 1979, covering a good time period for climatic analysis;
- the dataset will maintain continuity over time, allowing analyses able to be updated (this is important also for supporting the policies evaluation through indicators); moreover, data are released every two days, overcoming problems of availability of other datasets;
- further improvements and enrichment of the variables provided in the Copernicus project are planned.

The variables selected in ERA5 (atmosphere) are described in table 1.

The phenological database of the IPHEN network⁶ has been used to extract weekly observational data of the grapevine phenological phases on 33 sites, distributed all over the country, for the period 2006-2018.

The data used for the impact indicator derive from damages declarations recognized by the State as due to

Tab. 1. Variables selected in ERA5 for the context analysis.

Name of variable in ERA5	Abbreviation	Measure unit	Transformation of derived variables
2m temperature	2T	K	°C
2m dewpoint temperature	2D	K	Relative umidity min and max (%)
10m u-component of wind	10U	m s-1	Wind speed (m s-1)
10m v-component of wind	10V	m s-1	
Surface solar radiation downwards	SSRD	J m-2	MJ m-2
Total Precipitation	TP	m	mm
Orography	OROG	m2 s-1	Altitudine (m s.l.m.)

natural disasters, as assigned by the National solidarity fund for disasters in agriculture of MIPAAF (legislative decree 102/2004). Information from Italian ministerial decrees of damages due to “adverse events” is collected in a database now managed by CREA, reporting data from the 1980s on the date and the kind of event, the location (at level of municipalities) and the declared economic damages on production (at least 30% of losses), farm structures (such as irrigation systems, animal shelters, greenhouses, etc.) or infrastructures connected to agricultural activities (mostly collective drainage and irrigation channels, rural roads, etc.). For the present study, only the weather adverse events have been considered (for instance, earthquakes and volcanic eruptions have been not included). The definition of “adverse event” in the Italian law is an adverse weather such as frosts, storms and hail, ice, heavy rains or severe droughts that destroy more than 30 percent of the average annual production calculated on the basis of the previous three years or a three-year average based on the previous five years, excluding the lowest value e the highest one (legislative decree n. 102/2004). The general criteria used by the Ministry to declare a disaster due to adverse events are the aforementioned threshold of damages and the statistical exceptionality of the event (not the same in the previous 5 years in the same territory), but each case can be differently evaluated. The declara-

⁶ <https://www.reterurale.it/fenologia>.

tion assigns also an economic damage associated to the event in order to compensate farmers.

Moreover, the ISTAT data of the “Surveys on the structure and production of agricultural holdings (SPA)” have been used for the UAA data available for the analysis period⁷.

Methods

With reference to the context analysis, among the ETCCDI core indices, four “extreme events” indicators have been selected (warm and cold spell duration indices, a modified version of frost days and very wet day fraction). Moreover, the standardized precipitation evapotranspiration index - SPEI has been calculated because of the importance of monitoring drought events in agriculture. This indicator covers also the issue “changes in precipitation and in temperatures” proposed by the EC policy brief, being the two variables strictly linked in its definition and calculation. An increasingly widespread use of these indicators and indices can be found in the scientific literature, also referred to risk assessment and adaptation policies support (EEA, 2017; Klein Tank et al., 2009; Donat et al., 2013a, b; Russo et al., 2014; Zhang et al., 2011; Zolina et al., 2009). Less references can be found in the agricultural sector, most of them referring to drought indices, although a general increase of the studies in this field has been observed in the last decade (EEA, 2019; Cogato et al. 2019; Blauhut et al. 2015).

A further context indicator is the First flowering date, very important for agricultural productions and practices. Basing on the data availability, the chosen indicator has been calculated for the Grapevine Chardonnay variety.

Finally, an original impact-vulnerability indicator has been defined, mainly based on the economic value of damages affecting production, farm structures and infrastructures.

All the indicators have been aggregated at the NUTS1 region level using the official administrative boundaries from the Italian National Institute of Statistics (ISTAT), updated to the 1st of January 2019⁸ and transformed from the projected EPSG: 32632 to the geographical EPSG: 4326 reference system⁹, the same adopted by the data distributed through Copernicus climate data store. Data have been spatially aggregated, using the median value of the cells intercepted by the administrative boundaries, unless for the SPEI index, for which the

10th percentile has been adopted (Bachmair et al., 2015), with the aim to investigate the link with the impact-vulnerability indicator values.

Data processing has been performed through specific libraries of the R software (“climdex.pcic” and “SPEI”). R is an open source statistical software released under the GNU general public license (GPL)¹⁰.

Warm spell duration index - WSDI

The warm spell duration index is the yearly number of days belonging to warm spells, defined as at least 6 consecutive days with maximum temperature higher than the 90th percentile of the distribution of maximum daily temperatures in the same period of the year over the 30 years of climate. Recently, the negative correlation between wine quality and the incidence of heat waves has been investigated by Blanco-Ward et al., 2017.

Cold spell duration index - CSDI

The cold spell duration index is the yearly number of days belonging to cold spells, defined as at least 6 consecutive days with minimum temperature less than the 10th percentile of the distribution of minimum daily temperatures in the same period of the year over the 30 years of climate. This index is generally calculated within a set of indices (see references above), in some cases strictly associated to WSDI (Song et al., 2018).

Late frost days - LFD

Starting from the original indicator FD of ECCTDI, this indicator is based on the count of the frost days limited to the period March -April, when most of crops are in the phenological phase most sensitive to frost (flowering), with reference to the area study and as reported by Gobin (2018), who analysed the spring frost days during the sensitive crop stages. The indicator is expressed as the yearly deviation from the climate values [$LFD_{year} - LFD_{Climate}$], which correspond to the median of the distribution of the annual values during the climate period.

As frost days are considered all the days with a minimum temperature equal to or less than 0 °C. This generic threshold of 0 °C is due to the purpose of the analysis, that doesn't consider local conditions and specific crops. Furthermore, to detect the wheat's frost-susceptibility, this threshold has also been adopted by Zheng et al. (2015).

⁷ <http://dati.istat.it/>.

⁸ <https://www.istat.it/it/archivio/222527>.

⁹ <https://www.epsg-registry.org/>.

¹⁰ <https://cran.r-project.org>.

Very wet day fraction - R95pTOT

This indicator represents the yearly amount (in millimetres) of the daily precipitation above the 95th percentile of the distribution of daily rainfall of the wet days (greater precipitation than 1 mm) in the climate period. The values are also expressed as percentage contribution of R95pTOT to annual total precipitation. This index has been already used to investigate the impacts of heavy rains on wheat (Li et al., 2016) and rice (Subash et al., 2011).

For this indicator, an additional analysis has been carried out to compare the mean value resulted in the analysis period to the mean value calculated for the previous not-overlapping period 1981-2002.

Standardized precipitation evapotranspiration index at time scale of 6 months – 6-month SPEI

SPEI represents a simple climatic water balance (CWB), also known as “effective precipitation”, calculated as difference between total precipitation and potential evapotranspiration (PET), here estimated through the Penman-Montheit equation (Allen et al., 1998).

The indicator has two important peculiarities. The first is that it can be computed at different time scales, incorporating the influence of the past values (Vicente - Serrano S.M. et al., 2010). Thus, the value calculated for each month considers the values of the previous months, with a different time scale (from 1 to 48 months) which depends on the aims of the analysis (assessment of meteorological, agricultural or hydrological drought). In the study, the time scale chosen is 6-month, considered more suitable to describe water stresses during the agricultural season. The second peculiarity is that the SPEI calculation is based on the comparison between the CWB recorded in an interval of t months (where $t = 1, 2, \dots, 48$ months) with the distribution of the CWB in the climate period for the same interval. For each cell, the time series of cumulative effective precipitation is interpolated by means of a log-Logistic theoretical probability distribution with the unbiased fitting method probability weighted moments (Vicente - Serrano S.M. et al., 2010), assuming a rectangular kernel that assigns the same weight to all months of the interval of 6 months. The tail values of SPEI <-2.5 and SPEI $>+2.5$ have been cut according to what suggested in literature, mainly when short time series are considered (Vicente-Serrano S. M. et al., 2016).

The SPEI drought index is classified by the scientific community in different classes of intensity¹¹ (WMO and GWP, 2016) (Tab. 2).

Tab. 2. Classes of values of SPEI.

Classes of intensity	SPEI values
EW - Extreme wet	≥ 2.00
SW - Severe humidity	$1.50 \div 1.99$
MW - Moderate humidity	$1.00 \div 1.49$
N - Near normal	$-0.99 \div 0.99$
MD - Moderate drought	$-1.00 \div (-1.49)$
SD - Severe drought	$-1.50 \div (-1.99)$
ED - Extreme drought	$\leq (-2.00)$

The elaborations are here reported with the values of March as representative of the recharge seasons (October-March) and with the single values from April to September, useful to monitor the drought during the growing seasons.

Grapevine first flowering date -FFD (cv. Chardonnay)

The indicator is expressed as yearly deviation from the climate values [$FFD_{year} - FFD_{Climate}$], which corresponds to the median of the first flowering dates during the climate period. The first flowering corresponds to the 61 value of the BBCH scale (Meier, 2001). The FFD indicator is calculated using the IPHEN phenological model for the estimation of grapevine flowering dates for each year both of the analysis and climate periods. The model, adopted by CREA for producing a weekly phenological bulletin at a national scale¹², has been developed within the IPHEN project (Mariani et al., 2013; Cola *et al.*, 2012). It is based on the calculation of normal heat hours (NHH) (Wang and Engel, 1998; Weikai and Hunt, 1999). The accumulation of NHH is converted to phenological phases, according to the BBCH scale, through empirical equations obtained by regression on both historical NHH and phenological data detected in the field.

To check the IPHEN model performance in simulating flowering dates, the mean absolute error-MAE between the flowering dates simulated and those observed in the field has been calculated.

Considering that the altitudes of ERA5 cells and phenological observation sites may be dissimilar, the

¹¹ <https://spei.csic.es/home.html>.

¹² <https://www.reterurale.it/bollettinofeno>.

link between the differences of elevation and those of flowering date (MAE errors) has been investigated, by a linear regression, with the aim of verifying whether this uncertainty source can affect the model performance.

Damages attributed to natural disasters

Referring to the impact-vulnerability indicator, the chosen indicator “Economic damages attributed to disasters on utilized agricultural area” (euro/hectare of UAA) is based on the above-mentioned database on data of damages recognized by the State as due to natural disasters, as assigned by the National solidarity fund for disasters in agriculture of MIPAAF.

The calculation of the economic value of impacts on production is based on the UAA involved and the official prices at the time of the event of the affected crops, while for structures and infrastructures is based on the physical damages and the prices of rebuilding/repairing. These data produced with the same criteria are an important point of reference to assess the impacts in different periods and areas. Nevertheless, it is important to specify that they are slightly underestimated in terms of absolute values because of the exclusion of insured crops (foreseen by the law, but less than 18% of national production in 2015) (Pontrandolfi et al., 2016).

The UAA data from ISTAT have been used for creating a complete series from 2003 to 2018. As original data cover only the years 2003, 2005, 2007, 2010, 2013, 2016¹³, missing annual data have been covered by the nearest previously available value: e.g. 2003 data applied also to 2004 and so on.

The geographical reference units for the elaborations are the NUTS1 regions and the indicator has been calculated as yearly values of total damages per hectare of UAA.

Further elaborations are presented referring to the kind of damages (on production, farm structures or infrastructures) and to the kind of events producing damages.

RESULTS

The SPEI data in figure 1 show two cases of widespread severe and extreme drought phenomena: 2003 and 2017, with extreme drought in 2003 in Centre and North and in 2017 in Centre, South and Islands. Another similar phenomenon, although of lower intensity, is noticeable for 2007 and 2012; it involved almost

all NUTS1 regions, unless the Islands. This latter region was instead affected by a moderate/severe drought during 2016. In some cases, drought conditions, at least moderate, affected the recharge periods (March) almost all over the country, mainly in 2007, 2012 and 2017. A prolonged drought condition interested the Northern regions from 2003 to 2007 and 2011-2012 in northern and central Italy but with less intensity. As regards wetness events during the observed period, only few cases are remarkable: South in 2009, Centre in 2010, Centre and North-East in 2013, Centre in 2018 show wetness conditions from moderate to severe. These phenomena resulted to affect mainly Centre.

The results of warm and cold spell indices are reported in the figure 2. Referring to the warm spells, the most critical years result to be 2011 and 2003, followed by 2007 and 2015. In details, in 2011 the maximum values were reached in the northern and central regions, with a peak of 45 in North-East. In 2003, warm spells were widespread all over the country, with WSDI values of at least 30 in 4 of the 5 NUTS1 regions. On the contrary, the years less interested by warm spells were 2004, 2005, 2008 and 2010. In general, the second half of the analysis period results to be more continuously affected by these phenomena.

The cold spells are in general less widespread all over the country and the values result to be lower than warm spells in terms of days. Few years show the occurrence of these phenomena: the most relevant in the North-West, with peaks of 15 days in 2012 and 10 in 2005; single events of cold spells occurred in northern regions (2003), South (2006, 2009 and 2017), Islands (2005 and 2009). It is noticeable that almost all events are concentrated in the first 10 years of analysis.

The results on late frost days are shown in the figure 3. The data show positive anomalies in 2005 in all the regions and in 2010 in the North. The number of late frosts is below average in 2007-2009 and after 2013 there is a clear tendency to reduction of late frosts (each year below the average), most accentuated in the north-eastern and central areas. A different behaviour is present in the Islands, where the late frost days are near normal, except a weak positive anomaly in 2005.

In figure 4, the indicator R95pTOT (very wet days) is represented in millimeters and as the percentage fraction of the total annual precipitation, in order to allow a better comparison among the different cases. The distribution of these phenomena shows that, even though different rainfall regimes are present within the country, a heavy rain fraction is always represented among the years and the areas, with an average of 20% and a range between 10 and 31%. In general, the percentage

¹³ <http://dati.istat.it/>.

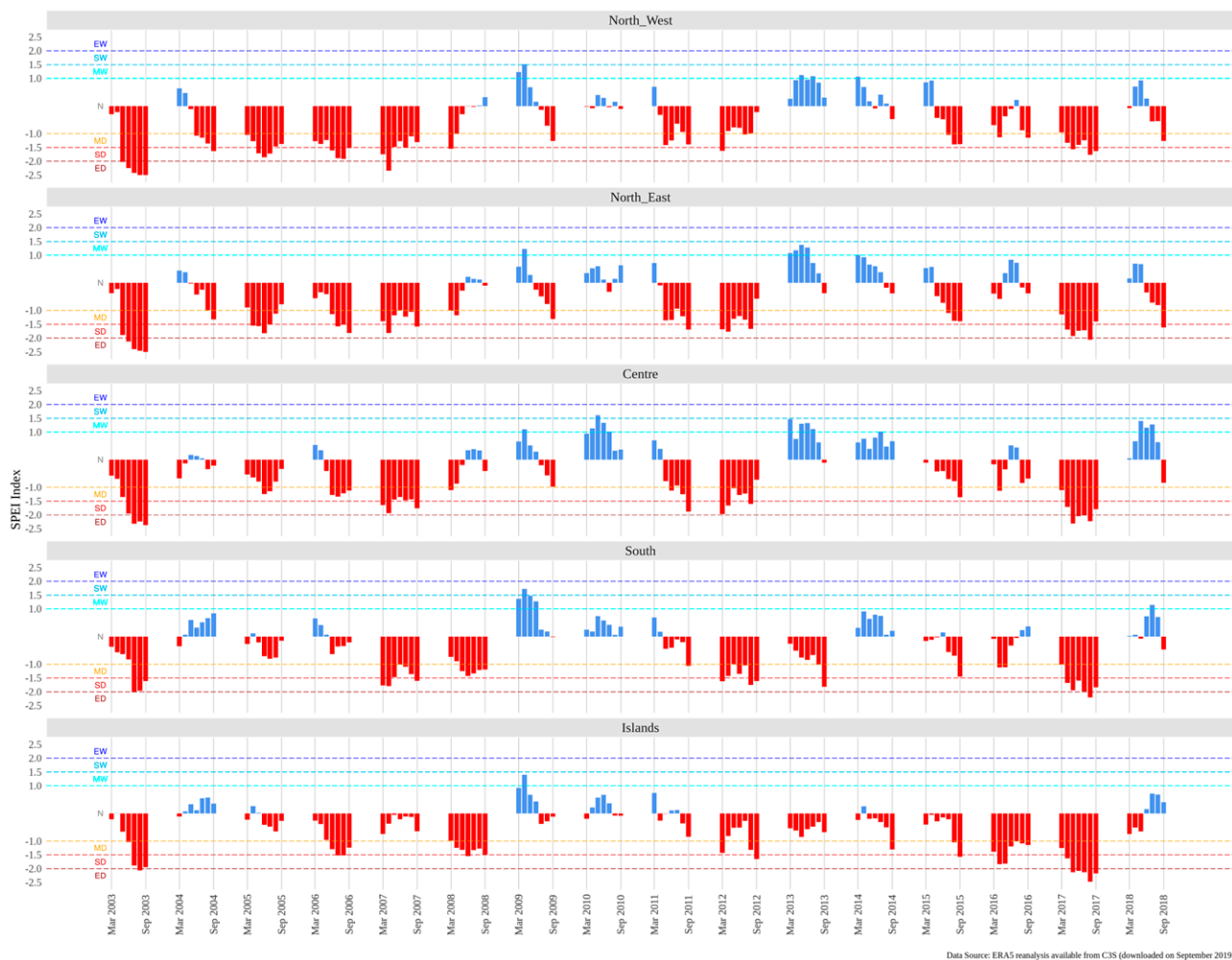


Fig. 1. Standardized precipitation evapotranspiration index – 6-month SPEI, monthly values in the period 2003-2018 (class description in Tab. 2).

values vary among regions, but they all show high values, from 24% in the Centre to 30% in North-West and Islands, in the year 2010 (the second rainiest year in the period). Another important indication is that in the 16 years period the heavy rain amounts have been most relevant in South and Islands, with a mean value significantly higher than in the previous period 1981-2002: the increase is equal to 42.4% ($p.value$ 0.0006) and 44.7%, ($p.value$ 0.003) in South and Islands respectively.

At last, the indicator of first flowering date shows between-year variability in terms of deviation from average (Fig. 5). Anomalies can be observed in 2004 with generalized late flowering around 7–12 days and in 2007 with generalized early flowering around 10-16 days. From 2012, Centre, South and Islands present a widespread advanced flowering until 16 days. In 2013 and 2016 a significant latitudinal gradient of temperatures

divided Italy in two parts, with the northern regions presenting a late flowering while the central, southern and island regions an advanced one. The median MAE value has resulted to be equal to 5 days at a national scale and significantly affected by the differences in elevation between gridded and site dataset. In fact, the relationship between MAE and differences in elevation has showed that the 65% of FFD variability can be explained by these differences (adjusted r-squared= 0.65, $p.value$ $<2.2e^{-16}$).

Referring to the indicator of impacts, the results show significant damages due to natural disasters meteorological-related all over the country in 2003 and 2017, corresponding to the most severe droughts, followed by 2012 (Fig. 6). In these years, the highest values range from 300 to 600 euro of damages per hectare of UAA. The most affected region is North-East, with highest

damages per hectare in 2003 and 2012 and the second highest in 2017, after Centre (with 614 €/ha). The persistent conditions of drought in the period 2004-2007 in the North of the country (Fig. 1) don't correspond to the damages, less pronounced. On the contrary, in 2003-2007, South and Islands show relevant damages although with no or moderate and less persistent drought than in North.

In total, it has been calculated a damage of 27.837 billion euros declared in the 16 years, 76% of which are damages on productions, 18% on farm structures and 8% on infrastructures connected to the agricultural activities (Tab. 3). The highest absolute values of damages affected the Islands and the South, followed by the North-East. The Islands also suffered the major damages on productions and on farm structures and the South on

infrastructures. These data, comparing to the intensity of the events, in terms of hazard showed before, seem define the Islands and the South of Italy more vulnerable to damages than exposed to the hazards.

The kind of event affects differently areas and type of damages (Fig. 7). The number of events declared as natural disaster classified per type of damage show that the episodes of heavy and/or prolonged rain are frequent and affect all three productions, structures and infrastructures (these ones almost exclusively hit by heavy rain), while several strong winds and tornados mainly hit the farm structures. The damages on productions are due to several kind of events, mainly drought, hail and heavy rain.

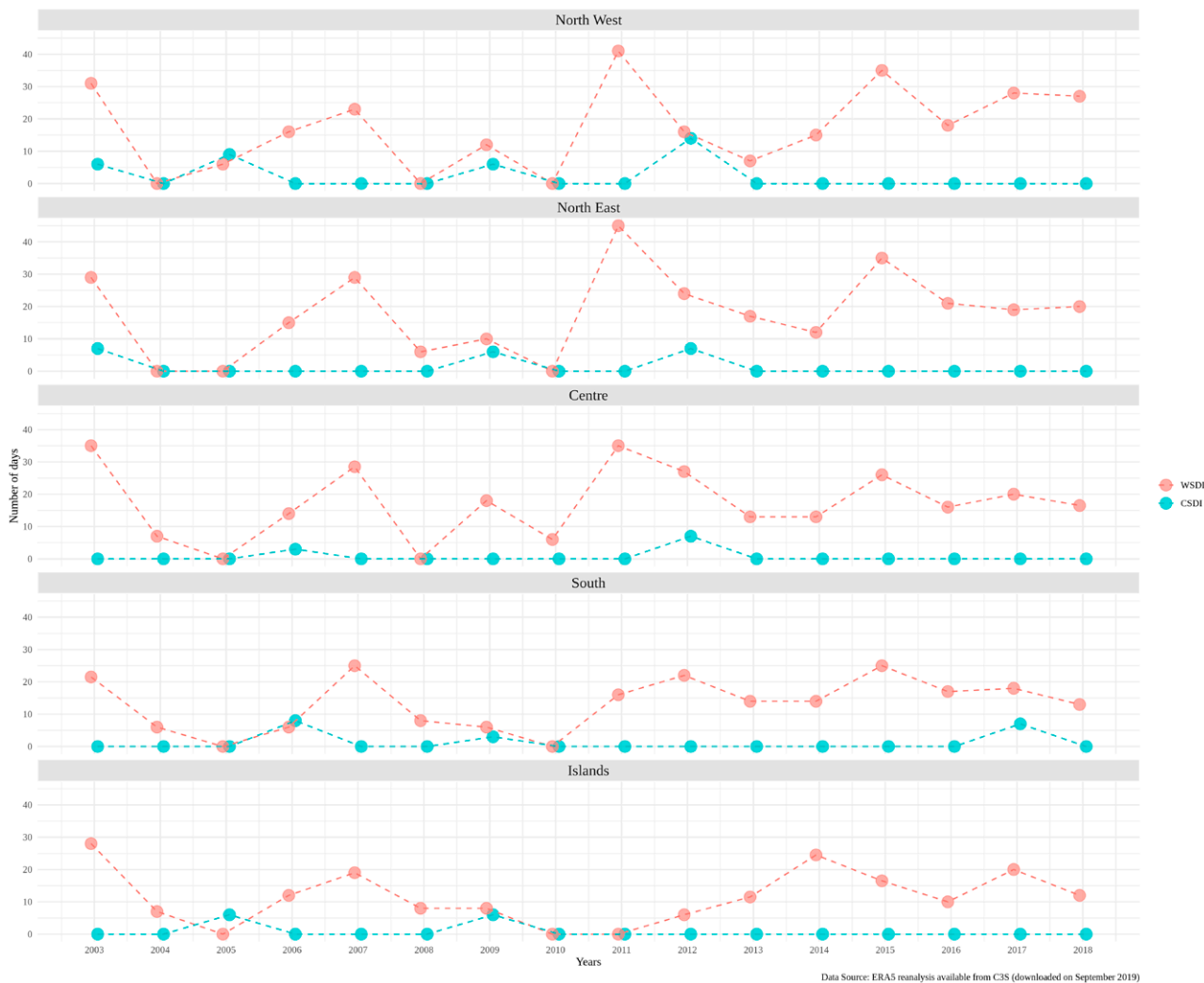


Fig. 2. Warm spells and cold spells, number of days per year in the period 2003-2018.

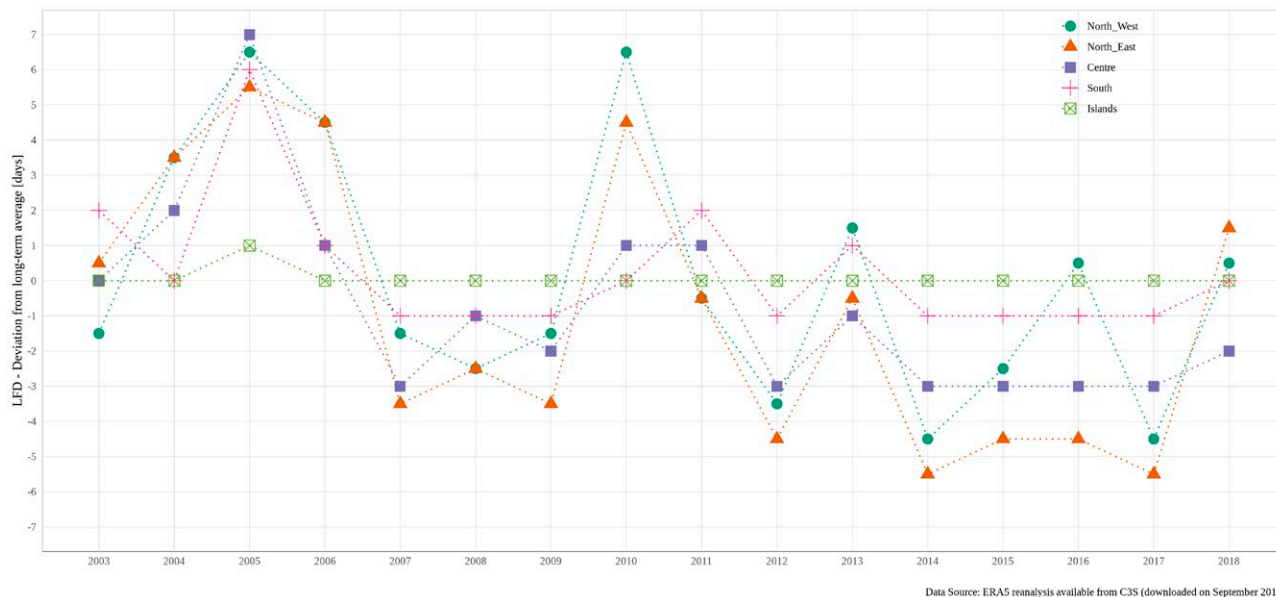


Fig. 3. Late frosts days, deviation from the climate per year in the period 2003-2018.

DISCUSSION

The context analysis here presented provides a first description of the relationships between damages on agriculture and weather-climate conditions, despite the small scale necessary for the National Strategic Plan.

In particular, the results show that drought has been the most impacting hazard and a frequent condition affecting all the country around every 4-5 years, with extreme peaks in 2003 and 2017. Moreover, considering the climatic characteristics of the different areas of the country, in South and Islands the drought events are less extreme than in North, in terms both of hazard and impacts (see Fig. 1 and 7). The positive relationship between drought and damages did not occur everywhere: for example, lower damages have been recorded for the persistent drought occurred in the northern areas in the period 2004-2007 (Fig. 1), while relevant damages occurred in South and Islands in 2003-2007, although these areas showed no or moderate and less persistent drought in relation to North. These results confirm that the link between drought and impacts is time variant and region specific (as already noticed by EEA, 2017; Bachmair et al., 2015 and Blauhut et al., 2015). In the investigation of this link, it would be also important to consider other factors such as the level of spatial aggregation (i.e. NUTS1), mainly in climatically heterogeneous areas, and the type of agricultural production (Parsons et al., 2019; Gobin, 2018).

The second most important event is heavy rain: the results show that the country has a general intense and concentrated precipitation hazard. The concentrated precipitation in average is equal to 20% of annual total precipitation. Overall, there is a variability of this phenomenon during the analysis period and among the different NUTS1 regions. In particular, the heavy rain amounts have been most relevant in South and Islands, with a mean value for the analysis period significantly higher than in the previous period 1981-2002, meaning a change of pattern in precipitation distribution in time.

Heavy rain is the hazard that affects at the same time productions, farm structures and infrastructures and in some cases, as in Islands for 2012 and 2015, these phenomena during the year are associated to drought events, with potential huge impacts on entire agricultural seasons.

Another significant indication comes from the warm spells, which affected the whole period, with a major frequency in its second half, while the cold spells are rarer, with few events concentrated in the first 10 years of analysis, even though the general threshold adopted for this index (0 °C) is not suitable to investigate the different hazards due to late frosts, which vary with the site, the season and the crops.

The late frost days after 2013 show a clear tendency to reduction (all the years below the average), most accentuated in the north-eastern and central areas.

The results on the indicator of first flowering show a generalized early flowering from 2012 in the Centre, South and Islands.

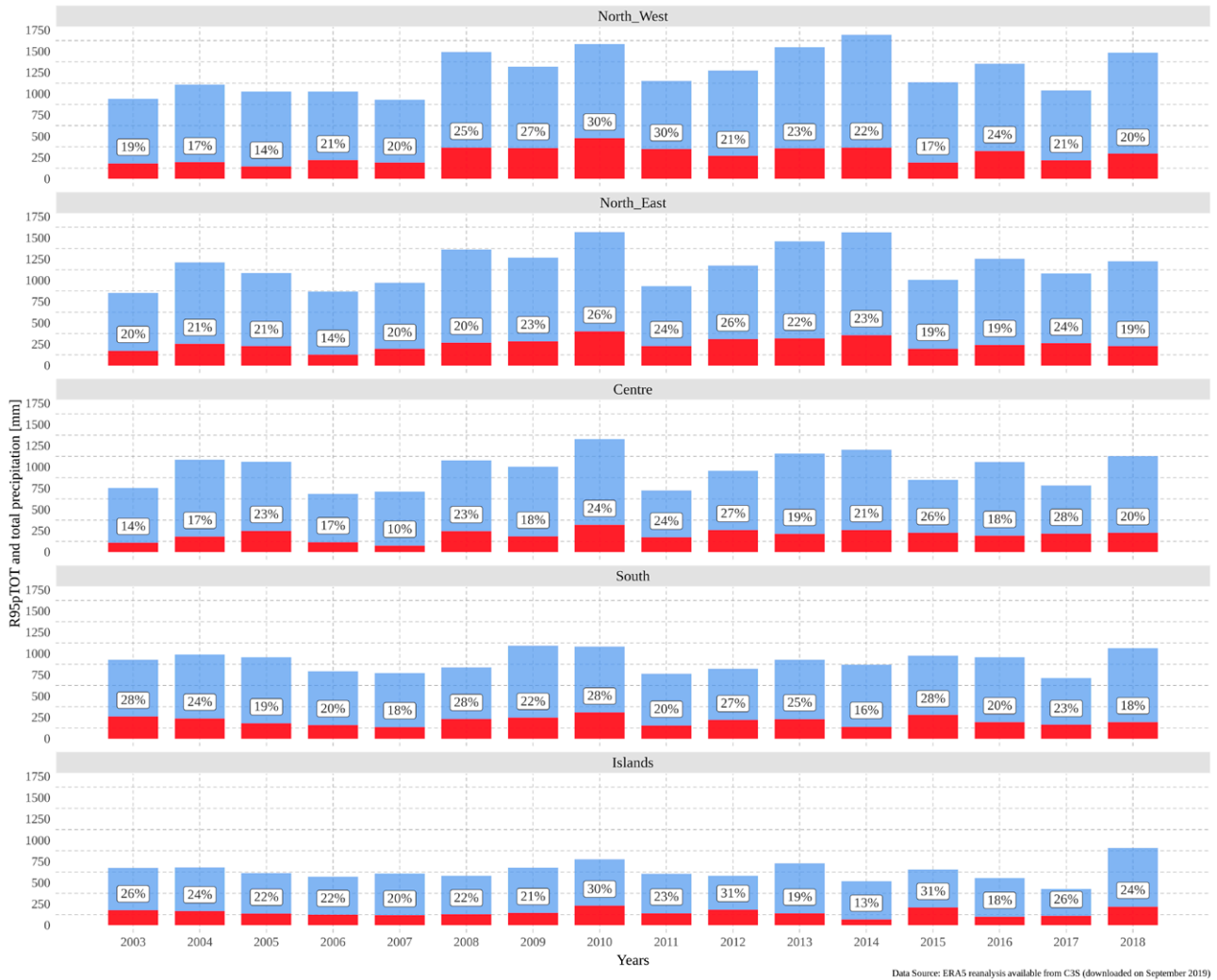


Fig. 4. Annual total precipitation (blue bar) and precipitation fraction due to very wet days (red bar and %) per year in the period 2003-2018.

The joint analysis of some hazard indicators highlights some consistent signals in relation to particular years or sub-periods. In 2004, the relevant delay of first flowering is consistent with the almost absence of warm spells, on the contrary, a negative link between flowering and warm spells is evident, all over the country in 2007 and mainly for northern regions in 2011. In addition, a persistent advanced flowering in the second part of the analysis period is consistent with a general increase of warm spells, especially in South and Islands.

As regards the choice of indicators, some of them need to be assessed at a more detailed spatial scale and to be focused on the specific requirements of the different crops. In addition, local specific thresholds could improve the analyses.

The results of SPEI, late frost days, first flowering date and warm spells seem strictly linked to the undisputed increase of average temperatures in the last years also in Italy (ISPRA, 2019).

In general, the country shows a high vulnerability to weather events leading to disasters, with a huge amount of damages declared (almost 30 billion euros) in these 16 years and frequent high values, normalized to the hectares of UAA, which are greater than about 300 up to 600 euros. The highest absolute values of damages affected the Islands and the South, followed by the North-East and these data, cross-read with the intensity of the events, seem define the Islands and the South of Italy more vulnerable to damages than exposed to the hazards. For instance, in terms of kind of event, the highest damages are due to drought events, while the most

frequent events are others, such as hail and heavy rain (both frequent and damaging), while other events are more frequent and less damaging (strong wind).

A crucial point in this analysis is the choice of metrics (i.e. median or 10th percentile) for spatial aggregation: in fact, it is important to choose the most effective metric to highlights the phenomena, particularly

in a very orographically complex area like Italy. Some uncertainties are due to the resolution of input data, as in the case of first flowering: the correlation of phenological model errors (MAE) with differences in elevation between the ERA5 cells and observation sites confirms such uncertainty, as suggested by Fehlmann et al. (2019).

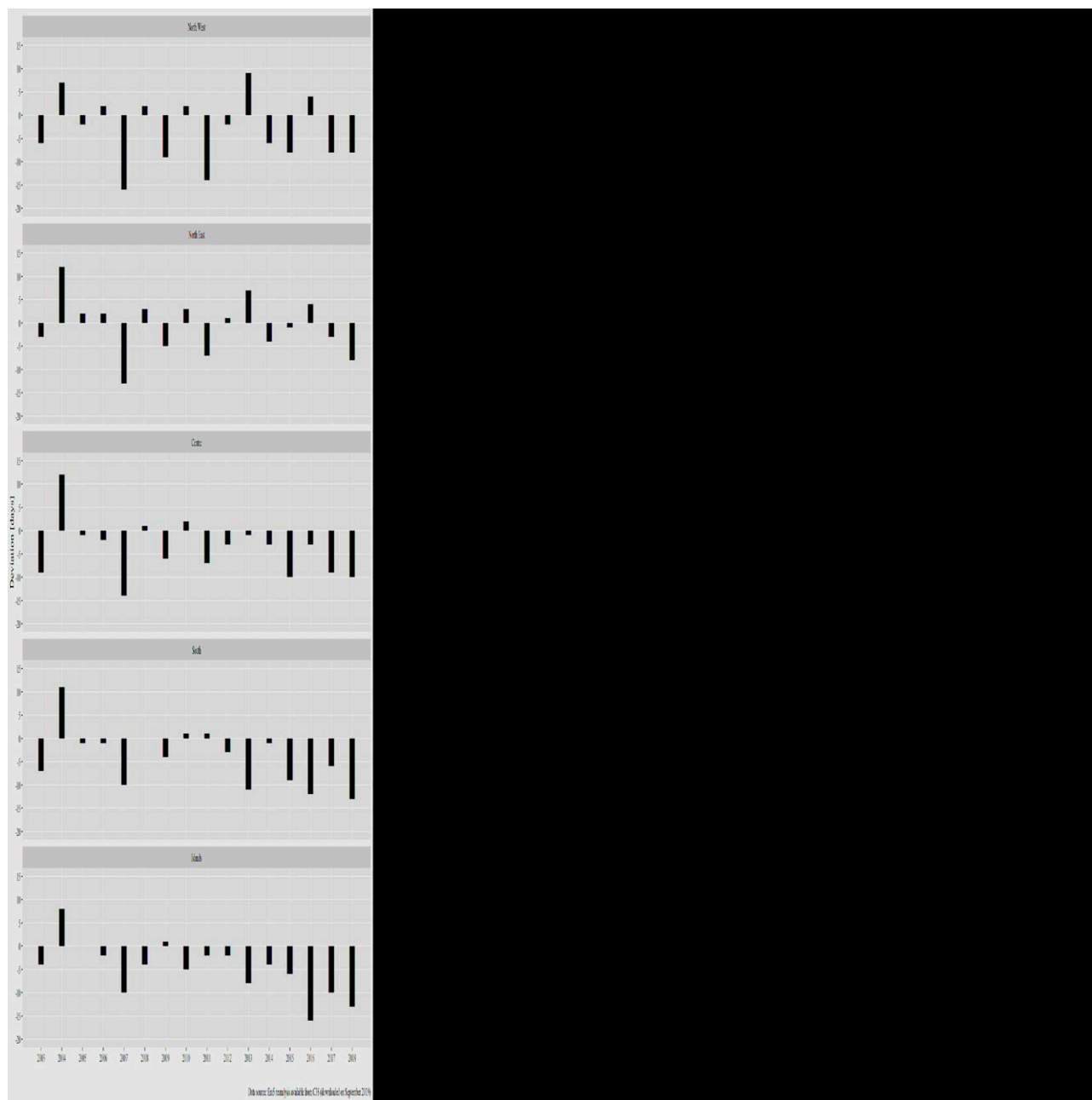


Fig. 5. Annual deviation of first flowering dates from the median (corresponding to 0 value on the y axis) of the climate period. The median dates correspond to 3 of June (DOY, day of the year = 154) for the North West, 27 of May (DOY=147) for the North-East, 28 of May (DOY=148) for Centre, 25 of May (DOY=145) for the South and 16 of May (DOY=136) for the Islands.

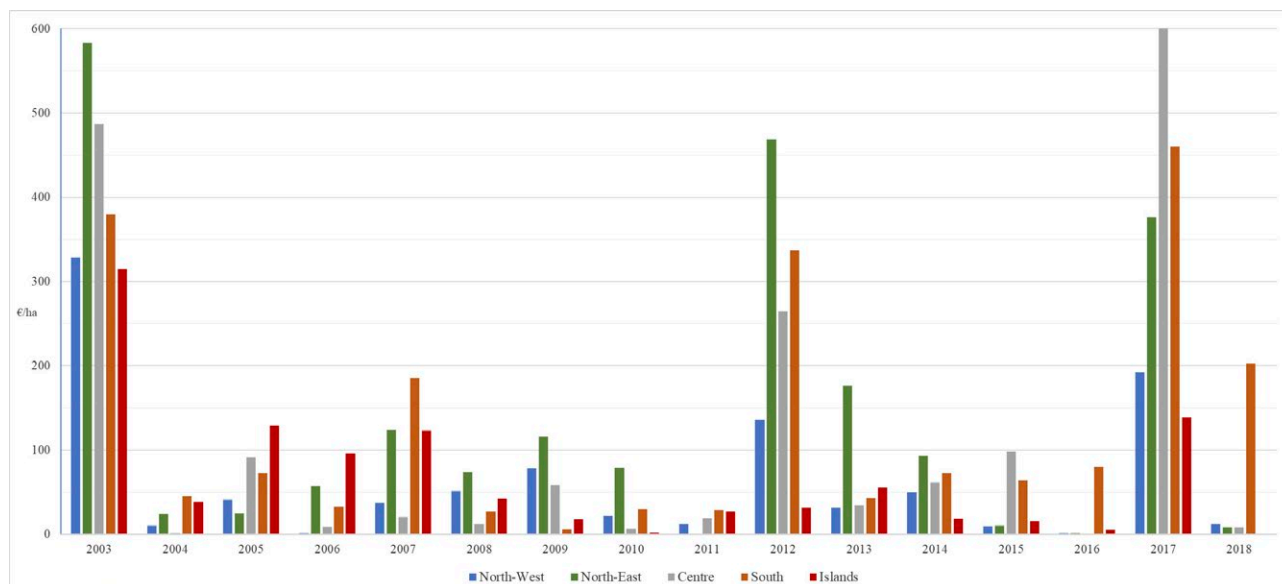


Fig. 6. Damages attributed to natural disasters per NUTS 1 region per year in the period 2003-2018 (values in €/ha UAA).

CONCLUSIONS

Referring to the aims and the context of the study, the results suggest the adoption of policy measures designed through objective analyses instead of simple “perception” of hazard and risks. This aspect has emerged by cross-reading the results of the hazard indicators in terms of intensity and occurrence in time and space and those of the impact indicator (damages due to natural disasters), that in some cases confirm, but not in others, the relationship between hazard and impacts. Moreover, the policy measures need to be enhanced at local level in terms of risk reduction where the agricultural systems are highly vulnerable (the hazard and the impacts are not aligned) and in terms of

adaptation to CC and disaster management where the impacts are linked to objective high hazards. For future studies it will be important also to consider indicators for events such as hail and strong wind and some indicators correlating more directly the hazards and the vulnerabilities at territorial level for each kind of adverse event.

A possible weakness of the study is the spatial resolution of the input meteorological data, that could be not completely suitable for agrometeorological analyses. In addition, the NUTS1 spatial aggregation chosen due to the needed synthesis for the national context could flatten the phenomena too much; better indications for policy choices could derive from a regional/sub-regional aggregation (NUTS2/NUTS3).

Nevertheless, the study indicates good potentialities of the ERA5 data source for the purpose above explained (Italian national context analysis). In order to give more specific indications for agricultural policy decisions other options will be explored for future studies, such as ERA5-Land which provides higher resolution¹⁴, but shorter time series (from 2001 onwards).

Further improvements are also planned in terms of time scale, for instance using a seasonal approach, important for programming adaptation actions of the agricultural activities.

Tab. 3. Damages attributed to natural disasters in the period 2003-2018 per NUTS 1 region (values in billion euros).

NUTS 1 Region	Damages on productions	Damages on farms structures	Damages on infrastructures for agriculture	Total
North-West	1,542	0.298	0.290	2,131
North-East	4,716	0.433	0.350	5,499
Centre	3,088	0.629	0.232	3,950
South	5,566	1,201	0.447	7,214
Islands	6,369	2,350	0.323	9,043
Italy	21,283	4,912	1,642	27,837

¹⁴ <https://cds.climate.copernicus.eu/cdsapp#!dataset/reanalysis-era5-land?tab=overview>.

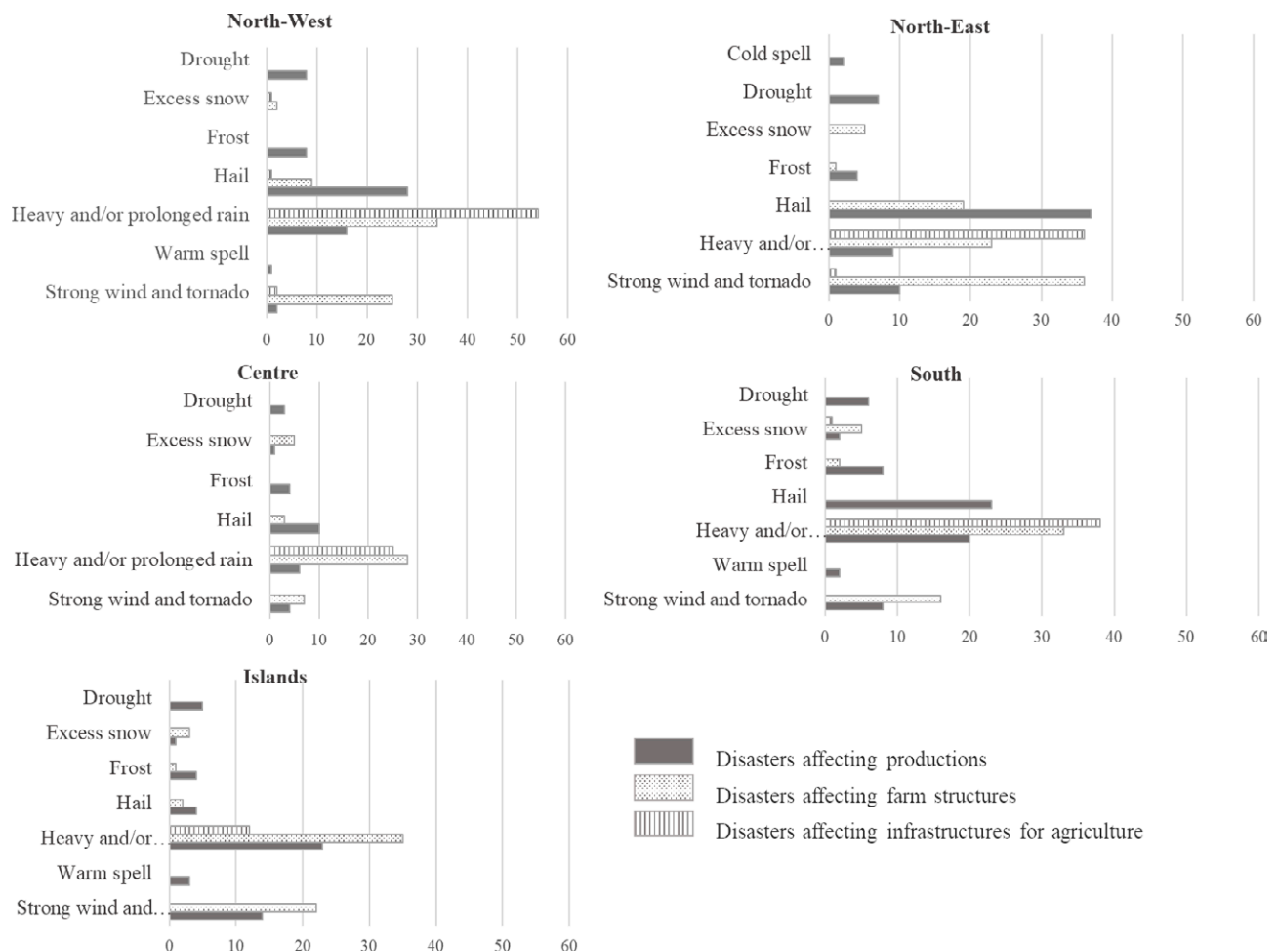


Fig. 7. Number of disasters declared per NUTS 1 region, type of event and type of damages in the period 2003-2018.

ACKNOWLEDGEMENTS

The study has been produced within the project National Rural Network, financed by MIPAAF. A special acknowledgment goes to the project coordinator Alessandro Monteleone for the involvement of the working group on Agrometeorology of CREA - Research Centre for Agriculture and Environment. Moreover, datasets on specific indicators have been provided within the Agri-Digit-AgroModelli project (DM n. 36502 of 20/12/2018), funded by MiPAAF.

REFERENCES

- Allen R.G., Pereira R.S., Raes D., Smith M., 1998. Crop evapotranspiration – Guidelines for computing crop water requirements. FAO Irrigation and Drainage Paper No. 56, Roma Italy, 300 pp.
- Bachmair S., Kohn I., Stahl K., 2015. Exploring the link between drought indicators and impacts. *Natural Hazards and Earth System Science*. 15: 1381-1397 DOI: 10.5194/nhess-15-1381-2015.
- Beguiría S., Vicente-Serrano S.M., Reig F., Latorre F., 2014. Standardized precipitation evapotranspiration index (SPEI) revisited: parameter fitting, evapotranspiration models, tools, datasets and drought monitoring. *Int. J. Climatol.* 34: 3001-3023 DOI: 10.1002/joc.3887.
- Blanco-Ward D., Monteiro A., Lopes M., Borrego C., Silveira C., Viceto C., Rocha A., Ribeiro A., Andrade J., Feliciano M., Castro J., Barreales D., Carlos C., Peixoto C., Miranda A., 2017. Analysis of climate change indices in relation to wine production: A case study in the Douro region (Portugal). *BIO Web Conf.* 9 01011. DOI: 10.1051/bioconf/20170901011.
- Blauhut V., Gudmundsson L. and Stahl K., 2015. Towards pan-European drought risk maps: Quantifying the link between drought indices and reported drought

- impacts. *Environmental Research Letters*. 10(1): 014008 doi: 10.1088/1748-9326/10/1/014008.
- C3S Copernicus Climate Change Service, 2017. ERA5: Fifth Generation of ECMWF Atmospheric Reanalyses of the Global Climate. Copernicus Climate Change Service Climate Data Store (CDS).
- Cogato A., Meggio F., De Antoni Migliorati M. and Marinello F., 2019. Extreme Weather Events in Agriculture: A Systematic Review. *Sustainability* 2019, 11, 2547 DOI:10.3390/su11092547.
- Cola G., Mariani L., Dal Monte G., Alilla R., Epifani C., Failla O., 2012. A thermal based model for vegetative and reproductive phenology of grapevine. In *Atti del XV Convegno Nazionale di Agrometeorologia*, Palermo 5-7 Giugno 2012, Italian Journal of Agrometeorology, Patron Ed. Bologna, Italy, 69-70 ISBN: 978-88-555-3175-7.
- Donat M.G., Alexander L.V., Yang H., Durre I., Vose R., Dunn R.J.H., Willett K.M., Aguilar E., Brunet M., Caesar J., Hewitson B., Jack C., Klein Tank A.M.G., Kruger A.C., Marengo J., Peterson T.C., Renom M., Oria Rojas C., Rusticucci M., Salinger J., Elrayah A.S., Sekele S.S., Srivastava A.K., Trewin B., Villarreal C., Vincent L. A., Zhai P., Zhang X. and Kitching S., 2013a. Updated analyses of temperature and precipitation extreme indices since the beginning of the twentieth century: The HadEX2 dataset. *J. Geophys. Res. Atmos.* 118: 2098–2118 DOI: 10.1002/jgrd.50150.
- Donat M.G., Alexander L.V., Yang H., Durre I., Vose R. and Caesar J., 2013b. Global Land-Based Datasets for Monitoring Climatic Extremes, *Bull. Amer. Meteor. Soc.* 94, 997–1006 DOI: 10.1175/BAMS-D-12-00109.1.
- Donat M.G., Sillmann J., Wild S., Alexander I.V., Lippmann T., Zwier F.W., 2014. Consistency of temperature and precipitation extremes across various global gridded in situ and reanalysis datasets. *J. Clim.* 27: 5019–5035 <https://doi.org/10.1175/JCLI-D-13-00405.1>.
- EC European Commission, 2019. CAP specific objective: Agriculture and climate mitigation. https://ec.europa.eu/info/food-farming-fisheries/key-policies/common-agricultural-policy/future-cap/key-policy-objectives-future-cap_en.
- EEA European Environment Agency, 2017. Climate change adaptation and disaster risk reduction in Europe Enhancing coherence of the knowledge base, policies and practices. EEA Report No 15/2017 Publications Office of the European Union, 2019 DOI:10.2800/938195.
- EEA European Environment Agency, 2019. Climate change adaptation in the agriculture sector in Europe. EEA Report No 04/2019. Publications Office of the European Union, 2019 DOI:10.2800/537176.
- European Parliament, 2018. Proposal for a regulation of the European Parliament and of the Council establishing rules on support for strategic plans to be drawn up by Member States under the Common agricultural policy (CAP strategic plans) and financed by the European Agricultural Guarantee Fund (EAGF) and by the European Agricultural Fund for Rural Development (EAFRD) and repealing Regulation (EU) No 1305/2013 of the European Parliament and of the Council and Regulation (EU) No 1307/2013 of the European Parliament and of the Council. COM(2018) 392 1.6.2018 <https://cds.climate.copernicus.eu/cdsapp#!/home> (accessed September 2019).
- Fehlmann M., Gascón E., Rohrer M., Schwarb M., Stoffel M., 2019. Improving medium-range forecasts of rain-on-snow events in prealpine areas. *Water Resources Research*, 55 <https://doi.org/10.1029/2018WR024644>
- Gobin, A., 2018. Weather related risks in Belgian arable agriculture. *Agricultural Systems* 159: 225-236 DOI: 10.1016/j.agsy.2017.06.009.
- Hargreaves G.H., Samani Z.A., 1982. Estimating potential evapotranspiration. *J. Irrig. Drain. Div.*, 108 (3): 225–230.
- Hui-Meana F., Yusopa Z., Yusofb F., 2018. Drought analysis and water resource availability using standardised precipitation evapotranspiration index, *Atmospheric Research* 201: 102–115 <http://dx.doi.org/10.1016/j.atmosres.2017.10.014>.
- IPCC Intergovernmental Panel on Climate Change, 2007. *Climate Change 2007: Impacts, Adaptation and Vulnerability*. Contribution of Working Group II to the Fourth Assessment Report of the Intergovernmental Panel on Climate Change, IPCC Geneva.
- IPCC Intergovernmental Panel on Climate Change, 2012. *Managing the Risks of Extreme Events and Disasters to Advance Climate Change Adaptation*. A Special Report of Working Groups I and II of the Intergovernmental Panel on Climate Change [(eds.)], Cambridge University Press, Cambridge, UK, and New York, NY, USA, 582 pp.
- Istituto Superiore per la Protezione e la Ricerca Ambientale – ISPRA, 2019. *Gli indicatori del clima in Italia*. Stato dell'ambiente 88/2019. ISPRA Roma ISBN 978-88-448-0955-3.
- Klein Tank A. M. G., Zwiers F. W. and Zhang X., 2009. *Guidelines on Analysis of extremes in a changing climate in support of informed decisions for adaptation*. Climate Data and Monitoring WCDMP-No. 72. World Meteorological Organization, Geneva.

- Li C., Wang R., Ning H., Luo Q., 2016. Changes in climate extremes and their impact on wheat yield in Tianshan Mountains region, northwest China. *Environ Earth Sci* 75:1228 DOI: 10.1007/s12665-016-6030-6.
- Mariani L., Alilla R., Cola G., Dal Monte G., Epifani C., Puppi G., Failla O., 2013. IPHEN a real time network *IJBiom* 57: 881-893 DOI:10.1007/s00484-012-0615-x.
- Mariani S., Braca G., Romano E., Lastoria B., Bussetti M., 2018. Linee guida sugli indicatori di siccità e scarsità idrica da utilizzare nelle attività degli osservatori permanenti per gli utilizzi idrici. Stato attuale e prospettive future. CREIAMO PA 2018, <https://urly.it/334f9>.
- Meier U. (ed), 2001. Growth stages of mono- and dicotyledonous plants. BBCH. Monograph, 2nd edn. Federal Biological Research Centre of Agriculture, Germany.
- Parsons D.J., Rey D., Tanguy M., Holman I.P., 2019. Regional variations in the link between drought indices and reported agricultural impacts of drought. *Agricultural Systems* 173:119-129.
- Pontrandolfi A., Capitanio F., Pepe A.G., 2016. Vulnerability of agricultural areas to climatic risk and effectiveness of risk management policy scheme in Italy. *International Journal of Safety and Security Engineering*. 6(2): 150-160, WIT Press DOI: 10.2495/SAFE-V6-N2-150-160.
- R Core Team, 2018. R: A language and environment for statistical computing. R Foundation for Statistical Computing, Vienna, Austria. <https://www.R-project.org/>.
- Russo S., Dosio A., Graversen R. G., Sillmann J., Carrao H., Dunbar M. B., Singleton A., Montagna P., Barbola P. and Vogt J. V., 2014. Magnitude of extreme heat waves in present climate and their projection in a warming world. *J. Geophys. Res. Atmos.* 119: 12.500–12.512 DOI:10.1002/2014JD022098.
- Song S., Li F., Lu Y., Kifayatullah K., Xue J. and Leng P., 2018. Spatio-Temporal Characteristics of the Extreme Climate Events and their Potential Effects on Crop Yield in Ethiopia. *J. Resour. Ecol.* 2018 9(3): 290-301 DOI: 10.5814/j.issn.1674-764x.2018.03.009.
- Sonkoué D., Monkam D., Fotso-Nguemo T.C., Zéphirin D., Vondou D.A., 2018. Evaluation and projected changes in daily rainfall characteristics over Central Africa based on a multi-model ensemble mean of CMIP5 simulations. *Theoretical and Applied Climatology*. 137(3-4): 2167-2186 DOI:10.1007/s00704-018-2729-5.
- Subash N., Singh S.S., Priya N., 2011. Extreme rainfall indices and its impact on rice productivity. A case study over sub-humid climatic environment. *Agricultural Water Management*. 98(9): 1373-1387 DOI: <https://doi.org/10.1016/j.agwat.2011.04.003>.
- UNISDR United Nations Office for Disaster Risk Reduction, 2015. Making Development Sustainable: The Future of Disaster Risk Management. Global Assessment Report on Disaster Risk Reduction. Geneva, Switzerland: United Nations Office for Disaster Risk Reduction ISBN: 978-92-1-132042-8.
- Vicente-Serrano S.M., Beguería S., 2016. Short Communication Comment on 'Candidate distributions for climatological drought indices (SPI and SPEI)' by James H. Stagge et al. *Int. J. Climatol.* 36: 2120–2131 DOI: 10.1002/joc.4474.
- Vicente-Serrano S.M., Beguería S., Lopez-Moreno J.I., 2010. A Multiscalar Drought Index Sensitive to Global Warming: The Standardized Precipitation Evapotranspiration Index. *J. Climate*. 23: 1696-1718 DOI: 10.1175/2009JCLI2909.1.
- Wang E., Engel T., 1998. Simulation of phenological development of wheat crops. *Agric Syst.* 58(1):1–24.
- Weikai Y., Hunt L.A., 1999. An equation for modeling the temperature response of plants using only the cardinal temperatures. *Ann Bot.* 84:607–614.
- WMO World Meteorological Organization and Global Water Partnership, 2016. Handbook of Drought Indicators and Indices (M. Svoboda and B.A. Fuchs). Integrated Drought Management Programme (IDMP), Integrated Drought Management Tools and Guidelines Series 2. Geneva. ISBN: 978-92-63-11173-9.
- WMO World Meteorological Organization, 2017. WMO Guidelines on the calculation of climate normals. WMO-No. 1203. ISBN: 978-92-63-11203-3 https://library.wmo.int/doc_num.php?explnum_id=4166.
- Zhang X., Alexander L., Hegerl G.C., Jones P., Klein Tank A., Peterson T. C., Trewin B. and Zwiers F.W., 2011. Indices for monitoring changes in extremes based on daily temperature and precipitation data. *WIREs Clim. Change*. 2(6): 851–870 DOI:10.1002/wcc.147.
- Zheng, B., Chapman S.C., Christopher J.T., Frederiks T., Chenu K., 2015. Frost Trends and their Estimated Impact on Yield in the Australian Wheatbelt. *Journal of experimental botany*. 66(12): 3611-3623 DOI: 10.1093/jxb/erv163.
- Zolina O., Simmer C., Belyaev K., Kapala A. and Gulev S., 2009. Improving Estimates of Heavy and Extreme Precipitation Using Daily Records from European Rain Gauges. *Journal of Hydrometeorology*. 10(3): 701-716. www.jstor.org/stable/24912001.



Citation: A. Ahrar, F. Paknejad, S. A. Tabatabaei, F. Aghayari, E. Soltani (2020) Evaluation of forage Amaranth (*Amaranthus hypochondriacus* L.) yield via comparing drought tolerance and susceptibility indices. *Italian Journal of Agrometeorology* (1): 31-40. doi: 10.13128/ijam-868

Received: March 3, 2020

Accepted: April 26, 2020

Published: June 23, 2020

Copyright: © 2020 A. Ahrar, F. Paknejad, S. A. Tabatabaei, F. Aghayari, E. Soltani. This is an open access, peer-reviewed article published by Firenze University Press (<http://www.fupress.com/ijam>) and distributed under the terms of the Creative Commons Attribution License, which permits unrestricted use, distribution, and reproduction in any medium, provided the original author and source are credited.

Data Availability Statement: All relevant data are within the paper and its Supporting Information files.

Competing Interests: The Author(s) declare(s) no conflict of interest.

Evaluation of forage Amaranth (*Amaranthus hypochondriacus* L.) yield via comparing drought tolerance and susceptibility indices

ALIREZA AHRAR¹, FARZAD PAKNEJAD^{1,*}, SEYED ALI TABATABAEI², FAYAZ AGHAYARI¹, ELIAS SOLTANI³

¹ Department of Agronomy, Karaj Branch, Islamic Azad University, Karaj, Iran

² Seed and Plant Improvement Research Department, Yazd Agricultural and Natural Resources and Education Center, AREEO, Yazd, Iran

³ Department of Agronomy and Plant Breeding (Abureyhan), University of Tehran, Tehran, Iran

*Corresponding author email: farzadpaknejad@yahoo.com, <https://orcid.org/0000-0003-0951-2072>.

Abstract. In order to investigate the influence of different drought stress levels on the quality and quantity yield of forage Amaranth, a set of split-plot analysis were carried out in randomized blocks design with three replicates during the 2018 and 2019 growing seasons. The main factor of this study was different irrigation levels (50, 60, 70, and 80 % of the plant available water depletion) and the sub-factor was considered to be three different forage Amaranth genotypes, including Cim, Kharkovski, and Loura. The results revealed that an increase in irrigation intervals especially in 80 % water-deficit condition, will lead to a decrement in the fresh and dry yields (62 and 50 %), a reduction of WP factor (50 %) and an increase of the dry matter and crude protein percentages regarding the control treatment. Furthermore, to specify the most significant stress indices from Principal Component analysis in different drought stress levels, Harmonic Mean was chosen as the best index to examine the tolerance of Amaranth cultivars to the drought condition. According to the 3D graph of the opted index correlation with the yields, it was concluded that while Loura presents a better yield under mild stress conditions, the Cim genotype has the highest performance under moderate and severe drought stress conditions.

Keywords. *Amaranthus hypochondriacus*, Forage, Drought, Stress tolerance indices.

INTRODUCTION

Amaranth (*Amaranthus spp.*) which is originally a native plant in Mexico and Central America is considered as a weed in many regions (Khan et al., 2019). However, for many others, it has proved to be a highly tolerant and valuable plant which brings about many different human usages. Since the Spanish conquest, it has been considered as cuisine and the main ingredient for various beverages due to the high rich content of protein, and the dietary minerals such as calcium, magnesium, phosphorus, and potassium (Adhikary et al., 2020; Svirskis, 2003). Moreover, not only because of the plant's excellent tolerance in harsh climates and its short growth period but also due to the relatively high yields compared to the seeding rate, there is a worldwide trend for using it as a forage crop for ruminants, rabbits, pigs, and poultry (Leukebandara et al., 2019; Oba et al., 2012; Peiretti, 2018; Purwin et al., 2019).

In Nigeria, the effects of intercropping and fertilizer applications on the yield and nutritive value of Amaranth and maize were studied as a forage crop. The study revealed that the fertilizer which is used augments the Dry Matter yields and Crude Protein concentration of Amaranth and Amaranth/maize intercropping mixtures (Olorunnisomo and Ayodele, 2009). In another study, Sokoto and Johnbosco (2017) examined the yield and growth of Amaranths also in Nigeria. They applied 2 varieties of the plant with four different seed rates. Their findings indicated that although the plant height is not severely affected by the seed rates at 2 Weeks After Planting but at 4, 6, and 8 WAP the plants with a higher seed rate were obviously taller than the others. The effect of organic fertilizers on the same factors (yield and growth) also was investigated by Dlamini et al., (2020), they recommended stillage as a good choice for the farmers who prefer organic fertilizers in planting Amaranths.

On the other hand, ever since there was agriculture, drought was always considered a problem in the hot and dry regions of the world. The drought stress can affect the plant from morphological, physiological and biochemical aspects (Anjum et al., 2011; Gao et al., 2020). A study was conducted by Liu and Stützel (2002) to observe the leaf water relations and osmotic adjustment of Amaranth in dry soil conditions. Two years later in another research, they examined biomass production, partitioning, and water use efficiency of four different genotypes of Amaranth. They stated that the Specific Leaf Area and Water Use Efficiency of the plant were affected by the lack of water in all types but not with identical behavior (Liu and Stützel, 2004).

Despite Amaranths mentioned outstanding applications, research on the responses of forage Amaranths to the drought stresses was not carried out, adequately. But in other species of Amaranth, for example, grain for human consumption, a study was conducted in Brazil on the response of two Amaranth species (*Amaranthus caudatus* and *Amaranthus cruentus*) to water deficit stress. The results showed that with increasing the stress the amount of root dry mass decreased while the shoot part augmented. Also in the *A. cruentus* specimen water productivity decreased with increasing water stress (Da Silva et al., 2019).

In Japan, four vegetable Amaranth cultivars were examined under the drought stress conditions. It was seen that due to its fine supply of the necessary elements under stress conditions, the plant could be an appropriate crop in semi-arid and dry regions and also during dry seasons, but it was highly dependent on the genotypes (Sarker and Oba, 2018). In Russia, also Amaranth responses to the soil drought in a greenhouse were investigated by Valdayskikh et al. (2019). Furthermore, Jamalluddin et al. (2019) tried to evaluate the Transpiration Efficiency of Amaranth in response to drought. They explored the TE factor for 9 accessions belonging to Amaranths and stated that the TE factor was much higher in the water-deficient plants compared to the water-sufficient plants. In another investigation Grantz et al., (2019) examined the tolerance to ozone and drought in *Amaranthus tuberculatus*. Although in their study, Amaranth was considered as a weed, but according to their results, the plant productivity, Leaf mass per unit area, and root mass per unit leaf area were not significantly affected by the drought.

Due to the increasing demand for animal feed and the lack of fodder Amaranth scientific investigations, it seems essential to study different qualifications and specifications of the plant. Thereby, regarding the inadequacy of awareness about the drought stress on the Amaranth as forage, this study aimed to investigate the quantity and quality of leaves and stems of three Amaranth cultivars for forage usage and it was tried to evaluate the resistance and performance of this plant when sown under different levels of water deficit, via comparisons of stress tolerance and susceptibility indices. Also, in this research, we sought to achieve maximum water productivity with a non-significant statistical reduction in forage yield.

MATERIALS AND METHODS

Plant materials and growth conditions

Seeds of three forage Amaranth cultivars were used in this study namely Cim, Kharkovski and Ioura. Seeds

Tab. 1. Meteorological data of the experimental sites. (During the experiments).

Month	Temperature (°C)				Relative Humidity (%)	Evaporation Rate (mm)	Monthly Rainfall (mm)
	Mean of Max.	Mean of Min.	Daily ave.	Mean of soil (0-30 cm)			
May 2018	34.9	21.0	28.3	30.1	19.7	12.6	7.8
June 2018	39.8	24.7	33.1	36.1	8.5	15.9	0
July 2018	39.2	25.8	33.0	37.4	11.2	16.3	0
May 2019	30.7	18.3	24.7	27.4	28.7	9.8	8.5
June 2019	39.0	25.2	32.4	35.5	12.6	15.0	0
July 2019	39.3	24.3	32.9	35.8	7.4	16.0	0

Tab. 2. physicochemical properties of the soil in the field before planting (0–30 cm depth).

Year	K (p.p.m)	P (p.p.m)	N (%)	O.C (%)	S.A.R	pH	EC (dS/m)	FC Θ_v	PWP Θ_v	Soil texture
2018	157	13.6	0.017	0.205	3.63	7.2	4.9	24.4	10.8	Sandy clay loam
2019	138	7.3	0.021	0.254	2.8	7.2	4.5	-	-	Sandy clay loam

O.C: Organic Carbon, S.A.R: Sodium Adsorption Ratio, EC: Electrical Conductivity, FC: Field Capacity, PWP: Permanent Wilting Point, Θ_v : Volumetric Humidity.

were planted at Agricultural Research Station located in Yazd, Iran (31°54'30''N and 54°16'20''W). The station is located at 1215 m above the sea level and according to Koppen climate classification (Kottek et al. 2006), it has summers with dry and warm climates (See Table 1). The genotypes were planted in the first week of May during 2018 and 2019 in 40m² plots (fifteen 4-meter-long rows). The spacing was 10 cm and 60 cm between the plants and the rows, respectively (Planting density =166000 plants.ha⁻¹). In addition, the soil properties of the study site are listed in Table 2.

Treatments

One of the factors was devised to be the four levels of soil moisture: 1. No drought stress (i.e. 50 % moisture depletion of plant available water, normal condition), 2. Mild water deficit (60 % moisture depletion), 3. Medium water deficit (70 % moisture depletion) and 4. Severe water deficit (80 % moisture depletion). Soil moisture was checked with TDR (Connector and Buri-able Probes, 6050X1 TRASE System I Analyzer, Soil-moisture Equipment Corp., United States). In the first step, Field Capacity (FC) and Permanent Wilting Point (PWP) were calculated in the field and the pots, respectively (table 2), and afterwards, Plant Available Water

(PAW) was computed from PAW=FC-PWP (Kirkham, 2005).

Firstly, all test cases were irrigated at the same time from planting to the seedling establishment stage as designed in the control conditions (50% moisture depletion of plant available water). Afterwards, the stress treatments were applied (60, 70 and 80 % moisture depletion of plant available water). The amount of irrigation was determined by the irrigation meter of each plot, and Table 3 presents the number of irrigation times and the amount of irrigation in two years.

Another factor was the three different Amaranth genotypes used in this study. All of the specimens belong to the *Amaranthus hypochondriacus* specie. It is worth mentioning that these cultivars were selected, according to the available species of Amaranth in Iran recommended by the Iranian state organization (AREEO)¹, and also due to the conservation of genetic diversity. Seeds of all cultivars had a yellow cream color, and unlike Kharkovski's green color; the Loura and Cim plants were a spectrum of the red color (Rahnama and Safaeie, 2017).

¹ Agricultural Research, Education and Extension Organization

Tab. 3. The number of irrigation times and the amount of irrigation in two years.

Irrigation treatments	Number of irrigation times		The cumulative amount of irrigation (m ³ ha ⁻¹)	
	Year: 2018	Year: 2019	Year: 2018	Year: 2019
Normal condition (50% moisture depletion)	12	12	12307	12000
Mild stress (60% moisture depletion)	11	11	11282	11000
Medium stress (70% moisture depletion)	10	10	10256	10000
Severe stress (80% moisture depletion)	9	9	9230	9000

Yield parameters

Plants per experimental plot were harvested to obtain biologic yield at 50 % flowering. The Sampling process was carried out from four middle lines of each sub-plot with 4 m² by removing the marginal effect. Then, in order to obtain the dry weight of the plant, the samples were incubated for 48 hours in the oven at 75 ° C. At the same time, fresh and dry weights of the leaves and stems of some random bushes were measured (Rahnama and Safaeie, 2017).

For agricultural systems, Water Productivity (WP) is a factor that indicates the production rate of a plant with respect to the consumed water. In this survey, water productivity was calculated by the following equation.

$$WP = \frac{\text{fresh forage yield}}{\text{consuming water}} \text{ (kg m}^{-3}\text{)} \text{ (Cook et al., 2006)}$$

Also, the Leaf to Stem Ratio (LSR) in Amaranth is obtained from the division of fresh leaf to fresh stem weight (Rahnama and Safaeie, 2017). Likewise, the dry matter (DM) content of the crop represents the amount of residual dry material when the water content of the plant has been deducted, which is obtained from the ratio of dry plant yield to fresh plant yield (Olorunniyomo and Ayodele, 2009). The Kjeldahl method was applied to calculate the total nitrogen content for the plants with a ratio of 1: 1 leaf and stem (Kjeldahl, 1883). Then the amount of Crude Protein (CP) was calculated based on the nitrogen value (Onyango, 2010).

Tab. 4. Various drought stress index equations.

Mean Production	$MP = (Y_p + Y_s)/2$	(Rosielle and Hamblin 1981)
Tolerance Index	$Tol = Y_p - Y_s$	(Rosielle and Hamblin 1981)
Geometric Mean Productivity	$GMP = \sqrt{Y_s \cdot Y_p}$	(Fernandez 1992)
Stress Index	$SI = 1 - (\bar{Y}_s / \bar{Y}_p)$	(Fischer and Maurer 1978)
Stress Susceptibility Index	$SSI = (1 - Y_s/Y_p)/SI$	(Fischer and Maurer 1978)
Stress Tolerance Index	$STI = (Y_s \cdot Y_p) / (\bar{Y}_p)^2$	(Fernandez 1992)
Yield Stability Index	$YSI = Y_s/Y_p$	(Bouslama and Schapaugh 1984)
Harmonic Mean	$HM = (2 \cdot Y_p \cdot Y_s) / (Y_p + Y_s)$	(Fernandez 1992)
Yield reduction ratio	$Yr = 1 - (Y_s/Y_p)$	(Gavuzzi et al. 1997)
Relative Drought Index	$RDI = (Y_s/Y_p) / (\bar{Y}_s/\bar{Y}_p)$	(Bidingier et al. 1987)

Drought indices

Various stress indices were applied in this study to carry out the drought stress analysis in different fodder genotypes of Amaranths. The plants' drought stress sensitivity and tolerance are investigated using the following equations.

In the above equations, and are the mean yields of a given genotype evaluated under the drought stress and non-stress conditions, respectively. Also, and are the mean seed yields overall genotypes evaluated under the drought stress and non-stress conditions, respectively.

Experimental design and data analysis

A split-plot analysis was applied in some randomized complete blocks design in two successive years. The main factor was four levels of water stress and the sub-factor was three cultivars of forage Amaranth. Each treatment was repeated three times and wherever significant differences were obtained by the ANOVA, a comparative Duncan test ($P \leq 0.05$) was carried out. Bartlett test was applied to ensure the homogeneity of error variances (Bartlett, 1937). All of the traits were analyzed by combined analysis because of homogeneous error variances for two consecutive years. Furthermore, the obtained data were analyzed using SAS v 9.4 (SAS Institute Inc. USA), and the principal component analysis

was done using the Statgraphics 18 Software (Statgraphics Technologies, Inc. The Plains, Virginia).

RESULTS AND DISCUSSION

Yield Parameters

According to table 5, no significant difference was observed in the studied behaviors of the cases in the two test years (i.e. 2018 and 2019). Moreover, amongst all other active parameters of the main factor (various levels of the drought stress) a significant difference ($p < 0.01$) was observed. Besides, the forage fresh and dry yields, as well as the water productivity in the Control condition (50 % of the plant available water depletion) were clearly higher than those of other treatments, which was also reported by several other researchers (Alvar-Beltrán et al., 2019; Jaleel et al., 2009). Since our target product was the leaves and stems of the plants and the plant's life cycle was relatively short, therefore the drought stress durations after the establishment of the seedlings were quite short, which leads to a decrement of WP with an increment of the drought stress levels. However, in the 3 other parameters (LSR, DM, and CP) the results in the 80% water-depletion treatment were relatively higher than the other treatments.

Also in the genotypes factor, differences ($p < 0.05$) were obtained in the LSR, CP and fresh yield parameters between treatments, which is due to the genetic diversity of the genotypes. According to the field experiments, the LSR and fresh yield parameters of Cim and Loura genotypes were remarkably higher than Kharkovski but on the other hand, the Crude Protein percentage of the Kharkovski genotype was significantly higher than the others.

The interactions of drought stress levels and cultivars revealed that in the control condition Cim and Loura genotypes offered the best results in the fresh and dry yield parameters, while they had a significant difference with Kharkovski. But, it was interesting to see, although Loura had the highest result in the control condition, the genotype was quite weak facing the drought stress. It was seen that the rate of decrement in the fresh and dry yields of the genotypes subjected to the drought stress was much steeper for Loura. Meanwhile, Cim offers an acceptable productivity level in the control condition and also it shows a better tolerance to the water deficit under moderate and severe drought stresses. The reduction of plants' yields under drought stress conditions has been reported vastly by other researchers in the open literature (Bidinger et al., 1987; Da Silva et al., 2019; Sarker and oba, 2018). Under mild drought stress, Loura water productivity did not show any significant difference to

Cim and Loura genotypes in the control condition. With the augmentation of the drought stress level, we witness a decrease in water productivity in all cultivars which is also verified by other researchers (Da Silva et al., 2019). In this parameter also Cim presented a better performance facing the drought stress, regarding Loura and Kharkovski genotypes.

However, the three different genotypes of Amaranth show different behaviors from the fresh weight of leaves to the stem ratio per plant parameter point of view. As was observed in the control condition, Cim cultivar offers the highest LSR, but Loura didn't show a distinguishable difference between its control and the 80 % water deficit conditions. It goes without saying that LSR is a division of two independent parameters (leaf to stem). In the control condition due to the maximum growth and competition of the plants, the numerator (fresh leaf weight) of the fraction exceeds the denominator. On the other hand, in the 80% water-deficit case, despite remarkable leaf and stem weight drops, the stem weight decreased more drastically. Hence, the denominator reduces and it causes the no-significance difference level between the control and severe stress conditions.

Furthermore, Kharkovski cultivar offered a relatively higher percentage of crude protein in the 80% water-deficit condition with respect to the other genotypes × drought stress levels. The CP behavior with a mild variation rate decreases from the severe stress to control condition in all genotypes. This trend also was reported by others (Kuchenmeister et al., 2013). Besides, Nabhan (1986) stated that in some wild cultivars of the canopy, the nitrogen levels are increased but prolonging the drought condition can cause a decrement in the nitrogen content of leaves due to the nitrogen transport to the foliage and seeds. Also, the dry matter percentage did not show any significant difference between the cases.

Comparison of the genotypes based on tolerance indices

The most popular tolerance and susceptibility index equations which are presented in Table 4 were applied to investigate the resistance of Amaranths different genotypes to the drought stress. It is also worth mentioning that the best usage of Amaranths plant is as fresh or silage fodder (Stordahl et al. 1999), thus in this research the stress indices are used for the fresh forage, only and the results can be seen in table 6.

It is known that for RDI, SSI, TOL, and Yr indices, lower values represent higher resistance of the plant to the drought stress, while for YP, YS, GMP, MP, YSI, STI, and HM indices higher values are representing higher tolerance. However, for a better understanding of the

Tab. 5. Effect of water stress on the yield parameters of three genotypes of forage Amaranth in the two successive years.

Treatment	Fresh Yield (ton ha ⁻¹)	Dry Yield (ton ha ⁻¹)	Water Productivity (kg m ⁻³)	Leaf to Stem Ratio	Dry Matter (%)	Crude Protein (%)
Year						
2018	35.52	5.63	3.21	0.51	16.56	15.27
2019	36.71	5.56	3.39	0.50	15.76	15.16
significance	ns	ns	ns	ns	ns	ns
Drought stress level						
water-deficit 50%	53.65 a	7.59 a	4.42 a	0.51 b	14.16 c	13.50 d
water-deficit 60%	41.72 b	6.30 b	3.74 b	0.50 bc	15.11 c	14.62 c
water-deficit 70%	28.98 c	4.78 c	2.86 c	0.49 c	16.66 b	15.66 b
water-deficit 80%	20.12 d	3.74 c	2.21 d	0.54 a	18.75 a	17.11 a
significance	**	**	**	**	**	**
Genotype						
Cim (C)	38.55 a	5.91	3.54	0.53 a	15.81	14.66 b
Kharkovski (Kh)	31.99 b	5.04	2.94	0.46 b	16.22	15.94 a
Loura(L)	37.82 a	5.86	3.44	0.54 a	16.47	15.07 b
significance	*	ns	ns	*	ns	*
Interaction						
water-deficit 50%×(C)	56.24 a	8.08 a	4.63 ab	0.60 a	14.38	13.02 h
water-deficit 50%×(Kh)	46.32 bc	6.56 bc	3.81 c	0.35 g	14.15	14.35 f
water-deficit 50%×(L)	58.40 a	8.14 a	4.81 ab	0.58 b	13.93	13.13 h
water-deficit 60%×(C)	42.19 c	6.20 cd	3.79 c	0.46 f	14.67	13.95 g
water-deficit 60%×(Kh)	36.24 d	5.56 de	3.25 d	0.53 c	15.41	14.86 e
water-deficit 60%×(L)	46.74 b	7.13 b	4.19 bc	0.49 de	15.26	15.05 e
water-deficit 70%×(C)	33.15 d	5.23 e	3.27 d	0.50 de	15.79	14.79 e
water-deficit 70%×(Kh)	27.51 e	4.86 ef	2.72 e	0.46 f	17.71	16.56 c
water-deficit 70%×(L)	26.28 ef	4.25 fg	2.59 ef	0.52 d	16.47	15.65 d
water-deficit 80%×(C)	22.62 fg	4.15 fg	2.48 ef	0.55 c	18.42	16.88 b
water-deficit 80%×(Kh)	17.88 h	3.16 h	1.96 g	0.49 e	17.61	17.98 a
water-deficit 80%×(L)	19.85 gh	3.92 gh	2.18 fg	0.58 b	20.21	16.47 c
significance	*	*	*	**	ns	**
CV (%)	12.02	12.98	12.86	14.56	7.04	5.02

Values within one column followed by different letters are significantly different at $P < 0.05$ according to Duncan's test. ns, no significance ($P < 0.05$). *, **, significance at $P < 0.05$, $P < 0.01$, respectively.

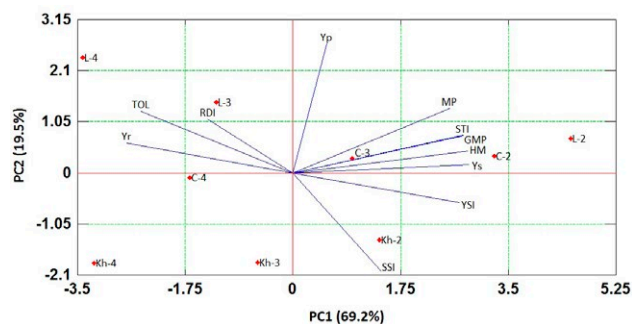


Fig. 1. Biplot principal component analysis (PCA) of various drought resistance indices in three forage Amaranth cultivars. Note: PC1 and PC2; First and second principal component respectively. C: Cim, KH: Kharkovski, L: Loura. 2, 3 and 4: 60, 70 and 80% plant available water depletion, respectively.

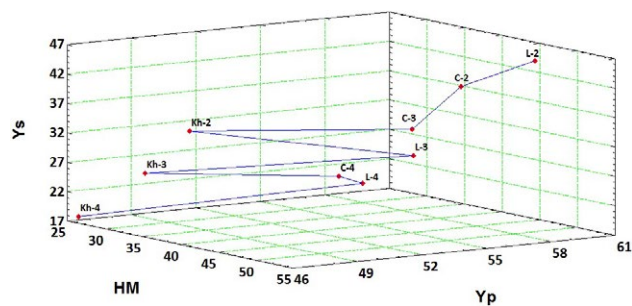


Fig. 2. Graphic display 3D biplot of the best genotypes for Harmonic Mean and potential (control) yield and fresh forage yield under drought stress. Note: C: Cim, KH: Kharkovski, L: Loura. 2, 3 and 4: 60, 70 and 80% plant available water depletion, respectively.

results of table 6, it is required to investigate the mutual relationship of these indices together.

Principal Component Analysis simplifies complex data via converting several associated variables into a smaller number of variables as main components. The first component indicates the maximum variability in the data as compared to the others. This is while in this study, Component 1 and 2 accounted for approximately 89% of the variation (Supplementary Table 7).

Table 8 presents the correlation results of the average values for the three genotypes in two successive years between the fresh forage yield and stress indices in the normal and stress condition, independently. In the mild stress condition HM, STI, GMP, TOL, MP indices and in the moderate stress condition Yr, Ysi, MP, TOL indices had the highest correlation with the yield of the no-stress condition Yp. Also in the severe stress condition, Tol and Mp indices presented the strongest correlation to the control yield. On the other hand, while in

Tab. 6. Tolerance and susceptibility indices three genotypes of forage Amaranth under conditions of drought stress in the two successive years.

Genotype	Yp	Ys	MP	TOL	GMP	SSI	STI	YSI	HM	Yr	RDI
Tolerance and susceptibility indices under mild drought stress											
Cim	56.24	42.19	49.21	14.05	48.65	0.98	2370.16	0.76	48.09	0.24	1.01
Kharkovski	46.32	36.24	41.28	10.08	40.81	0.94	1671.91	0.80	40.36	0.20	1.02
Loura	58.40	46.74	52.57	11.66	52.16	1.00	2735.08	0.81	51.76	0.19	1.00
Tolerance and susceptibility indices under moderate drought stress											
Cim	56.24	33.15	44.70	23.09	43.08	0.99	1861.41	0.59	41.54	0.41	1.01
Kharkovski	46.32	27.51	36.91	18.81	35.65	0.99	1282.43	0.60	34.43	0.40	1.01
Loura	58.40	26.28	42.34	32.12	38.73	0.80	1515.89	0.46	35.56	0.54	1.02
Tolerance and susceptibility indices under severe drought stress											
Cim	56.24	22.62	39.43	33.63	35.32	0.98	1270.19	0.41	31.81	0.59	1.00
Kharkovski	46.32	17.88	32.10	28.44	28.66	0.99	833.49	0.39	25.64	0.61	1.01
Loura	58.40	19.85	39.13	38.55	33.46	0.99	1144.34	0.35	28.88	0.65	1.02

Yp, fresh mean yield of the genotype under non-stress conditions; Ys, fresh mean yield of the genotype under stress conditions; MP, mean productivity; TOL, tolerance; GMP, geometric mean productivity; SSI, stress susceptibility index; STI, stress tolerance index; YSI, yield stability index; HM, harmonic mean; Yr, Yield reduction rate; RDI, relative drought index.

all drought stress levels Tol, SSI, YSI, Yr, RDI indices did not have any significant correlation with the yield of the stress condition (Ys), other indices of Mp, GMP, STI, HM demonstrated a positive correlation ($P < 0.01$) to Ys.

In order to specify the most applicable indices, the Principal Component Analysis (PCA) was carried out. According to the biplot graph of figure 1, the first and second components represented 69.2 and 19.5 % of the variation with the different attributes, respectively. Additionally, since Ys and HM indices in the first component and Yp index in the second component can probe the variations in the best way, they were applied in this study.

Also for a precise study of the cultivars, their Harmonic Mean (HM) index is investigated in the no-stress and under-stress conditions. The result is illustrated in figure 2, in which the horizontal axis indicates the cultivars' priority from the HM index point of view. It is obvious at the first look, that Loura possesses the highest yield in the mild stress condition, but it can be seen that its tolerance to the drought stress is much weaker regarding other genotypes. On the other hand, not only Cim offers the highest HM index in the severe stress condition, but also its performance in the moderate stress condition is higher than Kharkovski in the mild stress condition. This can prove that Cim cultivar provides much better resistance to drought stress with relatively high productivity.

CONCLUSIONS

Despite its tolerance to the harsh weather and wonderful applications in both food and forage industries in

Tab. 7. Principal component analysis of stress tolerance indices in three genotypes of forage Amaranth under conditions of drought stress.

Indices	Component				
	1	2	3	4	5
Yp	0.069	0.628	-0.319	0.180	0.311
Ys	0.361	0.039	0.080	-0.043	-0.120
MP	0.321	0.313	-0.079	0.046	0.043
TOL	-0.311	0.300	-0.249	0.139	0.283
GMP	0.349	0.184	-0.031	0.075	-0.033
SSI	0.181	-0.477	-0.416	0.747	0.006
STI	0.348	0.181	-0.057	-0.036	-0.597
YSI	0.340	-0.145	0.254	-0.053	0.464
HM	0.358	0.108	0.002	0.071	-0.063
Yr	-0.340	0.145	-0.254	0.053	-0.464
RDI	-0.175	0.261	0.720	0.607	-0.119
Eigenvalue	7.604	2.142	1.106	0.132	0.014
Percent of Variance	69.126	19.476	10.054	1.200	0.144
Cumulative Percentage	69.126	88.602	98.656	99.856	100

the world, it seems that the forage Amaranth plant is not appreciated by many researchers. In the present study, the growth and yield of three different genotypes of forage Amaranth were investigated under various drought stress levels in Yazd - Iran in two successive years. The results revealed that the plant is highly affected by water deficit and the water productivity parameter (WP) expe-

Tab. 8. The correlation coefficient between the different levels of tolerance and susceptibility to water deficit in the average of three genotypes of forage Amaranth in the two successive years.

Tolerance and susceptibility indices under mild drought stress										
	YS	MP	TOL	GMP	SSI	STI	YSI	HM	Yr	RDI
YP	0.52*	0.91**	0.72**	0.88**	0.43ns	0.88**	-0.58*	0.84**	0.58*	-0.48*
YS		0.82**	-0.21ns	0.86**	-0.31ns	0.86**	0.38ns	0.9**	-0.38ns	0.28ns
MP			0.38ns	0.99**	0.14ns	0.99**	-0.21ns	0.99**	0.21ns	-0.19ns
TOL				0.31ns	0.74**	0.31ns	-0.97**	0.24ns	0.97**	-0.77**
GMP					0.09ns	0.99**	-0.14ns	0.99**	0.14ns	-0.13ns
SSI						0.09ns	-0.82**	0.04ns	0.82**	-0.97**
STI							-0.13ns	0.99**	0.13ns	-0.13ns
YSI								-0.07ns	-1**	0.83**
HM									0.07ns	-0.07ns
Yr										-0.83**
Tolerance and susceptibility indices under moderate drought stress										
	YS	MP	TOL	GMP	SSI	STI	YSI	HM	Yr	RDI
YP	-0.04ns	0.82**	0.83**	0.54*	0.16ns	0.54*	-0.66**	0.28ns	0.66**	-0.39ns
YS		0.82**	-0.21ns	0.86**	-0.31ns	0.86**	0.38ns	0.9**	-0.38ns	0.28ns
MP			0.36ns	0.93**	-0.11ns	0.92**	-0.11ns	0.78**	0.11ns	0.06ns
TOL				-0.01ns	0.37ns	-0.01ns	-0.96**	-0.3ns	0.96**	-0.69**
GMP					-0.24ns	0.99**	0.27ns	0.96**	-0.27ns	0.34ns
SSI						-0.23ns	-0.47*	-0.32ns	0.47*	-0.87**
STI							0.26ns	0.96**	-0.26ns	0.33ns
YSI								0.52*	-1**	0.78**
HM									-0.52*	0.52*
Yr										-0.78**
Tolerance and susceptibility indices under severe drought stress										
	YS	MP	TOL	GMP	SSI	STI	YSI	HM	Yr	RDI
YP	0.09ns	0.83**	0.8**	0.48*	-0.36ns	0.48*	-0.4ns	0.23ns	0.4ns	-0.28ns
YS		0.82**	-0.21ns	0.86**	-0.31ns	0.86**	0.38ns	0.9**	-0.38ns	0.28ns
MP			0.33ns	0.88**	-0.43ns	0.88**	0.18ns	0.73**	-0.18ns	0.24ns
TOL				-0.15ns	0.14ns	-0.15ns	-0.87**	-0.4ns	0.87**	-0.73**
GMP					-0.36ns	0.99**	0.61**	0.96**	-0.61**	0.61**
SSI						-0.36ns	-0.11ns	-0.29ns	0.11ns	-0.37ns
STI							0.6**	0.96**	-0.6**	0.61**
YSI								0.79**	-1**	0.9**
HM									-0.79**	0.76**
Yr										-0.9**

ns, no significance ($P < 0.05$). *, **, significance at $P < 0.05$, $P < 0.01$, respectively.

rienced a significant drop of 15, 35, and 50 % for mild, moderate and severe drought stress conditions, respectively. It was also observed that despite its short life cycle, Amaranth plant offers acceptable quantity and quality of fodder which is why it is considered an excellent forage in many regions of the world. Moreover, the Principal Component analysis indicated that the HM index is one of the main components for the genotypes and according to this index, while Cim cultivar yield

was higher than the other two genotypes, Kharkovski showed the weakest results. Since in this study the irrigation treatments were chosen according to the customary farming of the region. It seems that applying milder treatments in future researches could be effective in increasing water productivity. It may also lead to an increment in the yield.

REFERENCES

- Adhikary D., Khatri-Chhetri U., and Slaski J., 2020. Amaranth: An Ancient and High-Quality Wholesome Crop. In Nutritional Value of Amaranth. IntechOpen.
- Alvar-Beltrán J., Saturnin C., Dao A., Dalla Marta A., Sanou J., Orlandini S., 2019. Effect of drought and nitrogen fertilisation on quinoa (*Chenopodium quinoa* Willd.) under field conditions in Burkina Faso. *Italian Journal of Agrometeorology* (1), 33-43.
- Anjum S.A., Xie X.y., Wang L.c., Saleem M.F., Man C., Lei W., 2011. Morphological, physiological and biochemical responses of plants to drought stress. *African Journal of Agricultural Research* 6(9), 2026-2032.
- Bartlett M.S., 1937. Properties of sufficiency and statistical tests. *Proceedings of the Royal Statistical Society, Series A* 160, 268-282.
- Bidinger F., Mahalakshmi V., Rao G.D.P., 1987. Assessment of drought resistance in pearl millet (*Pennisetum americanum* (L.) Leeke). II. Estimation of genotype response to stress. *Australian Journal of Agricultural Research* 38(1), 49-59.
- Bousslama M., Schapaugh W., 1984. Stress tolerance in soybeans. I. Evaluation of three screening techniques for heat and drought tolerance 1. *Crop Science* 24(5), 933-937.
- Cook S., Gichuki F., Turrall H., 2006. Water productivity: Estimation at plot, farm and basin scale. *People and Agro-Ecosystems Research for Development Challenge*; CIAT: Cali, Colombia, 144.
- Da Silva J.G., Bianchini A., Costa P.M.C., de Almeida Lobo F., de Almeida J.P.M., de Moraes M.F., 2019. Amaranth Response to Water Stress. *Journal of Experimental Agriculture International*, 1-9.
- Dlamini S.N., Masarirambi M.T., Wahome P.K., Oseni T.O., 2020. The Effects of Organic Fertilizers on the Growth and Yield of Amaranthus (*Amaranthus hybridus* L.) Grown in a Lath House. *Asian Journal of Advances in Agricultural Research*, 1-10.
- Fernandez G.C., 1992. Effective selection criteria for assessing plant stress tolerance, 257-270.
- Fischer R., Maurer R., 1978. Drought resistance in spring wheat cultivars. I. Grain yield responses. *Australian Journal of Agricultural Research* 29(5), 897-912.
- Gao S., Wang Y., Yu S., Huang Y., Liu H., Chen W., He, X., 2020. Effects of drought stress on growth, physiology and secondary metabolites of Two *Adonis* species in Northeast China. *Scientia Horticulturae* 259, 108795.
- Gavuzzi P., Rizza F., Palumbo M., Campanile R., Ricciardi G., Borghi B., 1997. Evaluation of field and laboratory predictors of drought and heat tolerance in winter cereals. *Canadian Journal of Plant Science* 77(4), 523-531.
- Grantz D.A., Paudel R., Shrestha A., 2019. Tolerance of ozone and drought in common waterhemp (*Amaranthus tuberculatus*). *Journal of Crop Improvement* 33(2), 236-253.
- Jaleel C.A., Manivannan P., Wahid A., Farooq M., Al-Juburi H.J., Somasundaram R., Panneerselvam, R., 2009. Drought stress in plants: a review on morphological characteristics and pigments composition. *Int. J. Agric. Biol* 11(1), 100-105.
- Jamalluddin N., Massawe F.J., Symonds R.C., 2019. Transpiration efficiency of Amaranth (*Amaranthus* sp.) in response to drought stress. *The Journal of Horticultural Science and Biotechnology* 94(4), 448-459.
- Khan M.G., Abate M., Endris S., Chaka A., 2019. A Critical Appraisal of Amaranths and Chenopodium Weeds for Their Harmful and Beneficial Aspects in Context to Food Security in Pastoral Area. *Daagu International Journal of Basic & Applied Research-DIJBAR* 1(1), 58-69.
- Kirkham M., 2005. Field capacity, wilting point, available water, and the non-limiting water range. *Principles of soil and plant water relations*, 101-115.
- Kjeldahl J., 1883. Neue methode zur bestimmung des stickstoffs in organischen körpern. *Zeitschrift für analytische Chemie* 22(1), 366-382.
- Kottek M., Grieser J., Beck C., Rudolf B., Rubel F., 2006. World map of the Köppen-Geiger climate classification updated. *Meteorologische Zeitschrift* 15(3), 259-263.
- Kuchenmeister K., Kuchenmeister F., Kayser M., Wrage M.N., Isselstein J., 2013. Influence of drought stress on nutritive value of perennial forage legumes. *International journal of plant production* 7(4), 693-710.
- Leukebandara I., Premaratne S., Peiris B., Madugith T., Wimalasiri S., 2019. Study on Milk Parameters of Saanen Goats Fed with Diet Containing Amaranth (*Amaranthus Hypochondriacus*) Seeds. *International Journal of Agricultural Science* 4, 45-56.
- Liu F., Stützel H., 2002. Leaf water relations of vegetable Amaranth (*Amaranthus* spp.) in response to soil drying. *European Journal of Agronomy* 16(2), 137-150.
- Liu F., Stützel H., 2004. Biomass partitioning, specific leaf area, and water use efficiency of vegetable Amaranth (*Amaranthus* spp.) in response to drought stress. *Scientia Horticulturae* 102(1), 15-27.
- Nabhan G.P., 1986. *Gathering the Desert*, University of Arizona Press. USA. page: 99-100.
- Obua B., McAlbert F., Okoro B., Efenie S., 2012. Survey of the diversity of forage Plants used in feeding Pigs in smallholder farms in Southeastern Nigeria. *Int'l Journal of Agric. and Rural Dev* 15(3), 1310-1316.

- Olorunnisomo O., Ayodele O., 2009. Effects of intercropping and fertilizer application on the yield and nutritive value of maize and Amaranth forage in Nigeria. *Grass and forage science* 64(4), 413-420.
- Onyango C., 2010. Preharvest and postharvest factors affecting yield and nutrient contents of vegetable Amaranth (Var. *Amaranthus hypochondriacus*). Thesis, Wageningen University, 129.
- Peiretti P.G., 2018. Amaranth in animal nutrition: A review. *Livestock Research for Rural Development*, 30(5).
- Purwin C., Gugolek A., Strychalski J., Fijałkowska M., 2019. Productivity, Nutrient Digestibility, Nitrogen Retention, and Meat Quality in Rabbits Fed Diets Supplemented with *Sida hermaphrodita*. *Animals* 9(11), 901.
- Rahnama A., Safaeie A.R., 2017. Performance Comparison of Three Varieties of Amaranth (*Amaranthus Hypochondriacus* L.) at Different Harvest Time. *Journal of Asian Scientific Research* 7(6), 224-230.
- Rosielle A., Hamblin J., 1981. Theoretical aspects of selection for yield in stress and non-stress environment 1. *Crop Science* 21(6), 943-946.
- Sarker U., Oba S., 2018. Response of nutrients, minerals, antioxidant leaf pigments, vitamins, polyphenol, flavonoid and antioxidant activity in selected vegetable Amaranth under four soil water content. *Food Chemistry*, 252, 72-83.
- Sokoto M., Johnbosco O., 2017. Growth and yield of Amaranths (*Amaranthus* spp.) as influenced by seed rate and variety in Sokoto, Nigeria. *Archives of Agriculture and Environmental Science* 2(2), 79-85.
- Stordahl J., DiCostanzo A., Sheaffer C., 1999. Variety and maturity affect Amaranth forage yield and quality. *Journal of production agriculture* 12(2), 249-253.
- Svirskis A., 2003. Investigation of Amaranth cultivation and utilization in Lithuania. *Agronomy Research* 1(2), 253-264.
- Valdayskikh V.V., Voronin P.Y., Artemyeva E.P., Rymar V.P., 2019. Amaranth responses to experimental soil drought. In *AIP Conference Proceedings*, Vol. 2063, No. 1, p. 030023.



Citation: E. Kitta, N. Katsoulas (2020) Effect of shading on photosynthesis of greenhouse hydroponic cucumber crops. *Italian Journal of Agrometeorology* (1): 41-48. doi: 10.13128/ijam-871

Received: March 4, 2020

Accepted: April 18, 2020

Published: June 23, 2020

Copyright: © 2020 E. Kitta, N. Katsoulas. This is an open access, peer-reviewed article published by Firenze University Press (<http://www.fupress.com/ijam>) and distributed under the terms of the Creative Commons Attribution License, which permits unrestricted use, distribution, and reproduction in any medium, provided the original author and source are credited.

Data Availability Statement: All relevant data are within the paper and its Supporting Information files.

Competing Interests: The Author(s) declare(s) no conflict of interest.

Effect of shading on photosynthesis of greenhouse hydroponic cucumber crops

EVANGELINI KITTA, NIKOLAOS KATSOULAS

University of Thessaly, Department of Vegetal Production and Rural Environment, Phytokou Street, 38444 Volos, Greece

Abstract. In this work an attempt was made to investigate the effect of shading on photosynthesis rate, transpiration rate and stomatal conductance of a cucumber cultivation in a greenhouse. To this end, autumnal hydroponic cultivation of cucumbers was installed in three same arched greenhouses with lateral ventilation openings at the University of Thessaly experimental farm in Velestino, Greece. One of the greenhouses was used as a control (without shading), the other two were shaded using two different shading nets (shading intensity of 35% and 50%). In the hydroponic cucumber cultivation, a series of crop photosynthesis measurements were performed for two months on leaves of randomly selected plants per greenhouse under natural illumination and using artificial illumination conditions of $1000 \mu\text{mol m}^{-2} \text{s}^{-1}$ with the LCpro+ instrument. Statistical processing of the results showed that shading reduced photosynthesis of the cucumber leaf almost linearly. Furthermore, artificial illumination measurements allowed us to conclude that shaded plants do not acclimate to shade conditions and respond directly to lighting conditions which practically enhances the usefulness of periodic shading as a tool for improving the microclimate in greenhouses.

Keywords. Photosynthesis, greenhouse, shading, hydroponic crops, cucumber.

INTRODUCTION

Various methods can be used to cool the greenhouse. The use of nets or screens is a typical practice in the whole Mediterranean basin. It is considered a low-cost method of decreasing radiation and the concomitant energy load during warm periods (Kitta, 2014). Mobile shading allows improvement of greenhouse climate, especially during the noon hour. It reduces canopy transpiration and water uptake, and increases remarkably water use efficiency (Lorenzo *et al.*, 2006). The use of shading screens in greenhouses became a common practice during the last decade (Cohen *et al.*, 2005; Castellano *et al.*, 2008) because it is a flexible and efficient method of reducing the energy load inside the greenhouse (Teitel and Segal, 1995), especially in climates characterized by high evaporative demand and limited water resources (Lorenzo *et al.*, 2006). The optical properties of the screens (mainly shade factor) can modify the diffuse-to direct radiation ratio (Baille *et al.*, 2001; Raveh *et al.*, 2003; Cohen *et al.*, 2005) and cooling performance (Willits, 2001), while reducing air and crop temperature (Smith *et al.*, 1984; Fernandez-Rodriguez *et al.*, 2000). The modifications arising from the optical properties of the screens can affect radiation absorbed by the crop, stomatal conductance, and net CO₂ assimilation, and consequently crop growth and productivity. Nevertheless, adaptation of plants to light conditions depends also on the specific behavior of the plant species grown in greenhouses (Raveh *et al.*, 2003; Barradas *et al.*, 2005; Romacho *et al.*, 2006). Shade can increase total and marketable yield of tomato grown in hot climates. Depression of crop yield is frequently observed under Mediterranean conditions when high solar radiation and low air humidity conditions prevail. El-Gizawy *et al.* (1993) mention that the highest tomato crop production was obtained under 35% shading, while increasing shading intensity decreased by up to 100% the incidence of sunscald on fruit. Concerning the effect of shading on cucumber crop, Naraghi and Lofti (2010) observed that increasing shading density up to 35% led to an increase in the number of fruits per plant. However, the number of fruits tended to decrease as shading density increased to 60%. Furthermore, the above authors mention that shading intensity greatly influenced the physiological disorders like sun-scald of cucumber fruits.

A better understanding of plant responses to shading is of great interest for greenhouse crops. With respect to the Mediterranean greenhouses, more information is needed mainly on plant responses to the time of application, including both commencement and termination of shading dates. So, an important issue not

yet fully investigated in shaded greenhouses concerns plant acclimation to the light regime imposed by the screen.

Therefore, in this paper we are trying to investigate the effect of shading on photosynthesis rate and plant acclimation of a hydroponic cucumber crop, which is of great economic interest for the Mediterranean countries.

MATERIAL AND METHODS

Greenhouses and plant material

The experiments have been performed in three similar arched roof greenhouses, with vertical side walls, covered with a single sheet of 180 µm thick PE film, N-S oriented, located at the University of Thessaly near Volos, (Velesino: Latitude 39° 22', longitude 22° 44', altitude 85 m), Eastern Greece. The geometrical characteristics of the greenhouses were as follows: eaves height of 2.4 m; ridge height of 4.1 m; total width of 8 m; total length of 20 m; ground area of 160 m², and volume of 572 m³. The soil of each greenhouse was totally covered by double-side coloured plastic mulch. The greenhouses were equipped with two side roll-up vents controlled automatically and ventilation set point temperature was set at 23°C. An autumn hydroponic cultivation of cucumber (*Cucumis sativus cv. Stamina*) was planted, which was transplanted on September 1 and expired on November 12. The plants were grown in slabs (1 m long, 0.3 m wide) filled with perlite sacks (1 m long, 0.3 m wide, 0.2 m high) and planting density was 2.4 plants / m².

Plants were arranged in four duplicate rows, spaced between the lines 0.33 m and 0.80 m apart. The supply of a standard nutrition solution for cucumber (Sonneveld, 2002) was automatically controlled by a fertigation computer and pH set point was at 5.6 with small fluctuations aimed to maintain the pH between 5.5 and 6.5 in the drainage solution. The plants were pruned according to the umbrella training system (Klieber *et al.*, 1993) and all other cultural practices inside the greenhouse (plant protection, harvesting, etc.) were similar to those practiced commonly by local greenhouse cucumber producers.

Three levels of greenhouse shading were tested in the greenhouses, obtained using no net in one of the greenhouses and shade nets made by polypropylene strips (C. Vellis S.A., Piraeus, Greece) differing in hole size. The fixed nets were installed over the external surface of the cover in the two shaded greenhouse. In particular, the three shading treatments were as follows:

- 0% shading (Gr_{0%}), greenhouse transmission to solar radiation approximately 79%).

- 35% shading ($Gr_{35\%}$) (net hole size 2X 8 mm), greenhouse with 35% shading intensity (SI) and transmission to solar radiation of approximately 50% and
- 50% shading ($Gr_{50\%}$) (net hole size 2 X 8 mm), greenhouse with 50% shading intensity (SI) and transmission to solar radiation of approximately 38%.
- The values of greenhouse transmission to solar radiation are the mean values calculated using the ratio of inside to outside solar radiation during the experimental period.

Shading was installed immediately after transplanting and maintained up to the end of the experiment.

Measurements

Climate measurements

For the purpose of the experiment total solar radiation (W/m^2) was recorded by means of pyranometers (model Middleton EP08-E, Brunswick Victoria, Australia), located 2 m above the ground in the center of each of the three greenhouses (Control greenhouse $Gr_{0\%}$, 35% shaded greenhouse $Gr_{35\%}$, and 50% shaded greenhouse $Gr_{50\%}$) and outside (Out) 15 m away from the greenhouse on a mast 3.5 m above the ground.

Photosynthesis Parameters Measurements

For the photosynthesis measurements in the experiment, a closed type LCpro+ photosynthesis system (model LCpro+, ADC BioScientific Ltd., Hertfordshire, England) was used, and the photosynthesis rate (A , $\mu mol.m^{-2}.s^{-1}$), transpiration rate (E , $mmol.m^{-2}.s^{-1}$) and stomatal conductance (g_c , $mol.m^{-2}.s^{-1}$) were measured. The photosynthesis measurements were done for two months, October and November. For photosynthesis measurements, 16 plants/greenhouse were randomly selected. The photosynthesis measurements were carried out approximately every 10 days on a random healthy, well-developed leaf that was about the middle of the total plant height each time. A total of 48 photosynthesis measurements were made every ten days. Two sets of measurements were made. The first series was in sunny days under natural light conditions inside the greenhouses. The second one was made over cloudy days, with artificial constant illumination conditions to evaluate whether cultures in different shading conditions (control, 35% shading and 50% shading) were adapted (acclimated) and reacted differently or not. Constant irradiation measurements, were performed with the use

of the integrated PAR control and adjustment mechanism using LED diodes provided by the LCpro+ measuring device. The illumination intensity was set at the intensity level of $1000 \mu mol.m^{-2}.s^{-1}$ for both the control greenhouse and the two shaded greenhouses in the PAR area.

Six (6) complete sets of measurements were made during the experiment, four (4) in sunshine conditions and two (2) in cloudy conditions.

Calculation of Vapor pressure deficit

Furthermore, Vapor Pressure Deficit (VPD_C) in the leaf chamber air of the LCpro+ device can be calculated from (Allen et al., 2005):

$$VPD_C = e_{sat,c} - e_{ref} \quad (1)$$

Where:

VPD_C = Vapor Pressure Deficit in leaf chamber, kPa

$e_{sat,c}$ = saturation vapor pressure in air temperature, kPa

e_{ref} = partial pressure of the water vapor in the air in leaf chamber, kPa

$e_{sat,c}$ and e_{ref} can be calculated from the following relations (Howell and Dusek, 1995):

$$e_{sat,c} = 0.611 * e^{\frac{(17.27 * T_{a,c})}{(T_{a,c} + 73) - 36}} \quad (2)$$

$$e_{ref} = \frac{RH}{100} * e_{sat,c} \quad (3)$$

where: $T_{a,c}$ = air temperature in the leaf chamber ($^{\circ}C$) and RH = relative humidity of the air in the leaf chamber.

Collection, storage and processing of measurements

Solar radiation measurements were collected on four (4) data loggers (ZEN0*3200, Coastal Environmental Systems, Inc., Seattle, Wash.) Measurements were taken every 30 s and averaged 10 min.

With regard to photosynthesis, transpiration and stomatal conductance measurements, the closed type LCpro+ photosynthesis measurement system had its own recording and storage system.

Descriptive and inferential statistics were performed with SPSS 25.0. One way ANOVA was used for comparisons, along with Fisher's Least Significant Difference (LSD) test for post-hoc analysis. Level of statistical significance was set at $p=0.05$.

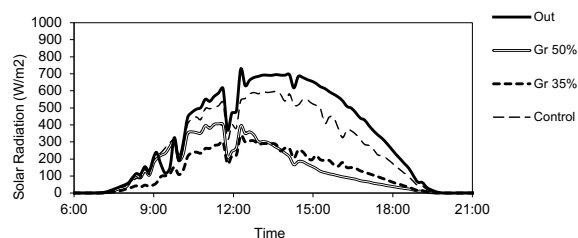


Fig 1. Daily sunlight outside the greenhouses, in the control greenhouse ($Gr_{0\%}$), in the 35% shaded greenhouse ($Gr_{35\%}$) and in the 50% shaded greenhouse ($Gr_{50\%}$), on 19 September.

RESULTS

Solar radiation measurements

Fig. 1 shows the daily course on 19th September of the incident and incoming solar radiation in the three greenhouses. The mean values of solar radiation are 275 W.m^{-2} , 231 W.m^{-2} , 129 W.m^{-2} and 111 W.m^{-2} for the external environment, the control greenhouse, the 35% greenhouse and the 50% greenhouse respectively. Similar results were found throughout the experiment.

Photosynthesis parameters measurements

As already described, photosynthesis rate (A), transpiration rate (E) and stomatal conductance (g_c) measurements concerned leaf measurements of plants exposed to different shading conditions.

Measurements in natural solar radiation conditions

Processing of measurements made during September- November in natural conditions, gave the following results.

Tab. 1. Results of Analysis of Variance (ANOVA) for Photosynthesis Rate A measurements in $Gr_{0\%}$, $Gr_{35\%}$ and $Gr_{50\%}$ during September-November.

Greenhouse	Mean $\mu\text{mol.m}^{-2}.\text{s}^{-1}$	SD $\mu\text{mol.m}^{-2}.\text{s}^{-1}$	F	p
Control	14.50	3.76	12.54	0.000
Shading 35%	11.74	4.06		
Shading 50%	9.51	2.87		

SD= Standard Deviation.

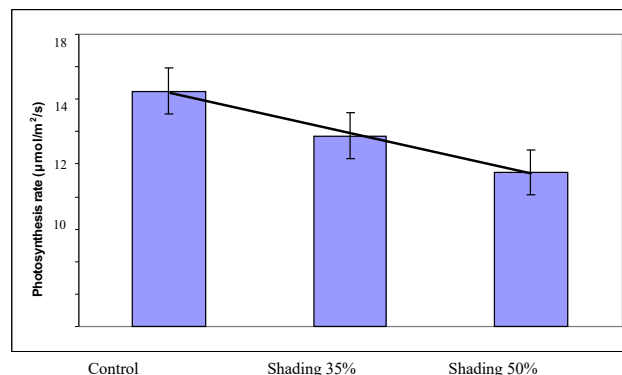


Fig 2. Mean values of Leaf Photosynthesis Rate in greenhouses $Gr_{0\%}$, $Gr_{35\%}$ and $Gr_{50\%}$.

Effect of shading on photosynthesis rate

One- way ANOVA results for the photosynthesis rate A in greenhouses appear in Table 1. From this Table is concluded that photosynthesis rate A differ statistically between the 3 greenhouses.

Fig. 2 shows, also, the descriptive statistics of photosynthesis rate A for the three greenhouses. It can be seen from this Figure that photosynthesis rate decreases as shading intensity increases.

Furthermore, Post Hoc analysis with LSD test for the dependent variable A, showed that the three greenhouses differ statistically from each other, for a significance level of 0.05, with the control greenhouse having the highest photosynthesis rate and the greenhouse with the highest 50% shading having the least photosynthesis (Table 2).

Effect of shading on leaf transpiration rate

Table 3 shows the results of ANOVA analysis of the leaf transpiration rate E in greenhouses.

Tab. 2. Results of multiple comparisons for the depended variable Photosynthesis Rate A in $Gr_{0\%}$, $Gr_{35\%}$ and $Gr_{50\%}$ according to Least Significant Difference (LSD) test for significant level 0.05 for measurements during September- November period

	Greenhouse (I)	Greenhouse (II)	Mean Difference (I-II)	p
LSD	Control	Shading 35%	2.75	0.007
		Shading 50%	4.98	0.000
	Shading 35%	Control	-2.75	0.007
		Shading 50%	2.23	0.028
	Shading 50%	Control	-4.98	0.000
		Shading 35%	-2.23	0.028

Tab. 3. Results of Analysis of Variance (ANOVA) for Transpiration Rate E measurements in Gr_{0%}, Gr_{35%} and Gr_{50%} during September-November.

Greenhouse	Mean mmol.m ⁻² .s ⁻¹	SD mmol.m ⁻² .s ⁻¹	F	p
Control	6.29	1.74		
Shading 35%	4.64	1.55	8.29	0.001
Shading 50%	5.12	1.05		

SD= Standard Deviation.

Tab. 4. Results of multiple comparisons for the depended variable Transpiration Rate E in Gr_{0%}, Gr_{35%} and Gr_{50%} according to Least Significant Difference (LSD) test for significant level 0.05 for measurements during September- November period.

	Greenhouse (I)	Greenhouse (II)	Mean Difference (I-II)	p
LSD	Control	Shading 35%	1.65	0.000
		Shading 50%	1.17	0.006
	Shading 35%	Control	-1.65	0.000
		Shading 50%	-0.48	0.253
	Shading 50%	Control	-1.17	0.006
		Shading 35%	0.48	0.253

It can be seen that there are statistically significant differences between the E averages. Post Hoc analysis with LSD test (Table 4) found that the unshaded greenhouse had a statistically greater transpiration rate than shaded greenhouses.

For no statistical differences in transpiration E between 35% and 50% shading greenhouses it should be considered whether there were differences in the air saturation deficit in the leaf chamber between 35% and 50% greenhouses.

Calculating from the experimental measurements data, vapor pressure deficit (VPDc) in the leaf chamber according to the previous equations (1), (2) and (3), we performed an ANOVA analysis for the dependent variable VPDc to determine if there were differences in the three greenhouses. The results are presented in the following Tables 5 and 6.

Vapor pressure deficit appears to be lower in the greenhouse with 35% shading than the 50% shaded greenhouse and the control. Given that cucumber leaves were in good condition, out of stress, the greater vapor

Tab. 5. Results of Analysis of Variance (ANOVA) for Vapor Pressure Deficit, VPDc in the leaf chamber at the three greenhouses Gr_{0%}, Gr_{35%} and Gr_{50%} during September-November.

Greenhouse	Mean mol.m ⁻² .s ⁻¹	SD mol.m ⁻² .s ⁻¹	F	p
Control	3.32	0.46		
Shading 35%	2.73	0.85	6.39	0.003
Shading 50%	3.19	0.48		

SD= Standard Deviation.

Tab. 6. Results of multiple comparisons for the depended variable Vapor Pressure Deficit, VPDc in the leaf chamber at Gr_{0%}, Gr_{35%} and Gr_{50%} according to Least Significant Difference (LSD) test for significant level 0.05 for measurements during September- November period.

	Greenhouse (I)	Greenhouse (II)	Mean Difference (I-II)	p
LSD	Control	Shading 35%	0.59	0.001
		Shading 50%	0.13	0.462
	Shading 35%	Control	-0.59	0.001
		Shading 50%	-0.46	0.006
	Shading 50%	Control	-0.13	0.462
		Shading 35%	0.46	0.006

pressure deficit in the leaf chamber under the 50% shaded greenhouse chamber probably explains the higher transpiration values in this greenhouse in relation to the corresponding transpiration values in the 35% shaded greenhouse, despite the greater intensity of the incoming radiation load in this greenhouse.

Effect of shading on leaf stomatal conductance

Concerning the values of stomatal conductance g_c for the three greenhouses, it was found that the mean g_c values of the hydroponic cucumber leaves were almost similar for the three greenhouses and there are no statistically significant differences between the greenhouses (Table 7).

Measurements in artificial lighting conditions. Effect of shading on photosynthesis rate

The purpose of these measurements was to investigate how plants in the three greenhouses exposed to

Tab. 7. Results of Analysis of Variance (ANOVA) for leaf Stomatal Conductance g_c measurements in $Gr_{0\%}$, $Gr_{35\%}$ and $Gr_{50\%}$ during September-November.

Greenhouse	Mean $\text{mol.m}^{-2}.\text{s}^{-1}$	SD $\text{mol.m}^{-2}.\text{s}^{-1}$	F	p
Control	0.97	0.46	0.51	0.950
Shading 35%	1.04	0.82		
Shading 50%	0.98	1.02		

SD= Standard Deviation.

Tab. 8. Results of Analysis of Variance (ANOVA) for photosynthesis rate A measurements under constant illumination conditions in $Gr_{0\%}$, $Gr_{35\%}$ and $Gr_{50\%}$ during September-November.

Greenhouse	Mean $\mu\text{mol.m}^{-2}.\text{s}^{-1}$	SD $\mu\text{mol.m}^{-2}.\text{s}^{-1}$	F	p
Control	11.58	4.29	1.43	0.245
Shading 35%	12.09	2.81		
Shading 50%	10.58	2.79		

SD= Standard Deviation.

different shading conditions responded to the same incident light intensity of $1000 \mu\text{mol.m}^{-2}.\text{s}^{-1}$. That is, whether they were adapted or not to shading conditions.

The following Table 8 shows the ANOVA results for photosynthesis rate A with constant illumination in the three greenhouses.

From this Table it appears that no statistical differences exist for photosynthesis rate between the three greenhouses. So, under constant illumination conditions of $1000 \mu\text{mol m}^{-2} \text{s}^{-1}$ the photosynthesis of cucumber leaves grown on a perlite substrate is not affected by shading for a significance level of 0.05.

DISCUSSION

Photosynthesis rate

The value of the photosynthesis rate in the control greenhouse (Table 1) is almost the same as this found by Mavrogiannopoulos et al. (1999) for melon cultivation in a greenhouse in Heraklion, Crete, Greece and by

Lykoskoufis et al. (2005) on hydroponic greenhouse pepper cultivation in Athens area. The results of the experiments on the effect of shading on photosynthesis rate showed that shading affects almost linearly the photosynthesis of cucumber leaves (Figure 1). Thus from $A = 14.5 \mu\text{mol m}^{-2}.\text{s}^{-1}$ in the control greenhouse it fell to $A = 11.7 \mu\text{mol.m}^{-2}.\text{s}^{-1}$ in the 35% shading greenhouse and to $A = 9.5 \mu\text{mol.m}^{-2}.\text{s}^{-1}$ in the 50% shading greenhouse. It, therefore, appears that 35% shading reduces the rate of photosynthesis by 20% and 50% shading reduces it by 34%. Thus the ratio of photosynthesis-shading is almost linear, which allows us to conclude that a 10% increase in shading induces a decrease in the rate of photosynthesis by $0.80 \mu\text{mol.m}^{-2}.\text{s}^{-1}$. Similar results were also found by Schwartz et al. (2002) when they made photosynthesis measurements in a hydroponic tomato culture in a growth chamber at the University of Georgia, USA, and found that a reduction in radiation level of 35% resulted in a decrease in leaf photosynthesis by $0.84 \mu\text{mol.m}^{-2}.\text{s}^{-1}$.

Furthermore, although photosynthesis rate measurements showed a clear difference between the three greenhouses, at the same time leaf stomatal conductance was statistically the same in all three greenhouses. The reduction in the rate of A under shading is reasonable, since the radiation regime inside the non-shaded greenhouse during September and October was relatively high but below the saturation point for cucumber crop, which ranges between $800\text{-}1000 \mu\text{mol.s}^{-1}.\text{m}^{-2}$ (Turcotte and Gosselin, 1989; Drew et al., 1990). The restriction of net photosynthesis in the shaded greenhouses was not due to limitations in the diffusion of CO_2 to the mesophyll through the stomata aperture, as indicated by the lack of any effect of shading on g_c . Hence, it is reasonable to conclude that in the shaded greenhouses net photosynthesis was inhibited at the chloroplast level due to limitations in light energy perception by the photosystem I. A similar response on net photosynthesis owing to sub-optimal light availability was also reported by Robbins and Pharr (1987) and by Hao and Papadopoulos (1999).

Transpiration rate and stomatal conductance

The leaf transpiration values presented in Table 3 are greater than the values found by Lykoskoufis et al., 2005, for pepper cultivation. These values, however, are very close to the values found by Medrano et al., 2005, who found transpiration values per m^2 of leaf in a greenhouse with autumn cucumber cultivation in perlite, from 10:00 to 14:00 of the order of $250\text{-}300 \text{g.m}^{-2}.\text{h}^{-1}$, corresponding to a transpiration rate of $4.6 - 5.6 \text{mmol.m}^{-2}.\text{s}^{-1}$, which are similar to our values from Table 3. The same researchers found that transpiration rate

values were linearly affected by the levels of incoming solar radiation, thus confirming the effect of shading on the transpiration rate found in our experiment. Also, close to the values of Table 4 are the results of Nederhof et al., 1992, who found for sweet pepper cultivation mean leaf transpiration rate values around 200 W.m^{-2} , that is, about $4.5 \text{ mmol.m}^{-2}.\text{s}^{-1}$ (Hanan, 1998).

For stomatal conductance g_c the values found in the greenhouses of our experiment are similar to those found by Mavrogiannopoulos et al, (1999) in hydroponic melon culture and higher than those found by Lykoskoufis et al. (2005) in pepper cultivation.

The values in Table 7 show leaf stomatal conductance values for our experiment conditions of the order of $1 \text{ mol.m}^{-2}.\text{s}^{-1}$, corresponding to stomatal conductance of about 22.3 mm.s^{-1} (Rosenberg et al., 1983). This value is close to the values of Katsoulas et al. (2001), who found values for the stomatal conductance of the order of 20 mm.s^{-1} for rose cultivation in a shaded roof greenhouse in Volos-Greece region. Similar values were given by Nederhof et al. (1992) who gave values for stomatal conductance of $15\text{-}20 \text{ mm.s}^{-1}$ for hydroponic sweet pepper cultivation in a greenhouse in the Netherlands.

It is well known that stomatal conductance values above 20 mm.s^{-1} , such as g_c values for cucumber leaves in our three experimental greenhouses in autumn, correspond to normal state of free transpiring plants that are outside stress and their stomata are open (Hanan, 1998). Since, in such conditions their transpiration rate is a function of the incident solar radiation on the leaves and the air vapor pressure deficit in the leaf chamber (Katsoulas, 2002), greater transpiration in the control greenhouse is justified by the higher solar radiation intensity.

Photosynthesis acclimation

Finally, the lack of any difference in photosynthesis rates A between plants from the three shading treatments when the measurements were conducted at light saturation with a constant illumination conditions of $1000 \mu\text{mol.m}^{-2}.\text{s}^{-1}$, despite the long term exposure to different light conditions shows that shading up to 50% does not affect permanently the leaf photosynthetic apparatus (Table 8). These results indicate that greenhouse cucumber does not adapt to reductions in light up to 50%. Hence, automated application of intermittent shading depending on current solar radiation intensity does not seem to affect the photosynthetic potential of greenhouse cucumber due to acclimation. This is in accordance with the results of Smith et al. (1993) for tomato crop who found that leaf photosynthetic capacity along a fruit-

bearing shoot is mainly driven by the sink demand of the most proximal fruit, and not by light acclimation.

CONCLUSIONS

The analysis of photosynthesis measurements made during autumn hydroponic cucumber cultivation showed that photosynthesis rate is reduced proportionally by shading while, shading does not seem to have a permanent effect on leaves and this illustrates the usefulness of the periodic shading by placing shading for periods of high solar radiation (summer) and removing shading when the intensity of solar radiation decreases (mid-autumn-winter) without photosynthetic cost.

REFERENCES

- Allen R.G., Walter I.A., Elliott R.L., Howell T.A., Itenfisu D., Jensen M.E., Snyder R.L., 2005. The ASCE Standardized Reference Evapotranspiration Equation. American Society of Civil Engineers, 216 pp.
- Baille, A., Kittas, C. and Katsoulas, N. 2001. Influence of whitening on greenhouse microclimate and crop energy partitioning. *Agr. For. Meteorol.* 107:193-306.
- Barradas, V.L., Nicolás, E., Torrecillas, A. and Alarcón, J.J., 2005. Transpiration and canopy conductance of young apricot (*Prunus armeniaca* L.) trees subjected to different PAR levels and water stress. *Agr. Wat. Man.* 77:323-333.
- Castellano, S., Scarascia, G. M., Russo, G., Briassoulis, D., Mistriotis, A., Hemming, S., Waaijenberg, D., 2008. Plastic nets in agriculture: A general review of types and applications. *Applied Engineering in Agriculture*, 24(6): 799-808.
- Cohen, S., Raveh, E., Li, Y., Grava, A. and Goldschmidh, E.E. 2005. Physiological response of leaves, tree growth and fruit yield of grapefruit trees under reflective shading screens. *Sci. Hort.* 107:15-35.
- Drew, M.C., Hole, P.S. and Piccioni, G.A. 1990. Inhibition by NaCl of net CO₂ fixation and yield of cucumber. *J. Am. Soc. Hort. Sci.* 115:472-477.
- El-Gizawy, A. M., Abdallah, M. M. F., Gomaa, H. M., Mohamed, S. S., 1993. Effect of different shading levels on tomato plants 2: Yield and fruit quality. *Acta Horticulturae*, 323(1): 349-354.
- Fernandez-Rodriguez, E.J., Fernandez-Vadillos, J., Camacho-Ferre, F., Vazquez, J.J. and Kenig, A. 2000. Radiative field uniformity under shading screens under greenhouse versus whitewash in Spain. *Acta Hort.* 534:125-130.

- Hanan J.J. 1998. *Advanced Technology for Protected Horticulture*. Taylor & Francis Inc., 720 pp.
- Hao, X. and Papadopoulos, A. 1999. Effects of supplemental lighting and cover materials on growth, photosynthesis, biomass partitioning, early yield and quality of greenhouse cucumber. *Sci. Hort.* 80:1-18.
- Howell T. and Dusek D., 1995. Comparison of vapour-pressure-deficit calculations methods-southern high plains. *Journal of Irrigation and Drainage Engineering*, 121: 191-198.
- Katsoulas N., Baille A., Kittas C., 2001. Effect of misting on transpiration and conductances of a greenhouse rose canopy. *Agricultural and Forest Meteorology*, 106, 233-247.
- Katsoulas N., 2002. Effect of climate factors on rose transpiration under cover. PhD Dissertation, University of Thessaly, 216 pp.
- Kitta E., 2014. *Ecophysiological and Agronomic Response of Horticultural Crops Grown under Screens in a Mediterranean Climate*. PhD Dissertation, Polytechnical University of Cartagena, Spain, 84 pp.
- Klieber, A., W.C. Lin, P.A. Jolliffe, and Hall, J.W., 1993. Training systems affect canopy light exposure and shelf life of long English cucumber. *J. Amer. Soc. Hort. Sci.* 118:786-790.
- Lorenzo P, Garcia L.M, Sanchez-Guerro C.M, Medrano E, Caparros I., Giménez M., 2006. Influence of mobile shading on yield, crop transpiration and water use efficiency. *Acta Horticulturae* 719: 471-478.
- Lycoskoufis I.H., Savvas D., Mavrogiannopoulos F., 2005. Growth gas exchange and nutrient status in pepper (*Capsicum annum L.*) grown in recirculating nutrient solution as affected by salinity imposed to half of the root system. *Scientia Hort.* 106: 147-161.
- Mavrogiannopoulos G.N., Spanaikis J., Tsikalas P., 1999. Effect of carbon dioxide enrichment and salinity on photosynthesis and yield in melon. *Scientia Horticulturae*, 79: 51-63.
- Medrano E., Lorenzo P, Sánchez-Guerrero M.C., Montero J.I., 2005. Evaluation and modelling of greenhouse cucumber-crop transpiration under high and low radiation conditions. *Scientia Horticulturae*, 105: 163-175.
- Naraghi, M., Lotfi, M., 2010. Effect of different levels of shading on yield and fruit quality of cucumber (*Cucumis sativus*). *Acta Horticulturae*, 871(1): 385-388.
- Nederhoff E.M., Rijdsdijk, de Graaf R., 1992. Leaf conductance and rate of crop transpiration on greenhouse grown sweet pepper (*Capsicum annum L.*) as affected by carbon dioxide. *Scientia Horticulturae*, 52:283-301.
- Raveh, E., Cohen, S. Raz, T. Grava, A. Goldschmidt, E.E., 2003. Increased growth of young citrus trees under reduced radiation load in a semi-arid climate. *Journal of Experimental Botany* 54(381): 365-373.
- Robbins, N.S. and Pharr, D.M. 1987. Regulation of photosynthetic carbon metabolism in cucumber by light intensity and photosynthetic period. *Plant Phys.* 85:592-597.
- Romacho, I., Hita, O., Soriano, T., Morales, M. I., Escobar, I., Suarez-Rey, E. M., Hernandez, J., Castilla, N., 2006. The growth and yield of cherry tomatoes in net covered greenhouses. *Acta Horticulturae*, 719(2): 529-534.
- Rosenberg N.J., Blad B.L., Verma S.B., 1983. *Microclimate: The Biological Environment*. John Wiley & Sons, USA, 495 pp.
- Smith, I.E., Savage, M.J. and Mills, P. 1984. Shading effects on greenhouse tomatoes and cucumbers. *Acta Hort.* 148:229-237.
- Sonneveld, C., 2002. Composition of nutrient solution. In: *Hydroponic Production of Vegetables and Ornamentals* (Savvas, D. and Passam, H.C., Eds.). Embryo Publications, Athens, Greece, 179-210.
- Schwartz D., Kläring H.-P., van Iersel M.W., Ingram K.T., 2002. Growth and photosynthetic response of tomato to nutrient solution concentration at two light levels. *J. Amer. Soc. Hort. Sci.*, 127(6): 984-990.
- Teitel, M., Segal, I., 1995. Net thermal radiation under shading screens. *Journal of Agricultural Engineering Research*, 61(1): 19-26.
- Turcotte, G. and Gosselin, A. 1989. Influence of continuous and discontinuous supplemental lighting on the daily variation in gaseous exchange in greenhouse cucumber. *Sci. Hort.* 40:9-22.
- Willits, D. H. 2001. The effect of cloth characteristics on the cooling performance of external shade cloths for greenhouses. *Journal of Agricultural Engineering Research*, 79(3): 331-340.



Citation: P. Garofalo, D. Ventrella, M. Mastrorilli, A. D. Palumbo, P. Campi (2020) An empirical framework for modelling transpiration use efficiency and radiation use efficiency of biomass sorghum in Mediterranean environment. *Italian Journal of Agrometeorology* (1): 49-62. doi: 10.13128/ijam-855

Received: February 12, 2020

Accepted: April 25, 2020

Published: June 23, 2020

Copyright: © 2020 P. Garofalo, D. Ventrella, M. Mastrorilli, A. D. Palumbo, P. Campi. This is an open access, peer-reviewed article published by Firenze University Press (<http://www.fupress.com/ijam>) and distributed under the terms of the Creative Commons Attribution License, which permits unrestricted use, distribution, and reproduction in any medium, provided the original author and source are credited.

Data Availability Statement: All relevant data are within the paper and its Supporting Information files.

Competing Interests: The Author(s) declare(s) no conflict of interest.

An empirical framework for modelling transpiration use efficiency and radiation use efficiency of biomass sorghum in Mediterranean environment

PASQUALE GAROFALO*, DOMENICO VENTRELLA, MARCELLO MASTRORILLI, ANGELO DOMENICO PALUMBO, PASQUALE CAMPI

Council for Agricultural Research and Economics, Research Center for Agriculture and Environment (CREA-AA), Via Celso Ulpiani 5, 70125 Bari, Italy

*Corresponding author. E-mail: pasquale.garofalo@crea.gov.it

Abstract. In this experimental-modelling research, the potential biomass achievable by sorghum to be converted in bioethanol was assessed and then formalized into the radiation use efficiency (*RUE*) and transpiration use efficiency (*TUE*). Dry above-ground biomass (harvested at the flowering stage) ranged between 22.6 t ha⁻¹ and 28.34 t ha⁻¹ over two growing seasons with a total water consumption of 382 mm and 504 mm, respectively. Starting from sampling measurements, the empirical framework allowed to reproduce daily data of dry biomass, canopy development, intercepted photosynthetically active radiation and transpiration related efficiencies. *RUE* and *TUE* resulted 4.98 g MJ⁻¹ and 7.45 kg m⁻³, respectively. Their robustness (as stable parameters) was assessed through the validation process. Finally, the multiple linear regression approach, was applied to screen among limiting factors. It was pointed out that although sorghum was grown under irrigated regime, water demand resulted not fully fulfilled to achieve the full performance of the crop.

Keywords. Energy crop, crop modelling, bioethanol, biomass, water consumption.

INTRODUCTION

In the search for renewable energy sources, also promoted by the recent European directives (Renewable Energy Directive, RED I and RED II) sorghum (*Sorghum bicolor* L. (Moench)) is seen as one of the main crops to produce bio (ethanol) energy.

Sorghum is highly efficient in using the available soil water, nitrogen and growing inputs. Indeed, in Mediterranean environment the crop showed higher efficiency respect to the agro-energy inputs, improving the energy performance and energy use efficiency of the bioethanol supply chain (Garofalo et al., 2015).

To assess the suitability of a crop for energy purpose, the potential biomass needs to be estimated, considering the consequences of the pedo-climatic context coupled to the soil-crop management on yield. This allows to screen and to rank the crops deputed to feed the energy supply chain and their requirements in water, solar radiation, nutrients.

Indeed, the growth and development of a crop is driven by several environmental components such as water availability, intercepted solar radiation and temperature. These factors affect all the hierarchically structured processes involved in the leaf gas exchange (CO_2 and H_2O), the storage of photosynthates, the accumulation of biomass and finally the yield (Garofalo and Rinaldi, 2015).

The strong relationship among crop water transpiration, solar radiation interception and biomass accumulation is made explicit by two empirical parameters: transpiration use efficiency (*TUE*) and radiation use efficiency (*RUE*). The photosynthetically active radiation (*PAR*; 400-700 nm waveband) is intercepted at canopy level to provide the radiant energy at chloroplast level to drive both CO_2 assimilation and H_2O transpiration processes.

The correlations between aboveground dry plant matter (*ADM*) and water used by the crop, as well as the radiation intercepted by the canopy, tend to remain linear in both well-watered and water deficit conditions (Hsiao, 1993; Hsiao and Bradford, 1983; Monteith, 1977; Tanner and Sinclair, 1983). The robustness of *RUE* and *TUE* resulted in their implementation (individually or both) in most of the crop simulation models as conservative parameters. A group of these models uses a crop growth module relying on *RUE* (*i.a.*, CERES, Ritchie et al. 1985; Jones and Kiniry 1986; Jones et al. 2003; EPIC, Jones et al. 1991; and STICS, Brisson et al. 2003).

TUE represents the driving parameter for another group of crop simulation models. It is the case of PARCH (Hess et al., 1997) and AquaCrop (Steduto et al., 2009). While CropSyst (Stöckle et al., 2003) estimates

the crop biomass accumulation on the basis of both *TUE* and *RUE* parameters.

The estimation of *RUE* and *TUE* should be carried out under optimal-growing conditions, since their values are estimated based on the potential biomass accumulation and canopy development under a specific environment. Heat and/or water stresses that can occur during the growing period, negatively impact on the canopy development resulting in a reduction of the intercepted radiation, water transpired and anticipated senescence and as a result, on biomass.

Under Mediterranean environment, soil water shortage and high air temperature do occur during the spring-summer period, determining a high variability of estimated *RUE* and *TUE*.

Indeed, different values were reported for estimated *RUE* in Mediterranean environment, ranging from 3.4 g of *ADM* per MJ^{-1} of intercepted *PAR* (*iPar*; Mastrorilli et al., 1995) to 4.7 g MJ^{-1} (Perniola et al., 1996) or between 1.89 g MJ^{-1} and 3.81 g MJ^{-1} (Garofalo and Rinaldi, 2011).

On the other hand, further investigations on the water use efficiency in sorghum (*WUE*) reported values that ranged from 4.4 to 5.5 kg of *ADM* per m^{-3} of water used by the crop (Steduto and Albrizio, 2005) or from a minimum of 4.0 kg m^{-3} to a maximum 8.49 kg m^{-3} (Garofalo and Rinaldi, 2013).

In addition, uncertainty in *RUE* and *TUE* may arise according to the methods applied for their estimation.

Although *RUE* and *TUE* are commonly recognized as the slopes of the linear predictor function between the explanatory variable (*iPAR* or *Tr*) and the response variable (*ADM*), the extent of approximation is strictly dependent on the number of observations of such variables. The more data available, the better the estimate is.

In this context *ADM*, canopy cover (*CC*), *iPAR* and *Tr* collected on daily basis, would represent the optimal dataset, but technical, human or environmental constraints could not allow for daily sampling. In the light of that, most of the researches to estimate *RUE* and/or *TUE* relied on time-spaced samples or even on the data collected at harvest (Rinaldi and Garofalo, 2011; Kemanian et al., 2004; Kiniry et al., 2005, Garofalo and Rinaldi, 2015; Yimam et al., 2015; Liu and Stützel, 2004).

Dataset coming from samplings spaced in time may not adequately draw the dynamics of growth, leading to an incorrect estimate of *RUE* and *TUE*.

However, empirical models can render a gradual transition from one phase of the growth to the next, at daily scale, by smoothing within a certain extent of approximation any sampling flaws (Yin et al., 2003).

Thus, in this paper is reported an empirical approach to develop a framework to artificially repro-

duce daily data on growth and development of sorghum. The experimental dataset collected over two growing years was functional to both calibration and validation process of the algorithms provided for the empirical approach. The artificial data at daily scale shaped by the system, allowed us to estimate *RUE* and *TUE* of sorghum. Finally, the multiple linear regression statistics allowed to assess if solar radiation or soil water availability were the main constraint for achieving the potential crop performance.

MATERIALS AND METHODS.

Experimental site

The field experiment was carried out over 2-year period from 2013 to 2014 in Rutigliano (lat: 40° 59' N, long: 17° 01' E, alt: 147 m a.s.l.), Southern Italy, in the experimental farm belonging to the Council for Agricultural Research and Economics (CREA).

Soil texture was classified as clay-loam (USDA, 2010) with physical-chemical characteristics of soil were reported in Table 1. At 0.6 m in depth, the parent rock reduces the capacity of the root systems to expand beyond this layer and the capillary rise from deeper soil layers. As a consequence, the impact of the groundwater to the rooting zone is totally negligible.

The experimental site is under the Mediterranean climate (UNESCO-FAO classification, 1963), characterized by warm and dry summers, with daily minimum air temperature ranging from 0-5°C and daily maximum temperature from 32 to 43°C. Annual rainfall (average 535 mm) is mostly concentrated during the winter months and class 'A pan' evaporation exceeds 7.5 mm day⁻¹ during the summer months. Daily meteorological data - temperatures, humidity, rainfall, wind velocity and solar radiation - were recorded by the local meteorological station.

Finally, initial soil water content at sowing time was of 0.324 m³ m⁻³ and 0.312 m³ m⁻³ (0-0.6 m depth) in the first year and second year, respectively.

Field experiment

Biomass sorghum (cv. Bulldozer) was sown at the beginning of June in 2013 and in late May in 2014, in rows 0.45 m apart and 0.1 m between seeds in each row (7 kg of seeds per hectare). Sorghum was harvested before heading (when the crop achieved the maximum dry matter yield) or the second half of September in both years. The experimental trial was arranged a sin-

Tab. 1. Main physical-chemical characteristics of soil of the experimental site.

Parameter	Unit	Average	Standard deviation (±)
Sand	g 100g ⁻¹	21	0.6
Silt	g 100g ⁻¹	37	2.9
Clay	g 100g ⁻¹	42	3.6
Soil electrical conductivity 1:1	dS m ⁻¹	0.6	0.05
Field Capacity	m ³ m ⁻³	0.36	0.03
Wilting Point	m ³ m ⁻³	0.22	0.02
Soil Organic Content	g kg ⁻¹	14	1.1
Total Nitrogen	g kg ⁻¹	1.5	0.2
Available Phosphorus	mg kg ⁻¹	71	3.1
Exchangeable Potassium	mg kg ⁻¹	540	61

gle plot of 80 m² size, 14 rows per plot. Water distribution was supplied by drip irrigation system: one line for each plant row; 4 L h⁻¹ per dripper; 0.3 m dripper spacing. Irrigation volumes were measured by flow meters (one per plot). Before sowing, 120 kg ha⁻¹ of N and 90 kg ha⁻¹ of P₂O₅ were supplied as diammonium phosphate. Mouldboard plow, disk harrow and rotary tiller were used to prepare the soil for the sowing, similarly to local farmer practices. Weeds were controlled by herbicides before sowing and by hand-hoeing during the first part of growing cycle. The health of the plants was ensured by chemicals when required.

During the experimental seasons, weather data were measured by means of a meteorological station located in the experimental farm. Maximum and minimum temperatures, global solar radiation (*R_g*), precipitation, wind speed and relative maximum and minimum air humidity were collected on a daily basis.

Growth analysis

Plants from 1- linear meter were sampled eight times during both sorghum seasons and each sample was replicated three times. The above ground biomass was obtained by adding stems and leaves. The plant material was dried at 80 °C until the weight was constant. At harvest, biomass samples covered a surface area of 2 m x 2 m and dry weight of stem and leaf determined accordingly.

To investigate the dynamic of the dry matter accumulated during the growing period, the sigmoid model

(Vannella, 1998) was calibrated on the observed data of the most favourable (in terms of accumulated biomass and canopy development) growing season (2014):

$$ADM_i = \frac{ADM_{max}}{(1 + e^{(t_i - t_h)/b})} \quad (1)$$

where ADM_i is the above dry biomass ($t \text{ ha}^{-1}$) at day i , ADM_{max} the maximum achievable value of ADM , t_i the time expressed in days after sowing, t_h represents the time between sowing and time to reach 50% of the ADM_{max} and b the fitting parameter of the model.

The green leaf area index (GAI , $\text{m}^2 \text{ m}^{-2}$) was measured at each sampling date with a LI-COR 2000 portable area meter (LI-COR Biosciences, Lincoln, NE, USA). For each sampling, figures were derived by the average of six measurements carried out below the plant canopy, during the 12:00 to 02:00 p.m. daytime and for each of the three replications within the main plot.

Daily green leaf area index (GAI_i) was estimated by fitting the field data with a beta function (Yin et al., 2003):

$$GAI_i = GAI_{max} * \left(1 + \frac{t_e - t_i}{t_c - t_m}\right) * \left(\frac{t_i}{t_e}\right)^{\frac{t_i}{t_e - t_m}} \quad (2)$$

where GAI_{max} is the maximum GAI , t_m represents the time between sowing and time to achieve GAI_{max} , t_e the time at the end of canopy growth.

The values of the parameters involved in Eqs (1, 2) were achieved by iterative procedure implemented in Excel (Solver add-in program) using the Generalized Reduced Gradient (GRG) Nonlinear algorithm as solving method.

Daily canopy cover (CC_i ; 0-1) was estimated with the equation:

$$CC_i = 1 - e^{(-k * GAI_i * cf)} \quad (3)$$

where k is the light extinction coefficient (-0.75; Rinaldi and Garofalo, 2013) and cf is the clumping factor (Nilsson 1971; Lang 1986, 1987), as follow:

$$cf = 0.75 + (0.25) * (1 - e^{(-0.35 * GAI_i)}) \quad (4)$$

Intercepted radiation and radiation use efficiency

The fraction of PAR intercepted by the canopy at daily scale ($iPAR_i$; MJ m^{-2}) was estimated as:

$$iPAR_i = CC_i * Rg_i * 0.48 \quad (5)$$

where Rg_i (daily global radiation) was measured with a thermophile pyranometer (305–2800-nm wavelength range) and 0.48 the fraction of solar radiation photosynthetically active.

RUE (g MJ^{-1}) was calculated as the slope of the linear regression between the cumulated daily values of ADM and $iPAR$ by forcing the intercept (b) to zero:

$$RUE = \frac{ADM_{i\text{par}}}{\sum_{i=\text{sowing}}^{i=\text{harvest}} iPAR_i} \quad (6)$$

Irrigation, transpiration and transpiration use efficiency

The reference evapotranspiration (ET_0 , in mm), was calculated using the FAO-Penman-Monteith model (Allen et al., 1998).

Irrigations were scheduled according the crop evapotranspiration (ET_c , mm), restoring the water used by sorghum whenever the 30 mm threshold was reached (subtracting rainfall).

ET_c was calculated as follow:

$$ET_c = ET_0 * Kc \quad (7)$$

where Kc is the crop coefficient as reported by Rinaldi and Garofalo (2011) and ET_0 , the reference evapotranspiration

Daily transpiration at day i (Tr_i) was calculated as:

$$Tr_i = CC_i * (Kc * ET_0) \quad (8)$$

Finally, TUE (kg m^{-3}) was calculated as the slope of the linear regression between cumulative ADM and water consumed by transpiration (Eq. (9):

$$TUE = \frac{ADM_{itr}}{\sum_{i=\text{sowing}}^{i=\text{harvest}} Tr_i} \quad (9)$$

with b (intercept) forced to 0.

Temperature limitation on growth

To account for the effect of temperature on growth and canopy development, the " T_{lim} " factor was calculated which describes the effect of daily average temperature T_m on biomass accumulation, as reported by Montieth (1977). T_{lim} was assessed as follow:

$$T_{lim} = 0 \text{ when } \begin{cases} T_m < T_b; \\ T_m > T_x \end{cases}$$

$$T_{lim} = 1 \text{ when } T_m = T_{opt}$$

$$T_{lim} = \frac{T_m - T_b}{T_{opt} - T_b} \text{ when } T_b \leq T_m \leq T_{opt} \quad (10)$$

$$T_{lim} = \frac{T_{opt} - T_b}{T_m - T_b} \text{ when } T_{opt} \leq T_m \leq T_x$$

where T_b is the base temperature (8 °C), T_{opt} the optimal temperature for growth (25 °C) and T_x the maximum temperature threshold for growth (33 °C; Alagarswamy and Ritchie 1991; Hammer et al. 1993; Rinaldi and Garofalo, 2011; Djanaguiraman et al., 2014).

Thus, the fitting of the parameters reported in Eq (1) occurred in two steps. The first one, involved a preliminary estimate of ADM_{max} , t_m and b on observed data, after which ADM_i and GAI_i resulting from Eqs. (1-2) were recalculated multiplying their values by T_{lim} . Finally, a second fitting procedure of parameters was carried out based on daily ADM_i and GAI_i corrected for T_{lim} to refit their figures to the values observed at sampling date.

The plant development rate was expressed by the growing degree days, GDD (°C) which measures that measured the heat accumulation calculated as the difference between the daily mean temperature and T_b .

Validation of the framework

To check the robustness of the framework, Eqs. (1) and (2) were replicated on the 2013 growing season, keeping the values of their parameters, unchanged. The outcomes were adjusted by T_{lim} calculated based on the climatic pattern of 2013 and compared with the observed data.

Finally, for 2013 $iPAR_i$ was estimated with Eqs. (3-5) and Tr_i with Eqs. (8) and (9) to validate ADM radiation-dependent and ADM transpiration-dependent adjusted by T_{lim} by means of RUE and TUE values assessed in the calibration step, when the 2014 data-set was used.

Biomass- RUE dependent and biomass- TUE simulated with this approach, were compared with the 2013 observed data to validate the reliability of RUE and TUE computed with the calibration step.

RESULTS

Meteorological patterns

In 2013, during the first part of growing period, climate was characterized by peaks of maximum temperature (T_{max}) up to 33 °C, up to 19 °C for minimum temperature (T_{min}). Cooler temperatures characterized the period from late June until the third decade of July, where T_{max} remained below 28 °C and T_{min} below 18 °C (Fig. 1).

Except for some very hot days (daytime temperature up to 37 °C), the second part of the growing peri-

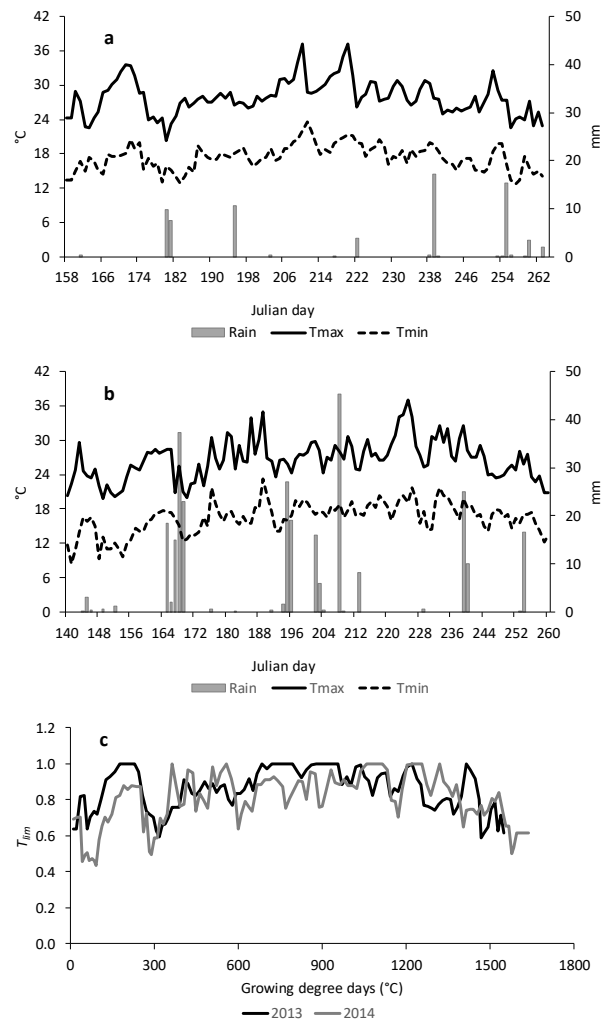


Fig. 1. Maximum temperature (T_{max} ; continuous line), minimum temperature (T_{min} ; dashed line), rain (grey columns) recorded in 2013 (a) and 2014 (b) growing season and T_{lim} (see text) behaviour.

od recorded temperature below 30 °C (T_{max}) and 19 °C (T_{min}) in August, to remain below 25 °C and 18 °C in September (hotter temperature in some days at the beginning of September, were observed).

Total rainfall in 2013 growing season was 72.4 mm, spaced over time, with two fairly rainy events, one at the end of August and the other in mid-September (Fig. 1).

The crop growing period of 2014 was warmer than in 2013, especially from 16th to 51st day after sowing (from June 4th to July 10th) with peaks of T_{max} that exceeded 31 °C for several days and some events of T_{min} above 20 °C.

Conversely, the middle part of the growing period was cooler in 2014 than in 2013, with T_{max} rarely above 30 °C as well as T_{min} which remained below 18 °C.

However, for the most of the second part of the growing season, temperature reached maximum peaks of 2-3 degrees above 30 °C, whereas T_{min} was cooler than the first period of the growing period; the last part of the growing cycle in 2014, was slightly hotter than 2013, with T_{max} that ranged from 23 to 27 °C and T_{min} below 15 °C.

Rainfall in 2014 cultivation time frame was much higher than 2013 (157 mm vs 72 mm) with 96 mm falling on four consecutive days in June and 76 mm recorded from from 21st July to 1st.

Two following events for a total of 35 mm of rainfall characterized the end of August, whereas a single event of 17 mm concluded the growing period in 2014.

Crop growth and development analysis

The daily growth and canopy development curves of the 2014 growing season, resulting from the calibration of Eq. (1) and Eq. (2), were well fitted to the observed values of ADM ($R^2 = 0.976$) and GAI ($R^2 = 0.97$; fig. 2). It should be pointed out that the values of parameters of both models were preliminary calibrated to fit the estimated ADM and GAI to the observed values and recalibrated on daily values of ADM and GAI corrected by T_{lim} . In this way, parameters of Eq. (1) and (2) were predicted net of the effect of temperature on growth.

Over the 2014 growing season (year used for the calibration of the empirical models), the average temperature rarely achieved optimal values and T_{lim} was close to 1.

This trend was particularly noticeable from the middle to the final part of the growing season, where T_{lim} showed values between 0.9 and 0.7 or even below 0.7, mainly due to mean temperatures which remained below the optimal value (25 °C) rather than above the maximum threshold (33°C).

From 300 GDD to 1000 GDD, was observed a first growing phase characterized by an exponential convex growth, followed by a second phase (between 1000 GDD and 1500 GDD) identified by a concave senescent growth. The inflection point (transaction between the first and second growing phase) at which the development rate reached its maximum value (t_h) was formalized 78 days after sowing. Finally, the potential dry biomass achievable at harvest (net of limitations due to temperatures not optimal for the crop) was estimated as 32 t ha⁻¹, whereas the actual ADM at harvest was 28.32 t ha⁻¹. Such figure is consistent with the yield values reported in the international literature: in Greece (from 17 t ha⁻¹ to 31 t ha⁻¹; Dercas and Liakatas, 2007), in Spain (18.38 t ha⁻¹, Farrè and Faci, 2006), in Italy (from 40.97 t ha⁻¹ to 23.22 t ha⁻¹, Rinaldi and Garofalo, 2011)

As regards the development of canopy (GAI), the beta function curve highlighted the highest expansion rate in the first period of growing season (from 300 GDD to 700 GDD) with tm achieved at 65 days after sowing. After that, followed a near-linear development of the canopy (from 700 GDD to 1050 GDD) to reach the maximum value of 6.8 m² m⁻² (5.2 m² m⁻² when accounting for T_{lim} during the growing cycle) at 92 days after sowing (te), time to end the plant growth.

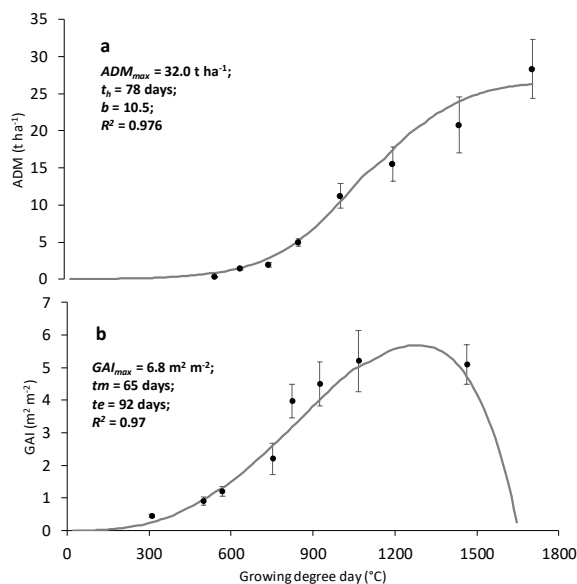


Fig. 2. Dynamic of total above dry matter (ADM a; line), green area index (GAI b; line) and experimental data (circle) observed during 2014 growing season. Vertical bars indicate \pm standard deviation. The values of parameters of the empirical models are shown (see text).

Canopy radiation interception and radiation use efficiency

Sorghum reached a high value of CC (0.9) quite rapidly, or 64 days after sowing.

Basically, this value was reached with GAI of $3.34 \text{ m}^2 \text{ m}^{-2}$ keeping a high efficiency in radiation interception for more than 50% of its growing cycle (Fig. 3a) with performance in line with Fletcher et al. (2013) but slightly lower than Rinaldi and Garofalo (2013).

At the end of growing season, cumulative $iPAR$ was of 568 MJ m^{-2} , with a linear increment of intercepted radiation from emergence to harvest (Fig. 3b), consistent with the value indicated by Narayanan et al. (2013) but less than that reported by Ceotto et al. (2013).

The strong correlation between dry biomass accumulated during the growing season and the radiation intercepted by the canopy is drawn by figure 3c. The slope of the linear regression between $iPAR$ and ADM was equal to 0.0481, confirming the sorghum high efficiency (4.81 g MJ^{-1}) in converting the intercepted solar energy in photosynthates.

Our results pointed out a higher RUE compared to recent studies (e.g. 3.48 g MJ^{-1} reported by Ceotto et al., 2013; 3.23 g MJ^{-1} found out by Garofalo et al., 2011) but consistent with previous investigations (4.7 g MJ^{-1} , Perniola et al., 1995).

Obviously, the forcing to reproduce a logistic growth pattern through a linear regression model produces bias. A polynomial fitting would have matched the growth curve more accurately but would not have led to the formalization of a single parameter (RUE) of quick understanding and easy application.

Plant transpiration and transpiration use efficiency

Total water supplied with irrigation in 2014 amounted to 225 mm, split in one application (15 mm) before sowing to restore the water field capacity and seven applications (30 mm each) over the 2014 growing season.

Rainfall plus water supply indicated a total water consumption (soil evaporation, drainage and crop, drainage and crop transpiration) equal to 475 mm (Fig. 4 a), in line with the finding (489 mm-517 mm) reported by Hao et al. (2014), or (446 mm-683 mm) indicated by Yimam et al. (2015) both calculated under well-watered regimes. It should be pointed out that to account for the effect of closed canopy on rainfall interception, a 22% reduction of water amount from precipitation in calculating WU (Kozak et al., 2007) was applied after CC reached 0.9.

The water daily transpired by the crop raised rapidly from 28 days after sowing to reach peaks of 7-10 mm between 80 and 100 days after sowing (Fig. 3a).

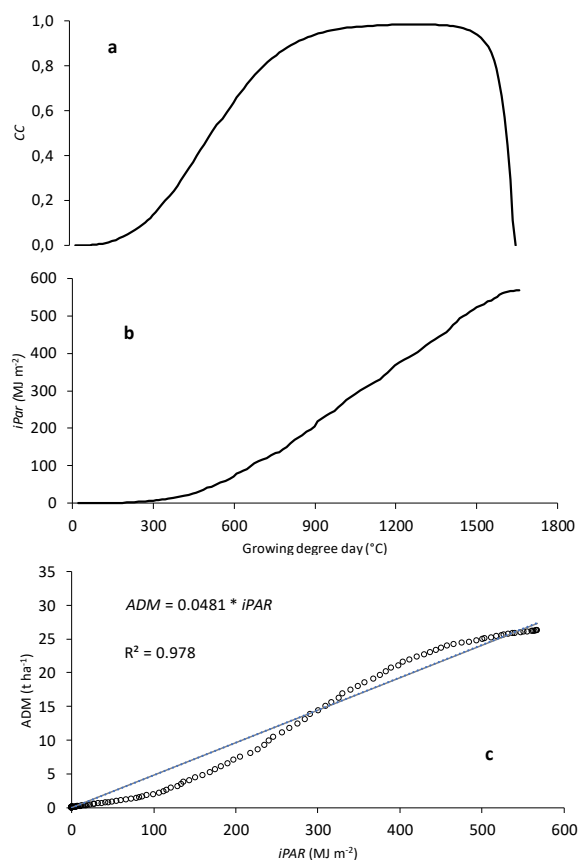


Fig. 3. Trend of the intercepted radiation ($iPAR$; a), canopy cover (CC ; b) during the 2014 growing season and linear regression between $iPAR$ and aboveground dry matter (ADM ; c).

The reported value of Tr_i was due to combined effect of the rapid expansion of canopy (in the early phenological stages) and the evaporative demand of the atmosphere (Fig 3a). On the other hand, the cumulative water transpired by the crop (see Eq. (8)) was 399 mm, with a trend synchronized with the canopy development (Fig. 3b). The discrepancy between Tr and the total water consumption represented the loss of water by evaporation and drainage, otherwise called not productive water, which was estimated to range between 61 mm and 280 mm in sorghum (Garofalo and Rinaldi, 2013).

Most of the abovementioned difference was accounted in the first part of the growing season, due to the evaporation from bare soil or partially covered by the canopy other than the crop transpiration. Once achieving GAI of $3.0 \text{ m}^2 \text{ m}^{-2}$ or a CC close to 0.9, WU was due to the plant transpiration, if the soil was completely shaded by canopy and so evaporation was negligible (Ritchie, 1972).

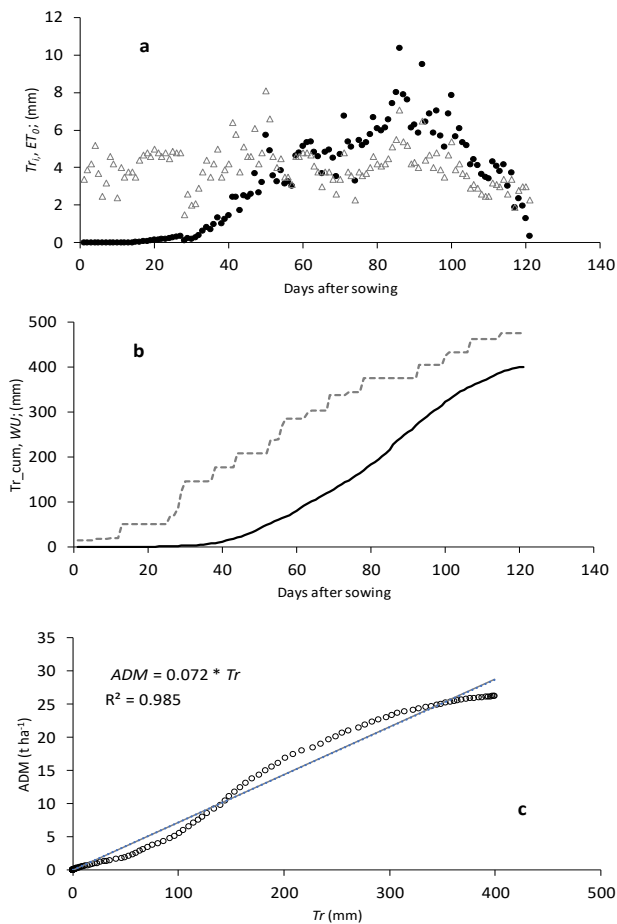


Fig. 4. Daily transpiration and reference evapotranspiration (Tr , ET_0 a), cumulative transpiration (Tr_{cum} , continuous line) vs total water consumption (WU, dashed line; b) and linear regression between Tr and aboveground dry matter (ADM; c), in 2014 growing season.

At the end of the growing period the gap between the total water consumption and water transpired by the canopy was 76 mm.

The slope between the transpiration (net of water loss by evaporation or drainage) and cumulative dry biomass on daily basis was of $0.072\ t\ mm^{-1}$ or $7.2\ kg\ m^{-3}$ (Fig. 3c) a value higher than those reported by other researches (Thapa et al., 2017; Reddy and Angira, 2015) but consistent with other investigations (Garofalo and Rinaldi, 2013).

Validation of the empirical framework

To check the robustness of this framework, from the formalization of biomass accumulation and canopy

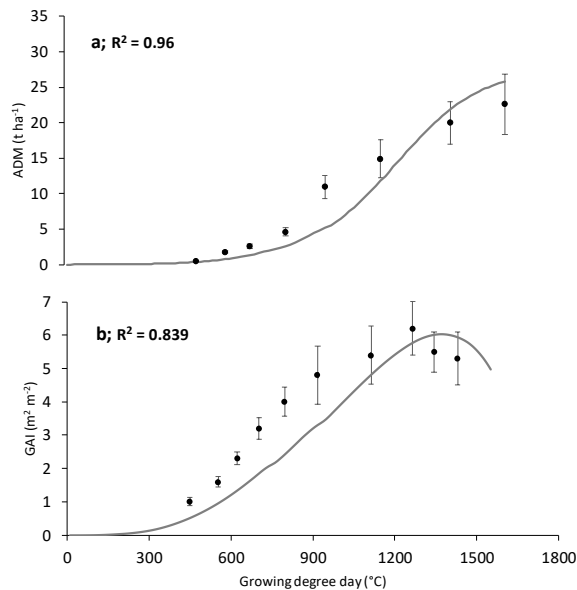


Fig. 5. Dynamic of total above dry matter (ADM a; line), green area index (GAI b; line) and experimental data (circle) observed during the growing season. Vertical bars indicate \pm standard deviation.

development to the accuracy of the estimated RUE and WUE , the empirical structure was verified on experimental data collected over the 2013 growing season.

Basically, the parameters of Eqs. (1-5) and Eqs. (7-8) remained unchanged excepting for Rg and ET_0 , as well as T_{lim} , that varied according to 2013 climate trend.

Validation process pointed out a satisfying matching between the experimental data of ADM and GAI with figures replicated by the empirical model ($R^2 = 0.96$ for ADM, Fig. 5a; $R^2 = 0.839$ for GAI; Fig 5b).

Water transpired by the crop in 2013 had a pattern close to that computed in 2014; indeed, the daily transpiration grew up rapidly from 30 to 80 days after sowing, passing from 1 mm to 6 mm and then settle between 6-8 mm at maximum canopy expansion and decline rapidly once reached the reproductive phase (Fig. 6a).

Cumulative Tr in 2013 was slightly lower than 2014 (- 29 mm), but WU was 22% lesser compared to the first growing season (Fig. 6b). A shorter distance between WU and Tr in 2013 was due to a lower amount of rainfall in this year compared to 2014 (reduced water loss by drainage) and lower evaporative demand of the environment (ET_0 ; Fig. 6a).

Once it was established that the framework was suitable to replicate the growth of the crop and development of the canopy, ADM of 2013 was estimated on the basis of computed Tr and $iPAR$ (2013) and TUE and RUE of 2014.

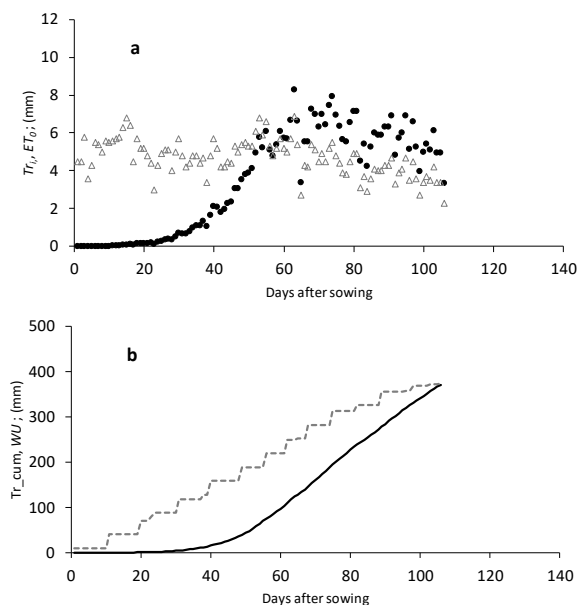


Fig. 6. Daily transpiration and reference evapotranspiration (Tr_i , ET_0 a), cumulative transpiration (Tr_{cum} , continuous line) vs total water consumption (WU, dashed line; b) in 2013 growing season.

This procedure (validation step) allowed us to assess the stability and effectiveness of these parameters (RUE and TUE) as well as the empirical approach here proposed, in estimating the potential productivity of sorghum.

Formalization of ADM dependent on RUE ($ADM-RUE$) as well as ADM dependant on TUE ($ADM-TUE$) and T_{lim} acting on potential ADM , was congruent with the experimental data collected in 2013 (Fig. 7).

Effect of available water and radiation on plant performance

A sensitivity analysis was aimed at assessing whether the biomass accumulation was mainly affected by the intercepted radiation or by transpiration or by both drivers interacting each other, or again, if both parameters had the same weight. Specifically, the standardized multiple linear regression (Myers, 1990) was applied, with cumulative ADM_i as dependent response variable and cumulative Tr_i and cumulative $iPar_i$ as predictors for both years, as single factors and in interaction. In this way, it was assessed whether the daily increase in biomass was more sensitive to the daily amount of water used by the crop or to the intercepted radiation or, in other words, which was the limiting factor (if any).

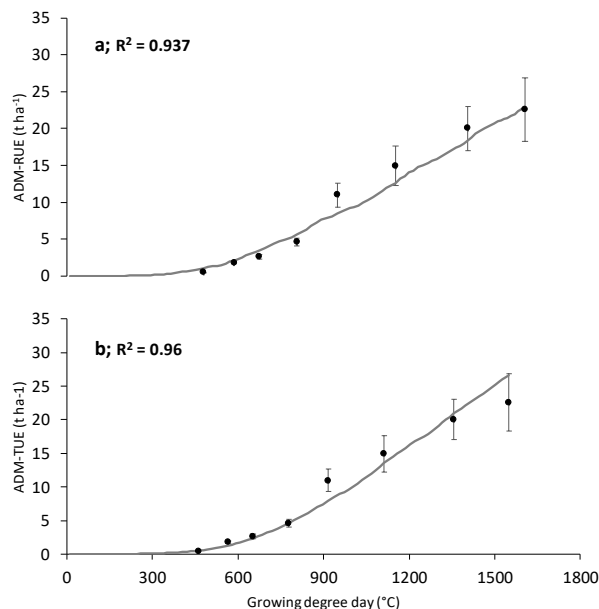


Fig. 7. Comparison between the trend of observed (full circle) aboveground dry matter (ADM) and ADM dependent on RUE ($ADM-RUE$; grey line, a) and ADM dependent on TUE ($ADM-TUE$, b) in 2013 growing season.

The standardized regression coefficients (β) pointed out that transpiration was the main driver in regulating the accumulation of biomass and that interaction between Tr and $iPar$ was not significant (Fig. 8).

DISCUSSION

Our experimental data confirmed the high capability of sorghum to produce high amount of biomass under well-watered irrigation regime, as reported in other investigations (Zegada-Lizarazu and Monti, 2012). However, the ability of this crop to thrive also under suboptimal conditions is well documented (Garofalo and Rinaldi, 2013) where other crops would struggle (Woods, 2001).

In addition, sorghum is known for being a low demanding N crop, even compared to other C4 crops. For example, it was highlighted that sorghum requires up to 40% less nitrogen fertilization than maize (Smith and Buxton, 1993), whereas Garofalo et al. (2015) pointed out the lack of statistical differences between the biomass productivity of sorghum under well-fertilized regime compared to halved N doses (150 kg N ha⁻¹ vs 75 kg N ha⁻¹) or even no N fertilization. The same authors also indicated comparable performance between sor-

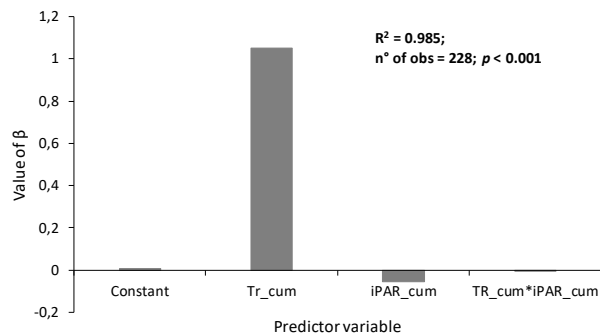


Fig. 8. Standardized regression coefficients (β) of cumulative transpiration (Tr_cum), cumulative intercepted solar radiation (iPAR_cum) and the combined effect on biomass accumulation. The higher the value, the higher their contribution.

ghum cultivated under conventional soil practices compared with no-tillage soil management.

High biomass productivity even with reduced agro-inputs result in a high energy efficiency and energy performance of a specific energy crop, which are the key points to make the sorghum suitable for energy purposes (Garofalo et al., 2018).

However, the assessment of the performance (e.g. biomass, yield or energy harvest) of a crop using only the “productivity” (biomass or yield) parameter, net of the environmental impacts that lead to its value, may determine assessment bias.

Radiation, available water and air temperature are the main weather-related variables affecting the biophysical processes related to the growth and development of a crop. If these processes are recognized as a hierarchical pyramid structure in which the complexity is reduced as we move from the base to the tip, *RUE* and *TUE* are located at top, including and integrating the mechanisms and climatic constrains for plant growth and development (Garofalo and Rinaldi, 2015).

Although, *RUE* and *TUE* are known to be crop-specific parameters (Hughes et al., 1987; Russell et al., 1989; Monteith, 1994), other studies pointed out as these variables can vary according to environmental factors and management (i.e. nitrogen and water supply, plant density, cultivars; Sinclair and Horie, 1989; Rosenthal and Gerik, 1991; Cosentino et al., 2016).

However, here we assume that *RUE* and *TUE* should be easy to read and quick to understand and maintain their robustness and effectiveness inside the modelling frameworks or modelling solutions as stable parameters.

This implies the calculation of *TUE* and *RUE* as fixed indices of the potential crop performance, on which “limiting factors” afterwards act.

In the Mediterranean environment the factors constraining the plant growth are the water scarcity and heat waves, especially in spring-summer cropping systems, not the solar radiation.

Thus, in this experimental-modelling research drought conditions were mitigated through irrigation; as for temperature, the T_{lim} correction allowed to separate its effect when *RUE* and *TUE* were estimated.

As previously stated, in other investigations, the data of biomass used for the estimation of *RUE* or water use efficiencies were collected from sampling during the growing season; out-of-scale values could lead to overestimation or underestimation of these parameters.

Thus, in this research the empirical framework was set up to replicate daily biomass accumulation of sorghum, starting from sampling data. Although flaws in sampling may occur, the proposed approach is adequate to dampen such biases, since it models the growth dynamics between two figures through a curvilinear instead of a linear transition.

The approach proposed in this research led to results that can also be considered valid in other pedo-climatic and management contexts comparable to those from which the data for this research were obtained. Significant variations in terms of canopy development and/or biomass accumulation, intercepted radiation and transpiration can occur with crop and soil management substantially different from our field trials (i.e. sub-optimum fertilization, sprinkler system instead of drip irrigation, no-tillage instead of conventional tillage, etc.)

In other researches, the efficiency to convert water in biomass was estimated without partitioning the water consumption in soil evaporation and crop transpiration or accounting for the rainwater intercepted by the closed canopy, whose amount is not gathered from soil and not available for the transpiration process (Moroke et al., 2011; Hao et al., 2014; Chimonyo et al., 2016). Water loss by evaporation as well as rainfall intercepted by closed canopy and not available for the water requirement of the crop are not involved in the bio-physical processes of the plant and their inclusion in water use efficiency may lead to underestimation of this parameter.

In this paper is indicated a procedure that reproduce the daily canopy development (Eqs. (2-4)) and the water daily transpired by the canopy itself (Eqs. (7-8)) taking into account the effect of closed canopy on rainfall interception. Thus, water transpired by the crop fitted linearly with daily biomass accumulation, led to the estimation of *TUE*.

The replicability of this empirical structure has proved feasible through the validation step and *RUE* and *TUE* calibrated in 2014 accurately formalized the bio-

mass accumulation observed in 2013 (validation year).

This let us to discuss on the most suitable index (*RUE* or *TUE*) to replicate the growth of the crop as a function of intercepted radiation or water transpired by the canopy.

If the available water or radiation are alternatively the limiting factors, the choice of the parameter to simulate the plant growth should be linked to the limiting factor itself; *RUE* if radiation is limiting for the optimal growth or *TUE* if the crop is under sub-optimal watered regime.

In the experimental trials carried out for this investigation, the water management was aimed at maintaining the crop under well-watered condition to avoid possible water stresses. On the other hand, in the Mediterranean environment, solar radiation did meet the energy demand for photosynthesis.

Results from the standardized multiple linear regression suggested that the accumulation of crop biomass over the two growing seasons, was mainly driven or affected by the water used by the sorghum rather than by the intercepted radiation as a single factor or in interaction with transpiration. Such result paves the way to three hypotheses: i) solar radiation was not a limiting factor; ii) during the two growing seasons, the sorghum crop experienced the soil water shortage; iii) all the biophysical processes are water-dependent. For the latter, some authors reported that *RUE* was strongly correlated to the water consumed by the crop (Derkas and Liacatas, 2007; Rinaldi and Garofalo, 2011). However, we assumed that *RUE* (as well as *TUE*) should be a stable parameter as a predictor of potential sorghum performance

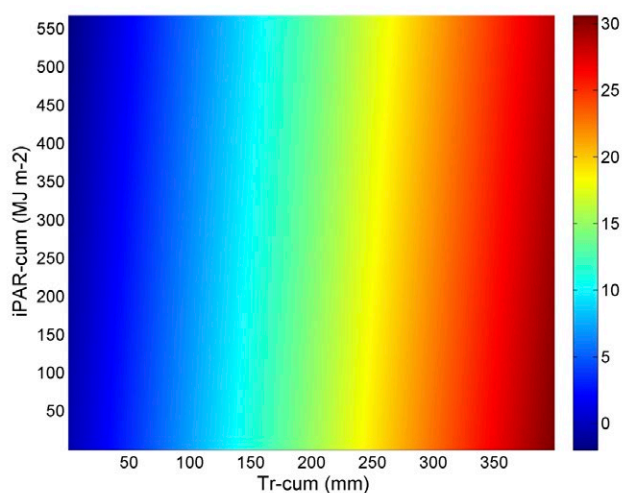


Fig. 9. Interaction response surface of the cumulative ADM (right bar) as it depends on cumulative intercepted solar radiation (iPAR-cum) and cumulative transpiration (Tr-cum).

and that limiting factors (such as the water availability) should act in reducing the potential biomass computed by *RUE* and/or *TUE*. This assumption is further evidenced by the surface response plot (Fig. 9) which pointed out that the accumulation of biomass occurred mainly in response to *Tr_cum* rather than *iPar_cum*.

CONCLUSIONS

Our experimental-modelling research proposes an empirical framework to formalize the daily growth and development of sorghum as well as *RUE* and *TUE* as a function of intercepted radiation and transpiration on daily basis. Under well-watered regime and in Mediterranean pedo-climatic conditions (as in our experimental trials), sorghum proved to be high performant in biomass yielding even with less water requirements respect to other energy crops (Triana et al., 2014), such as giant reed (1161 mm) or miscanthus (991 mm). This turned in the capability of sorghum to fully take advantage from solar radiation and water supply, providing high values of *RUE* and *TUE*, thus making this crop suitable for energy purposes (high energy yield in response to the agro-inputs management).

The estimate of *RUE* and *TUE* was the conclusive step in the whole empirical procedure, which starting from sampling carried out over the growing season, led to the projection of data at daily scale involved in the estimation of the efficiency of the plant to convert radiation and water into biomass.

This framework is easy to replicate also in other pedo-climatic contexts and for other crops, since few inputs are required for specification and parametrization (i.e. weather data and crop coefficient of the species under investigation).

The modelling approach used for this research was empirical and all the relationship among the analysed parameters (biomass and canopy development as a function of temperature, and intercepted radiation and transpiration) were quantified by means of regression models. Therefore, this approach excluded any process-based analysis underlying these relationships which could be deepened through mechanistic crop simulation models.

In addition, for the experimental trials the crop was grown under optimal level of nitrogen fertilizer as well as conventional soil tillage; by varying these two conditions the results and discussions reported so far could also undergo significant changes. Changes that could also be induced by climate change scenarios, where prolonged or repeated drought or heat waves conditions could undermine the crop growth-water or the crop

growth-radiation dependence, which in turn are *TUE* and *RUE*.

Although the water supply was aimed at satisfying the water demand of sorghum, the regression analysis highlighted that the water requirement was likely not fully met.

This leads to the final considerations: i) in our experimental trials, sorghum did not reach its full performance and that; ii) other irrigation scheduling and distribution methods in addition with investigations on different soil tillage schemes, different nitrogen doses, plant densities or sowing times should be assessed to attain also at the farm scale the findings collected so far.

ACKNOWLEDGMENTS

This work was supported by the Italian Ministry of Agriculture (MiPAAF) under the AGROENER project (D.D. n. 26329, 1 April 2016) - <http://agroener.crea.gov.it/>

REFERENCES

- Alagarswamy G., Ritchie J.T., 1991. Phasic development in CERES-sorghum model. In 'Predicting crop phenology'. Ed. T Hodges. pp. 143-152. CRC Press: Boca Raton, FL.
- Allen R.G., Pereira L.S., Raes D., Smith M., 1998. Crop evapotranspiration. Guidelines for computing crop water requirements. Irrig Drain Paper No. 56, FAO, Rome. 301 pp.
- Brisson N., Gary C., Justes E., Roche R., Mary B., Ripoche D., Zimmer D., Sierra J., Bertuzzi P., Burger P., Bussiere F., Cabidoche Y.M., Cellier P., Debaeke P., Gaudillere J.P., Henault, C., Maraux F., Seguin B., Sinoquet H., 2003. An overview of the crop model STICS. *Eur. J. Agron.* 18: 309-332. doi:10.1016/S1161-0301(02)00110-7.
- Ceotto E., Di Candilo M., Castelli F., Badeck F.W., Rizza E., Soave C., Volta A., Villani G., Marletto V., 2013. Comparing solar radiation interception and use efficiency for the energy crops giant reed (*Arundo donax* L.) and sweet sorghum (*Sorghum bicolor* L. Moench). *Field Crops Res.* 149: 159-166.
- Chimonyo V.G.P., Modi A.T., Mabhaudhi, T. 2016. Water use and productivity of a sorghum-cowpea-bottle gourd intercrop system. *Agri. Water Manag.* 165: 82-96.
- Cosentino S.L., Patanè C., Sanzone E., Testa G., Scordia D., 2016. Leaf gas exchange, water status and radiation use efficiency of giant reed (*Arundo donax* L.) in a changing soil nitrogen fertilization and soil water availability in a semi-arid Mediterranean area. *Eur. J. Agron.* 72: 56-69.
- Dercas N., Liakatas A., 2007. Water and radiation effect on sweet sorghum productivity. *Water Resour. Manag.* 21: 1585-1600.
- Djanaguiraman M., Prasad P.V.V., Murugan M., Perumal M., Reddy U.K., 2014. Physiological differences among sorghum (*Sorghum bicolor* L. Moench) genotypes under high temperature stress. *Environ. Exp. Bot.* 100: 43:54.
- European Commission, 2009a. Directive 2009/28/EC of the European Parliament and of the Council of 23 April 2009 on the promotion of the use of energy from renewable sources and amending and subsequently repealing Directives 2001/77/EC and 2003/30/EC. *Off. J. Eur. Union* (140/16 of 05.06.2009). <https://eur-lex.europa.eu/legal-content/EN/TXT/PDF/?uri=CELEX:32009L0028&from=EN>, (accessed June 2019).
- European Commission, 2016. Proposal for a DIRECTIVE OF THE EUROPEAN PARLIAMENT AND OF THE COUNCIL on the promotion of the use of energy from renewable sources, COM/2016/0767 final/2 - 2016/0382 (COD). <https://eur-lex.europa.eu/legal-content/EN/TXT/?uri=CELEX:52016PC0767R%2801%29>, (accessed, June 2019).
- Triana F., Nasso N., Ragolini G., Roncucci N., Bonari E., 2014. Evapotranspiration, crop coefficient and water use efficiency of giant reed (*Arundo donax* L.) and miscanthus (*Miscanthus × giganteus* Greef et Deu.) in a Mediterranean environment. *G.C.B. Bioenergy*, pp. 1-9.
- Farrè I., Faci J.M., 2006. Comparative response of maize (*Zea mays* L.) and sorghum (*Sorghum bicolor* L. Moench) to deficit irrigation in a Mediterranean environment. *Agric. Water Manag.* 83: 135-143.
- Fletcher A.L., Johnstone P.R., Chakwizira E., Brown H.E., 2013. Radiation capture and radiation use efficiency in response to N supply for crop species with contrasting canopies. *Field Crops Res.* 150: 126-134.
- FAO-UNESCO, 1963. Bioclimatic map of the Mediterranean Zone, explanatory notes. Paris, France.
- Garofalo P., Vonella A.V., Ruggieri S., Rinaldi M., 2011. Water and radiation use efficiencies of irrigated biomass sorghum in a Mediterranean environment. *Ital. J. Agron.* 6: 133-139.
- Garofalo P., Rinaldi M., 2013. Water-use efficiency of irrigated biomass sorghum in a Mediterranean environment. *Span. J. Agric. Res.* 11: 1153-1169.
- Garofalo P., Campi P., Vonella A.V., Mastroianni M., 2018. Application of multi-metric analysis for the evaluation of energy performance and energy use efficiency

- of sweet sorghum in the bioethanol supply-chain: A fuzzy-based expert system approach. *Appl. Energy*, 220: 313-324.
- Garofalo P., Rinaldi, M., 2015. Leaf gas exchange and radiation use efficiency of sunflower (*Helianthus annuus* L.) in response to different deficit irrigation strategies: From solar radiation to plant growth analysis. *Eur. J. Agron.* 64: 88-97.
- Garofalo P., D'Andrea L., Vonella A.V., Rinaldi M., Palumbo A.D, 2015. Energy performance and efficiency of two sugar crops for the biofuel supply chain. Perspectives for sustainable field management in southern Italy. *Energy* 93: 15-24.
- Hamdi, Q.A., Harris, D., Clarck, J.A., 1987. Saturation deficit, canopy formation and function in *Sorghum bicolor* (L.). *J. Exp. Bot.* 38: 1272-1283.
- Hammer G.L., Carberry P.S., Muchow R.C. 1993. Modeling genotypic and environmental control of leaf area dynamics in grain sorghum. Whole plant level. *Field Crops Research* 33: 293-310.
- Hao B., Xue Q., Bean B.W., Rooney W.L., Becker J.D., 2014. Biomass production, water and nitrogen use efficiency in photoperiod-sensitive sorghum in the Texas High Plains. *Biomass Bioenerg.*, 62: 108-116.
- Hess T.M., Stephens W., Crout N.M.J., Young S.D., Bradley R.G., 1997. PARCH-user guide. Sutton Bonnington, University of Nottingham, UK.
- Hsiao T.C., 1993. Growth and productivity of crops in relation to water status. *Acta Hort.* 335: 137-148.
- Hsiao T.C., Bradford K.J., 1983. Physiological consequences of cellular water deficits: an overview. In: Limitations to efficient water use in crop production (Taylor H, Jordan W, Sinclair T, eds). *Am. Soc. Agron.*, Madison, WI, USA. pp. 227-265.
- Hughes G., Keatinge J.D.H., Copper P.J.M., Dee N.F., 1987. Solar radiation interception and utilization by chickpea crops in northern Syria. *J. Agric. Sci. Cambridge.* 108: 419-424.
- Jones C.A., Dyke P.T., Williams J.R., Kiniry J.R., Benson C.A., Griggs R.H., 1991. EPIC: an operational model for evaluation of agricultural sustainability. *Agric. Syst.* 37: 341-350.
- Jones C.A., Kiniry J.R., 1986. CERES-Maize: a simulation model of maize growth and development. Texas A&M University Press: College Station, TX.
- Jones J.W., Hoogenboom G., Porter C.H., Boote K.J., Batchelor W.D., Hunt L.A., Wilkens P.W., Singh U., Gijssman A.J., Ritchie J.T., 2003. The DSSAT cropping system model. *Eur. J. Agron.* 18: 235-265.
- Kemanian A.R., Stöckle C.O., Huggins D.R., 2004. Variability of barley radiation-use efficiency. *Crop Sci.* 44: 1662-1672.
- Kiniry J.R., Simpson C.E., Schubert A.M., Reed J.D., 2015. Peanut leaf area index, light interception, radiation use efficiency, and harvest index at three sites in Texas. *Field Crop Res.* 91: 297-306.
- Kozak A.J., Ahuja L.R., Green T.G., Ma L., 2007. Modeling crop canopy and residue rainfall interception effects on soil hydrological components for semi-arid agriculture. *Hydrol. Process.* 21: 229-241.
- Liu F., Stützel H., 2004. Biomass partitioning, specific leaf area, and water use efficiency of vegetable amaranth (*Amaranthus* spp.) in response to drought stress. *Sci Hortic.* 102, 1: 15-27.
- Mastrorilli M., Katerji. N, Rana. G, Steduto P., 1995. Sweet sorghum in Mediterranean climate: radiation use and biomass water use efficiencies. *Ind. Crops Prod.* 3: 253-260.
- Monteith J.L., 1977. Climate and the efficiency of crop production in Britain. *Philos. Trans. R. Soc. Lond. B. Biol.* 281: 277-294.
- Monteith J.L., 1994. Validity of the correlation between intercepted radiation and biomass. *Agric. For. Meteorol.* 6: 213-220.
- Moroke T.S., Schwartz R.C., Brown K.W., Juo A.S.R., 2011. Water use efficiency of dryland cowpea, sorghum and sunflower under reduced tillage. *Soil Tillage Res.* 112: 76-84.
- Myers R.H., 1990. Classical and modern regression with applications. PWS-Kent Publishing, Boston.
- Narayanan S., Aiken R.M., Vara Prasad P.V., Xin Z., Yu J., 2013. Water and radiation use efficiencies in sorghum. *Agron. J.* 105: 649-656.
- Perniola, M., Tartaglia, G., Tarantino, E., 1996. Radiation Use Efficiency of sweet sorghum and kenaf under field condition. Proc. 9th. Eur. Bioenergy Conf., Copenhagen, Denmark, p. 156 (abstr.).
- Reddy B., Angira B., 2015. Transpiration efficiency of grain sorghum and maize under different planting geometries. *J. Crop Improv.* 29, 5: 619-635.
- Rinaldi M., Garofalo P., 2011. Radiation-use efficiency of irrigated biomass sorghum in a Mediterranean environment. *Crop Pasture Sci.* 62: 830-839.
- Ritchie J.T., 1972. Model for predicting evaporation from a row crop with incomplete cover. *Water Resour. Res.* 8: 1204-1212.
- Ritchie J.T., Godwin D.C., Otter-Nacke, S., 1985 CERES-Wheat: a simulation model of wheat growth and development. Texas A&M University Press: College Station, TX.
- Rosenthal W.D., Gerik T.J., 1991. Radiation use efficiency among cotton cultivars. *Agron. J.* 83: 655-658.
- Russell G., Jarvis P.G., Monteith J.L., 1989. Absorption of radiation by canopies and stand growth. In: Russell,

- G., Marshall, B., Jarvis, P.G. (Eds.), *Plant Canopies: Their Growth, Form and Function*. Cambridge University Press, Cambridge, pp. 21-39.
- Sinclair T.R., Horie T., 1989. Leaf nitrogen photosynthesis, and crop radiation use efficiency: a review. *Crop Sci.* 29: 90-98.
- Steduto P., Albrizio R., 2005. Resource use efficiency of field-grown sunflower, sorghum, wheat and chickpea. II. Water use efficiency and comparison with radiation use efficiency. *Agr. Forest Meteorol.* 130: 269-281.
- Steduto P., Hsiao T.C., Raes D., Fereres E., 2009. AquaCrop- The FAO crop model for predicting yield response to water: I. Concepts and underlying principles. *Agron. J.* 101: 426-437.
- Stöckle C.O., Donatelli M., Nelson R., 2003. CropSyst, a cropping systems simulation model. *Eur. J. Agron.* 18: 289-307.
- Tanner C.B., Sinclair T.R., 1983. Efficient water use in crop production: research or re-search. In: *Limitations to efficient water use in crop production* (Taylor HM et al., eds). ASA, Madison, WI, USA. pp. 1-27.
- Thapa S., Stewart B.A., Xue Q., 2017. Grain sorghum transpiration efficiency at different growth stages. *Plant Soil Environ.*, 63: 70-75.
- Soil Survey Staff "Keys to Soil Taxonomy", 11th ed. USDA-Natural Resources Conservation Service, Washington DC., 2010. Available in https://www.nrcs.usda.gov/wps/portal/nrcs/detail/soils/survey/class/taxonomy/?cid=nrcs142p2_053580.
- Woods J., 2001. The potential for energy production using sweet sorghum in southern Africa. *Energ. Sustain. Dev.* 1: 31-38.
- Yimam Y.T., Ochsner T.E., Kakani, V.G., 2015. Evapotranspiration partitioning and water use efficiency of switchgrass and biomass sorghum managed for biofuel. *Agric. Water Manag.* 155: 40-47.
- Yin X., Goudriaan J., Lantinga E.A., Vos J., Spiertz H.J., 2003. A flexible sigmoid function of determinate growth. *Ann. Bot.* 91: 361-371.
- Zegada-Lizarazu W., Monti A., 2012. Are we ready to cultivate sweet sorghum as a bioenergy feedstock? A review on field management practices. *Biomass Bioenerg.* 40: 1-12.



Citation: A. Dao, A. Guira, J. Alvar-Beltrán, A. Gnanda, L. Nebie, J. Sanou (2020) Quinoa's response to different sowing periods in two agro-ecological zones of Burkina Faso. *Italian Journal of Agrometeorology* (1): 63-72. doi: 10.13128/ijam-731

Received: November 25, 2019

Accepted: April 10, 2020

Published: June 23, 2020

Copyright: © 2020 A. Dao, A. Guira, J. Alvar-Beltrán, A. Gnanda, L. Nebie, J. Sanou. This is an open access, peer-reviewed article published by Firenze University Press (<http://www.fupress.com/ijam>) and distributed under the terms of the Creative Commons Attribution License, which permits unrestricted use, distribution, and reproduction in any medium, provided the original author and source are credited.

Data Availability Statement: All relevant data are within the paper and its Supporting Information files.

Competing Interests: The Author(s) declare(s) no conflict of interest.

Quinoa's response to different sowing periods in two agro-ecological zones of Burkina Faso

ABDALLA DAO^{1,*}, AMIDOU GUIRA², JORGE ALVAR-BELTRÁN³, ABDOU GNANDA², LOUIS NEBIE², JACOB SANOU¹

¹ Institut de l'Environnement et de Recherches Agricoles (INERA), Bobo Dioulasso BP910, Burkina Faso

² Institut de Développement Rural (IDR), Université Nazi Boni, Bobo-Dioulasso, Burkina Faso

³ Department of Agriculture, Food, Environment and Forestry (DAGRI)-University of Florence, 50144 Florence, Italy

* Corresponding author. Email: adao@wacci.ug.edu.gh

Email address: guira.amidou@yahoo.fr; jorge.alvar@unifi.it; gnandaabdou@gmail.com; nebielouis@yahoo.fr; jacobsanou17@gmail.com

Abstract. The Soudano-Sahelian and Soudanian agro-climatic zones of Burkina Faso extent over 150,000 km² and 55,000 km², respectively, equivalent to 75 % of the country's total surface area. Food security throughout the country is constantly threatened due to inter/intra annual fluctuations on crop production. Climate resilient and highly nutritional crops (*Chenopodium quinoa* Willd.) are of increasing interest in regions exposed to environmental stresses and having high undernourishment rates. This study examines quinoa's adaptability in two agro-ecological zones of Burkina Faso (Soudano-Sahelian and Soudanian zones). Four quinoa genotypes (Pasankalla, Negra Collana, Titicaca and Puno) are tested for different sowing periods (from October to January) in two agro-ecological zones, and their effect on crop growth is evaluated. Results show a significant effect of sowing dates on plant phenology in both agro-climatic zones. Photoperiod, temperature and wind speed are the major environmental factors explaining variation in terms of crop growth and development between sowing dates. Emerging findings show that short cycle varieties (Titicaca and Puno) can be highly performing (above 3 t ha⁻¹) when sowing between November-December and October-December in the Soudano-Sahelian and Soudanian zones, respectively. Other genotypes (Pasankalla), can respond better to strong Harmattan winds, besides having similar yields to those reported for Titicaca and Puno. Pasankalla and Negra Collana tend to be susceptible to heat-stress conditions occurring in March-April because of their long cycle (around 120 days).

Keywords. Quinoa, agrometeorology, adaptability, climate-resilient crops, abiotic factors, Sahel.

INTRODUCTION

In recent years, the expansion of quinoa beyond traditionally grown agro-ecological zones has increased scientific attention. Portrayed as a highly nutritional crop, quinoa's spread is the result of an optimal adaptation to adverse environmental conditions. High tolerance to heat and drought-stress conditions, and great performance under saline and unfavourable soils have been reported within the Mediterranean, Middle East and North African (MENA) and Sahel regions (Hirich *et al.*, 2012; Coulibaly and Martinez, 2015; Bazile *et al.*, 2016; Dao *et al.*, 2016; Habsatou, 2016; Mosseddaq *et al.*, 2016). The great adaptability of quinoa to abiotic stresses is the result of a wide genetic diversity (Bazile, 2015). The recent discover of the quinoa genome sequence has open new opportunities for identifying desirable genotypes for specific regions (Jarvis *et al.*, 2017). The great genetic diversity of quinoa shows that there is space for developing new and more productive varieties that can cope with more intensified and recurrent environmental stresses (Gandarillas *et al.*, 2015).

To optimize the productivity of the crop, it is important to identify the most suitable sowing dates by adjusting ontogenesis (chronology of phenological stages) to the best environmental conditions. Sometimes, environmental stresses are unavoidable; therefore, minimizing the effects of adverse environmental conditions at plant's most sensitive stages (flowering and seed germination) becomes imperative. However, determining the most appropriate sowing dates of highly sensitive crop's to photoperiodicity is more complex. This is the case of quinoa, with genotypes ranging in cycle from 80 days to more than 200 days (Bertero, 2001; Rojas *et al.*, 2015). For this crop, it is widely accepted that the shorter the photoperiod the more rapid the plants flower, being its sensitivity to photoperiod and temperature a function of origin (Jacobsen, 2003). It is accepted that genotypes growing in the tropics are more sensitive to photoperiod and have a longer vegetative phase when compared to genotypes grown by the sea and at the Andean altiplano (Jacobsen, 2003). However, other experiments, under controlled environmental conditions, have shown that different genotypes are highly sensitive to day length, with very little differences on the time to flowering; but having great variances on time to maturity (Christiansen, 2010; Bertero, 2015a). Also, some affirm that day lengths over 12 hours tend to have an undesirable effect on the development of the plant (Jacobsen, 2015). This is the case of genotype Titicaca, with a time to maturity of 134 days in Germany (34 °N) and less than 90 days in Burkina Faso (11 °N) (Präger *et al.*, 2018; Alvar-Beltrán *et al.*, 2019a).

Quinoa is a new crop recently introduced in Burkina Faso (Dao *et al.*, 2016) and up until now, there has not yet been a study examining the adaptation of quinoa to the different agro-ecological zones. Hence, this study was carried out with the objectives to evaluate the effect of sowing dates on phenological and agronomic traits of quinoa, to evaluate plant growth and grain yield performance of quinoa varieties in two agro-ecological zones and to determine the optimal growing calendars in Burkina Faso.

MATERIALS AND METHODS

Experimental set-up and statistical analysis

These trials were conducted simultaneously in two agro-climatic zones of Burkina Faso between October 2017 and June 2018 (Figure 1). The Institut de l'Environnement et Recherches Agricoles (INERA)-Farako-Ba research station (11°05' N and 4°20' W; 405 masl) was characterised for having a tropical savannah climate (Soudanian agro-climatic zone). While, INERA-Saria research station (12°16' N and 2°09' W; 311 masl) was located within hot-semi arid climates (Soudano-Sahelian agro-climatic zone), with a well-defined rainy season (from June to October). Four sowing dates were



Fig. 1. Location of Farako-Ba (Soudanian zone) and Saria (Soudano-Sahelian zone) research stations within Burkina Faso.

tested, every month from 17th October 2017 until 17th January 2018, while four genotypes of quinoa were examined, namely Titicaca, Puno, Pasankalla and Negra Collana. Each treatment contained three replicates, with a total of 12 experimental plots per research site and sowing date. To test the different factors (sowing dates and genotypes), a completely randomized block-Fisher experimental design was used, with plots sizing 9 m², with 7 rows spacing each other by 0.50 m and with plants separated by 0.10 m. The ANOVA and the Student-Newman-Keuls post-hoc tests were used to assess the differences between means. All the statistics were done using the Statistical Analysis Software (SAS, version 9).

The soil was prepared manually and prior to sowing the soil was amended using compost at a rate of 5 t ha⁻¹ (1.1 % N content). NPK fertilization (14-23-14) was applied during sowing at a rate of 100 kg ha⁻¹, while 30 days after sowing (DAS) urea, CO(NH₂)₂ (46 % N content), was spread at a rate of 100 kg ha⁻¹. Prior to sowing, the seeds were treated with insecticides (Permethrin 25 g kg⁻¹ and Thirame 250 g kg⁻¹), and 3 to 5 seeds were introduced per hole at 10 mm depth. At 15 DAS, quinoa plants were thinned to leave 1 plant per hole, giving a plant density of 20 plant m⁻². Both trials were fully irrigated twice a week using a drip-irrigation system.

Measurements

Different crop parameters were selected to test the

effect of different agro-climatic regions and latitude on crop development and performance. For each plot, 10 plants were selected and the following parameters were measured: days after sowing to flowering (Flo₅₀ in days) and days after sowing to physiological maturity (PM in days), branches per plant (BP in number), plant height at harvest (PH in m), grain yield (GY in g plant⁻¹) and thousand grain weight (TGW in g). All the plant measurements were taken from the middle rows to avoid side effects.

The Agence National de la Météorologie (ANAM) provided this research with the necessary meteorological information to compare both research sites. Maximum, minimum and mean air temperatures (°C), just like precipitation (mm) and average wind speeds (km h⁻¹) were recorded daily to evaluate the effect of weather phenomenon's on plant growth and development in both experimental sites. The day length information, for each day of the growing season, was adjusted according to the latitude and longitude of interest using an excel spreadsheet provided by the National Atmospheric and Oceanic Administration (NOAA).

RESULTS

The soil texture is characterised for being sandy-loam at both research stations (0-0.20 m), while turning into sandy-clay-loam at lower depths (0.20-0.40 m) (Table 1). In both locations, the soils are acidic (pH value

Tab. 1. Physic-chemical properties of the soil at different depths (0-0.2, 0.2-0.4 and 0.4-0.6 m) at Saria (Soudano-Sahelian zone) and Farako-Ba (Soudanian zone).

Parameter	Units	Saria			Farako-Ba		
		0-0.2	0.2-0.4	0.4-0.6	0-0.2	0.2-0.4	0.4-0.6
Sand	%	78.4	60.8	39.2	73.5	56.8	46.0
Silt	%	13.7	15.7	13.7	16.0	15.1	13.1
Clay	%	7.9	23.5	47.1	10.5	28.1	40.9
USDA class		Sandy-Loam	Sandy-Clay-Loam	Clay	Sandy-Loam	Sandy-Clay-Loam	Clay-Loam
pH (H ₂ O)		5.4	5.2	6.8	5.5	5.2	5.3
C	%	0.34	0.28	0.21	0.31	0.30	0.26
Org. matter	%	0.58	0.48	0.36	0.52	0.51	0.54
N	%	0.034	0.031	0.022	0.029	0.030	0.23
C/N		10.0	9.0	9.0	10.0	10.5	10.5
P total	mg kg ⁻¹	146	120	137	108	121	123
P _{Bray1}	mg kg ⁻¹	11.5	2.4	0.6	8.3	1.2	0.4
K total	mg kg ⁻¹	940	1380	1575	1575	1941	2307
K available	mg kg ⁻¹	41.4	29.5	44.4	80.7	86.6	62.8

of 5.5), with a slightly higher organic matter and nitrogen (N) content in Saria when compared to Farako-Ba. Low carbon nitrogen ratios (C:N 10 at 0-0.20 m) have been reported in both sites, showing a fast rate of decomposition of in the soil due to high temperatures. The availability of Phosphorus (P) in the first layer of the soil is higher in Saria than Farako-Ba (11.5 mg kg⁻¹

and 8.3 mg kg⁻¹, respectively); whereas the availability of Potassium (K) in the top layer is double at Farako-Ba than in Saria (80.7 mg kg⁻¹ and 41.4 mg kg⁻¹, respectively).

Warm mean-temperatures (between 24 °C and 33 °C) have been consistent during the growing period of quinoa in both sites and for all sowing dates, with slightly higher mean-temperatures at Saria than Farako-

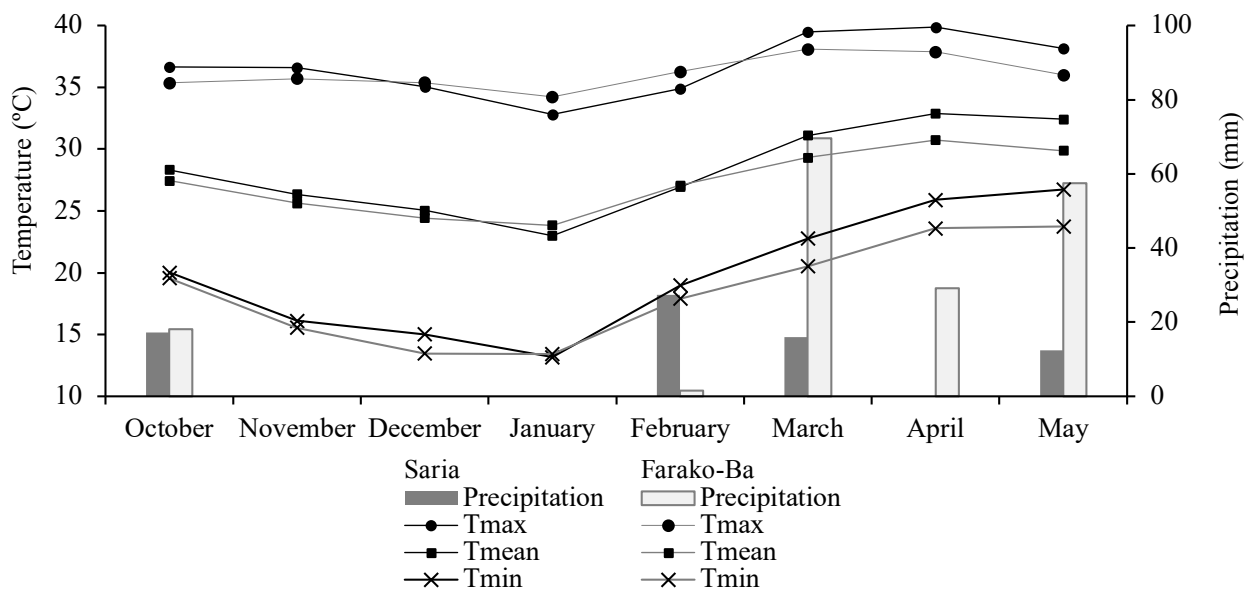


Fig. 2. Maximum/minimum mean monthly and average monthly temperatures (°C) and precipitation (mm) at Saria (Soudano-Sahelian zone) and Farako-Ba (Soudanian zone).

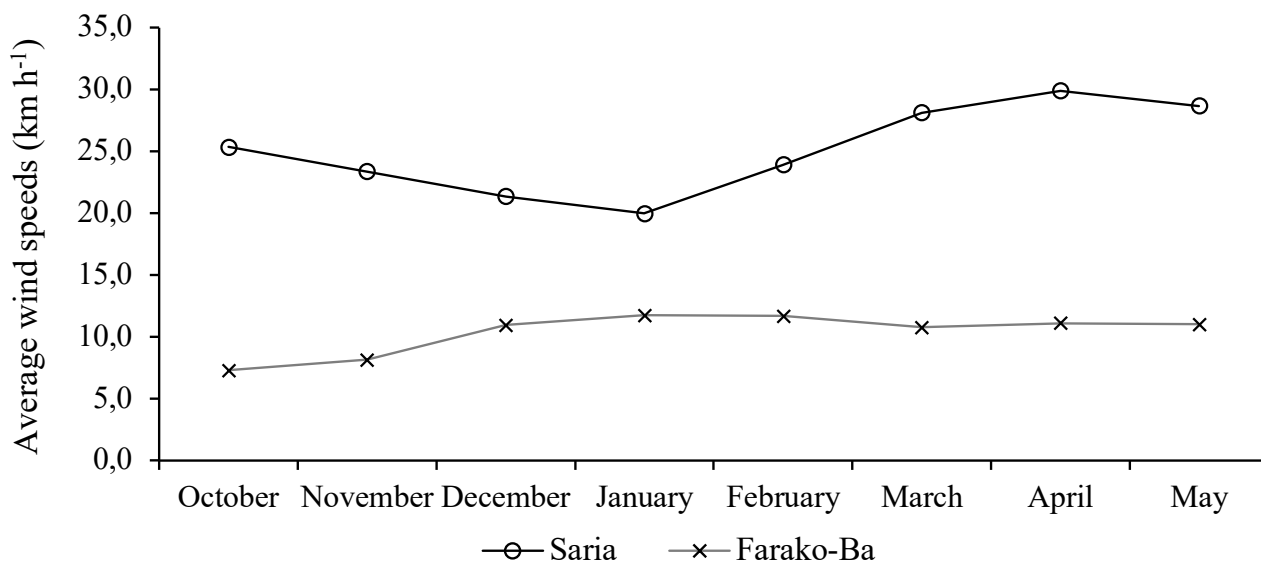


Fig. 3. Monthly average wind speeds (km h⁻¹) at Saria and Farako-Ba research stations.

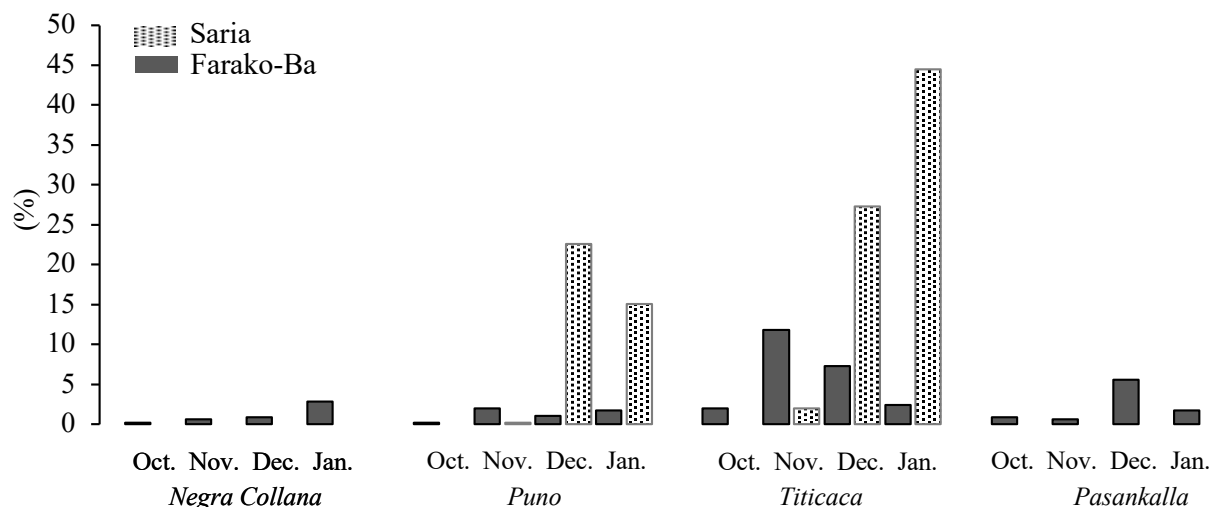


Fig. 4. Percentage of plants flattened by wind gusts for the different sowing dates (October, November, December and January), genotypes (Negra Collana, Puno, Titicaca and Pasankalla) in both experimental sites (Farako-Ba and Saria research stations).

Ba (Figure 2). Maximum monthly mean temperatures oscillated between 35 °C and 40 °C, particularly between October-November and February-May. Atypical precipitation for the time of the year has been reported in both sites, being exceptional the values recorded in March at Farako-Ba (70 mm) and during February and March at Saria (27 mm and 16 mm, respectively). Strong Harmattan winds (prevailing winds from the north) have been observed in both sites, being more intense in Saria during the warmest months of the year (March and April). Much higher average wind speeds have been reported in Saria than Farako-Ba, with mean wind speeds of 25 km h⁻¹ and 10 km h⁻¹, respectively during the growing period (Figure 3). The impact of high wind speeds at Saria has resulted in a high number of plants flat-

tened by winds (Figure 4). The most affected genotypes by wind have been Titicaca and Puno at Saria, with 45 % of the Titicaca plants flattened in January and 23 % of the Puno plants flattened in December. These genotypes are characterised for having a smaller stem diameter, root development and lower number of branches than Pasankalla and Negra Collana (Alvar-Beltrán *et al.*, 2019a, Dao *et al.*, 2019).

Even though quinoa is a highly sensitive plant to changes in photoperiodicity, this research trials have been conducted in two sites with small differences in latitude (Farako-Ba at 11°N and Saria at 12°N). Therefore no impact on time to reach physiological maturity has been reported among sites (Figure 5). However, there is a positive correlation between sowing dates and time

Tab. 2. Over all means (± SE) of six traits for the four quinoa genotypes in both experimental sites (Farako-Ba and Saria).

Site	Variety	Crop parameters					
		Flo50 (days)	PM (days)	BP (number)	PH (m)	GYP (g plant ⁻¹)	TGW (g)
Saria	Puno	38.7±7.4c	78.7±20.7c	27.1±7.2a	0.86±0.12b	7.6±6.8a	1.9±0.6c
	Titicaca	36.2±8.2d	76.9±21.7d	22.4±7.1b	0.76±0.14c	7.0±7.2a	2.4±0.7a
	Pasankalla	48.1±6.8a	113.4±20.0b	21.7±8.1b	1.11±0.16a	9.4±5.1a	2.1±0.7b
	Negra Collana	47.4±6.8b	125.1±23.0a	21.1±8.3b	0.92±0.16b	0.5±1.5b	1.7±0.7c
Farako-Ba	Puno	39.5±13.1b	78.3±25.1c	14.1±4.3a	0.61±0.18a	3.2±2.2b	1.6±0.5a
	Titicaca	38.3±13.4b	77.5±25.5c	16.1±4.2a	0.62±0.19a	4.7±2.2a	2.0±0.5a
	Pasankalla	53.6±12.7a	113.5±24.9b	9.9±4.3b	0.71±0.19a	1.3±2.3c	1.6±0.5a
	Negra Collana	53.7±12.8a	125.8±26.6a	11.2±4.2b	0.65±0.19a	1.1±2.3c	1.6±0.5a

Legend: means that do not share a letter are statistically significant different (p<0.05).

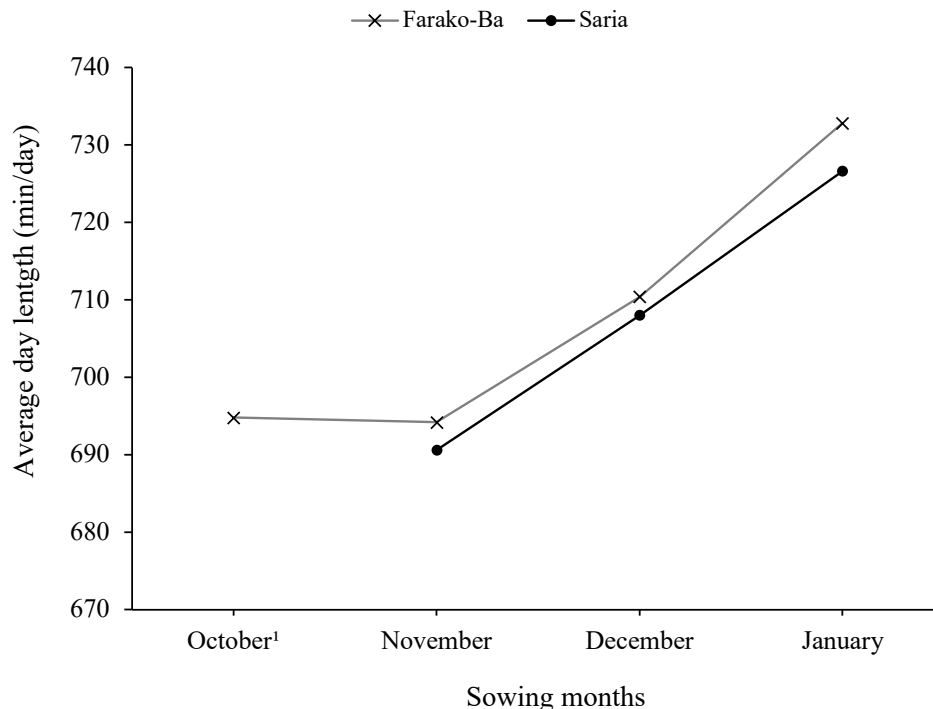


Fig. 5. Average photoperiodicity (minutes day⁻¹) during the growing cycle for the four sowing dates at Farako-Ba and Saria research stations.

to maturity, with a similar observed pattern in both sites (Table 3). For instance, at Farako-Ba, a shorter time to maturity has been noticed among plants sown in October, and which have been exposed to average (from sowing to maturity) day lengths of 695 min day⁻¹. On the opposite, if sowing in January, the average (from sowing to maturity) day lengths are of 733 min day⁻¹ and have resulted in a mean time to maturity of 125 days. Statistical differences on time to maturity have been depicted between short and long cycle genotypes, with Puno and Titicaca reaching maturity at 80 DAS, while Pasankalla and Negra Collana after 113-125 DAS (Table 2).

The time for reaching flowering of diverse genotypes of quinoa is significant different (Table 2). While Negra Collana and Pasankalla have attained flowering 50 DAS, Titicaca and Puno have only taken 40 DAS. In Saria, significant differences in time to flowering have been reported between all genotypes, being longest for Pasankalla (48 DAS) and shortest for Titicaca (36 DAS). Whereas for Farako-Ba statistical differences have only been reported between short cycle (Titicaca and Puno) and long cycle varieties (Negra Collana and Pasankalla), but not amongst them.

The number of primary branches varied among genotypes, and is affected by sowing dates and sites (Tables 2 & 3). The average of four sowing dates shows

that the number of primary branches of the early maturing genotypes (Puno, Titicaca) tend to have a high number of primary branches than the late maturing genotypes (Pasankalla, Negra Collana) (Table 2). Difference between the two sites in plant branching was also found, with a twofold increase between Farako-Ba and Saria from 12.8 to 23.1 branches plant⁻¹, respectively (Table 3). There has been significant differences in terms of plant height between genotypes. For instance, at Saria, Pasankalla had had an average height of 1.11 m, Negra Collana 0.92 m, Puno 0.86 m and Titicaca 0.76 m. A similar genotype-height order has been reported at Farako-Ba. Nevertheless, much smaller plants have been reported at Farako-Ba (0.65 m) than Saria (0.91 m), average of all genotypes, with a 30 % difference between sites. In addition, in both locations, there is a positive relationship between sowing dates and plant height, with higher plants found in December and January (Table 3). The average day length, from the sowing to maturity of the plants, is longer during the sowing of these months (December and January) than in October and November, resulting in a longer vegetative stage among plants exposed to longer photoperiods (Figure 5).

Results are displaying significant differences in yield (average of all genotypes) between sowing dates and locations (Table 3). For the differences between

sites, results show a twofold increase in terms of yield between Farako-Ba and Saria, from 2.57 g plant⁻¹ to 6.13 g plant⁻¹, respectively (average of all genotypes). More in detail, Pasankalla, Puno and Titicaca have shown a high performance in Saria with 9.4 g plant⁻¹, 7.6 g plant⁻¹ and 7.0 g plant⁻¹. For the sowing dates (Table 2), remarkable differences are observed in Saria, with average yields dropping from 16 g plant⁻¹ to 1.3 g plant⁻¹, respectively between November and December sowing dates (Table 3). High temperature conditions occurring at flowering are responsible for non-fertilised plants, particularly in Saria where temperatures are higher than in Farako-Ba (Figure 2). In both sites, the most affected genotype by extreme temperatures, in terms of yield per plant, has been Negra Collana (0.8 g plant⁻¹, average of the two sites), which had the longest cycle out of the four geno-

types in study. In fact, long cycle varieties (Negra Collana and Pasankalla) sown in December and January have been the most affected by temperatures occurring at flowering, 50 DAS. For the previous sowing dates, flowering has occurred when temperatures are highest in the Soudanian and Soudano-Sahelian zone (March and April). However, at Farako-Ba, with milder temperatures than Saria, small differences in yield have been reported between October and December sowing dates, with yields starting to drop from January onwards (Table 3).

Finally, genotype Titicaca has shown the greatest kernel weight (mass of 1000 seeds) in both sites with 2.2 g (Table 2). For both locations, there is a positive relationship with significant differences among sowing dates and kernel weight, having a much higher seed weight plants sown in October/November than in January/February.

Tab. 3. Means (\pm SE) and mean squares of six traits for the different sowing dates in both experimental sites (Farako-Ba and Saria).

Site	Sowing date	Crop parameters					
		Flo50 (days)	PM (days)	BP (number)	PH (m)	GYP (g plant ⁻¹)	TGW (g)
Saria	October ¹	-	-	-	-	-	-
	November	37.3 \pm 4.3c	85.8 \pm 18.6c	22.9 \pm 3.2b	0.85 \pm 0.12b	16.4 \pm 2.7a	2.8 \pm 0.4a
	December	43.1 \pm 3.7b	100.8 \pm 30.9b	28.3 \pm 4.6a	0.98 \pm 0.17a	1.3 \pm 0.6b	1.6 \pm 0.9b
	January	47.5 \pm 9.2a	109.0 \pm 17.4a	18.7 \pm 9.8c	0.96 \pm 0.17a	3.1 \pm 2.1b	1.4 \pm 0.1c
	<i>Sowing date</i>	317.2 ***	1669.5 ***	243.0 ***	541.3 **	477.2 ***	6.9 ***
	<i>Variety</i>	330.0 ***	5375.7 ***	68.9 **	1633.9 ***	3.30 NS	1.5 ***
	<i>Sowing date x Variety</i>	49.8 ***	250.6 ***	156.0 ***	117.9 NS	9.6 *	0.9 ***
	<i>Residual error</i>	0.47	0.47	2.99	7.96	1.52	0.17
	μ	42.61	98.53	23.14	0.93	7.19	2.06
	CV (%)	1.11	0.48	12.94	8.57	21.09	8.11
Farako-Ba	October	41.6 \pm 6.3c	84.0 \pm 14.7d	12.0 \pm 3.5b	0.56 \pm 0.15c	2.4 \pm 1.2b	2.0 \pm 0.6a
	November	40.7 \pm 3.7c	89.2 \pm 17.6c	10.0 \pm 4.1c	0.46 \pm 0.12d	2.7 \pm 1.4ab	2.1 \pm 0.2a
	December	43.4 \pm 4.4b	101.4 \pm 31.1b	15.0 \pm 2.6a	0.72 \pm 0.13b	3.7 \pm 3.1a	1.4 \pm 0.6b
	January	59.3 \pm 18.0a	120.6 \pm 26.3a	14.8 \pm 3.9a	0.84 \pm 0.08a	0.2 \pm 0.2c	1.3 \pm 0.1b
	<i>Sowing date</i>	928.6 ***	3172.8 ***	60.4 ***	3440.8 ***	7.9 **	1.8 ***
	<i>Variety</i>	873.4 ***	7277.9 ***	84.3 ***	350.9 *	13.6 ***	0.4 NS
	<i>Sowing date x Variety</i>	180.1 ***	236.8 ***	4.9 *	268.6 *	4.9 **	0.2 NS
	<i>Residual error</i>	1.78	1.23	2.31	9.89	1.00	0.41
	μ	46.25	98.79	12.98	0.64	2.36	1.70
	CV (%)	3.86	1.24	17.80	15.35	42.39	24.09

Legend: ¹No data has been collected in October sowing date at Saria due to external factors.

Legend: means that do not share a letter are statistically significant different ($p < 0.05$).

Legend: $p < 0.001$ (***), $p < 0.01$ (**), $p < 0.05$ (*), no significance (NS).

ruary (Table 2). Significant differences have been noticed between genotypes in Saria, having Titicaca a kernel weight of 2.4 g, Pasankalla 2.1 g, Puno 1.9 g and Negra Collana 1.7 g (Table 2). However, for Farako-Ba no differences have been depicted between the different genotypes. Overall, the genotype Negra Collana has had the lowest performance, in terms of kernel weight, out of all genotypes, with just 1.65 g (average value of both sites).

DISCUSSION

Pasankalla, Puno and Titicaca are displaying great production, with yields of 16.4 g plant⁻¹ (potential yield of 3.28 t ha⁻¹) when sown in November at Saria (Soudano-Sahelian zone). These potential values are similar to the observed yields for Pasankalla in the altiplano and coastal areas of Peru (4.5 t ha⁻¹) (Mujica, 2015). All genotypes of study have shown a strong negative relationship with lower yields under higher temperatures at flowering, notably when sown in January at Farako-Ba (0.2 g plant⁻¹) and in December and January at Saria (1.3 g plant⁻¹ and 3.1 g plant⁻¹). Therefore, this research results are not in line with Hinojosa's et al., 2019, findings using cultivars from Chile; but rather in line with experiments affirming that quinoa is highly susceptible to temperatures above 35 °C, which result in pollen sterility (Bertero *et al.*, 1999b; Bertero, 2015b; Pulvento, 2015; Alvar-Beltrán *et al.* 2019b). In addition, differences in soil characteristics could have been responsible for differences in yield between sites. Razzaghi *et al.*, 2012, have reported higher yields under sandy-loam soils when compared to sandy soils. However, in this research, the main differences in yields between sites are attributed to a higher nitrogen and organic matter content in the soil at Saria than in Farako-Ba. In this line, Alvar-Beltrán *et al.*, 2019b, reported a high bulk density (1.66 x 10⁻³g/mm³) at Farako-Ba research station, being a restrictive factor for root development.

Overall, the behaviour of genotype Titicaca under Soudanian environmental conditions is similar to that observed by Alvar-Beltrán *et al.*, 2019a. For instance, the average observed kernel weight of this research (2.2 g) is similar to that observed in the previous experiment in November and December (1.9 g). The values for genotype Titicaca are also in harmony with those observed (2.1 g) in the Mediterranean region when sown in May (Pulvento, 2015). Whereas this research's kernel weight for Negra Collana is higher (1.6 g) to that previously reported in the Soudanian agro-climatic zone (1.0 g) (Alvar-Beltrán *et al.*, 2019b). Other growth parameters, such as plant height and yield, are in line with those

reported by Coulibaly and Martinez, 2015, Dao, 2016, and Habsatou, 2016, under similar agro-climatic conditions (Mali, Burkina Faso and Niger, respectively). For instance, the reported plant height is around 0.80 m for Puno and Titicaca, whereas yield varies from 4 t ha⁻¹ to 3 t ha⁻¹, respectively. Emerging findings have shown that these two varieties can attain 18.8 g plant⁻¹ (Titicaca) and 16.8 g plant⁻¹ (Puno) if sown in November at Saria (potential yield of 3.8 t ha⁻¹ and 3.4 t ha⁻¹, respectively). In Kenya, significant differences are reported in the number of branches between 24 cultivars (Khaemba, 2015); whereas in this research, very few differences have been reported between genotypes.

Although, Hirich *et al.*, 2014, have reported longer growing periods among plants exposed to shorter photoperiods and lower solar radiations, our research is in line with the following studies (Bertero, 2001; Jacobsen 2003; Noulas, 2015; Rojas *et al.*, 2015). In fact, quinoa has had a more rapid growth and reached flowering faster under shorter photoperiods. Several studies have observed that time to flowering under different photoperiods does not vary much among genotypes. In fact, quinoa's response to different day lengths is reported after, at time to maturity and on plant height (Fuller, 1949; Christiansen, 2010; Bertero, 2015a). In both cases, plant height and time to maturity is positively affected by day length. Other plant parameters that react positively to longer day lengths are the number of leaves, but this parameter has not been considered in the present study (Bertero, 1999a). The present investigation has also observed significant differences when genotypes interact with sowing dates, having different photoperiods (particularly between November, December and January). These differences are depicted in terms of time to flowering, time to maturity and plant height, showing a positive relationship between time and height with the duration of the day.

CONCLUSION

The different genotypes of quinoa tested in this research have been exposed to a range of adverse conditions and have consequently responded differently. The multiple cultivars of quinoa have shown a high sensitivity to photoperiodicity, adapted to its ecotype of origin, just like differing between them: Puno and Titicaca from Denmark (maturity 80 DAS), while Negra Collana and Pasankalla from Peru (maturity 113-125 DAS). High-temperature stresses have had a major impact on long cycle varieties (Pasankalla and Negra Collana), when compared to short cycle varieties (Titicaca and Puno). Wind gusts have had devastating consequences in the

Soudano-Sahelian zone, often more exposed to strong Harmattan winds than the Soudanian agro-climatic zone. Genotypes with a less developed aboveground biomass and architecture of its root system (Titicaca and Puno) have been more exposed to winds than those fully developed and robust plants (Pasankalla and Negra Collana).

Emerging findings are important for developing crop calendars and need to be tailored according to the different agro-climatic zones. Selection of the most suitable crop varieties and improving existing crop management practices are also crucial. This research results bring to light the need to grow during the coldest period of the year (December and January) in order to avoid heat-stress at flowering and benefit the most of optimal temperatures for growth. Also, because the growing of quinoa during the rainy period (June to September) in these regions has not yet been successful (unpublished data). For this reason, sowing dates should target October and November in the Soudano-Sahelian zone and from October to December in the Soudanian zone. The previous genotype, together with Titicaca and Puno are more performing than Negra Collana under given agro-climatic conditions and therefore should be prioritized. Finally, considering the direction of the furrows with regards to the prevailing winds (North to South) in this time of the year is critical for diminishing the effect of strong winds on crop development and for maximizing plant density at harvest.

ACKNOWLEDGEMENTS

To the Food and Agriculture Organization (FAO) for the seed and fund provision for carrying out this experiment under the technical cooperation programs TCP/SFW/3404 and TCP/RAF/3602.

REFERENCES

- Alvar-Beltrán, J., Dao, A., Marta, A. D., Saturnin, C., Casini, P., Sanou, J., & Orlandini, S. 2019a. Effect of Drought, Nitrogen Fertilization, Temperature, and Photoperiodicity on Quinoa Plant Growth and Development in the Sahel. *Agronomy*, 9(10), 607.
- Alvar-Beltrán, J., Saturnin, C., Dao, A., Dalla Marta, A., Sanou, J., & Orlandini, S. 2019b. Effect of drought and nitrogen fertilisation on quinoa (*Chenopodium quinoa* Willd.) under field conditions in Burkina Faso. *Italian Journal of Agrometeorology*, (1), 33-43.
- Bazile, D. 2015. Chapter 1.4. The dynamics of the global expansion of quinoa growing in view of its high biodiversity. In: Bazile Didier (ed.), Bertero Hector Daniel (ed.), Nieto Carlos (ed.). State of the art report on quinoa around the world in 2013. Santiago du Chili: FAO, CIRAD, pp. 42-55.
- Bazile, D., Pulvento, C., Verniau, A., Al-Nusairi, M. S., Ba, D., Breidy, J., & Sepahvand, N. A. 2016. World-wide evaluations of quinoa: preliminary results from post international year of quinoa FAO projects in nine countries. *Frontiers in Plant Science*, 7, 850.
- Bertero, H. D., King, R. W., & Hall, A. J. 1999a. Photoperiod-sensitive development phases in quinoa (*Chenopodium quinoa* Willd.). *Field Crops Research*, 60(3), 231-243.
- Bertero, H. D., King, R. W., & Hall, A. J. 1999b. Modelling photoperiod and temperature responses of flowering in quinoa (*Chenopodium quinoa* Willd.). *Field crops research*, 63(1), 19-34.
- Bertero, H. D. 2001. Effects of photoperiod, temperature and radiation on the rate of leaf appearance in quinoa (*Chenopodium quinoa* Willd.) under field conditions. *Annals of Botany*, 87(4), 422-434.
- Bertero, H.D. 2015a. Chapter 5.5: Argentina. In: Bazile Didier (ed.), Bertero Hector Daniel (ed.), Nieto Carlos (ed.). State of the art report on quinoa around the world in 2013. Santiago du Chili: FAO, CIRAD, p. 524-533.
- Bertero, H.D. 2015b. Chapter 2.1. Environmental control of development. In: Bazile Didier (ed.), Bertero Hector Daniel (ed.), Nieto Carlos (ed.). State of the art report on quinoa around the world in 2013. Santiago du Chili: FAO, CIRAD, pp. 120-130.
- Christiansen, J. L., Jacobsen, S. E., & Jørgensen, S. T. 2010. Photoperiodic effect on flowering and seed development in quinoa (*Chenopodium quinoa* Willd.). *Acta Agriculturae Scandinavica, Section B-Soil & Plant Science*, 60(6), 539-544.
- Coulibaly, A.k. & Martinez E.A. 2015. Chapter 6.3.1. Assessment and adaptation of quinoa (*Chenopodium quinoa* Willd.) to the agro-climatic conditions in Mali, West Africa: An example of South-North-South-Cooperation In: Bazile Didier (ed.), Bertero Hector Daniel (ed.), Nieto Carlos (ed.). State of the art report on quinoa around the world in 2013. Santiago du Chili: FAO, CIRAD, pp. 524-533.
- Dao A., Sanou J., Yaméogo C., Kando C., Bakoané A., Traoré S., Dagnoko M., Bazile D. 2016. Quinoa introduction in West Africa: experience of Burkina Faso. International Quinoa Conference 2016: Quinoa for Future Food and Nutrition Security in Marginal Environments, Dubai 6-8 December 2016 (Accessed on: 8/10/2019). Available at: www.quinoaconference.com.

- Dao A., Gnanda A., Sanou J., Guira A., & Nebié L. 2019. Réponses des paramètres agro-morphologiques et de la productivité du quinoa, à la fertilisation minérale et organique. *Science et technique*, 38 (1), 81-92.
- Fuller, H. J. 1949. Photoperiodic responses of *Chenopodium quinoa* Willd. and *Amaranthus caudatus* L. *American Journal of Botany*, 175-180.
- Gandarillas, A., Rojas, W., Bonifacio, A. & Ojeda, N. 2016. Chapter 5.1.a. Quinoa in Bolivia: the Proinpa Foundation's Perspective. In: Bazile Didier (ed.), Bertero Hector Daniel (ed.), Nieto Carlos (ed.). State of the art report on quinoa around the world in 2013. Santiago du Chili: FAO, CIRAD, pp. 344-361.
- Habsatou, B. 2016. Adaptability of quinoa to adverse climatic and soil conditions of Niger. *International Quinoa Conference 2016: Quinoa for Future Food and Nutrition Security in Marginal Environments*, Dubai 6-8 December 2016 (Accessed on: 8/10/2019). Available at: www.quinoaconference.com.
- Hinojosa, L., Matanguihan, J. B., & Murphy, K. M. 2019. Effect of high temperature on pollen morphology, plant growth and seed yield in quinoa (*Chenopodium quinoa* Willd.). *Journal of agronomy and crop science*, 205(1), 33-45.
- Hirich, A., Choukr-Allah, R., Jacobsen, S. E., & Benlhabib, O. 2012. Could quinoa be an alternative crop of wheat in the Mediterranean region: case of Morocco. *Les notes d'alerte du CIHEAM*, 86(2012), 1-8.
- Hirich, A., Choukr-Allah, R., & Jacobsen, S. E. 2014. Quinoa in Morocco—effect of sowing dates on development and yield. *Journal of Agronomy and Crop Science*, 200(5), 371-377.
- Khaemba, C. 2015. Chapter 6.3.2. Production and utilization of quinoa (*Chenopodium quinoa* Willd.) outside its traditional growing areas: the case of Kenya. In: Bazile Didier (ed.), Bertero Hector Daniel (ed.), Nieto Carlos (ed.). State of the art report on quinoa around the world in 2013. Santiago du Chili: FAO, CIRAD, pp. 534-548.
- Jacobsen, S. E. 2003. The worldwide potential for quinoa (*Chenopodium quinoa* Willd.). *Food reviews international*, 19(1-2), pp. 167-177.
- Jacobsen, S. E. 2015. Chapter 6.1.1. Adaptation and scope for quinoa in northern latitudes of Europe. In: Bazile Didier (ed.), Bertero Hector Daniel (ed.), Nieto Carlos (ed.). State of the art report on quinoa around the world in 2013. Santiago du Chili: FAO, CIRAD, pp. 436-453
- Jarvis, D. E., Ho, Y. S., Lightfoot, D. J., Schmöckel, S. M., Li, B., Borm, T. J., & Kharbatia, N. M. 2017. The genome of *Chenopodium quinoa*. *Nature*, 542(7641), 307.
- Mosseddaq, F., Bounsir, B., Khallouq, M., Benlhabib, O. 2016. Optimization of quinoa nitrogen nutrition under Mediterranean climatic conditions. *International Quinoa Conference 2016: Quinoa for Future Food and Nutrition Security in Marginal Environments*, Dubai 6-8 December 2016 (Accessed on: 8/10/2019). Available at: www.quinoaconference.com.
- Mujica, A. 2015. Chapter 5.2. Peru. In: Bazile Didier (ed.), Bertero Hector Daniel (ed.), Nieto Carlos (ed.). State of the art report on quinoa around the world in 2013. Santiago du Chili: FAO, CIRAD, pp. 378-387
- Noulas, C. 2015. Chapter 6.1.6. Greece. In: Bazile Didier (ed.), Bertero Hector Daniel (ed.), Nieto Carlos (ed.). State of the art report on quinoa around the world in 2013. Santiago du Chili: FAO, CIRAD, pp. 492-510
- Präger, A., Munz, S., Nkebiwe, P., Mast, B., & Graeff-Hönninger, S. 2018. Yield and quality characteristics of different quinoa (*Chenopodium quinoa* Willd.) Cultivars grown under field conditions in Southwestern Germany. *Agronomy*, 8(10), 197.
- Pulvento, C. 2015. Chapter 6.2. Quinoa in Italy: research and perspectives. In: Bazile Didier (ed.), Bertero Hector Daniel (ed.), Nieto Carlos (ed.). State of the art report on quinoa around the world in 2013. Santiago du Chili: FAO, CIRAD, pp. 454-565.
- Razzaghi, F., Plauborg, F., Jacobsen, S. E., Jensen, C. R., & Andersen, M. N. 2012. Effect of nitrogen and water availability of three soil types on yield, radiation use efficiency and evapotranspiration in field-grown quinoa. *Agricultural water management*, 109, 20-29.
- Rojas, W., Pinto, M., Alanoca, C., Gómez, L., León, P., Alercia, A., Diulgheroff, S., Padulosi, S, Bazile, D. 2015. Chapter 1.5. Quinoa genetic resources and ex-situ conservation. In: Bazile Didier (ed.), Bertero Hector Daniel (ed.), Nieto Carlos (ed.). State of the art report on quinoa around the world in 2013. Santiago du Chili: FAO, CIRAD, pp. 56-82



Citation: T. Mai Anh Tran, J. Eitzinger, A. M. Manschadi (2020) Response of maize yield under changing climate and production conditions in Vietnam. *Italian Journal of Agrometeorology* (1): 73-84. doi: 10.13128/ijam-764

Received: December 10, 2019

Accepted: February 6, 2020

Published: June 23, 2020

Copyright: © 2020 T. Mai Anh Tran, J. Eitzinger, A. M. Manschadi This is an open access, peer-reviewed article published by Firenze University Press (<http://www.fupress.com/ijam>) and distributed under the terms of the Creative Commons Attribution License, which permits unrestricted use, distribution, and reproduction in any medium, provided the original author and source are credited.

Data Availability Statement: All relevant data are within the paper and its Supporting Information files.

Competing Interests: The Author(s) declare(s) no conflict of interest.

Response of maize yield under changing climate and production conditions in Vietnam

THI MAI ANH TRAN^{1,*}, JOSEF EITZINGER², AHMAD M. MANSCHADI³

¹ Thai Nguyen University of Agriculture and Forestry, Quyet Thang commune, Thai Nguyen city, Vietnam

² Institute of Meteorology and Climatology, University of Natural Resources and Life Sciences, Gregor-Mendel-Straße 33, A-1180 Vienna, Austria

³ Division of Agronomy, Department of Crop Sciences, University of Natural Resources and Life Sciences, Konrad Lorenz-Straße 24, 3430 Tulln an der Donau, Austria

*Corresponding author. E-mail: maianhtnmt@gmail.com

Abstract. This study concerns rainfed maize (*Zea mays*. L) grown in two different (winter and spring) growing seasons under current and future climate conditions in north-east of Vietnam. The yield response of rainfed maize was investigated by applying the DSSAT CERES-Maize crop model and two climate scenarios according to Representative Concentration Pathways (RCPs), RCP 4.5 and RCP 8.5. The results show that maize responds with a wide range of yield-levels due to the different climatic and production conditions. On average, under RCP 8.5 climate scenario, annual maize yield (including both winter and spring maize yields) increases by 1.1% while under RCP 4.5 the increase is 3.6%. The annual balanced maize yield increase under both RCPs is based, however, on significant changes in the simulated winter and spring maize yields, respectively. Winter maize yield was simulated to rise up to 33.3% and 31.9% under RCP 4.5 and RCP 8.5, respectively. In contrast, simulated spring maize yield decreases under both RCP 4.5 and RCP 8.5 by 30.3% and 33.9%, respectively. From those findings, it can be concluded that rainfed maize yields under future changing climatic conditions maybe positively affected in winter growing season while it will be reduced in the spring growing season, mainly due to increasing drought stress. Therefore, irrigation will be crucial key for spring maize production in the future to mitigate the effects of changing climate on crop water availability.

Keywords. Maize production, crop model, DSSAT, CERES-Maize, climate scenario, drought, adaptation, Vietnam

INTRODUCTION

An increase in the frequency and intensity of drought events is considered a consequence of climate change impact in many regions of the world (Baldock et al., 2000; Powell and Reinhard, 2015; Steffen et al., 2015). In the north of Vietnam, the decrease in precipitation by 5 to 10% throughout the year (IMHEN, 2011) has recently been considered as the main reason for increasing drought events, causing negative effects on crop production such as for grain maize (Thi-Minh-Ha et al., 2011).

Maize originated in South America (Mangelsdorf, 1947) and the highlands of Mexico (Tenaillon and Charcosset, 2011; Mickleburgh and Pagán-Jiménez, 2012). Maize is the third largest crop after wheat and rice globally and is cultivated around the world under a wide range of climatic conditions, from the temperate to tropical zones (Hardacre and Turnbull, 1986). However, changing climate conditions, such as increasing droughts, could become limiting factor that negatively influence maize growth.

Concerning water requirement, maize shows a wide range of responses in different production and climatic regions, depending on factors such as potential evapotranspiration and cultivar specific characteristics (e.g. phenological development). For example, over a province in the north of Iran, the total water requirement for maize cultivation, derived from satellite and meteorological data, ranges from 345 to 384 mm (Kamali and Nazari, 2018) there's a need for further investigation on various crops to identify the optimum water requirements to avoid water wasting in regions that are already facing water shortage. The focus of this work is to determine water requirement maize farming Mazandaran Province in Northern Iran, located on the southern side of the Caspian Sea, using Landsat satellite data. In order to use SEBAL algorithm, the images were atmospheric calibrated. Evapotranspiration maps with RMSE values equals to 0.73, 1.38 and 0.74 mm/day were produced and compared to Reference Book (RB while it is approximately 423 mm in a region of Ethiopia (Araya et al., 2015) and gets much higher in another region near the river basin in Northwest China with 618 mm (Zhao et al., 2010) six methods for estimating ET_c have been applied to maize field in the middle Heihe River basin, China. The ET_c was estimated by the soil water balance and Bowen ratio-energy balance methods while the Priestley-Taylor, Penman, Penman-Monteith and Hargreaves methods were used for estimating the reference evapotranspiration (ET₀). These differences in water requirement for maize indicate that the response of maize not only depends on local weather conditions but also on genetics

and other factors, such as crop management, prevailing soil and topographic conditions.

To identify and analyze climate change or weather impacts on crop growth dynamics, crop yields and effects of different crop management options, process-oriented crop models are widely used (e.g. Devkota et al., 2013; Ebrahimi et al., 2016; Eitzinger et al., 2013a, Jones et al., 2003).

As a decision support system of several crop-specific simulation models, the DSSAT (Decision Support System for Agrotechnology Transfer) shell (MacCarthy et al., 2017) has been used for more than 30 years worldwide for various purposes (e.g. Kadiyala et al., 2015). In most studies, DSSAT has been approved that it is a useful tool for crop simulation (Soler et al., 2011). DSSAT crop models' performance and sensitivity analysis were carried out for the most important crops in many studies (Eitzinger et al., 2013b; Kisekka et al., 2017) However, calibration and validation do not cover all cultivars, weather conditions as well as soil conditions all over the world. The DSSAT crop model for maize used in our study, CERES-Maize, has been used in other studies to simulate grain yield, maximize the maize yield, and help to avoid yield losses (Iyanda et al., 2014; Jing et al. 2017; MacCarthy et al., 2017). However, DSSAT models have some limitations, for example Ngwira et al. (2014) proved that it performed well for no-till and crop residue impacts but poor for crop rotation effects.

Being the first crop simulation study on the impact of climate change on maize production in the central north of Vietnam, we first tested the performance of CERES-Maize model for simulating seasonal maize growth under local conditions. We then applied the model to simulate maize yields for 100 years from 2001-2100 under two climate change scenarios (CCSs) of RCP 4.5 and RCP 8.5, respectively, in order to determine the response of maize yields to climate change conditions in Thai Nguyen province, a mountainous region in the north of Vietnam.

MATERIAL AND METHODS

To run process-based crop models for a specific location, a set of minimum data is required (MacCarthy et al., 2017). These include daily meteorological data (from Thai Nguyen center for Hydro-Meteorological Forecasting), soil data (from Thai Nguyen Department of Environment and Resources), field experiment data (from field experiment by Nguyen(2008)) and crop management data (from The Department of Agriculture and Rural Development, Thai Nguyen).

Material

The meteorological data were obtained from two local weather stations covering together 55 years from 1961 to 2015, namely Dinh Hoa station and Thai Nguyen station. They both record daily maximum temperature, minimum temperature, solar radiation, rainfall, and relative air humidity. The observed daily weather data from Dinh Hoa weather station was only available for 30 years from 1961-1990 while the daily data from Thai Nguyen weather station were recorded for 25 years from 1990-2015. However, the monthly weather data from Thai Nguyen weather station was available for 35 years from 1980-2015, providing an overlapping period from 1980-1990 of both weather stations to support the observed trend of climate change in Thai Nguyen province.

Soil properties involving soil textures, pH (acidic water-based solution), OM (organic matter), total N (total nitrogen), CEC (Cation exchange capacity) were examined by additional soil profiles from maize fields to ensure the accuracy of crop simulation. Three main soil types were chosen to simulate maize yields based on the main local soil types namely Ferralsols, Acrisols and Fluvisols (Tab. 1). Generally, Ferralsols and Acrisols are the two main soil types in Thai Nguyen province, with Ferralsols occupying approximately 75% of the total land area (TNDNRE, 2015). However, according to the FAO soil classification, local soil properties in some regions may fit to Acrisol classification. In addition, Ferralsols and Acrisols, Fluvisols and Gleysols are commonly found near the river banks and are strongly affected by

flooding in the rainy season in the case of a poor water-drainage system; however, they only occupy tiny proportions.

Field experimental data, used for crop model calibration of 3 selected maize cultivars, were collected from a report published in Thai Nguyen scientific journal in 2008. In the field experiment, three maize cultivars (SX2010, SX5012, and LVN 47) were grown in spring and winter season in 2007/2008 under irrigated condition and optimized fertilizer application (Nguyen, 2008) (Tab. 2). Each field was planted by different maize hybrid cultivars in the area of 1 ha. The field experiment provided statistical significant data (P -value < 0.05) for five main genetic plant coefficients for crop model calibration for each cultivar, including total number of leaves per stem (LAIH), beginning peg stage (days after sowing) (R2AT), day of physiological maturity (harvest day) (MDAPs), leaf area index (LAIXS) and grain yields (HWAMS), (Nguyen, 2008).

For model validation de-trended reported annual yields from regional yield statistics of recent past 15 years were used, to meet recommended validation setups (e.g. Grassini et al., 2017). For this baseline period of 2000-2014, additional information on current crop management practices (common planting date, fertilizer dose and application schedule, irrigation system, irrigation schedule, pest management) was collected by the author, provided by 10 local agricultural experts from the Department of Agriculture and Rural Development, Thai Nguyen.

Tab. 1. Soil properties of examined soil profiles in the study region (Thai Nguyen province, Vietnam).

Profile	Depth (bottom) (cm)	Texture (%)		pH (KCl)	OM (%)	Total N (%)	CEC (cmol/kg)	Drained		Bulk density g/cm ³
		< 0.002	0.02-0.002					Lower limit	Upper limit	
Profile A – Dong Hy Gleyic Acrisol	0-20	15.1	49.8	5.2	1.49	0.05	11.5	0.064	0.143	1.2
	20-90	23.7	9.8	4.2	0.44	0.04	5.7	0.052	0.078	1.56
	90-120	23.7	9.1	4.3	0.37	0.03	4.3	0.051	0.075	1.58
Profile B - Vo Nhai Calcic-Acric-Ferralsols	0-20	15.2	33.3	4.5	0.6	0.03	11.5	0.065	0.132	1.42
	20-80	16.5	30.1	4.2	0.3	0.01	5.7	0.07	0.135	1.48
Profile D - Phu Binh Fluvisols	80-120	16.9	30.9	4.4	0.1	0.01	4.3	0.057	0.11	1.51
	0-20	18.2	33.5	6.0	1.7	0.06	18.1	0.147	0.283	1.29
	20-60	20.1	32.9	5.5	0.3	0.03	11.1	0.121	0.226	1.47
	60-120	17.8	35.1	5.0	0.1	0.01	9.4	0.106	0.209	1.48

(OM: Total organic matter; CEC: Cation exchange capacity).

Tab. 2. Calibration results of the DSSAT model for the spring maize season.

Genotype	SX2010		SX5012		LVN47	
	Observed	Simulated	Observed	Simulated	Observed	Simulated
Crop indices						
Planting date (DOY)	Spring	53	Spring	53	Spring	53
Silking (Beginning Peg stage) (*)	77	70	75	62	77	70
Physiological maturity (Harvest) (*)	117	105	121	99	125	105
Leaf index, at harvest	3.6	5.72	3.9	5.59	4.0	5.98
Number of leaves per stem	20.2	15.62	20.2	14.18	20.1	15.29
Yield (kg/ha)	5720	5993	6350	6144	5990	6202

(*) (days after planting).

Climate change scenarios

Two climate scenarios from the Representative Concentration Pathways (RCP), RCP 4.5 and RCP 8.5 were used in this study. They are stabilized to limit radiative forcing at 4.5 and 8.5 W m⁻², respectively. Both of them were created by Danish Meteorology Institute and derived from CORDEX (coordinated Regional Climate Downscaling Experiment <https://esg-dn1.nsc.liu.se/search/cordex/>). The scenarios were based on the driving GCM (global circulation model), namely ICHEC-EC-EARTH and the RCM (regional climate model) DMI-HIRHAM5.

Methods

Crop simulation

In this study, spring (from February to early May) and winter (from October to early January) maize yields were simulated by the crop model CERES-Maize.

The simulation was implemented by setting the different sowing time of winter and spring maize and the share of three soil types within the case study region (Tab.1). The crop management was the same in all simulations, except for irrigation. Irrigation in the simulation was applied only for model calibration and validation, to reflect support irrigation practice. Every single estimated annual maize yield is calculated as an average of two simulated seasonal maize yields in the year. Annual yields were calculated in order to validate the model performance between simulated and reported annual maize yield. The maize yields were available only at annual basis for Thai Nguyen province for 15 years (TNDNRE, 2015).

Crop model calibration and validation

To ensure and enhance the accuracy of simulation results, model parameter estimation is a critical aspect of crop modeling because simulation results heavily dependent on parameter values, particularly crop (growth) parameters. The calibration of this study was based on the above described maize experiment in winter and spring 2008.

Based on the cultivars related calibration settings, validation of simulated grain maize yields was carried out using regional yield statistic reports of Thai Nguyen province of annual maize yield during the period of 15 years from 2000-2014 (TNDNRE, 2015). The three main regional soils (Tab.1), historical weather data and common crop management practice was used as input data to simulate the seasonal grain maize yields.

Finally, model performance analysis was carried out by two statistical methods as follows:

The Normalized Root Square Error (NRMSE) was used to evaluate the performance of CERES Maize model using the simulated and observed maize yield as follows:

$$RMSE = \sqrt{\frac{1}{n} \sum_{i=1}^n (o_i - s_i)^2} \quad (1)$$

$$NRMSE = \frac{RMSE}{\bar{O}} \times 100 \quad (2)$$

where RMSE: root mean square error, NRMSE: normalized root mean square error, n: number of simulated years, s_i: simulated maize yield in year I, o_i: observed maize yield in year I, \bar{O} : the mean of observed maize yield

NRMSE gives a relative measure (%) of the difference between simulated and observed data. The smaller the value of RMSE, the better the model performance,

while a minimum of zero implies the perfect model fit. The simulation is considered excellent with a NRMSE less than 10%, good if the normalized RMSE is greater than 10% and less than 20%, fair if the NRMSE is greater than 20% and less than 30%, poor if the NRMSE is greater than 30% (Bannayan and Hoogenboom, 2009).

The second indicator used for estimating model performance was the Index of Agreement (d):

$$d=1-\frac{\sum_i^n(O_i-S_i)^2}{\sum_i^n(|S_i-\bar{O}|+|O_i-\bar{O}|)^2} \quad (3)$$

Where d: index of agreement, O_i : Observed yield in year i , S_i : Simulated yield in year i , \bar{O} : the mean of observed maize yield. The Index of Agreement (d) developed by Willmott (1981) is a standardized measure of the degree of model prediction error and varies between 0 and 1. A value of 1 indicates a perfect match, and 0 indicates no agreement at all (Willmott, 1981). Besides, the index of agreement can detect additive and proportional differences in the observed and simulated means and variances; however, it is overly sensitive to extreme values due to the squared differences (Legates and McCabe, 1999).

De-trending observed yields

Technological improvements that lead to more effective crop production techniques over time, e.g. during the validation period (2000-2014) add a yield impacting factor. These trends are normally not simulated in multi-year crop model application such as in our study. Therefore, to obtain a reliable comparison (for model validation) between multi-year regional yield reports and simulated yields, the observed yield trends caused by improved production technology were removed by de-trending the yield time series. The year to year residuals from the smoothed time series of observed maize yields were calculated by a 6-year running mean, as shown in equation (4):

$$y=\frac{x-\bar{x}}{\bar{x}}\times 100(\%) \quad (4)$$

Where y is the residuals, x is the actual value, and \bar{x} represents the smoothed 6- year running means.

RESULTS

Climate change in Thai Nguyen province

Local weather in Thai Nguyen province, Vietnam, revealed an increase in temperature and a reduction in

precipitation (Fig. 1) within the observed period (1990-2015).

Similarly, an increasing trend of temperature and a decreasing trend of precipitation conditions in the local area was figured out by the data from projected period (2001-2100) under two climate change scenarios (i.e. RCP 4.5 and RCP 8.5. The average annual temperature increases from 24.4 °C (1990-2015) to 25.9 °C (2001-2100) under RCP 4.5 and 26.5 °C (2001-2100) under RCP 8.5. In contrast, a substantial reduction in precipitation by approximately 67.4% and 47.7% under RCP 4.5 and RCP 8.5 was determined in comparison with the average precipitation during the observed period from 1990-2015. Further, the decreasing trend of precipitation seems logical by the increase in annual and monthly percentage of dry days (Fig. 2). The total number of dry days was projected to increase, especially under RCP 4.5 by 72.3%, followed by RCP 8.5 with the value of number dry days is 71.2%.

The performance of CERES-Maize model

The result of the calibrated CERES-Maize model with three regional representative cultivars was very good for simulating the grain yields in the spring season, 2008. The percentage similarity between the observed grain yield and simulated grain yield was approximately 98% for all three maize varieties. Crop development was simulated acceptable, where e.g. for silking the deviation was 7 days (2 cultivars) and 13 days for the third cultivar (SX5012). A restriction for that comparison was that the sowing date from the experiment was not reported and, therefore, was set according to expert assessment. However, the observed leaf area indices were lower than the simulated ones, whereas the observed numbers of leaves per stem were higher than the simulated ones (Tab.2). These results show that there was still a misbalance between observed and simulated leaf areas (overestimation by the model) and the number of leaves (underestimation by the model) probably due to a deviation of mean leaf size and specific leaf weight to reality. Unfortunately, there were no further experimental data available for clarification.

Similar to the results for spring maize, for winter maize the CERES-Maize model showed a good agreement between observed and simulated grain yields. The percentage of similarity, however, ranged only from 78 to 88% for the three varieties. Crop development was slightly better simulated than for spring maize, where e.g. for silking the deviation was 5-6 days (2 cultivars) and again 13 days for the third cultivar (SX5012). Nevertheless, the accuracy of the crop model was again low

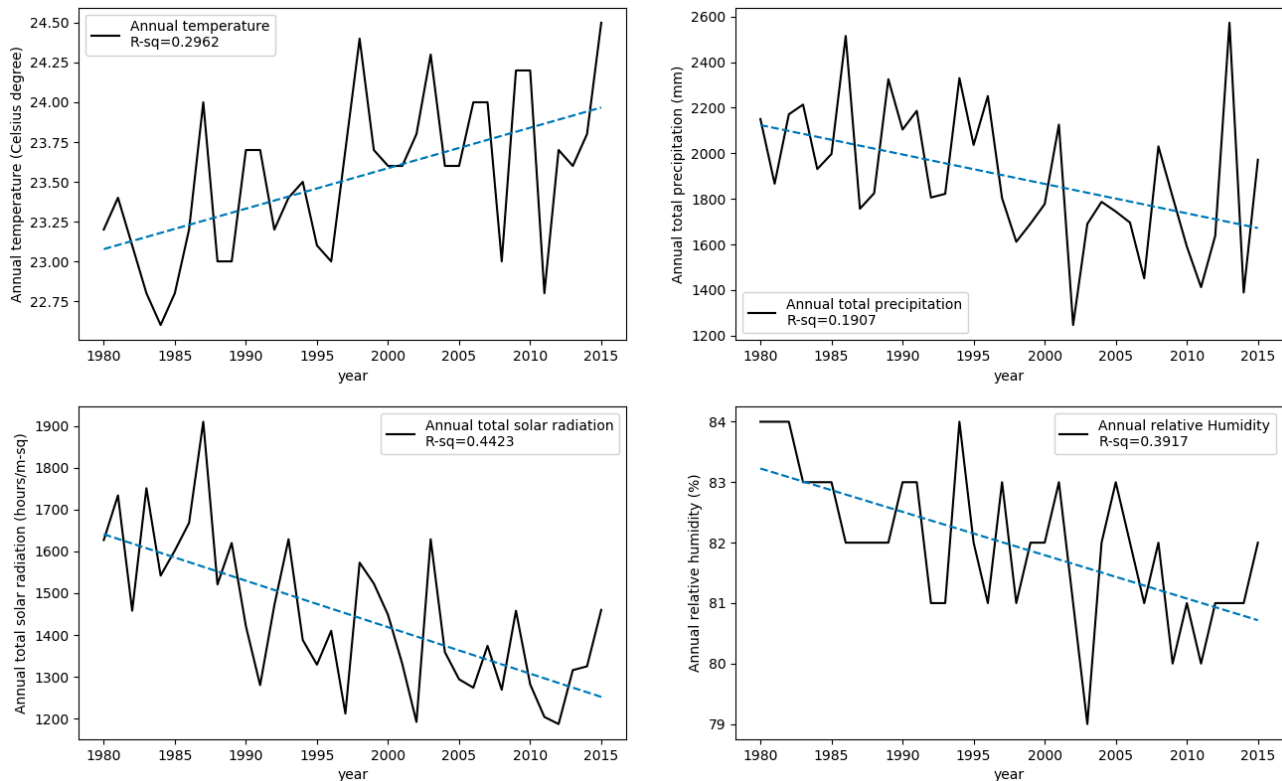


Fig. 1. Annual temperature and precipitation data from 1980-2014 in Thai Nguyen, Vietnam (R-sq termed R square).

in terms of leaf indices, in specific by a significant over-estimation of the leaf area index (Tab.3).

Based on these calibration results, we conclude that the CERES-Maize model was moderately good calibrated and acceptable for simulating maize grain yields in the region of interest with three representative cultivars. The genetic parameters for these maize cultivars are presented in Table 4.

CERES-Maize model validation under fixed irrigation

Due to a lack of suitable field experimental data, model validation was carried out on regional statistical grain maize yield reports (e.g. Grassini et al., 2015) of annual production, where no deviation between spring and winter maize is available. As in agricultural practice, maize is normally irrigated on demand, we validated CERES-Maize for irrigated simulation.

In general, moderately good performance of the CERES-Maize model was achieved with a NRMSE value for the annual maize yields of 10.3%. As the simulated yield level between spring and winter maize differs in most of the years, the comparison between the mean

simulated seasonal and mean annual reported yields shows a larger NRMSE value of 18.9% (spring maize) and 19.4% (winter maize) (Fig. 3).

Analysis of the performance of CERES-Maize by Index of Agreement (d) showed a moderate match between observed (statistical) annual maize yields and simulated annual maize yields with the (d) value of 0.77 (Fig.3).

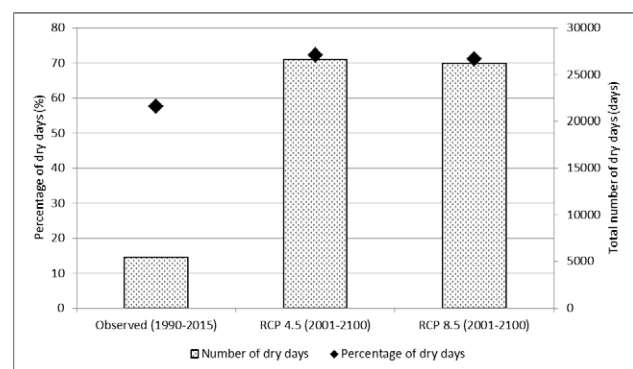


Fig. 2. Number of dry days from observed period (1990-2015) and projected period from 2001-2100 under RCP 4.5 and RCP 8.5.

Tab. 3. Calibration results of the DSSAT model for the winter maize season.

Genotype	SX2010		SX5012		LVN47	
	Observed	Simulated	Observed	Simulated	Observed	Simulated
Crop indices						
Planting date (DOY)	Winter	265	Winter	265	Winter	265
Silking(Beginning Peg stage) (*)	66	60	67	54	68	63
Physiological maturity (Harvest) (*)	120	133	123	122	123	136
Leaf index	2.9	5.66	2.4	5.68	2.9	5.76
Number of leaves per stem	19.6	15.49	19.9	16.22	19.5	16.07
Yield (kg/ha)	6440	7816	7370	8271	5660	8072

(*) (days after Planting date).

Concerning the technical improvement, the results reveal that the performance of CERES-Maize grain yield simulation between de-trended observed yields and simulated yields is better than the performance of the model between the real observed yields and simulated yields, shown by an increase of d-index from 0.77 to 0.86 and a decrease of the value of NRMSE from 10.3% to 7.3%. It was assumed that the detrended results are removed from climate-related influences such as new technologies in crop management or better cultivars.

Rainfed winter and spring maize yields under the selected climate scenarios

The simulated annual rainfed maize yields were mostly highest in the second 30-year period from 2035-2065, followed by the first 30-year period from 2001-2030. The lowest maize yields were received in the period 2070 – 2100. Besides, the average maize yields under both RCPs are quite similar. Under the RCP 4.5 scenario, the mean annual maize yield, the mean spring maize yield, and the mean winter maize yield are about 3957 kg/ha, 2483 kg/ha, and 5411 kg/ha, respectively, where under RCP 8.5 they are about 3854 kg/ha, 2353 kg/ha, and 5355 kg/ha, respectively (v. 4a-d).

In comparison with observed annual maize yields in the historical period (2000-2014), under the RCP 4.5 scenario, the mean annual rainfed maize yields over the 100 year period 2001-2100 increase by +3.6%, contributed by the increase in winter maize yields by +33.3% and a reduction of spring maize yields by 30.3%.

Under the RCP 8.5 scenario, the simulated spring maize also decreased in comparison with observed spring maize yield, and especially dramatic from 2070-2100 with a decline of 50.1% (w. 5). The simulated win-

Tab. 4. Calibrated crop coefficients for Thai Nguyen, Vietnam.

COEFF	Definitions	SX2010	SX5012	LVN47
P1	- Thermal time from seedling emergence to the end of the juvenile phase (expressed in degree days above a base temperature of 8 °C) during which the plant is not response to change in photoperiod.	140.4	121.0	125.0
P2	- Extent to which development (express as days) is delayed for each hour increase in photoperiod above the longest photoperiod at which development proceeds at a maximum rate (which is considered to be 12.5 h).	0.3	0.0	0.0
P5	- Thermal time from silking to physiological maturity (expressed in degree days above a base temperature of 8 °C).	685.0	685.0	685.0
G2	- Maximum possible number of kernels per plant.	907.9	907.9	907.9
G3	- Kernel filling rate during the linear grain filling stage and under optimum conditions (mg/day).	6.6	10.0	10.00
PHINT	- Phyllochron interval; the interval in thermal time (degree days) between successive leaf tip appearances.	44.92	38.9	38.9

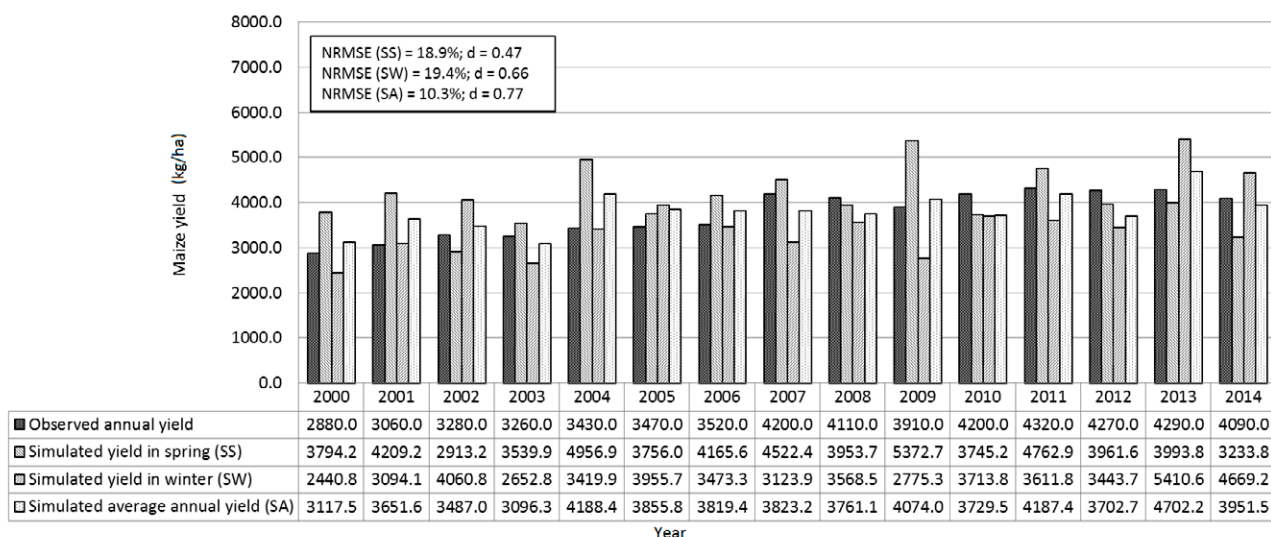


Fig. 3. Yield validation of spring and winter season maize 2000-2014 against statistically reported maize yields.

ter maize yield increased only by +18.2%, leading to a lower increase in annual maize yield compared to RCP 4.5 during the period 2001-2100 by +1.1% compared the observed yields 2000-2014.

DISCUSSION

To identify the impacts of climate parameters for maize yield potentials and trends in Vietnam under climate scenarios we focused on the simulation of rainfed maize only, although this does not fully represent current irrigation practice of occasional support irrigation.

The difference between spring and winter maize yields

On average, the simulated winter maize yields are significantly higher than spring yields. In reality, winter maize in northern Vietnam is sown after the end of the rainy season, where soils have still high water content. During winter maize growing season, precipitation is continuously decreasing, and effective solar radiation (data not shown) increases, forming ideal conditions for yield formation. The spring maize, sown in February, with low soil water contents often suffers drought stress during vegetative period, limiting its yield potential, so the spring maize yield stays lower on average than the yield of spring maize under current climate.

Climate change impacts on maize production in Vietnam and adaptation recommendations

Overall, under the two climate change scenarios in this study, RCP 4.5 and RCP 8.5, climate conditions are projected to be more extreme than in the past with higher temperature and lower seasonal precipitation. Both is expected to negatively impact maize production by a) shorter growing periods for annual crops due to higher temperatures and b) more drought stress conditions due to a higher number of dry days and higher evapotranspiration rates (forced again by higher temperatures).

Related to Thai Nguyen province, especially the spring maize season will suffer by increasing drought under future climate scenarios, while the winter growing season, despite increasing number of dry days, still remains with higher soil water content combined with increasing effective solar radiation. The study showed that annual rainfed maize yields in the 21st century will be slightly higher under two climate scenarios (RCP 4.5 and RCP 8.5) as in the reference period of 2000-2014, and only in the far future (period 2071-2100) would be generally lower than in the past, especially for spring season maize from 2070 to 2100 and under unchanged production technology. Although winter maize yield increase strongly, it could just outbalance the strong decreases in spring maize yields concerning annual yields under both applied climate scenarios. Other impacts on maize production, not considered in our simulation study, additionally can occur (e.g. reduced fertility, increased pest and disease challenges etc.). The influence of high temperature will become even more

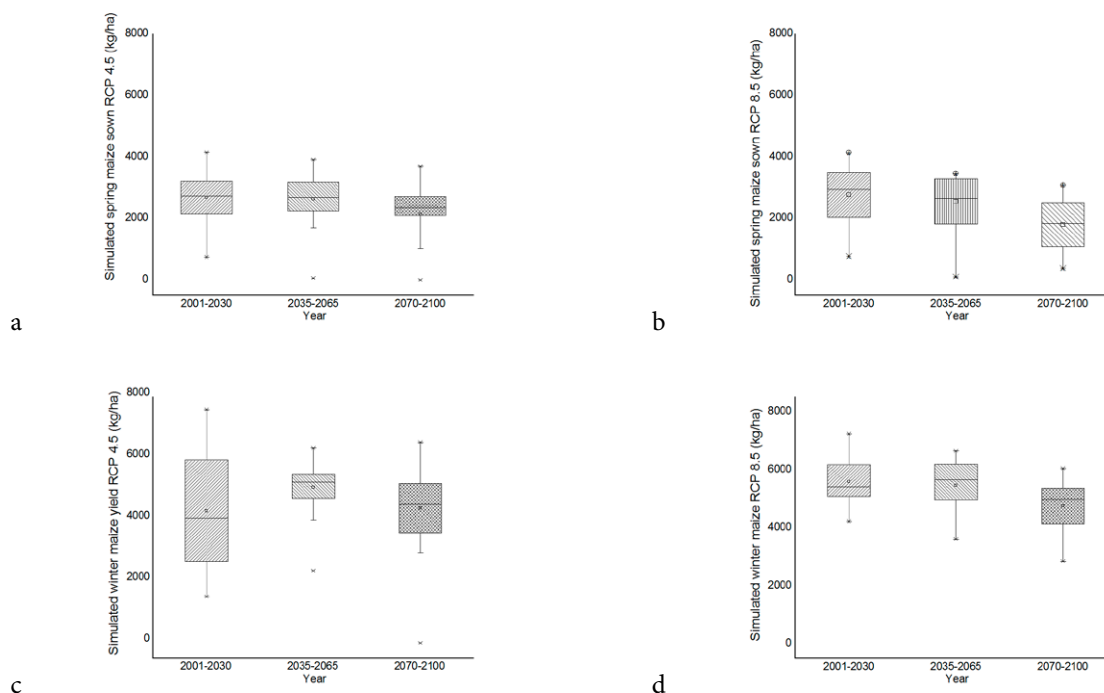


Fig. 4a-d. Simulated rainfed spring and winter season maize yields under the two different scenarios RCP 4.5 and RCP 8.5 for Thai Nguyen province, Vietnam. Boxes present 50% of all cases, including a horizontal line at the median and a dot at the mean.

extreme when it accompanies with water deficiency and drought stress. For example, in central Vietnam, maize yield decreased in dry seasons, driving farmers to change land use systems into other crops such as peanut, cassava or green bean (Uy et al., 2015).

Irrigation is considered globally as a crucial factor to mitigate the influence of drought stress on maize growth (van der Velde et al., 2010). Irrigation will become more important under the climate change perspective, especially in South Asia (Döll, 2002). Due to the typical characteristics of topography and hydrologic conditions of our study region Thai Nguyen, Vietnam, the irrigation system may expose to some difficulties in terms of water delivery in the dry season. Therefore, simultaneously building up an irrigation system, a system of dam or water storage in the local area might be a solution to store water in the rainy season and deliver water in the dry season.

In conjunction with irrigation, a shift in planting date also has positive influence in reducing drought stress impacts on maize production. Abraha & Gärn (2016) reported that flexible planting and rainwater harvesting have a substantial potential for reducing the negative impacts of climate change, and possibly even increasing outputs. In Southern Mali, earlier planting

date of maize in combination with recommended fertilizer rates and late-maturing varieties for medium farms were projected to decrease the impact of warming by 2.9 to 3.3 °C. Under controlled conditions, simulated maize grain yield even increased by 51-57% under current farmer fertilizer practices (Akinseye et al., 2017). Based on the local climate conditions (dry in early spring and late winter season), the planting date, therefore, may shift to be later in the spring season and sooner in the winter season to avoid the most extreme dry periods in early spring and late winter.

Limitations of the study

The uncertainties of our study can firstly be related to the availability of empirical data for crop model calibration and validation, however, fulfilling basic recommendations for crop model applications in data-poor countries (e.g. Grassini et al., 2015). Model validation was hampered by missing recorded seasonal maize yields that were not available in the local reports. Moreover, the recorded yields could have some mistakes that caused by the reporting local farmers and the local agriculture department. Another reason for deviations could be a difference in crop management between reality and

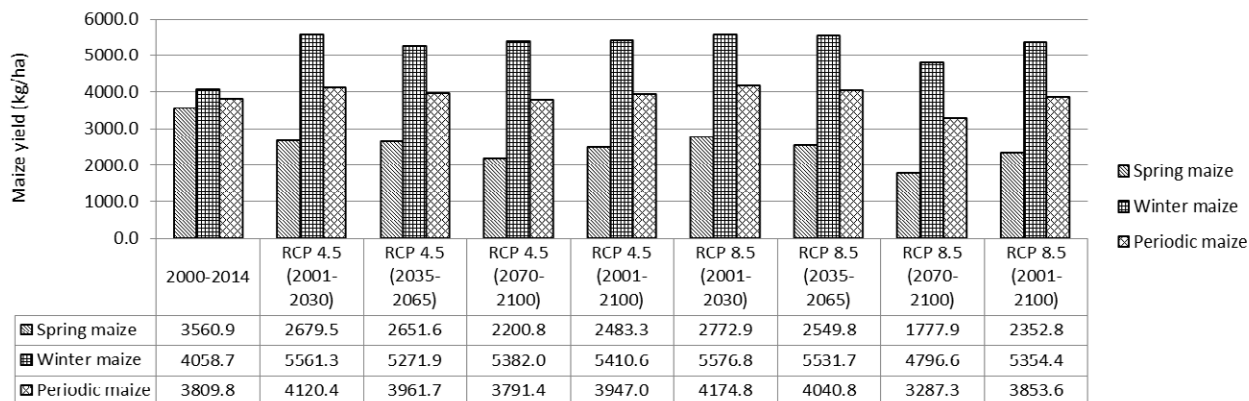


Fig. 5. Comparison of historical maize and simulated climate scenario periods rainfed maize yields.

simulation, for example, a different irrigation scheme between the simulation and reality in winter and spring seasons. In addition, the applied crop model may not be robust in simulating grain yield under extreme weather conditions, such as soil erosion occurring in the midland of the mountainous area or flooding which occurs in the fields located near the rivers. Further, the fact that we did not account for the potential CO₂-fertilizing effect (although limited for maize, but with complex and still uncertain environmental vs cultivar interactions (Adishesa et al., 2017) as well as crop rotation effects in the simulation (Ngwira et al., 2014), contribute to uncertainties in the results. In the study region, maize is usually cultivated with other crops in a flexible rotation to obtain the highest productivity. Additionally, the real maize yields and long term yield trends are also influenced by various elements that were not considered in the CERES-Maize model runs, such as occasional support irrigation, impacts of diseases and pests, future changes in production methods and technologies (fertilization, irrigation or new hybrid varieties or cultivars better adapted to drought conditions). All these effects are, however, ongoing in our case study region, which is still strongly developing towards more effective production.

CONCLUSIONS

Being the first crop simulation study on the impact of climate change on maize production in the central north of Vietnam, our study revealed important ongoing and potential future climatic changes of the two regional applied maize growing seasons, the spring and winter growing seasons. Main conclusions include especially an increasing rainfed yield difference between the two growing seasons with important implications for

increasing irrigation demand, especially for the spring season.

Although the CERES-Maize model applied in our study, showed good performance in estimating maize production under current conditions, several uncertainties remain, calling also for further research and data needs. First of all, there is still a gap on suitable, qualitative regional data bases for climate change impact studies, especially on experimental crop related data sets for model calibration and validation. This includes cultivar specific responses to various stresses such as drought, heat and nutrient based stresses and its combinations. Although the assimilation response to further increasing atmospheric CO₂-concentrations are considered as limited for C4 crops such as maize, uncertainties remain in relation to cultivar vs. environmental effects. More studies with complementary model approaches and ensemble simulations, based on improved and extended regional data bases of agricultural systems and ecosystems are needed to reduce potential uncertainties in future assessments.

ACKNOWLEDGEMENTS

The research for this paper was financially supported by the Vietnam International Education Cooperation Department (VIED) and Austrian agency for international mobility and cooperation in education, science and research (OeAD).

REFERENCES

Abraha G. and Gärn L., 2016. The effect of climate change and adaptation policy on agricultural production in Eastern Africa. *Ecological Economics*, 121: 54–64.

- Adishesha K., Janagoudar, B.S., Amaregouda, A., 2017. Response of maize (*Zea mays* L.) genotypes to elevated carbon dioxide and temperature regimes. *International Journal of Chemical Studies*, 5(5): 2448-2456.
- Araya, A., Hoogenboom, G., Luedeling, E., Hadgu, K. M., Kisekka, I., & Martorano, L. G., 2015. Agricultural and Forest Meteorology Assessment of maize growth and yield using crop models under present and future climate in southwestern Ethiopia. *Agricultural and Forest Meteorology*, 214–215: 252–265.
- Akinseye F.M., Adam M., Agele S.O., Hoffmann M P., Traore P.C.S., Whitbread A.M., 2017. Field Crops Research Assessing crop model improvements through comparison of sorghum (*sorghum bicolor* L. moench) simulation models: A case study of West African varieties. *Field Crops Research*, 201: 19–31.
- Bannayan M and Hoogenboom G., 2009. Using pattern recognition for estimating cultivar coefficients of a crop simulation model. *Field Crops Research*, 111(3): 290–302.
- Devkota K.P., Manschadi A.M., Devkota M., Lamers J.P.A., Ruzibaev E., Egamberdiev O., Amiri E., Vlek P.L.G., 2013. Simulating the impact of climate change on rice phenology and grain yield in irrigated drylands of Central Asia. *Journal of Applied Meteorology and Climatology*, 52: 2033-2050.
- Döll P., 2002. Impact of climate change and variability on irrigation requirements: A global perspective. *Climatic Change*, 54(3): 269-293.
- Ebrahimi E., Manschadi A.M., Neugschwandtner R.W., Eitzinger J., Thaler S., Kaul H.-P., 2016. Assessing the impact of climate change on crop management in winter wheat – A case study for eastern Austria. *The Journal of Agricultural Science, Cambridge*, 154(7): 1153-1170.
- Edalat M. and Kazemeini S.A., 2014. Estimation of cardinal temperatures for seedling emergence in corn, 8(7): 1072–1078.
- Eitzinger J., Trnka M., Semerádov D., Thaler S., Svobodová E., Hlavinka P., Siska B., Takáč J., Malatinská L., Nováková M., Dubrovsk, M., Zalud Z., 2013. Regional climate change impacts on agricultural crop production in Central and Eastern Europe – hotspots, regional differences and 34 common trends. *The Journal of Agricultural Science*, 151(6): 787-812.
- Eitzinger J., Thaler S., Schmid E., Strauss F., Ferrise R., Moriondo M., Bindi M., Palosuo T., Rötter R., Kersebaum K.C., Olesen J., Patil R., Saylan L., Caldag B., Caylak O., 2013b. Sensitivities of crop models to extreme weather conditions during flowering period demonstrated for maize and winter wheat in Austria. *J. Agric. Sci*, 151,:813-835.
- Eitzinger J., Trnka M., Hösch J., Žalud Z., Dubrovský M., 2004. Comparison of CERES, WOFOST and SWAP models in simulating soil water content during growing season under different soil conditions. *Ecological Modelling*, 171(3): 223–246.
- Eitzinger J., 2011. *Applied Agrometeorology*. Springer, Berlin, Germany, K. Stigter. xxxvii+1100 pp., ISBN 978-3-540-74697-3 (hardback).
- Grassini, P., Van Bussel. L.G.J., Van Werta, J., Wolf. J., Claessens, L., Yanga, H., Boogaarde, H., De Groote, H., Van Ittersum, H.K., Cassmana, K.G., 2015. How good is good enough? Data requirements for reliable crop yields simulations and yield-gap analysis. *Field Crops Research*, 177: 49-63.
- Hardacre A and Turnbull, H. L., 1986. The Growth and Development of Maize (*Zea mays* L.) at Five Temperatures. *Annals of Botany*, 58: 779-787.
- Iyanda R.A., Pranuthi G, Dubey S.K., Tripathi S.K., 2014. Use of dssatceres maize model as a tool of identifying potential zones for maize production in Nigeria. *International Journal of Agricultural Policy and Research*, 2: 69-75.
- Jing Q., Shang J., Huffman T., Qian B., Pattey E., Liu J., Tremblay N., 2017. Using the CSM-CERES-Maize model to assess the gap between actual and potential yields of grain maize. *Journal of Agricultural Science*, 155(2): 239–260.
- Jones J.W., Hoogenboom G., Porter C. H., Boote K. J., Batchelor W. D., Hunt L. A., Wilkens P.W., Singh U., Gijssman A. J., Ritchie J. T., 2003. The DSSAT cropping system model. *European Journal of Agronomy*, 18: 235–265.
- Kadiyala M.D.M., Jones J.W., Mylavarapu R.S., Li Y.C., Reddy M.D., 2015. Identifying irrigation and nitrogen best management practices for aerobic rice-maize cropping system for semi-arid tropics using CERES-rice and maize models. *Agricultural Water Management*, 149: 23–32.
- Kamali M.I. and Nazari R., 2018. Determination of maize water requirement using remote sensing data and SEBAL algorithm. *Agricultural Water Management*, 209: 197–205.
- Kisekka I., Schlegel A., Ma L., Gowda P. H., Prasad P. V.V., 2017. Optimizing preplant irrigation for maize under limited water in the High Plains. *Agricultural Water Management*, 187: 154–163.
- MacCarthy D. S., Adiku S. G., Freduah B. S., Kamara A. Y., Narh S., Abdulai A. L., 2017. Evaluating maize yield variability and gaps in two agroecologies in northern Ghana using a crop simulation model. *South African Journal of Plant and Soil*, 186: 1-11.

- Mangelsdorf P. C., 1947. The Origin and Evolution of Maize. Academic Press, In: M. B. T.-A. in G. Demerec (Ed.), 1: 161–207.
- Mickleburgh H. L and Pagán-Jiménez J. R., 2012. New insights into the consumption of maize and other food plants in the pre-Columbian Caribbean from starch grains trapped in human dental calculus. *Journal of Archaeological Science*, 39(7): 2468–2478.
- Nguyen H. H., 2008. Khả năng thích ứng của giống ngô lai trong 2 vụ xuân và đông năm 2008 tại Thái Nguyên, 62(13): 62–66.
- Ngwira A., Aune J, Thierfelder C., 2014. DSSAT modelling of conservation agriculture maize response to climate change in Malawi. *Soil and Tillage Research*, 143: 85-94
- Powell J. P and Reinhard S., 2015. Measuring the effects of extreme weather events on yields. *Weather and Climate Extremes*, 12: 69–79.
- IMHEN, Camau Peoples Committee, KienGiang Peoples Committee., 2011. Climate Change Impact and Adaptation Study in the Mekong Delta-Part A. In: Climate Change Vulnerability & Risk Assessment Study for Ca Mau and KienGiang Provinces, Vietnam. Institute of Meteorology, Hydrology and Environment of Vietnam, Hanoi, Vietnam, 250 pp.
- Soler C. M. T., Bado V. B., Traore K., Bostick W. M., Jones J. W., Hoogenboom G., 2011. Soil organic carbon dynamics and crop yield for different crop rotations in a degraded ferruginous tropical soil in a semi-arid region: a simulation approach. *The Journal of Agricultural Science*, 149(05): 579–593.
- Tenaillon M.I and Charcosset A., 2011. A European perspective on maize history. *Comptes Rendus Biologies*, 334(3): 221–228.
- TNDNRE (Thai Nguyen Department of Natural Resources and Environment)., 2015. Project report: Land degradation. People's Committee of Thai Nguyen province, Thai Nguyen, 237 pp.
- Thi-Minh-Ha H., Van-Tan P., Nhu-Quan L., Quang-Trung N., 2011. Extreme climatic events over Vietnam from observational data and RegCM3 projections. *Climate research*, 49: 87-100.
- Uy T. C., Limnirankul B., Chaovanapoonphol Y., 2015. Factors Impact on Farmers' Adaptation to Drought in Maize Production in Highland Area of Central Vietnam. *Agriculture and Agricultural Science Procedia*, 5: 75–82.
- Van der Velde M., Wriedt G., Bouraoui F., 2010. Estimating irrigation use and effects on maize yield during the 2003 heatwave in France. *Agriculture, Ecosystems & Environment*, 135(1): 90–97.
- Zhao W., Liu B., Zhang Z., 2010. Water requirements of maize in the middle Heihe River basin, China. *Agricultural Water Management*, 97(2): 215–223.



Citation: G. Ben Hamouda, F. Ventura (2020) Evaluation of some evapotranspiration estimation models under CO₂ increasing concentrations: A review. *Italian Journal of Agrometeorology* (1): 85-98. doi: 10.13128/ijam-831

Received: January 17, 2020

Accepted: May 3, 2020

Published: June 23, 2020

Copyright: © 2020 G. Ben Hamouda, F. Ventura. This is an open access, peer-reviewed article published by Firenze University Press (<http://www.fupress.com/ijam>) and distributed under the terms of the Creative Commons Attribution License, which permits unrestricted use, distribution, and reproduction in any medium, provided the original author and source are credited.

Data Availability Statement: All relevant data are within the paper and its Supporting Information files.

Competing Interests: The Author(s) declare(s) no conflict of interest.

Evaluation of some evapotranspiration estimation models under CO₂ increasing concentrations: A review

GHAIETH BEN HAMOUDA*, FRANCESCA VENTURA

Department of Agricultural and Food Sciences (DISTAL), Alma Mater Studiorum University of Bologna, Viale Fanin, 44, 40127, Bologna, Italy

*Corresponding author.

Email: ghaieth.benhamouda@unibo.it (G. Ben Hamouda), francesca.ventura@unibo.it (F. Ventura).

ORCID ID: 0000-0003-4182-0737 (G. Ben Hamouda), 0000-0003-0748-942X (F. Ventura)

Abstract. The total volume of CO₂ emissions is building up dramatically, and because of the effect of this gas on the growth, physiology, and biochemistry of plants, it is becoming increasingly necessary to look into the impact of the relentless rise of carbon dioxide. Although there are several developed approaches that tried to model the canopy resistance, many of these methodologies ignored the effect of CO₂ or were not incorporated with the existing evapotranspiration calculation methodologies, mainly due to the complexity of the modeling procedure and the short time framework of the conducted studies. This review explores the few models estimating crop water requirements that account for this effect and examines their assumptions and theories. The inclusion of canopy resistance models in evapotranspiration calculation may be of questionable utility without improvements in some modeling aspects, such as the relationship between the stomatal conductance and CO₂ and the climatic variables taken in consideration in the modeling process.

Keywords. Penman Monteith, ETo, carbon dioxide, canopy resistance, surface resistance, climate change.

INTRODUCTION

According to UNDESA (2017), the world population is foreseen to grow between 20-30% by 2050, going from 7.7 billion people in 2017 to between 9.2 and 10.2 billion. Naturally, the global demand for food production is also expected to increase by almost 60% by 2025 (Alexandratos and Bruinsma, 2012; OECD, 2012). On the other side, global water consumption has already known a leap of 600% over the last century (Wada et al., 2016), and it keeps increasing by 1% yearly (AQUASTAT n.d.). Water demand is currently evaluated at 4.600 km³ and could reach almost 6000 km³ by 2050 (Burek et al., 2016). All this will put more pressure on the agricultural sector, which is the actual largest world consumer of freshwater, mostly for irrigation, accounting for 70% of freshwater withdrawals, up to 90% by 2050 (WWAP, 2012). Agriculture is also expected to face a fierce competition for water resources from other sectors, resulting in a decrease in its share of total water use in developing countries from 86% in 1995 to 76% in 2025 (Rosegrant et al., 2002). In addition, global warming is meanwhile affecting the water cycle and shifting weather patterns (IPCC, 2014a). Therefore, the agricultural sector is in great need of creating strategies to improve water management and, consequently, attain greater levels of water savings in order to face these aforementioned challenges (de Fraiture and Wichelns, 2010).

One of the key components to improving the management of water resources is accurately determining the water requirements of irrigated crops. These needs depend on the management strategy chosen, and are based on the demand for atmospheric water, known as evapotranspiration. Evapotranspiration (ET) is a major component of the hydrological cycle and has an important effect on the quality of water, since in the evaporation process the water is purified. This clean H₂O restores about 60% of global land surface water. For vegetated ecosystems, it is also the main component of energy balance, employing more than 50% of absorbed solar radiation (Trenberth et al., 2009). In fact, evapotranspiration is a component of the energy budget involving incoming energy and outgoing water, occurring at the crop surface. The other components of the budget are net radiation, sensible heat flux, soil heat flux, and solar radiation stored as photochemical energy. This exchange process creates an atmospheric demand that is satisfied by transferring water out of the plant system through evapotranspiration. Such phenomenon is regulated by the principle of energy conservation or energy balance: energy arriving at the vegetation surface equal energy leaving the same surface for the same time peri-

od. The energy balance equation for an evaporating surface can be written as:

$$R_n - G - \lambda ET - H = 0 \quad (1)$$

where R_n is net radiation, H sensible heat, G soil heat flux and λET is the latent heat flux. Terms can be either positive or negative: positive R_n supplies energy to the vegetation surface and positive G , λET and H remove energy from the vegetation surface. The latent heat flux (λET) is the evapotranspiration fraction and can be derived from the energy balance equation, if all other components are known. ET is an important hydrological variable for irrigation water management, hydrological modeling and water balance calculations. Penman (1963) defines ET as the combination of two separate processes occurring simultaneously, evaporation from the soil surface and transpiration from the crop. Since the evapotranspiration is strongly affected by crop type, crop development and management practices, there was a need to find a concept to express the evaporative demand of the atmosphere independently of those factors. Hence, reference evapotranspiration (ET_o) was introduced for this purpose. ET_o is defined as the evapotranspiration rate from a well irrigated hypothetical grass reference crop with specific characteristics. It expresses the evaporating power of the atmosphere at a specific location and time of the year and does not consider crop characteristics and soil factors. Instead, it is driven by weather parameters, which are solar radiation, air temperature humidity and wind speed. A thorough understanding of ET_o is the first step to achieving efficient and effective water management and irrigation scheduling. The United Nations Food and Agriculture Organization (FAO) has adopted an updated Penman–Monteith equation (FAO-PM) as a global standard for estimating grass reference evapotranspiration (Allen et al., 1998). This equation was chosen as it provides a better prediction compared to other methods in a wide variety of geographic locations and climatic conditions (Kashyap and Panda, 2001; Yoder et al., 2005; López-Urrea et al., 2006; Suleiman and Hoogenboom, 2007; Adeboye et al., 2009; Rasul and Mahmood, 2009; Rácz et al., 2013). It includes all the different atmospheric variables that influence ET, which makes it suitable for climate change impact studies (Kingston et al., 2009; Islam et al., 2012; Priya et al., 2014). However, despite the completeness of this equation, it simulates poorly the effect of CO₂, that is represented by the “canopy resistance” or “surface resistance” term, r_c . In fact, daily r_c is fixed at 70 s m⁻¹ and is considered constant regardless of climate type and change in climate patterns, thus contradicting published reports

(Long et al., 2004; Damour et al., 2010). Although Allen et al. (2006) considered that fluctuation in its value would have a negligible effect on the ETo calculation, many experimental studies disagree with their statement on hourly, daily and seasonal scales (Steduto et al., 2003; Katerji and Rana, 2006, 2011, 2014; Yan et al., 2017). This is particularly true when the crop is under well-watered conditions, i.e. when the physiological component of r_c is at its minimum. The alarming increase of CO₂ concentrations due to climate change, the physiological effects that it would have on crop plants (Tubiello et al., 2000; Long et al., 2004; Mall et al., 2017) and the uncertainties affecting the calculation of ETo using the FAO-PM equation, have prompted many researchers to develop other approaches and models to estimate reference evapotranspiration, taking into account the variability of the canopy resistance r_c . Following a short discussion on the effect of rising CO₂ on crops evapotranspiration, this paper provides an overview of these different methods, delineating their main theories and assumptions, and exploring their strengths and weaknesses.

EFFECT OF CO₂ ON CROPS EVAPOTRANSPIRATION

Our planet's atmosphere witnessed a gradual change throughout history, experiencing a wide range of CO₂ concentration. Studies suggest that this concentration may have been about 4000 to 5000 ppm some 500 million years ago (Ehleringer et al., 2005). Then, this concentration decreased to around 1000 ppm between 35 and 55 million years ago, falling abruptly to about 390 ppm during Oligocene by approximately 32-25 million years ago (Tippie and Pagani, 2007). This decline in CO₂ limited the efficiency of photosynthesis, triggering the evolution of C₄ plants from ancestral C₃ species as a clever solution to the problem of low atmospheric CO₂. Since the pre-industrial era, anthropogenic greenhouse gas (GHG) emissions have been causing new increases in the atmospheric concentrations of carbon dioxide, going from 270 ppm before 1700 to about 410 ppm in 2020, reaching unprecedented levels in at least 800,000 years. The concentration will keep increasing if no additional efforts are made to reduce emissions (IPCC, 2014a, 2014b). These increasing concentrations have important physiological effects on plants, e.g. faster rate of photosynthesis, greater leaf area, increase in biomass and yield and decrease in stomatal conductance and transpiration rate (Allen, 1990; Ainsworth and Long, 2004; van der Kooi et al., 2016). The latter effect has been confirmed by several experimental studies conducted in open-top and closed-top chambers or using the Free-Air Carbon dioxide Enrich-

ment (FACE) method (Wullschleger et al., 2002; Shams et al., 2012). On the other hand, more biomass means more evapotranspiration because of a higher leaf area index (LAI) (Wand et al., 1999; Piao et al., 2010), potentially offsetting the effect of the reduction in stomatal conductance (Bernacchi et al., 2007). However, even under experimental conditions, there is a large uncertainty in the CO₂ induced change in stomatal conductance, especially when scaling from the single leaf to a full canopy where other factors affect the whole process (Polley, 2002). For example, CO₂ effect is significantly different between C₃ and C₄ plants and between trees and smaller plants (Taiz and Zeiger, 1991), but also seems to depend on the scale of the experiment (Jarvis and McNaughton, 1986; Bunce, 2004). In fact, most of the existing knowledge on plants response to higher CO₂ concentrations is based on small scale research experiments conducted in open field with controlled environment. Even if there are techniques such as FACE that allow the exposure of plants to elevated CO₂ concentrations under natural and fully open-air conditions, they can be difficult and expensive to construct and operate, which limits the inference space of these experiments with regards to the range of global ecosystems (Norby et al., 2016). Moreover, there could be an overestimation of the CO₂ effect due to artificial ventilation and advection from outside the FACE area (Kruijt et al., 2008). Given the complexity of the effect of CO₂-sensitivity of evapotranspiration on future climate simulations and the large uncertainty in the CO₂ induced change in stomatal conductance under experimental conditions (Kruijt et al., 2008), understanding plant responses to CO₂ is becoming increasingly important.

This review paper summarizes some of the most documented r_c models, precisely those directly used or modified to account for the effect of CO₂ on the evapotranspiration. The models presented (Table 1) have their limitations that the authors tried to underline. However, because the literature is limited regarding this particular topic, the primary purpose of this review was to provide a brief reference document for researchers and the scientific community in general on the different models developed so far and their main findings and challenges.

DESCRIPTION AND DISCUSSION OF EVAPOTRANSPIRATION APPROACHES ACCOUNTING FOR CO₂ EFFECT

Penman-Monteith method adapted to an increase in CO₂ concentrations

The standardized Penman–Monteith equation (FAO-PM) (Allen et al., 1998) is based on the Penman–Montei-

th equation (Monteith, 1965). It is the most widely used method and has been proven to be a good ETo estimator when compared with other methods, especially for daily computations (Chiew et al., 1995; Liu et al., 1997; Ventura et al., 1999; Jacobs and Satti, 2001; Garcia et al., 2004; Temesgen et al., 2005). For a grass reference surface and for a daily time step, this equation is expressed as:

$$ETo = \frac{0.408\Delta(R_n - G) + \gamma \frac{900}{T_{2m} + 273} \cdot u_2 (e_s - e_a)}{\Delta + \gamma(1 + 0.34u_2)} \quad (2)$$

where ETo is the reference evapotranspiration (mm day^{-1}); R_n is the net radiation at the crop surface ($\text{MJ m}^{-2} \text{day}^{-1}$); G is the soil heat flux density ($\text{MJ m}^{-2} \text{day}^{-1}$); T_{2m} is the mean daily air temperature at 2 m height ($^{\circ}\text{C}$); u_2 is the wind speed at 2 m height (m s^{-1}); e_s is the saturation vapour pressure (kPa); e_a is the actual vapour pressure (kPa); $(e_s - e_a)$ is the saturation vapour pressure deficit (kPa); Δ is the slope of the vapour-pressure curve ($\text{kPa } ^{\circ}\text{C}^{-1}$) and γ is the psychrometric constant ($\text{kPa } ^{\circ}\text{C}^{-1}$).

The canopy resistance r_c describes the resistance of vapour flow through the transpiring crop and evaporating soil surface. It is represented in the equation above by the value 0.34 in the denominator:

$$0.34u_2 = \frac{70}{208/u_2} = r_c/r_a \quad (3)$$

where r_a is the aerodynamic resistance (s m^{-1}), which describes the transfer of heat and water vapour from the evaporating surface into the air above the canopy. For a grass reference surface, assuming a constant crop height of 0.12 m and a standardized height for wind speed, temperature and humidity at 2 m, r_a becomes:

$$r_a = 208/u_2 \quad (4)$$

Under the same reference conditions, and knowing that the stomatal resistance r_s of an actively transpiring C_3 grass leaf surface has a value of about 100 s m^{-1} , r_c is represented as the following:

$$r_c = \frac{r_s}{0.5 \text{ LAI}} = \frac{100}{0.5 \times 2.88} = 69 \approx 70 \text{ s m}^{-1} \quad (5)$$

where LAI is the leaf area index of the upper half of dense clipped grass, which is generally the only part actively contributing to the surface heat and vapour transfer ($LAI = 24 \times \text{crop height (h)} = 24 \times 0.12 = 2.88$)

Assuming that the $r_c \approx 70 \text{ s m}^{-1}$ applies to a specific CO_2 concentration, estimating a new r_c value for higher CO_2 concentration provides a method to estimate possible impacts of higher CO_2 on ETo. Thus, the following form of FAO-PM equation should be adopted:

$$ETo = \frac{0.408\Delta(R_n - G) + \gamma \frac{900}{T_{2m} + 273} \cdot u_2 (e_s - e_a)}{\Delta + \gamma(1 + r_c/r_a)} \quad (6)$$

Lovelli et al. (2010) and Snyder et al. (2011) used this method in a Mediterranean climate, introducing in the equation published values regarding atmospheric CO_2 on stomatal conductance (Long et al., 2004; Ainsworth and Long, 2004), and considering the temperature increment effect on the reference evapotranspiration (ETo) variation. They concluded that the effect of increasing CO_2 concentration may be annulled by an increase in air temperature and subsequent increase in evapotranspiration rate. On the other hand, Moratitel et al. (2011) found out that the CO_2 increase from 372 ppm to 550 ppm would create a reduction of the ETo increment by half, from 11% to 5% in the next 50 years, as compared to the current situation in northern Spain. By recalibrating the canopy conductance for the widely acclaimed and recommended FAO-PM equation, this approach may be particularly effective in evaluating the effects of climate change on crop water use. However, The FAO-PM model is based on the “big leaf” approximation with constant

Tab. 1. Some of the models referenced in this work

Model	Reference	Simulation Period	CO_2 concentration
Penman Monteith with a modified r_c	Lovelli et al. (2010)	2071 - 2100	550 ppm
	Moratitel et al. (2011)	2007 - 2050	372 and 550 ppm
	Snyder et al. (2011)	2050	550 ppm
CO_2 -factor	Easterling et al. (1992)	Analog period: 1931 - 1940	330 and 660 ppm
	Ficklin et al., (2009)	NA	550 and 970 ppm
	Islam et al., (2012)	2010 - 2099	450 ppm to 900 ppm
	Wu et al., (2012)	2071 - 2100	330 and 660 ppm
	Fares et al., (2015)	NA	330, 550, 710 and 970 ppm
F factor	Olioso et al. (2010)	2020 - 2049 and 2070 - 2099	540, 703 et 836 ppm
	Salmon-Monviola et al. (2013)	1961-1990, 2010-2039, 2040-2069 and 2070-2099	330, 430, 545 and 640 ppm
Jarvis	Medlyn et al. (2001)	NA	350-700 ppm
Katerji and Perrier	Katerji et al. (2017)	1981 - 2006 and 2070 - 2100	600 and 850 ppm

canopy resistance, which is a simplistic assumption that could limit the accuracy of the predictions of the model. Considering the driving meteorological variables at a particular site, estimates made with the FAO-PM equation rely on the correct modeling of the effective values of both aerodynamic resistance r_a and canopy resistance r_c . Hence, the fixed value for r_c may be the cause of the tendency for the FAO-PM method to underestimate the higher values of measured ETo, and to overestimate the lower ETo values in semi-arid and windy areas with a high evaporative demand (Hussein, 1999; Ventura et al., 1999; Berengena and Gavilan, 2005). As r_a can be calculated from meteorological conditions, in order to provide more accurate estimations of evapotranspiration using the FAO-PM equation, it may be necessary to parameterise r_c as a primary factor in the evapotranspiration process (Monteith, 1965). Canopy resistance r_c is a physiological parameter with an aerodynamic component (Alves et al., 1998). It is difficult to estimate it for different climatic and crop water conditions, as it is influenced by solar radiation, temperature, vapor pressure deficit and soil water content (Lecina et al., 2003; Pereira et al., 1999). Nevertheless, a simple attempt to model this resistance may yield a better estimation when the FAO-PM equation is applied over both short and tall crops (Alves and Pereira, 2000; Pereira et al., 1999) and over other types of vegetation (Chávez and López-Urrea, 2019; Margonis et al., 2017). It could also be useful to incorporate the effects of the resistance due to vegetation into climatic and hydrological models (Yang et al., 2019; Bie et al., 2015).

In this context, some studies incorporated a “CO₂-factor” into the FAO-PM equation (Easterling et al., 1992; Ficklin et al., 2009; Parajuli, 2010; Islam et al., 2012; Wu et al., 2012; Priya et al., 2014; Fares et al., 2015). Then, equation (1) can be rewritten as:

$$ET_o = \frac{0.408\Delta(R_n - G) + \gamma \frac{900}{T_{2m} + 273} \cdot u_2 (e_s - e_a)}{\Delta + \gamma \left(1 + \frac{0.34u_2}{CO_2\text{-factor}}\right)} \quad (7)$$

where, in the denominator, a linear relationship for stomatal conductance as a function of CO₂ level is introduced. It was developed by Stockle et al. (1992), and based on 80 data sets comparing leaf conductance at 330 ppm and at 660 ppm of CO₂ concentration for a wide range of species including C₃ and C₄ crops:

$$g_{CO_2} = g \left[1.4 - 0.4 \frac{CO_2}{330}\right] \quad (8)$$

where g_{CO_2} is the leaf conductance modified to reflect CO₂ effects (m s⁻¹); g is the conductance without the

effect of CO₂ (m s⁻¹); CO₂ is the actual atmospheric CO₂ concentration (ppm) and 330 represents the baseline atmospheric CO₂ concentration (ppm). The new r_c is as follows:

$$r_c = \frac{1}{g_{CO_2} \times 0.5 LAI} \quad (9)$$

The “CO₂-factor” is based on experimental observations of a 40% linear decrease in stomatal conductance between 330 and 660 ppm CO₂ concentrations (Morison and Gifford, 1983). Islam et al. (2012) incorporated this model in the FAO-PM equation to evaluate the effects of possible future anthropogenic climate change on ETo. Results of the different simulation studies showed an increase in ETo with changing climate, but the impact of increasing temperatures was almost offset by increasing CO₂ levels. In fact, sensitivity analysis showed that the effect of a 1°C rise in temperature was offset by an increase in CO₂ levels up to 450 ppm, whereas the effect of a 2°C temperature rise was offset by CO₂ concentrations of 660 ppm, thus in close agreement with results found by Priya et al. (2014) using the same model. Authors pointed out that, due to its linearity, this “CO₂-factor” is only valid in the range of 330 to 660 ppm. For CO₂ concentrations beyond 660 ppm, factors for specific crops reported by Allen (1990) were used. The same remark was made by Ficklin et al. (2009) when increasing CO₂ concentration to 970 ppm and temperature by 6.4 °C caused watershed-wide average evapotranspiration, averaged over 50 simulated years, to decrease by 37.5%, resulting in an increase of water yield by 36.5%. They explained that the linear assumption of eq. (8) means that it is suitable for all plant species, which may lead to an overestimation of the aforementioned reduction in ETo in the presence of multiple types of land cover. They concluded that because of this broad simplification of the effects of CO₂ on plant growth, their analysis was still too uncertain for water management purposes. The presumed overestimation of ETo is because this “CO₂-factor” is based on the assumption that a doubling of CO₂ concentration would lead to a general decrease of 40% in stomatal conductance (Morison, 1987) irrespective of the land cover type. This reduction of conductance is assumed to be linear over the entire range of CO₂ concentrations between 330 ppm and 660 ppm (Morison and Gifford 1983). To overcome this issue, Wu et al. (2012) proposed an optimised equation:

$$g_{CO_2} = g \left[(1+p) - p \frac{CO_2}{330} \right] \quad (10)$$

where p is the percentage decrease in leaf conductance specific to vegetation types (Authors provided different values in their study). The modified equation inherently gave a better representation of this increasing CO₂ effects than the original equation by incorporating the CO₂ effects dynamically in more process-based details.

Olioso et al. (2010) suggested multiplying the FAO-PM ETo by another factor F to correct the daily values of reference evapotranspiration taking into account the effect of higher CO₂ concentrations. This factor was derived from evapotranspiration simulations of the ISBA-A-gs model (Calvet et al., 1998) at different CO₂ levels, and used in different studies (Martin et al., 2011; Lardy et al., 2012, 2014; Salmon-Monviola et al., 2013; Katerji et al., 2017):

$$F = 1.1403 - 3.8979 \times 10^{-4} \times [\text{CO}_2] \quad (11)$$

The value of F is approximately 1 when the mean annual value of the air CO₂ concentration is equal to 370 ppm. F decreases or increases when the CO₂ concentration is higher or lower than this threshold. For example, the decrease in ETo is approximately 8 and 20 % when the CO₂ concentration reaches 550 and 900 ppm, respectively (Olioso et al., 2010). The factor is also based on a linear relationship between the decrease of ETo and the increase of the CO₂ concentration, which raises the same concerns previously discussed.

According to Katerji et al. (2017), the issue of the approaches mentioned above is that they are insufficient to adapt the FAO-PM equation to the increasing concentrations of CO₂. These solutions always consider the resistance r_c to be constant by neglecting its reliance on climatic variables, which means that r_c parameterisation is required to reduce the difference between the directly measured ETo values, and those estimated using the FAO-PM model.

PENMAN-MONTEITH METHOD WITH VARIABLE CANOPY RESISTANCE MODELS

Jarvis Model

Jarvis model is a phenomenological and multiplicative empirical model that interprets field measurements of stomatal conductance g_{CO_2} in relation to environmental variables. It calculates g_{CO_2} by multiplying the maximum conductance g_{max} , which is a value which represents the highest g recorded under optimal conditions (Korner et al., 1979), with a number of empirical response functions, including one for CO₂-sensitivity,

and it is assumed that each variable acts independently (Jarvis, 1976; Whitehead, 1998):

$$g_{\text{CO}_2} = \frac{1}{r_s} = g_{\text{max}} f(I) f(T_a) f(C_a) f(\text{VPD}) f(\Psi) \quad (12)$$

where I is the absorbed photosynthetic photon flux density ($\mu\text{mol m}^{-2} \text{s}^{-1}$), T_a is the air temperature ($^{\circ}\text{C}$), C_a is the CO₂ concentration (ppm), VPD is the Vapour Pressure Deficit (kPa) and Ψ is the soil water potential (Pa).

Same as the aforementioned models, Jarvis model is also based on a linear function between the stomatal conductance g_{CO_2} and atmospheric CO₂. In fact, Jarvis (1976) concluded that g_{CO_2} decreased linearly when the increase in CO₂ concentration is within the range of 100-1000 ppm, and that it stays constant when the CO₂ concentration is <100 ppm or >1000 ppm. Also, equation (12) may underestimate g_{CO_2} when relative humidity (RH) is high because it correlates g_{CO_2} linearly to RH (Wang et al., 2009). In this case, a nonlinear function of RH or VPD may reduce the bias (Leuning, 1995; Wang et al., 2009).

Nevertheless, Jarvis model has been used in different forms in many studies (Hanan and Prince, 1997; Gharsallah et al., 2013; Zhang et al., 2016; Zhou et al., 2019). In the east coast region of North America, elevated atmospheric CO₂ was found to reduce ET at a rate of 0.84 mm/year between 1901 and 2008 when calculating stomatal conductance with a Jarvis-type equation in the Dynamic Land Ecosystem Model (DLEM) 2.0 (Yang et al., 2015). Using the same model in a global scale, Pan et al. (2015) concluded that increasing atmospheric CO₂ will lessen the positive effect of warming temperature and increasing precipitation on ET by the end of the 21st century. Medlyn et al. (2001) analysed data from 13 long-term (>1 year) field-based studies of the effects of elevated CO₂ concentration (350 ppm and 700 ppm) on European forest tree species by fitting data to two models namely Jarvis and Ball (Ball et al., 1987). Their meta-analysis indicated a significant decrease (21%) in stomatal conductance in response to growth in elevated CO₂ concentrations across all studies, resulting in a decrease of ET.

Some authors think that another limit of the Jarvis model is that each response function has to be adjusted to the data to be able to provide good predictions for any type of vegetation, since they are specific for only certain crops and climate conditions and they cannot be used for general purposes (Yu and Wang, 2010). Consequently, a site-specific calibration of the empirical response functions becomes necessary. Another criticism formulated against this approach is that the knowledge of stomatal resistance r_s alone may not be sufficient to

calculate ET because the FAO-PM equation requires r_c . Hence, the upscaling of r_s to the canopy level is required to calculate r_c , which could be quite challenging (Irmak et al., 2008). Besides, Alves and Pereira (2000) questioned the validity of the multiplicative model because it only includes the physiological component of r_c but not the aerodynamic component r_a and because of the assumption of environmental variables acting independently.

Katerji and Perrier (KP) model

Based on the fact that r_c , for well-watered crops, varies during the day with different climatological variables, Katerji et al. (1983) suggested a new semi-empirical procedure to determine both resistances r_c and r_a by applying the Buckingham π -theorem (Kreith and Bohn, 2001). They established a linear relationship between the canopy resistance r_c and the climatic resistance r^* (Monteith, 1965):

$$r_c/r_a = a r^*/r_a + b \quad (13)$$

where a and b are empirical calibration coefficients which vary with crop type but not with site (Rana et al., 1998). Parameter values for a few crops were provided by Katerji and Rana (2014). r^* ($s\ m^{-1}$) is represented by the following equation:

$$r^* = \frac{\Delta + \gamma \rho C_p D}{\Delta \gamma R_n - G} \quad (14)$$

where ρ is the air density ($kg\ m^{-3}$), C_p the specific heat of moist air ($J\ kg^{-1}\ C^{-1}$) and D is the vapor pressure deficit (VPD) (kPa).

However, this model still does not take into account the impact of the air CO₂ concentration value on the resistance r_c . After incorporating their model into the FAO-PM equation (PM-KP), Katerji et al. (2017) used a CO₂ correction factor (Olioso et al., 2010) with the PM-KP equation to compare it to the standard Penman-Monteith method (FAO-PM) with a fixed r_c value. PM-KP yielded better performances in forecasting the ETo directly measured by weighing lysimeters during the summer season for the measured period (1986–2006) in Apulia region in southern Italy (Katerji et al., 2017). The results demonstrated that the FAO-PM formula underestimated the measured ETo values by 20 %, whereas the underestimation is only 3 % for the PM-KP formula.

This semi-empirical KP approach has been widely used in the subsequent literature (Peterschmitt and Perrier, 1991; Alves and Pereira, 2000; Lecina et al., 2003; Steduto et al., 2003; Pauwels and Samson, 2006; Liu et

al., 2012b; Margonis et al., 2017). However, one of its main limitations is the need for a specific calibration, even if it can be unnecessary under certain circumstances (Rana et al., 1998, 2001; Katerji and Rana, 2008). Furthermore, Gharsallah et al. (2013) insisted that the model's performance would probably be improved calibrating the a and b parameters for the main phenological phases of crops, making the use of this model even more complicated. A second limitation is the fact that it depends on the temporary value of the Bowen ratio β , which is not readily available (Perez et al., 2006). Besides, the KP model seems to fail under irrigated conditions in semiarid to arid regions (Allen et al., 2006).

MODIFIED MAKKINK EQUATION

Makkink model (Makkink, 1957) is a simple empirical method for ETo estimation that uses only temperature and radiation parameters:

$$ET_o = \alpha \frac{S}{\lambda(S + \gamma)} K\downarrow \quad (15)$$

where $K\downarrow$ is the incoming short-wave (global) radiation ($W\ m^{-2}$), λ is the latent heat of vaporization of water ($J\ kg^{-1}$), S is the temperature-dependent gradient of the saturated vapour pressure curve ($Pa\ K^{-1}$) and α is an empirical coefficient ($= 0.65$).

This formula does not take into consideration the effects of CO₂. To fix that, Kruijt et al. (2008) multiplied eq. (15) with a correction factor c :

$$c = S_g \times S_T \times F_T \times \Delta_{CO_2} \quad (16)$$

$$S_g = (dg/g)/dCO_2 \quad (17)$$

$$S_T = (dT/T)/(dg/g) \quad (18)$$

where g is the stomatal conductance ($mol\ m^{-2}\ s^{-1}$), S_g is the sensitivity of g to CO₂ (ppm^{-1}), S_T is the relative sensitivity of transpiration T to g ($kg\ m^{-2}\ s^{-1}$), F_T is the transpiration share of evapotranspiration and Δ_{CO_2} is the change in atmospheric CO₂ concentration (ppm).

After parametrizing S_g , S_T and F_T based on the literature, Kruijt et al. (2008) provided correction factors applied to a projected additional increase of atmospheric CO₂ concentrations in 2050 and 2100 by 150 and 385 ppm respectively for various vegetation categories. Results of their study suggest that direct effects of CO₂ reducing evapotranspiration can be expected to be moderate, up to 5% in the coming 50 years and up to 15% by 2100. Applying their methodology in Central and

Eastern Europe resulted in a decrease in reference evapotranspiration rates compared with runs that did not consider increases in CO₂ levels (Eitzinger et al., 2013). Similarly, Huntington et al. (2016) concluded that crop evapotranspiration is projected to increase in all basins of Western United States, especially areas where perennial crops are grown, and with smaller increases in areas where annual crops are grown.

Based on the extensive number of manuscripts on the topic reviewed by the authors, there is an abundance of models with a modified canopy resistance r_c (e.g. Shuttleworth and Wallace, 1985; Massman, 1992; Stannard, 1993; Todorovic, 1999; Irmak and Mutiibwa, 2010). However, very few of them took in consideration the change in atmospheric CO₂, hence the small number of models discussed in this study. This is essentially because when the time span of the research is short, the change in atmospheric CO₂ concentration is very small and is generally ignored (Li et al., 2014; Zhang et al., 2008). Furthermore, some of these models were not even incorporated into the FAO-PM equation to estimate ET responses to increased CO₂ concentration (e.g. Ball et al., 1987; Wang and Wen, 2010). The main issue with the previously reviewed models is that the relationship between stomatal conductance and CO₂ concentration is assumed to be a simple linear one, which is an assumption only valid within the limited range of 330–660 ppm (Li et al., 2019). In fact, those models rarely went beyond that range where data are better fitted with a nonlinear curve. This observation is consistent with the findings of Health and Russell (1954), Morison and Gifford (1983) and Wang and Wen (2010). Thus, it is crucial and indispensable to validate the accuracy and reliability of these models when applying them into the FAO-PM equation especially when the CO₂ concentration is higher than 660 ppm, and to choose the appropriate one to improve the estimation of ET under elevated CO₂ concentration.

Although some studies applied modified simple empirical equations, such as Makkink (Kruijt et al., 2008) and Priestley-Taylor (Rosenzweig and Iglesias, 1998; Hatch et al., 1999; Strzepek et al., 1999) to account for the vegetation responses to an elevated atmospheric CO₂, the FAO-PM method has been always considered to be the most reliable one for various climatic conditions due to its physically based characteristic with incorporating both physiological and aerodynamic parameters (Xu et al., 2006). However, its use of a fixed canopy resistance of 70 s m⁻¹ is perceived as weakness, as surface resistance may change with climate and weather parameters, variation in day length, or differences between daytime and nighttime wind (Pereira et al., 1999). In fact, this fixed r_c hypothesis has not been veri-

fied in experimental trials carried out on irrigated grass surfaces which underlined significant variations in the canopy resistance r_c on daily and seasonal scales (Rana et al., 1994; Steduto et al., 2003; Katerji and Rana, 2006; Lecina et al., 2003; Perez et al., 2006). The same criticism applies to the models discussed above since they are replacing the constant daily values of the grass r_c with different but always constant values, or using a simple correction factor with the FAO-PM formula, which could be because of the complexity of the canopy resistance modelling (Katerji and Rana, 2006).

CONCLUSION

This paper provides an overview of surface resistance models found in literature that included the effect of CO₂ on crop evapotranspiration. The paper reports a brief explanation of the main theories and assumptions involved in the models' development and underlines their main characteristics. Using these models would help improving the accuracy of ET estimations. Yet, modeling canopy resistance is a difficult task as its value depends on vegetation type, climate, plant architecture and, in water scarcity conditions, on plant and/or soil water status (Shuttleworth and Gurney, 1990). This complexity caused the dissimilarity in results when using some of the aforementioned models in this review, which is also due to the conflicting effect that increase in CO₂ concentration has with increase in temperature. Hence, there is still a need to enhance the robustness of the resistance modeling procedure in order to be applied to different crops under different climatic conditions and under diverse future climate change scenarios. Actually, the great bulk of studies carried out on canopy resistance modelling compared the performance of these models with that of the FAO-PM approach or with different models for estimating ETo, and very few researchers have actually attempted to estimate future changes in ETo based on projected climate change scenarios and estimates of increased CO₂ concentrations. Furthermore, many models were not even tested with the FAO-PM equation, justifying Yang et al. (2019) statement that many present climate models do not account for vegetation responses to an elevated atmospheric CO₂, thus seriously questioning the claim of 'warming leads to drying' in earlier studies.

We note in conclusion that there is a growing need for improved surface resistance models, that may simulate better the changes in stomata physiological responses, thus enhancing the accuracy, reliability and applicability of ET estimates.

REFERENCES

- Adeboye O. B., Osunbitan J. A., Adekalu K. O., Okunade D. A., 2009. Evaluation of FAO-56 Penman-Monteith and temperature based models in estimating reference evapotranspiration using complete and limited data, Application to Nigeria. E-j. - CIGR 11:1-25.
- Ainsworth E. A., Long S. P., 2004. What have we learned from 15 years of free-air CO₂ enrichment (FACE)? A meta-analytic review of the responses of photosynthesis, canopy properties and plant production to rising CO₂. *New Phytol* 165:351-372. <https://doi.org/10.1111/j.1469-8137.2004.01224.x>.
- Alexandratos N., Bruinsma J., 2012. World agriculture towards 2030/2050: the 2012 revision. ESA Working paper No. 12-03. Rome, FAO.
- Allen L. H., 1990. Plant responses to rising carbon dioxide and potential interactions with air pollutants. *J. Environ. Qual* 19:15. <https://doi.org/10.2134/jeq1990.00472425001900010002x>
- Allen R. G., Pereira L. S., Raes D., Smith M., 1998. Crops evapotranspiration - Guidelines for computing crop requirements - Irrigations and Drainage Paper 56. FAO, Rome. 300, D05109.
- Allen R. G., Pruitt W. O., Wright J. L., Howell T. A., Ventura F., Snyder R., Itenfisu D., Steduto P., Berengena J., Basalga Yrisarry J., Smith M., Pereira L. S., Raes D., Perrier A., Alves I., Walter I., Elliott R., 2006. A recommendation on standardized surface resistance for hourly calculation of reference ETo by the FAO56 Penman-Monteith method. *Agric. Water Manage* 81:1-22. <https://doi.org/10.1016/j.agwat.2005.03.007>.
- Alves I., Pereira L. S., 2000. Modelling surface resistance from climatic variables?. *Agric. Water Manage* 42:371-385. [https://doi.org/10.1016/S0378-3774\(99\)00041-4](https://doi.org/10.1016/S0378-3774(99)00041-4).
- Alves I., Perrier A., Pereira L. S., 1998. Aerodynamic and surface resistances of complete over crops: how good in the "big leaf" approach?. *Trans. ASAE* 41(2):345-351. <https://doi.org/10.13031/2013.17184>.
- AQUASTAT (n.d) AQUASTAT website. FAO. fao.org/nr/water/aquastat/main/index.stm (Accessed January 2019).
- Ball J. T., Woodrow I. E., Berry J. A., 1987. A model predicting stomatal conductance and its contribution to the control of photosynthesis under different environmental conditions. *Progress in photosynthesis research*. Dordrecht, The Netherlands: Martinus-Nijhoff Publishers:221-224. https://doi.org/10.1007/978-94-017-0519-6_48.
- Berengena J., Gavilan P., 2005. Reference evapotranspiration estimation in a highly advective semi-arid environment. *J. Irrig. Drain. Eng. ASCE* 131(2):147-163. [https://doi.org/10.1061/\(ASCE\)0733-9437\(2005\)131:2\(147\)](https://doi.org/10.1061/(ASCE)0733-9437(2005)131:2(147)).
- Bernacchi C. J., Kimball B. A., Quarles D. R., Long S. P., Ort D. R., 2007. Decreases in stomatal conductance of soybean under open-air elevation of [CO₂] are closely coupled with decreases in ecosystem evapotranspiration. *Plant Physiol* 143:134-44. <https://doi.org/10.1104/pp.106.089557>.
- Bie W., Casper M. C., Reiter P., Vohland M., 2015. Surface resistance calibration for a hydrological model using evapotranspiration retrieved from remote sensing data in Nahe catchment forest area. *Proc. Int. Assoc. Hydrol. Sci* 368:81-86. <https://doi.org/10.5194/piahs-368-81-2015>.
- Bunce J. A., 2004. Carbon dioxide effects on stomatal responses to the environment and water use by crops under field conditions. *Oecologia* 140:1-10. <https://doi.org/10.1007/s00442-003-1401-6>.
- Burek P., Satoh Y., Fischer G., Kahil M. T., Scherzer A., Tramberend S., Nava L. F., Wada Y., Eisner S., Flörke M., Hanasaki N., Magnuszewski P., Cosgrove B., Wiberg D., 2016. Water Futures and Solution - Fast Track Initiative (Final Report). Available at: <http://pure.iiasa.ac.at/id/eprint/13008/>.
- Calvet J. C., Noilhan J., Roujean J. L., 1998. An interactive vegetation SVAT model tested against data from six contrasting sites. *Agric. For. Meteorol* 92:73-95. [https://doi.org/10.1016/S0168-1923\(98\)00091-4](https://doi.org/10.1016/S0168-1923(98)00091-4).
- Chávez J. L., López-Urrea R., 2019. One-step approach for estimating maize actual water use: Part I. Modelling a variable surface resistance. *Irrig. Sc.* 37(2):123-137. <https://doi.org/10.1007/s00271-018-0606-8>.
- Chiew F., Kamaladasa N., Malano H., McMahon T., 1995. Penman-Monteith, FAO-24 reference crop evapotranspiration and class-A pan data in Australia. *Agric. Water Manage* 28:9-21. [https://doi.org/10.1016/0378-3774\(95\)01172-F](https://doi.org/10.1016/0378-3774(95)01172-F).
- Damour G., Simonneau T., Cochard H., Urban L., 2010. An overview of models of stomatal conductance at the leaf level. *Plant Cell Environ* 33:1419-1438. <https://doi.org/10.1111/j.1365-3040.2010.02181.x>.
- De Fraiture C., Wichelns D., 2010. Satisfying future water demands for agriculture. *Agric. Water Manage* 97:502-511. <https://doi.org/10.1016/j.agwat.2009.08.008>.
- Easterling W. E., Rosenberg N. J., McKenney M. S., Jones C. A., Dyke P. T., Williams J. R., 1992. Preparing the erosion productivity impact calculator (EPIC) model to simulate crop response to climate change and the direct effects of CO₂. *Agric. For. Meteorol* 59:17-34. [https://doi.org/10.1016/0168-1923\(92\)90084-H](https://doi.org/10.1016/0168-1923(92)90084-H).

- Ehleringer J. R., Cerling T. E., Dearing D. M., eds. 2005. A history of atmospheric CO₂ and its effects on plants, animals, and ecosystems. Springer.
- Eitzinger J., Trnka M., Semerádová D., Thaler S., Svobodová E., Hlavinka P., Siska B., Takac J., Malatin-ska L., Novakova M., Dubrovsky M., Zalud Z., 2013. Regional climate change impacts on agricultural crop production in Central and Eastern Europe - hotspots, regional differences and common trends. *J. Agric. Sci* 151:787-812. <https://doi.org/10.1017/S0021859612000767>.
- Fares A., Awal R., Fares S., Johnson A. B., Valenzuela H., 2015. Irrigation water requirements for seed corn and coffee under potential climate change scenarios. *J. Water Clim. Change* 7:jwc2015025. <https://doi.org/10.2166/wcc.2015.025>.
- Ficklin D. L., Luo Y., Luedeling E., Zhang M., 2009. Climate change sensitivity assessment of a highly agricultural watershed using SWAT. *J. Hydrol* 374:16-29. <https://doi.org/10.1016/j.jhydrol.2009.05.016>.
- Garcia M., Raes D., Allen R., Herbas C., 2004. Dynamics of reference evapotranspiration in the Bolivian highlands (Altiplano). *Agric. For. Meteorol* 125:67-82. <https://doi.org/10.1016/j.agrformet.2004.03.005>.
- Gharsallah O., Facchi A., Gandolfi C., 2013. Comparison of six evapotranspiration models for a surface irrigated maize agro-ecosystem in Northern Italy. *Agric. Water Manage* 130:119-130. <https://doi.org/10.1016/j.agwat.2013.08.009>.
- Hanan N., Prince S., 1997. Stomatal conductance of West-Central supersite vegetation in HAPEX-Sahel: measurements and empirical models. *J. Hydrol* 188-189:536-562. [https://doi.org/10.1016/S0022-1694\(96\)03192-7](https://doi.org/10.1016/S0022-1694(96)03192-7).
- Hatch U., Jagtap S., Jones J., Lamb M., 1999. Potential effects of climate change on agricultural water use in the Southeast U.S. *J. Am. Water Resour. Assoc* 35:1551-1561. <https://doi.org/10.1111/j.1752-1688.1999.tb04237.x>.
- Huntington J. L., Morton C. G., McEvoy D., Bromley M., Hedgewisch K., Allen R., Gangopadhyay S., 2016. Historical and future irrigation water requirements for select reclamation project areas, Western U.S. Dissertation, Desert Research Institute. Available at: <https://www.usbr.gov/watersmart/baseline/docs/historicalandfutureirrigationwaterrequirements.pdf>.
- Hussein A. S. A., 1999. Grass ET estimates using Penman-type equations in central Sudan. *J. Irrig. Drain. Eng.*, 125(6):324-329. [https://doi.org/10.1061/\(ASCE\)0733-9437\(1999\)125:6\(324\)](https://doi.org/10.1061/(ASCE)0733-9437(1999)125:6(324)).
- IPCC., 2014a. Climate Change 2014: Impacts, adaptation, and vulnerability. working group ii contribution to the fifth assessment report of the intergovernmental panel on climate change, Cambridge, UK/New York: Cambridge University Press.
- Irmak S., Mutiibwa D., 2010. On the dynamics of canopy resistance: Generalized linear estimation and relationships with primary micrometeorological variables. *Water Resour. Res* 46. <https://doi.org/10.1029/2009WR008484>.
- Irmak S., Mutiibwa D., Irmak A., Arkebauer T. J., Weiss A., Martin D. L., Eisenhauer D. E., 2008. On the scaling up leaf stomatal resistance to canopy resistance using photosynthetic photon flux density. *Agric. For. Meteorol.* 148:1034-1044. <https://doi.org/10.1016/j.agrformet.2008.02.001>.
- Islam A., Ahuja L. R., Garcia L. A., Ma L., Saseendran A. S., 2012. Modeling the effect of elevated CO₂ and climate change on reference evapotranspiration in the semi-arid central great plains. *Trans. ASABE* 55:2135-2146. <https://doi.org/10.13031/2013.42505>.
- Jacobs J. M., Satti S. R., 2001. Evaluation of reference evapotranspiration methodologies and AFSIRS crop water use simulation model. Department of Civil and Coastal Engineering, University of Florida, Gainesville.
- Jarvis P. G., 1976. The interpretation of the variations in leaf water potential and stomatal conductance found in canopies in the field. *Philos Trans R Soc Lond B Biol Sci* 273:593-610. <https://doi.org/10.1098/rstb.1976.0035>.
- Jarvis P. G., McNaughton K., 1986. Stomatal control of transpiration: scaling up from leaf to region. *Adv. Ecol. Res* 15:1-49. [https://doi.org/10.1016/S0065-2504\(08\)60119-1](https://doi.org/10.1016/S0065-2504(08)60119-1).
- Kashyap P., Panda R., 2001. Evaluation of evapotranspiration estimation methods and development of crop-coefficients for potato crop in a sub-humid region. *Agric. Water Manage* 50:9-25. [https://doi.org/10.1016/S0378-3774\(01\)00102-0](https://doi.org/10.1016/S0378-3774(01)00102-0).
- Katerji N., Perrier A., Renard D., Aissa A. K. O., 1983. Modélisation de l'évapotranspiration réelle ETR d'une parcelle de luzerne: rôle d'un coefficient culturel. *Agronomie* 3:513-521. <https://doi.org/10.1051/agro:19830603>
- Katerji N., Rana G., 2006. Modelling evapotranspiration of six irrigated crops under Mediterranean climate conditions. *Agric. For. Meteorol* 138:142-155. <https://doi.org/10.1016/j.agrformet.2006.04.006>.
- Katerji N., Rana G., 2008. Crop evapotranspiration measurements and estimation in the Mediterranean region. INRA-CRA, Bari. ISBN 978:173.
- Katerji N., Rana G., 2011. Crop reference evapotranspiration: a discussion of the concept, analysis of the pro-

- cess and validation. *Water Resour. Manage* 25:1581-1600. <https://doi.org/10.1007/s11269-010-9762-1>.
- Katerji N., Rana G., 2014. FAO-56 methodology for determining water requirement of irrigated crops: critical examination of the concepts, alternative proposals and validation in Mediterranean region. *Theor. Appl. Climatol* 116:515-536. <https://doi.org/10.1007/s00704-013-0972-3>.
- Katerji N., Rana G., Ferrara R. M., 2017. Actual evapotranspiration for a reference crop within measured and future changing climate periods in the Mediterranean region. *Theor. Appl. Climatol* 129: 923-938. <https://doi.org/10.1007/s00704-016-1826-6>.
- Kingston D. G., Todd M. C., Taylor R. G., Thompson J. R., Arnell N. W., 2009. Uncertainty in the estimation of potential evapotranspiration under climate change. *Geophys. Res. Lett* 36. <https://doi.org/10.1029/2009GL040267>.
- Korner G., Schell J. A., Bauer H., 1979. Maximum leaf diffusive conductance in vascular plants. *Photosynthetica* 13 (1):45-82.
- Kreith F., Bohn M., 2001. Principles of heat transfer. New York: Brooks/Cole Eds.
- Kruijt B., Witte J-P M., Jacobs C. M., Kroon T., 2008. Effects of rising atmospheric CO₂ on evapotranspiration and soil moisture: A practical approach for the Netherlands. *J. Hydrol* 349:257-267. <https://doi.org/10.1016/j.jhydrol.2007.10.052>.
- Lardy R., Bachelet B., Bellocchi G., Hill D. R., 2014. Towards vulnerability minimization of grassland soil organic matter using metamodells. *Environ. Modell. Software* 52:38-50. <https://doi.org/10.1016/j.envsoft.2013.10.015>.
- Lardy R., Graux A. I., Bachelet B., Hill D. R., Bellocchi G., 2012. Steady-state soil organic matter approximation model: application to the Pasture Simulation Model. 6th Biennial Meeting of International Congress on Environmental Modelling and Software: Managing Resources of a Limited Planet: Pathways and Visions under Uncertainty. Leipzig, Germany:769-776.
- Lecina S., Martinez-Cob A., Pérez P. J., Villalobos F. J., Baselga J. J., 2003. Fixed versus variable bulk canopy resistance for reference evapotranspiration estimation using the Penman-Monteith equation under semiarid conditions. *Agric. Water Manage* 60:181-198. [https://doi.org/10.1016/S0378-3774\(02\)00174-9](https://doi.org/10.1016/S0378-3774(02)00174-9).
- Leuning R., 1995. A critical appraisal of a combined stomatal- photosynthesis model for C-3 plants. *Plant Cell Environ* 18(4):339-355. <https://doi.org/10.1111/j.1365-3040.1995.tb00370.x>.
- Li S. E., Hao X. M., Du T. S., Tong L., Zhang J. H., Kang S. Z., 2014. A coupled surface resistance model to estimate crop evapotranspiration in arid region of northwest China. *Hydrol. Processes* 28(4):2312-2323. <https://doi.org/10.1002/hyp.9768>.
- Li X., Kang S., Niu J., Huo Z., Liu J., 2019. Improving the representation of stomatal responses to CO₂ within the Penman-Monteith model to better estimate evapotranspiration responses to climate change. *J. Hydrol.* 572:692-705. <https://doi.org/10.1016/j.jhydrol.2019.03.029>.
- Liu G., Hafeez M., Liu Y., Xu D., Vote C., 2012a. A novel method to convert daytime evapotranspiration into daily evapotranspiration based on variable canopy resistance. *J. Hydrol* 414-415:278-283. <https://doi.org/10.1016/j.jhydrol.2011.10.042>.
- Liu G., Liu Y., Hafeez M., Xu D., Vote C., 2012b. Comparison of two methods to derive time series of actual evapotranspiration using eddy covariance measurements in the southeastern Australia. *J. Hydrol* 454-455:1-6. <https://doi.org/10.1016/j.jhydrol.2012.05.011>.
- Liu Y., Pereira L. S., Teixeira J. L., 1997. Update definition and computation of reference evapotranspiration comparison with former method. *J. Hydraul. Eng.*, 6:27-33.
- Long S. P., Ainsworth E. A., Rogers A., Ort D. R., 2004. Rising atmospheric carbon dioxide: plants FACE the future. *Annu. Rev. Plant Biol* 55:591-628. <https://doi.org/10.1146/annurev.arplant.55.031903.141610>.
- López-Urrea R., Martín de Santa Olalla F., Fabeiro C., Moratalla A., 2006. Testing evapotranspiration equations using lysimeter observations in a semiarid climate. *Agric. Water Manage* 85:15-26. <https://doi.org/10.1016/j.agwat.2006.03.014>.
- Lovelli S., Perniola M., Di Tommaso T., Ventrella D., Moriondo M., Amato M., 2010. Effects of rising atmospheric CO₂ on crop evapotranspiration in a Mediterranean area. *Agric. Water Manage* 97:1287-1292. <https://doi.org/10.1016/j.agwat.2010.03.005>.
- Makkink G. F., 1957. Testing the Penman formula by means of lysimeters. *J. Inst. Water Eng* 11:277-288.
- Mall R., Gupta A., Sonkar G., 2017. Effect of climate change on agricultural crops. *Cur. Develop. Biot. and Bioeng*:23-46. <https://doi.org/10.1016/B978-0-444-63661-4.00002-5>.
- Margonis A., Papaioannou G., Kerkides P., Bourazanis G., 2017. Parameterization of “canopy resistance” and estimation of hourly latent heat flux over a crop. *Eur. Water* 59:277-283.
- Martin G., Felten B., Duru M., 2011. Forage rummy: A game to support the participatory design of adapted livestock systems. *Environ. Modell. Software* 26:1442-1453. <https://doi.org/10.1016/j.envsoft.2011.08.013>.

- Massman W. J., 1992. A surface energy balance method for partitioning evapotranspiration data into plant and soil components for a surface with partial canopy cover. *Water Resour. Res* 28:1723-1732. <https://doi.org/10.1029/92WR00217>.
- Medlyn B., Barton C., Broadmeadow M., Ceulemans R., De Angelis P., Forstreuter M., Freeman M., Jackson S. B., Kellomäki S., Laitat E., Rey A., Roberntz P., Sigurdsson B. D., Strassmeyer J., Wang K., Curtis P. S., Jarvis P. G., 2001. Stomatal Conductance of Forest Species after Long-term Exposure to Elevated CO₂ Concentration: A Synthesis. *New Phytol* 149(2):247-264. <https://doi.org/10.1046/j.1469-8137.2001.00028.x>.
- Monteith J. L., 1965. Evaporation and environment. *Symp. Soc. Exp. Biol* 19:205-34.
- Moratiel R., Snyder R. L., Durán J. M., Tarquis A. M., 2011. Trends in climatic variables and future reference evapotranspiration in Duero Valley (Spain). *Nat. Hazards Earth Syst. Sci* 11:1795-1805. <https://doi.org/10.5194/nhess-11-1795-2011>.
- Morison J. I. L., 1987. Intercellular CO₂ Concentration and Stomatal Response to CO₂. *Stomatal Function*. Stanford University Press:229-251.
- Morison J. I., Gifford R. M., 1983. Stomatal sensitivity to carbon dioxide and humidity: a comparison of two C₃ and two C₄ grass species. *Plant Physiol* 71:789-96. <https://doi.org/10.1104/pp.71.4.789>
- Norby R. J., De Kauwe M. G., Domingues T. F., Duursma R. A., Elisworth D. S., Goll D. S., Lapola D. M., Luus K. A., MacKenzie A. R., Medlyn B. E., Pavlick, R., Rammig A., Smith B., Thomas R., Thornicke K., Walker A. P., Yang X., Zaehle S., 2016. Model-data synthesis for the next generation of forest free-air CO₂ enrichment (FACE) experiments. *New Phytol* 209:17-28. <https://doi.org/10.1111/nph.13593>.
- OECD., 2012. OECD environmental outlook to 2050, OECD Publishing, <https://dx.doi.org/10.1787/9789264122246-en>.
- Oliosio A., Huard F., Guilioni L., 2010. Prise en compte des effets du CO₂ sur le calcul de l'évapotranspiration de référence. *Climator 2010*. Versailles, France.
- Pan S., Tian H., Dangal S. R. S., Yang Q., Yang J., Lu C., Tao B., Ren W., Ouyang Z., 2015. Responses of global terrestrial evapotranspiration to climate change and increasing atmospheric CO₂ in the 21st century. *Earth's Future* 3:15-35. <https://doi.org/10.1002/2014EF000263>.
- Parajuli P. B., 2010. Assessing sensitivity of hydrologic responses to climate change from forested watershed in Mississippi. *Hydrol. Processes* 24:3785-3797. <https://doi.org/10.1002/hyp.7793>.
- Pauwels V. R., Samson R., 2006. Comparison of different methods to measure and model actual evapotranspiration rates for a wet sloping grassland. *Agric. Water Manage* 82:1-24. <https://doi.org/10.1016/j.agwat.2005.06.001>
- Penman H. L., 1963. Vegetation and hydrology. *Soil Sci* 96:357.
- Pereira, L. S., Perrier A., Allen R. G., Alves I., 1999. Evapotranspiration: concepts and future trends. *J. Irrig. and Drainage. Eng.*, 125(2):45-51. [https://doi.org/10.1061/\(ASCE\)0733-9437\(1999\)125:2\(45\)](https://doi.org/10.1061/(ASCE)0733-9437(1999)125:2(45)).
- Perez P. J., Lecina S., Castellvi F., Martínez-Cob A., Vilalobos F. J., 2006. A simple parameterization of bulk canopy resistance from climatic variables for estimating hourly evapotranspiration. *Hydrol. Processes* 20:515-532. <https://doi.org/10.1002/hyp.5919>.
- Peterschmitt J-M., Perrier A., 1991. Evapotranspiration and canopy temperature of rice and groundnut in southeast coastal India. Crop coefficient approach and relationship between evapotranspiration and canopy temperature. *Agric. For. Meteorol* 56:273-298. [https://doi.org/10.1016/0168-1923\(91\)90096-9](https://doi.org/10.1016/0168-1923(91)90096-9).
- Piao S., Ciais P., Huang Y., Shen Z., Peng S., Li J., Zhou L., Liu H., Ma Y., Ding Y., Friedlingstein P., Liu C., Tan K., Yu Y., Zhang T., Fang J., 2010. The impacts of climate change on water resources and agriculture in China. *Nature* 467:43-51. <https://doi.org/10.1038/nature09364>.
- Polley H. W., 2002. Implications of atmospheric and climatic change for crop yield and water use efficiency. *Crop Sci* 42:131-140. <https://doi.org/10.2135/cropsci2002.1310>.
- Priya A., Nema A. K., Islam A., 2014. Effect of climate change and CO₂ on reference evapotranspiration in Varanasi, India-A case study. *J Agrometeorol* 16:44-51.
- Ráczy C., Nagy J., Dobos A. C., 2013. Comparison of several methods for calculation of reference evapotranspiration. *Acta Silv. Lignaria Hung* 9:9-24. <https://doi.org/10.2478/aslh-2013-0001>.
- Rana G., Katerji N., Mastrorilli M., 1998. Canopy resistance modelling for crops in contrasting water conditions. *Phys. Chem. Earth* 23:433-438. [https://doi.org/10.1016/S0079-1946\(98\)00049-4](https://doi.org/10.1016/S0079-1946(98)00049-4).
- Rana G., Katerji N., Mastrorilli M., El Moujabber M., 1994. Evapotranspiration and canopy resistance of grass in a Mediterranean region. *Theor Appl Climatol*. 50(1-2):61-71. <https://doi.org/10.1007/BF00864903>.
- Rana G., Katerji N., Perniola M., 2001. Evapotranspiration of sweet sorghum: A general model and multilocal validity in semiarid environmental condi-

- tions. *Water Resour. Res* 37:3237-3246. <https://doi.org/10.1029/2001WR000476>.
- Rasul G., Mahmood A., 2009 Performance evaluation of different methods for estimation of evapotranspiration in Pakistan's climate. *Pak J Agr Sci* 5:25-36.
- Rosegrant M. W., Cai X., Cline S. A., 2002. World water and food to 2025: Dealing with scarcity. *Intl Food Policy Res Inst. Washington, DC*:322.
- Rosenzweig C., Iglesias A., 1998. The use of crop models for international climate change impact assessment. In *Understanding options for agricultural production*. Springer, Dordrecht:267-292. https://doi.org/10.1007/978-94-017-3624-4_13.
- Salmon-Monviola J., Moreau P., Benhamou C., Durand P., Merot P., Oehler F., Gascuel-Oudou C., 2013. Effect of climate change and increased atmospheric CO₂ on hydrological and nitrogen cycling in an intensive agricultural headwater catchment in western France. *Clim. Change* 120:433-447. <https://doi.org/10.1007/s10584-013-0828-y>.
- Shams S., Nazemosadat S. M. J., Haghghi A. A. K., Parsa S. Z., 2012. Effect of carbon dioxide concentration and irrigation level on evapotranspiration and yield of red bean. *J. Sci. Technol. Greenh. Cult* 2:1-10.
- Shuttleworth, W. J., Gurney, R. J., 1990. The theoretical relationship between foliage temperature and canopy resistance in sparse crops. *Q. J. R. Meteorol. Soc.* 116 (492):497-519. <https://doi.org/10.1002/qj.49711649213>
- Shuttleworth W. J., Wallace J. S., 1985. Evaporation from sparse crops-an energy combination theory. *Q. J. R. Meteorol. Soc* 111:839-855. <https://doi.org/10.1002/qj.49711146910>.
- Snyder R., Moratiel R., Song Z., Swelam A., Jomaa I., Shapland T., 2011. Evapotranspiration response to climate change. *Acta Hort* 922:91-98. <https://doi.org/10.17660/ActaHortic.2011.922.11>.
- Stannard D. I., 1993. Comparison of Penman-Monteith, Shuttleworth-Wallace, and modified Priestley-Taylor evapotranspiration models for wildland vegetation in semiarid rangeland. *Water Resour. Res* 29:1379-1392. <https://doi.org/10.1029/93WR00333>.
- Steduto P., Todorovic M., Calciando A., Rubino P., 2003. Daily reference evapotranspiration estimates by the Penman-Monteith equation in Southern Italy. Constant vs. variable canopy resistance. *Theor. Appl. Climatol* 74:217-225. <https://doi.org/10.1007/s00704-002-0720-6>.
- Stockle C. O., Williams J. R., Rosenberg N. J., Jones C. A., 1992. A method for estimating the direct and climatic effects of rising atmospheric carbon dioxide on growth and yield of crops: Part I—Modification of the EPIC model for climate change analysis. *Agric. Syst* 38:225-238. [https://doi.org/10.1016/0308-521X\(92\)90067-X](https://doi.org/10.1016/0308-521X(92)90067-X).
- Strzepek K. M., Major D. C., Rosenzweig C., Iglesias A., Yates D. N., Holt A., Hillel D., 1999. New methods of modelling water availability for agriculture under climate change: the U.S. Cornbelt 1. *J. Am. Water Resour. Assoc* 35:1639-1655. <https://doi.org/10.1111/j.1752-1688.1999.tb04242.x>.
- Suleiman A. A., Hoogenboom G., 2007. Comparison of Priestley-Taylor and FAO-56 Penman-Monteith for daily reference evapotranspiration estimation in Georgia. *J. Irrig. Drain. Eng* 133:175-182. [https://doi.org/10.1061/\(ASCE\)0733-9437\(2007\)133:2\(175\)](https://doi.org/10.1061/(ASCE)0733-9437(2007)133:2(175)).
- Taiz L., Zeiger E., 1991. *Plant physiology the benjamin. Cummings* Redwood City, CA.
- Temesgen B, Eching S, Davidoff B, Frame K (2005) Comparison of some reference evapotranspiration equations for California. *J. Irrig. Drain. Eng* 131:73-84. [https://doi.org/10.1061/\(ASCE\)0733-9437\(2005\)131:1\(73\)](https://doi.org/10.1061/(ASCE)0733-9437(2005)131:1(73)).
- Tipple B. J., Pagani M., 2007. The early origins of terrestrial C₄ photosynthesis. *Annu. Rev. Earth Planet Sci* 35:435-61. <https://doi.org/10.1146/annurev.earth.35.031306.140150>.
- Todorovic M., 1999. Single-layer evapotranspiration model with variable canopy resistance. *J. Irrig. Drain. Eng.*, 125:235-245. [https://doi.org/10.1061/\(ASCE\)0733-9437\(1999\)125:5\(235\)](https://doi.org/10.1061/(ASCE)0733-9437(1999)125:5(235)).
- Trenberth K. E., Fasullo J. T., Kiehl J., 2009. Earth's Global Energy Budget. *Bull. Am. Meteorol. Soc* 90:311-324. <https://doi.org/10.1175/2008BAMS2634.1>.
- Tubiello F. N., Donatelli M., Rosenzweig C., Stockle C. O., 2000. Effects of climate change and elevated CO₂ on cropping systems: model predictions at two Italian locations. *Eur. J. Agron* 13:179-189. [https://doi.org/10.1016/S1161-0301\(00\)00073-3](https://doi.org/10.1016/S1161-0301(00)00073-3).
- UNDESA (United Nations-Department of Economic and Social Affairs), 2017. World population prospects: The 2017 revision, key findings and advance tables. Working Paper No. ESA/P/WP/248.
- Van der Kooi C. J., Reich M., Löw M., De Kok L. J., Tausz M., 2016. Growth and yield stimulation under elevated CO₂ and drought: A meta-analysis on crops. *Environ. Exp. Bot* 122:150-157. <https://doi.org/10.1016/j.envexpbot.2015.10.004>.
- Ventura F., Spano D., Duce P., Snyder R. L., 1999. An evaluation of common evapotranspiration equations. *Irrig Sci* 18:163-170. <https://doi.org/10.1007/s002710050058>.
- Wada Y., Flörke M., Hanasaki N., Eisner S., Fischer G., Tramberend S., Sotah Y., van Vliet M. T. H., Yillia P,

- Burek P., Wiberg D., 2016. Modeling global water use for the 21st century: the Water Futures and Solutions (WFaS) initiative and its approaches. *Geosci. Model Dev* 9:175-222. <https://doi.org/10.5194/gmd-9-175-2016>.
- Wand S. J. E., Midgley G. F., Jones M. H., Curtis P. S., 1999. Responses of wild C₄ and C₃ grass (Poaceae) species to elevated atmospheric CO₂ concentration: a meta-analytic test of current theories and perceptions. *Global Change Biol* 5:723-741. <https://doi.org/10.1046/j.1365-2486.1999.00265.x>.
- Wang J. L., Wen, X. F., 2010. Modeling the response of stomatal conductance to variable CO₂ concentration and its physiological mechanism. *Acta Ecol. Sin.* 30 (17):4815-4820.
- Wang S. S., Yang Y., Trishchenko A. P., Barr A. G., Black T. A., McCaughey H., 2009. Modeling the response of canopy stomatal conductance to humidity. *J. Hydrometeorol* 10(2):521-532. <https://doi.org/10.1175/2008JHM1050.1>.
- Whitehead D., 1998. Regulation of stomatal conductance and transpiration in forest canopies. *Tree Physiol.* 18 (8-9):633-644. <https://doi.org/10.1093/treephys/18.8-9.633>.
- Wullschlegel S. D., Gunderson C. A., Hanson P. J., Wilson K. B., Norby R. J., 2002. Sensitivity of stomatal and canopy conductance to elevated CO₂ concentration - interacting variables and perspectives of scale. *New Phytol* 153:485-496. <https://doi.org/10.1046/j.0028-646X.2001.00333.x>.
- Wu Y., Liu S., Abdul-Aziz O. I., 2012. Hydrological effects of the increased CO₂ and climate change in the Upper Mississippi River Basin using a modified SWAT. *Clim. Change* 110:977-1003. <https://doi.org/10.1007/s10584-011-0087-8>.
- WWAP, 2012. The United Nations World Water Development Report 4: Managing water under uncertainty and risk. Paris, UNESCO.
- Xu C., Gong L., Jiang T., Chen D., Singh V., 2006. Analysis of spatial distribution and temporal trend of reference evapotranspiration and pan evaporation in Changjiang (Yangtze River) catchment. *J Hydrol* 327(1):81-93. <https://doi.org/10.1016/j.jhydrol.2005.11.029>.
- Yan H., Zhang C., Peng G., Darko R. O., Cai B., 2017. Modelling canopy resistance for estimating latent heat flux at a tea field in South China. *Exp. Agric* 54:563-576. <https://doi.org/10.1017/S0014479717000242>.
- Yang Q., Tian H., Li X., Tao B., Ren W., Chen G., Lu C., Yang J., Pan S., Banger K., 2015. Spatiotemporal patterns of evapotranspiration along the North American east coast as influenced by multiple environmental changes. *Ecohydrol.* :1-12, doi:10.1002/eco.1538.
- Yang Y., Roderick M. L., Zhang S., McVicar T. R., Donohue R. J., 2019. Hydrologic implications of vegetation response to elevated CO₂ in climate projections. *Nat. Clim. Change* 9:44-48. <https://doi.org/10.1038/s41558-018-0361-0>.
- Yoder R., Odhiambo L., Wright W., 2005. Evaluation of methods for estimating daily reference crop evapotranspiration at a site in the humid Southeast United States. *Appl. Eng. Agric* 21:197-202. <https://doi.org/10.13031/2013.18153>.
- Yu G., Wang Q., 2010. *Ecophysiology of plant photosynthesis, transpiration, and water use*. Beijing: Science Press, 2010:351-352.
- Zhang B. Z., Kang S. Z., Li F. S., Zhang L., 2008. Comparison of three evapotranspiration models to Bowen ratio-energy balance method for a vineyard in an arid desert region of northwest China. *Agric. For. Meteorol* 148 (10):1629-1640. <https://doi.org/10.1016/j.agrformet.2008.05.016>.
- Zhang B., Xu D., Liu Y., Li F., Cai J., Du L., 2016. Multi-scale evapotranspiration of summer maize and the controlling meteorological factors in north China. *Agric. For. Meteorol* 216:1-12. <https://doi.org/10.1016/j.agrformet.2015.09.015>.
- Zhou H., Kang S., Tong L., Ding R., Li S., Du T., 2019. Improved application of the Penman-Monteith model using an enhanced Jarvis model that considers the effects of nitrogen fertilization on canopy resistance. *Environ. Exp. Bot* 159:1-12. <https://doi.org/10.1016/j.envexpbot.2018.12.007>.

RIGOROUS PEER REVIEW

Each submission to IJAm is subject to a rigorous quality control and peer-review evaluation process before receiving a decision. The initial in-house quality control check deals with issues such as competing interests; ethical requirements for studies involving human participants or animals; financial disclosures; full compliance with IJAm's data availability policy, etc. Submissions may be returned to authors for queries, and will not be seen by our Editorial Board or peer reviewers until they pass this quality control check. Each paper is subjected to critical evaluation and review by Field Editors with specific expertise in the different areas of interest and by the members of the international Editorial Board.

OPEN ACCESS POLICY

The Italian Journal of Agrometeorology provides immediate open access to its content. Our publisher, Firenze University Press at the University of Florence, complies with the Budapest Open Access Initiative definition of Open Access: By "open access", we mean the free availability on the public internet, the permission for all users to read, download, copy, distribute, print, search, or link to the full text of the articles, crawl them for indexing, pass them as data to software, or use them for any other lawful purpose, without financial, legal, or technical barriers other than those inseparable from gaining access to the internet itself. The only constraint on reproduction and distribution, and the only role for copyright in this domain is to guarantee the original authors with control over the integrity of their work and the right to be properly acknowledged and cited. We support a greater global exchange of knowledge by making the research published in our journal open to the public and reusable under the terms of a Creative Commons Attribution 4.0 International Public License (CC-BY-4.0). Furthermore, we encourage authors to post their pre-publication manuscript in institutional repositories or on their websites prior to and during the submission process and to post the Publisher's final formatted PDF version after publication without embargo. These practices benefit authors with productive exchanges as well as earlier and greater citation of published work.

COPYRIGHT NOTICE

Authors who publish with IJAm agree to the following terms:

Authors retain the copyright and grant the journal right of first publication with the work simultaneously licensed under a Creative Commons Attribution 4.0 International Public License (CC-BY-4.0) that allows others to share the work with an acknowledgment of the work's authorship and initial publication in IJAm. Authors are able to enter into separate, additional contractual arrangements for the non-exclusive distribution of the journal's published version of the work (e.g., post it to an institutional repository or publish it in a book), with an acknowledgment of its initial publication in this journal.

Authors are allowed and encouraged to post their work online (e.g., in institutional repositories or on their website) prior to and during the submission process, as it can lead to productive exchanges, as well as earlier and greater citation of published work (See The Effect of Open Access).

PUBLICATION FEES

Unlike many open-access journals, the Italian Journal of Agrometeorology does not charge any publication fee.

WAIVER INFORMATION

Fee waivers do not apply at Firenze University Press because our funding does not rely on author charges.

PUBLICATION ETHICS

Responsibilities of IJAm's editors, reviewers, and authors concerning publication ethics and publication malpractice are described in IJAm's Guidelines on Publication Ethics.

CORRECTIONS AND RETRACTIONS

In accordance with the generally accepted standards of scholarly publishing, IJAm does not alter articles after publication: "Articles that have been published should remain extant, exact and unaltered to the maximum extent possible". In cases of serious errors or (suspected) misconduct IJAm publishes corrections and retractions (expressions of concern).

Corrections

In cases of serious errors that affect or significantly impair the reader's understanding or evaluation of the article, IJAm publishes a correction note that is linked to the published article. The published article will be left unchanged.

Retractions

In accordance with the "Retraction Guidelines" by the Committee on Publication Ethics (COPE) IJAm will retract a published article if:

- there is clear evidence that the findings are unreliable, either as a result of misconduct (e.g. data fabrication) or honest error (e.g. miscalculation)
- the findings have previously been published elsewhere without proper crossreferencing, permission or justification (i.e. cases of redundant publication)
- it turns out to be an act of plagiarism
- it reports unethical research.
- An article is retracted by publishing a retraction notice that is linked to or replaces the retracted article. IJAm will make any effort to clearly identify a retracted article as such.

If an investigation is underway that might result in the retraction of an article IJAm may choose to alert readers by publishing an expression of concern.

ARCHIVING

IJAm and Firenze University Press are experimenting a National legal deposition and long-term digital preservation service.

SUBMITTING TO IJAm

Submissions to IJAm are made using FUP website. Registration and access are available at: <https://riviste.fupress.net/index.php/IJAm/submission>
For more information about the journal and guidance on how to submit, please see <https://riviste.fupress.net/index.php/IJAm/index>

Principal Contact

Simone Orlandini, University of Florence
simone.orlandini@unifi.it

Support Contact

Alessandro Pierno, Firenze University Press
alessandro.pierno@unifi.it

GUIDE FOR AUTHORS

1. Manuscript should refer to original researches, not yet published except in strictly preliminary form.
2. Articles of original researches findings are published in Italian Journal of Agrometeorology (IJAm), subsequent to critical review and approval by the Editorial Board. External referees could be engaged for

particular topics.

3. Three types of paper can be submitted: original paper, review, technical note. Manuscript must be written in English. All pages and lines of the manuscript should be numbered.

4. First Name, Last Name, position, affiliation, mail address, telephone and fax number of all the Co-Authors are required. Corresponding Authors should be clearly identified.

5. The abstract should be no longer than 12 typed lines.

6. Full stop, not comma, must be used as decimal mark (e.g. 4.33 and not 4,33).

7. Figures, tables, graphs, photos and relative captions should be attached in separate files. All images must be vector or at least 300 effective ppi/dpi to ensure quality reproduction.

8. Captions should be written as: Fig. x – Caption title, Tab. x – Caption title. Images should be referred to in the text as (Fig. x), (Tab. x).

9. Proof of the paper (formatted according to the Journal style) will be sent to the Corresponding Author for proof reading just one time. Corrections can be made only to typographical errors.

10. All the references in the text must be reported in the "References" section and vice-versa. In the text, only the Author(s) last name must be present, without the name or the first letter of the name (e.g. "Rossi, 2003" and not "Federico Rossi, 2003" or "F. Rossi, 2003"). If two authors are present, refer to them as: "Bianchi and Rossi, 2003" in the text (do not use "&" between the surnames). If more than two Authors are present, refer to them as: "Bianchi et al., 2003" in the text.

For journals, references must be in the following form:

Bianchi R., Colombo B., Ferretti N., 2003. Title. Journal name, number: pages.

For books:

Bianchi R., Colombo B., Ferretti N., 2003. Book title. Publisher, publishing location, total number of pages pp.

Manuscripts "in press" can be cited.

BECOME A REVIEWER

Peer review is an integral part of the scholarly publishing process. By registering as a reviewer, you are supporting the academic community by providing constructive feedback on new research, helping to ensure both the quality and integrity of published work in your field. Once registered, you may be asked to undertake reviews of scholarly articles that match your research interests. Reviewers always have the option to decline an invitation to review and we take care not to overburden our reviewers with excessive requests.

You must login before you can become a reviewer.

If you don't want to be a reviewer anymore, you can change your roles by editing your profile.

COMPETING INTERESTS

You should not accept a review assignment if you have a potential competing interest, including the following:

- Prior or current collaborations with the author(s)
- You are a direct competitor
- You may have a known history of antipathy with the author(s)
- You might profit financially from the work

Please inform the editors or journal staff and recuse yourself if you feel that you are unable to offer an impartial review.

When submitting your review, you must indicate whether or not you have any competing interests.



Italian Journal of Agrometeorology

Rivista Italiana di Agrometeorologia

n. 1 – 2020

Table of contents

Serhan Yeşilköy, Levent Şaylan

Assessment and modelling of crop yield and water footprint of winter wheat by aquacrop 3

Barbara Parisse, Antonella Pontrandolfi, Chiara Epifani, Roberta Alilla, Flora De Natale

An agrometeorological analysis of weather extremes supporting decisions for the agricultural policies in Italy 15

Alireza Ahrar, Farzad Paknejad, Seyed Ali Tabatabaei, Fayaz Aghayari, Elias Soltani

Evaluation of forage Amaranth (*Amaranthus hypochondriacus* L.) yield via comparing drought tolerance and susceptibility indices 31

Evangelini Kitta, Nikolaos Katsoulas

Effect of shading on photosynthesis of greenhouse hydroponic cucumber crops 41

Pasquale Garofalo, Domenico Ventrella, Marcello Mastrorilli, Angelo Domenico Palumbo, Pasquale Campi

An empirical framework for modelling transpiration use efficiency and radiation use efficiency of biomass sorghum in Mediterranean environment 49

Abdalla Dao, Amidou Guira, Jorge Alvar-Beltrán, Abdou Gnanda, Louis Nebie, Jacob Sanou

Quinoa's response to different sowing periods in two agro-ecological zones of Burkina Faso 63

Thi Mai Anh Tran, Josef Eitzinger, Ahmad M. Manschadi

Response of maize yield under changing climate and production conditions in Vietnam 73

Ghaieth Ben Hamouda, Francesca Ventura

Evaluation of some evapotranspiration estimation models under CO₂ increasing concentrations: A review 85